Report No. BDK75 977-49 Date: December 2013
FINAL REPORT

Contract Title: Steel Shear Strength of Anchors with Stand-off Base Plates
UF Project No. 00093973
Contract No. BDK75 977-49

STEEL SHEAR STRENGTH OF ANCHORS WITH STAND-OFF BASE PLATES

Principal Investigators: Ronald A. Cook, Ph.D., P.E.
David O. Prevatt, Ph.D., P.E.

Graduate Research Assistant: Kenton E. McBride, E.I.

Project Manager: William Potter, P.E.

Department of Civil and Coastal Engineering
College of Engineering
University of Florida
Gainesville, FL 32611

Engineering and Industrial Experiment Station

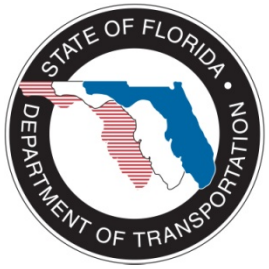

DISCLAIMER

The opinions, findings, and conclusions expressed in this publication are those of the authors and not necessarily those of the State of Florida Department of Transportation.

METRIC CONVERSION TABLE

SYMBOL	WHEN YOU KNOW	MULTIPLY BY	TO FIND	SYMBOL
		LENGTH		
in	inches	25.4	millimeters	mm
ft	feet	0.305	meters	m

SYMBOL	WHEN YOU KNOW	MULTIPLY BY	TO FIND	SYMBOL
		AREA		
in^2	square inches	645.2	square millimeters	mm^2
ft^2	square feet	0.093	square meters	m^2

SYMBOL	WHEN YOU KNOW	MULTIPLY BY	TO FIND	SYMBOL
		VOLUME		
fl oz	fluid ounces	29.57	milliliters	mL
gal	gallons	3.785	liters	L
ft^3	cubic feet	0.028	cubic meters	m^3
yd^3	cubic yards	0.765	cubic meters	m^3
NOTE: volumes greater than 1000 L shall be shown in m^3				

SYMBOL	WHEN YOU KNOW	MULTIPLY BY	TO FIND	SYMBOL
		MASS		
oz	ounces	28.35	grams	g
lb	pounds	0.454	kilograms	kg

SYMBOL	WHEN YOU KNOW	MULTIPLY BY	TO FIND	SYMBOL
		TEMPERATURE (exact degrees)		
°F	Fahrenheit	5 (F-32)/9 or (F-32)/1.8	Celsius	°C

SYMBOL	WHEN YOU KNOW	MULTIPLY BY	TO FIND	SYMBOL
		FORCE and PRESSURE or STRESS		
lbf	pound force	4.45	newtons	N
lbf/in^2	pound force per square inch	6.89	kilopascals	kPa
kip	1,000 pounds force	4.45	kilonewtons	kN
kip-ft	1,000 pounds force - feet	1.36	kilonewton-meter	kN-m
kip/in^2	1,000 pounds force per square inch	6.89	megapascals	MPa

TECHNICAL REPORT DOCUMENTATION PAGE

1. Report No.	2. Government Accession No.	3. Recipient's Catalog No.

4. Title and Subtitle	5. Report Date
Steel Shear Strength of Anchors with Stand-off Base Plates	September 2013
	6. Performing Organization Code 00093973
7. Author(s) K. E. McBride, R. A. Cook, and D. O. Prevatt	8. Performing Organization Report No. 2013/93973
9. Performing Organization Name and Address University of Florida Department of Civil and Coastal Engineering 365 Weil Hall / P.O. Box 116580 Gainesville, FL 32611-6580	10. Work Unit No. (TRAIS) 11. Contract or Grant No. BDK75 977-49
12. Sponsoring Agency Name and Address Florida Department of Transportation Research Management Center 605 Suwannee Street, MS 30 Tallahassee, FL 32301-8064	13. Type of Report and Period Covered DRAFT Final Report April 2011 – September 2013 14. Sponsoring Agency Code
15. Supplementary Notes	

16. Abstract

Sign and signal structures are often connected to concrete foundations through a stand-off annular base plate with a double-nut anchor bolt connection, which leaves exposed anchor bolt lengths below leveling nuts used in these connections. Cantilever sign and signal structures may experience high shear forces in anchor bolts due to torsion at the base connection resulting from wind loads. Grout pads, which may or may not be present in existing structures, offer additional restraint against these forces. Motivated by gaps in information and lack of uniformity in addressing anchor bolt steel shear strength in stand-off base plates, this research study was initiated to quantify the reduction in steel shear strength for anchors installed with stand-off base plates and develop draft design and maintenance guidelines for these systems.

To satisfy these objectives, a three-phase experimental study was undertaken. Phase 1 utilized direct shear methodology to establish relationships between stand-off distance and ultimate steel shear strength. Phase 2 contained torsion tests of ungrouted and grouted circular groups of 5/8 in. and 1 in. diameter anchor bolts. Phase 3 comprised four full-scale tests containing circular groups of six 1.25 in. diameter bolts. Decreases in anchor steel shear strength were observed for all levels of stand-off distance, including those within the current permissible range for ignoring strength reductions caused by bolt bending. Grouted tests contained higher shear strengths commensurate with flush-mounted strength at high levels of connection deformation, while an FRP retrofit around the perimeter of the grout pad resulted in higher strength at lower connection deformation. Design and maintenance recommendations include consideration for strength reduction of anchor bolts in all stand-off base plates, allowance for grout pad contributions to ultimate strength in double-nut connections, and use of grout pads as a viable retrofit for increasing the strength of existing ungrouted stand-off base plates.

17. Key Word	18. Distribution Statement
cantilever structures, anchor bolts, shear strength, base connection, base plates, annular plate, anchors, grout,	No restrictions

19. Security Classif. (of this report)	20. Security Classif. (of this page)	21. No. of Pages	22. Price
Unclassified	Unclassified	164	

Form DOT F 1700.7 (8-72) Reproduction of completed page authorized

ACKNOWLEDGMENTS

The authors are grateful to the Florida Department of Transportation (FDOT) for funding this multi-phase research study. Sincere thanks are extended to Josh Burkard, Kunal Malpani, and Andrew De Alba for their contributions to laboratory testing conducted at the University of Florida. Work conducted at the University of Florida was also supported by patient telephone and email correspondence on instrumentation, test methodology, and physical implementation of the experimental program by FDOT personnel. Testing conducted at the FDOT Marcus H. Ansley Structures Research Center was enabled by much appreciated support from FDOT personnel with specimen preparation, instrumentation setup, cleanup, and material testing.

EXECUTIVE SUMMARY

Sign and signal structures are often connected to concrete foundations through a stand-off annular base plate with a double-nut anchor bolt connection, which leaves exposed anchor bolt lengths below leveling nuts used in these connections. Cantilever sign and signal structures may experience wind-induced torsion from wind load, which transfers potentially high shear forces to individual anchor bolts. Grout pads, which may or may not be present in existing structures, offer additional restraint against these forces. Current code specifications do not account for strength reduction when the distance from the bottom of the leveling nut to the concrete surface is less than one anchor bolt diameter in ungrouted stand-off base plates. Code allowance of grout contribution to strength varies from no allowance to a simple reduction factor applied to equivalent connections where the base plate is fastened flush with the concrete surface. Gaps in information and uniformity in addressing anchor bolt steel shear strength in stand-off base plates served as the motivating factor for this experimental study, which was driven by two primary objectives:

- Quantify the reduction in steel shear strength for anchors installed with stand-off base plates.
- Develop draft design and maintenance guidelines for these systems.

To satisfy these objectives, the research program presented herein included a literature review, a comparison of existing code standards, a three-phase experimental study, and development of draft guidelines. Phase 1 utilized direct shear methodology to establish relationships between stand-off distance and ultimate steel shear strength, also addressing installation method, single- and double-bolt connections, and bolt diameter. Phase 2 contained torsion tests of ungrouted and grouted circular groups of 5/8 in. and 1 in. diameter anchor bolts installed in oversize holes. Stand-off distance, influence of grout, bolt pretensioning, size effect,

and the presence of a fiber-reinforced polymer (FRP) wrap were investigated for their influence on strength and behavior. Phase 3 comprised four full-scale tests containing circular groups of six 1.25 in. diameter bolts, again installed in oversize holes, testing the influence of grout pads, stand-off distance, and base plate type.

Statistically significant differences were produced between anchor bolts at *all* levels of stand-off distance, including within the permissible range for ignoring strength reductions caused by bolt bending. The strengths of flush-mounted torsion tests were slightly less than direct shear counterparts, which was attributed to the use of oversize holes in Phase 2. Grouted tests contained higher shear strengths commensurate with flush-mounted strength, but at higher levels of connection deformation than observed with flush-mounted plates. No difference in ultimate strength was observed between grouted base plate stand-off distances. An FRP retrofit around the perimeter of the grout pad provided higher strength at lower connection deformation. Similar reduction in the strength to direct shear and scaled torsion tests was seen in the ungrouted full-scale test. Grouted test behavior and strength were consistent with scaled torsion tests.

Design and maintenance recommendations include consideration for strength reduction of anchor bolts in *all* stand-off base plates, allowance for grout pad contributions to ultimate strength in double-nut connections, and use of grout pads as a viable retrofit for increasing the strength of existing ungrouted stand-off base plates. Recommendations for future work include further development of a bolt bending model in ungrouted stand-off base plates, experimental tests of anchor bolt strength in structures with various levels of combined loading, a parametric study of grout pad dimensions, and further investigation of FRP as a structural retrofit in grouted stand-off base plates.

TABLE OF CONTENTS

page

LIST OF FIGURES

Figure page

LIST OF TABLES

Table page

CHAPTER 1
INTRODUCTION

1.1 Problem Statement

Anchored steel base plates used to connect poles in sign and signal structures to concrete foundations often stand off of the foundation, resting on nuts threaded onto the anchor bolts that can be adjusted during erection to level the structure. A nut is subsequently tightened above the stand-off base plate on each bolt, forming a “double-nut” connection. As a result, an exposed length of the bolt is left between the top of the concrete surface and the bottom of the leveling nut. Shear forces on individual anchor bolts must transfer over the exposed length, resulting in axial stresses due to bolt bending over the exposed length in addition to the shear stresses. Correspondingly, shear strength and stiffness of anchor bolts in stand-off base plates is significantly lower than in equivalent flush-mounted base plates. Anchor bolts in cantilever sign and signal structures such as in Figure 1-1 experience high magnitudes of shear force, predominantly from wind-induced torsion forces transferred through the base plate.

Figure 1-1. Cantilever sign structure with an ungrouted stand-off base plate

Until 2008, the FDOT provided details for the use of grout pads underneath base plates in their design standards for cantilever sign structures (Index No. 11310) and cantilevered mast arm assemblies (Index No. 17745). Thus, both ungrouted and grouted stand-off base plates are currently in service in the state of Florida. While anchor bolt steel shear strength in ungrouted stand-off base plates is addressed in the AASHTO *Standard Specifications for Structural Supports for Highway Signs, Luminaires, and Traffic Signals* (AASHTO 2013b), bending is allowed to be ignored in exposed lengths of up to one anchor bolt diameter. ACI's *Building Code Requirements for Structural Concrete* (ACI 2011) and AISC's *Steel Construction Manual* (AISC 2010) do not include provisions for ungrouted stand-off base plates. For grouted stand-off base plates, AASHTO (2013b) does not allow grout to contribute to design strength, ACI (2011) applies a 0.8 factor to the shear strength of equivalent flush-mounted connections, and AISC (2010) simply states that anchor bolt bending must be considered when the design calls for shear transfer through the bolts. A survey of state DOTs in NCHRP 494 found that a majority of states refer to AASHTO for anchor bolt design. The survey also found that while foundation failure of sign and signal supports is not common, the majority of such failures were attributed to anchor bolts (Fouad et al., 2003). The absence of information and uniformity in addressing anchor bolt steel shear strength in stand-off base plates served as the motivating factor for this experimental study.

1.2 Components

A typical double-nut stand-off base plate connection with an annular base plate welded to a steel pole is shown in Figure 1-2. The NCHRP 494 survey found that signal and sign structures are connected predominantly to reinforced drilled shafts and spread footings. The base plate containing prefabricated holes is set over the anchors. Pretensioning of anchor bolts, which

FDOT employs, was practiced in only 7% and 11% of reporting states for sign and signal structures, respectively (Fouad et al., 2003).

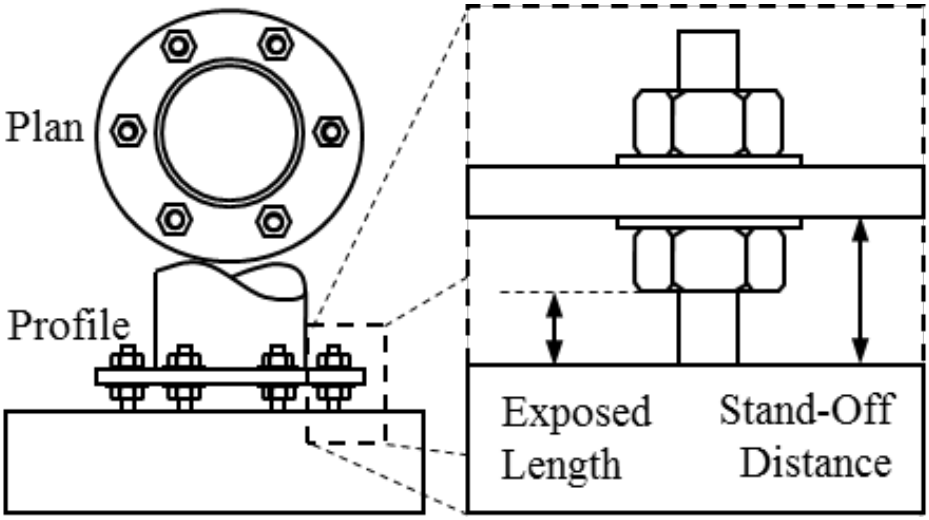

Figure 1-2. Typical double-nut annular stand-off base plate plan (left) and profile (right) views

Cast-in-place (CIP) anchors may have a forged head or nuts, a plate washer, or a hooked or bent end to develop embedment strength against anchor bolt tension forces. A wide variety of post-installed anchors also exist that utilize different combinations of mechanical, adhesive, and friction mechanisms for load transfer from the base plate to the concrete. The majority of states reported using straight headed bolts for sign structures and hooked bolts for signal structures. Anchor bolts ranged in diameter from 0.5 in. to 3.5 in, with reported averages of 1.88 in. and 1.54 in. for cantilevered sign and signal structures, respectively.

1.3 Connection Types

For the purposes of this study, these connections are broken into three categories: flush-mounted base plates, ungrouted stand-off base plates, and grouted stand-off base plates. Figure 1-3 provides a schematic illustration of each. Subsequent paragraphs define and describe the installation each of these connection types.

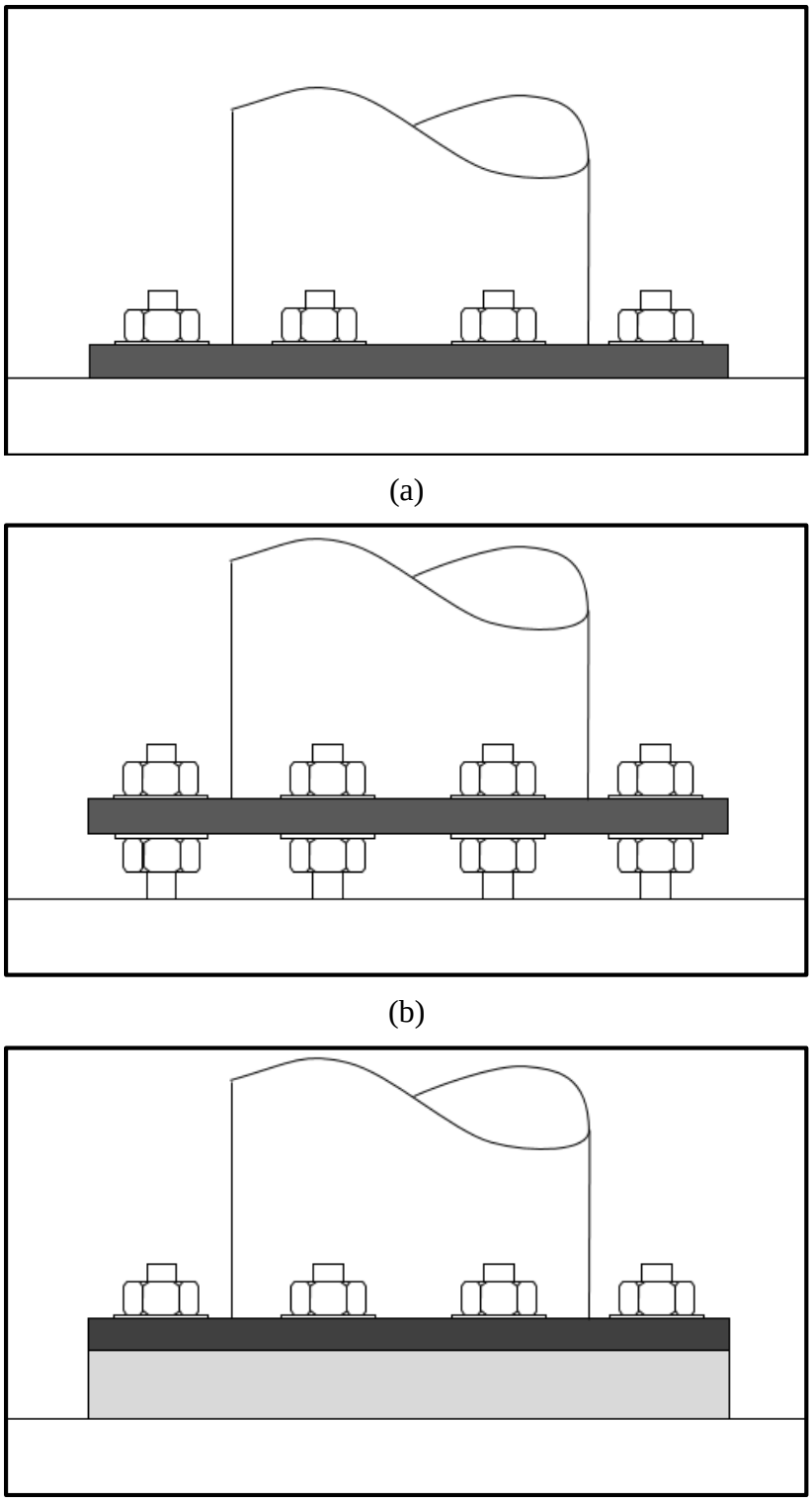

Figure 1-3. Schematic illustrations of (a) flush-mounted, (b) ungrouted stand-off, and (c) grouted stand-off base plates

Flush-mounted base plates are set directly on a finished concrete surface with anchors protruding from the concrete. Nuts (structural washers may be present) fasten the base plate to the anchors. Tightening the nuts engages the bolts in tension through a depth of the foundation concrete.

Ungrouted stand-off base plates contain leveling nuts placed on the anchor bolts protruding from the concrete. The base plate is set on the leveling nuts, after which tightening nuts are threaded onto the top of the base plate, forming a double-nut connection. Tightening the nuts places tension only in the length of the bolt between the nuts, i.e. within the thickness of the base plate and/or washers. An ungrouted stand-off base plate connection could also be achieved without leveling nuts by setting the base plate on shim stacks or a leveling plate, but examples of such connections have not been found in the literature.

Grouted stand-off base plates are used in both column and signal/sign connections. The base plate is first leveled on leveling nuts, shim stacks, or a setting plate. After the base plate has been erected and fastened, grout is placed to enclose the void between the base plate and the concrete surface. Tightening top nuts prestresses bolts within the thickness of the base plate in double-nut connections and through the grout into the concrete in single-nut grouted connections.

1.4 Modes of Load Transfer

Loads on sign and signal structures are predominantly induced by wind or seismic events and self-weight. In cantilever sign structures, a resultant lateral load produces global overturning moment, torsion, and direct shear at the base of the pole which are transferred through the annular base plate to anchor bolts. All of these forces resolve to combinations of axial and shear forces within individual anchor bolts within the group depending on their position within the base plate. Axial forces in individual bolts result from the superimposition of equally shared base

plate axial loads and unequally distributed axial forces from base plate overturning moments. The magnitude of axial force from overturning moment is related to the anchor bolt position relative to the neutral axis of the base plate moment. Shear force on individual anchor bolts is the resultant vector from equally distributed direct shear and resolved base plate torsion forces as shown in Figure 1-4. Resultant wind loads acting on signs in cantilever structures produce individual bolt forces from torsion V_t on the order of ten times the direct shear force V_v.

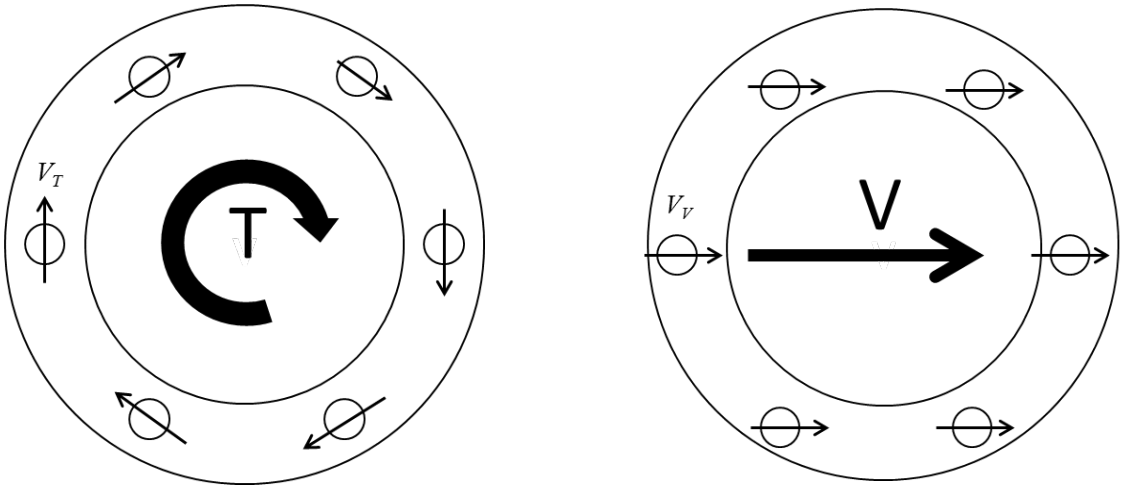

(a) (b)

Figure 1-4. Transfer of base plate torsion and direct shear forces into individual shear forces on anchor bolts

Connection type dictates the mechanisms of load transfer from the base plate to the concrete foundation. In flush-mounted connections, compression forces are transferred directly from the base plate to the concrete. Tension forces are transferred fully through the anchors and into the supporting concrete foundation. Overturning moments are resolved into compression forces acting on the concrete alone and tension forces in the anchors. Base plate rigidity plays a role in the distribution of compression and tension forces from overturning moment. However, for the purposes of this study, it is assumed that base plates are fully rigid elements. Direct shear

and torsional force is taken by a combination of the resistance of the steel anchors and friction between the base plate and the concrete surface.

Ungrouted stand-off base plates transfer all compression and tension forces through anchor bolts. Overturning moment, then is taken by both tension and compression in the bolts depending on the position of the bolts relative to the neutral axis of bending. The force in individual bolts is proportional to the distance from the neutral axis over the moment of inertia of the bolt group. Shear forces (V_t and $V_v$in Figure 1-4) act over a lever arm in the bolts. As a result of the shear force acting over this distance, localized bending produces bending stresses in the bolts in addition to the constant shear force, the most extreme stresses at the top and bottom of the lever arm where rotation is restrained on both sides. If one end is free to rotate as in some single-bolt connections, the bolt acts as a "flagpole" with extreme bending moments at the point of restraint. Figure 1-5 illustrates the transfer of shear force into anchor bolt shear and moment forces assuming a beam bending model with moment restraint at the top and the bottom of the exposed length of the anchor bolt.

In grouted connections, compression forces may be transferred directly from the base plate to the concrete or through the anchor bolts in double-nut connections. Tension forces are transferred fully through the anchors and into the supporting concrete foundation. Overturning moments may be resolved into compression forces acting on the grout and concrete or through the anchor bolts in double nut connections and into tension forces in the anchors. Direct shear and torsional force is taken by a combination of the resistance of the steel anchors and any frictional forces that might exist between the base plate and the concrete/grout surface.

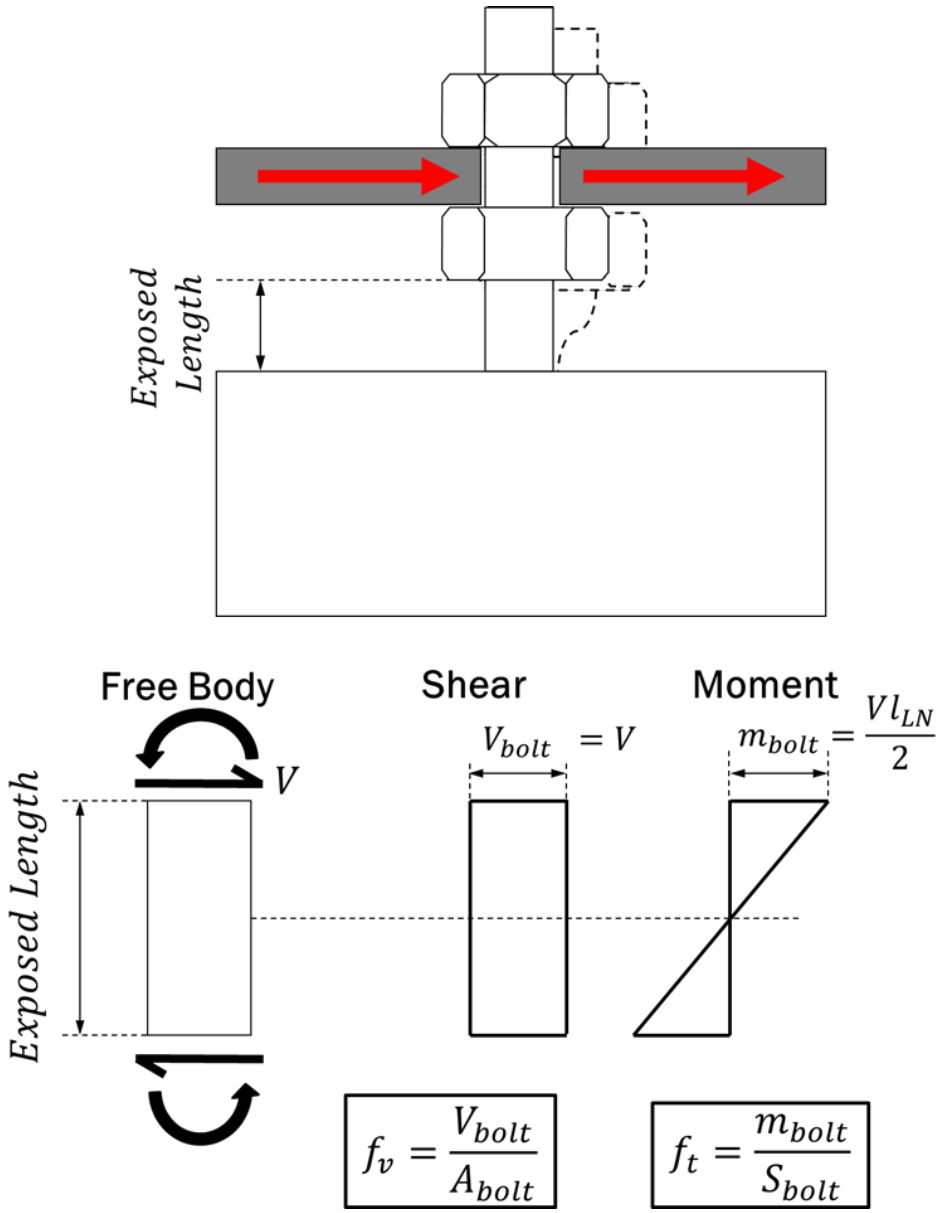

Figure 1-5. Schematic illustrations shear force transfer through double-nut ungrouted stand-off base plate connection

1.5 Focus of Study and Report Organization

Beyond steel failure, several other tension and shear failure modes related to the embedded portion of the anchor are defined by ACI 318-11 Appendix D (ACI 2011). All potential failure modes are shown in Table 1-1 and need to be considered in the design of an anchor bolt. The basis for the definitions of failure and their corresponding designs comes from Fuchs et al. (1995), Eligehausen and Balogh (1995), and Eligehausen et al. (2006a). This project focuses on

the steel shear strength and behavior of anchor bolts in ungrouted and grouted stand-off base plates. As such, all other failure modes were not considered.

Table 1-1. Tension and shear failure modes defined by ACI (2011)

Tension Failure Modes	Shear Failure Modes
steel	steel
concrete breakout	concrete breakout
adhesive bond	concrete pryout
pullout	
side-face blowout	
concrete splitting	

This report presents a three-phase experimental study of the steel shear strength of anchor bolts in ungrouted and grouted stand-off base plate connections in six chapters. Chapter 1 provides background information and definitions introducing the problem that this research addresses along with basic definition of components and the mechanics of load transfer in these connections. Chapter 2 provides a review of related research studies, including the tension, shear, and combined steel strength and behavior of steel-to-steel connections, single-bolt steel-to-concrete connections, and bolt group connections to concrete. Chapter 3 discusses how forces experienced by anchor bolts in flush-mounted, ungrouted, and grouted stand-off base plate connections are addressed in design. Chapter 4 describes the materials, methods, and experimental designs used for all three experimental phases within the study. Chapter 5 details the results from these phases and presents comparisons of current code provisions to test data. Finally, Chapter 6 summarizes the results and provides conclusions, recommendations for design and maintenance, and recommendations for future work relating to the steel strength of anchor bolts. Appendices A, B, and C provide load-displacement behavior for the tests conducted in Phases 1, 2, and 3, respectively. Appendix D contains the draft version of design guidelines for anchor bolt steel strength and Appendix E contains revised FDOT grout pad specifications based on the findings of this research.

CHAPTER 2
LITERATURE REVIEW

2.1 Introduction

This chapter provides a review of research reports and articles on the steel strength of anchor bolts. Other potential failure modes related to the embedment (concrete breakout, pullout, pryout, etc.) are not covered since they were not within the scope of this study. Design information on embedment failure modes is available in ACI 318-11.

2.2 Individual Bolt Steel Strength in Flush-mounted Steel-to-steel Connections

2.2.1 Axial

The tensile strength of threaded bolts is equal to the ultimate tensile stress capacity of the bolts multiplied by the net tensile area of the cross-section. In threaded regions, the net tensile stress area given in Equation (2-1) is based on the provisions of ANSI B1.1 as provided in Table 7-17 in AISC (2010). According to Yura et al. (1987), this slightly underrepresents the tensile stress area. Nonetheless, it is used in this report due to its general acceptance in practice. The variables factored into net tensile stress area for common threaded rod sizes as well as the gross and net tensile areas are presented in Table 2-1 as provided by Table 7-17 of AISC (2010). In addition, Table 2-1 contains ratios of the threaded area to the gross bolt area for these bolt sizes, which range from 0.72 to 0.80 for 0.5 in. to 2 in. diameter bolts, respectively.

$$A_{nt} = \frac{\pi}{4} * (d_b - \frac{0.9743}{n})^2 \quad (2\text{-}1)$$

where A_{nt} = net tensile area of the anchor, in.^{2}
d_b = unthreaded bolt diameter, in.
n = number of threads per inch

Table 2-1. Threaded rod section properties

Bolt Dia., d_b (in.)	Gross Bolt Area, A_b (in.^{2})	Threads per in., n	Net Tensile Area, A_{nt} (in.^{2})	A_{nt}/A_b
0.5	0.196	13	0.142	0.72
0.625	0.307	11	0.226	0.74
0.75	0.442	10	0.334	0.76
0.875	0.601	9	0.462	0.77
1	0.785	8	0.606	0.77
1.125	0.994	7	0.763	0.77
1.25	1.227	7	0.969	0.79
1.375	1.485	6	1.155	0.78
1.5	1.767	6	1.405	0.80
1.75	2.405	5	1.899	0.79
2	3.142	4.5	2.498	0.80

While it has been shown to have no impact on ultimate tensile strength, pretensioning by the "turn-of-the-nut" method brings the tensioned length of bolt into the initial stages of yield behavior (Kulak et al. 1987) and is recommended in NCHRP 469 (Dexter and Ricker 2002) for better anchor bolt performance under fatigue loading for sign and signal structures. The Federal Highway Administration *Guidelines for the Installation, Maintenance, and Repair of Structural Supports for Highway Signs, Luminaires, and Traffic Signals* (FHWA 2002) provides a procedure for tightening anchor bolts in a star pattern using the turn-of-the-nut method.

2.2.2 Shear

Shear strength of steel bolts is generally expressed as a constant proportion of the tensile strength. The elastic yield stress of a steel element exposed to shear forces can be derived using the von Mises formulation in Equation (2-2). With unidirectional shear, all normal stresses as well as the shear stresses in the other two directions reduce to zero. The reduced formulation, then, may be expressed as shown in Equation (2-3). While this formulation is applicable only in the linear-elastic range of stress-strain steel behavior, it serves as a good approximation for

inelastic strength. Setting the effective stress equal to the tensile yield stress of the steel, a yield shear stress, τ, of 0.577 of the tensile yield stress is predicted.

$$\sigma_{eff} = \sqrt{\frac{1}{2}((\sigma_x - \sigma_y)^2 + (\sigma_y - \sigma_z)^2 + (\sigma_z - \sigma_x)^2 + 6(\tau^2{}_{xy} + \tau^2{}_{yz} + \tau^2{}_{zx}))} \quad (2\text{-}2)$$

$$\sigma_{eff} = \sqrt{\frac{1}{2} * 6(\tau^2))} = \sqrt{3} * \tau \quad (2\text{-}3)$$

where $\sigma_x, \sigma_y, \sigma_z$ = directional normal stresses on the element
$\tau_{xy,}\tau_{yz,}\tau_{zx}$ = directional shear stresses on the element

To determine the shear strength of bolt materials experimentally, Wallaert and Fisher (1965) conducted tests on individual 7/8 in. diameter and 1 in. diameter ASTM A325, A354, and A490 bolts installed in two test configurations. Configuration type, grade, diameter, and grip length were studied for their influence, finding that only the test setup condition affected the shear strength of these steel materials. Kulak et al. (1987) state that the test setup producing the lower-bound ratio of 0.62 should be used as a basis for determining pure shear strength experimentally of bolt materials. The American Institute of Steel Construction *Steel Construction Manual* (AISC 2010) uses the 0.62 value from the lower-bound test configuration in Wallaert and Fisher (1965). Kulak also stated that pretensioning the bolts had no influence on shear strength, as the low-magnitude axial strains incurred in the preload process are overcome and their stresses discharged in tests of ultimate shear strength.

The ratio of threaded shear strength to unthreaded shear strength in bolts is frequently assumed to be equal to the ratio of the net tensile area (2-1) to the gross bolt area. Yura et al. (1987), however, conducted several tests on ASTM A325 and A490 bolts with threads included and excluded from the shear plane, finding that the ratio of threaded to unthreaded strength was

0.83, higher than the net tensile area to nominal area of 0.77 for the 7/8 in. and 1 in. bolts tested. It was stated that the shear area is larger than the tensile area for the threaded portion of bolts, accounting for the higher values.

2.2.3 Combined Axial and Shear

Chesson et al. (1965) conducted bolt steel strength tests on 3/4 in. and 1 in. dia. ASTM A325 and A354 bolts under combinations of tension and shear loading. Tests were conducted using 7 tension-to-shear ratios ranging from pure tension to pure shear in an angled load application approach. In addition to the ratio of tensile stress to shear stress, presence of threads in the failure plane, bolt material, test block material, and bolt diameter were also considered for their influence on the tests. Based on the work by Chesson et al. (1965), Kulak et al. (1987) suggested the following relationship to describe the strengths of all steel-to-steel fasteners subjected to combined tension and shear given in Equation (2-4).

$$\left(\frac{x}{0.62}\right)^2 + y^2 = 1.0 \qquad (2\text{-}4)$$

where $x =$ ratio of shear stress to tensile stress capacity
$y =$ ratio of tensile stress to tensile stress capacity

2.3 Individual Bolt Steel Strength in Steel-to-concrete Connections

2.3.1 Axial

The axial steel strength of anchor bolts in steel-to-concrete connections is the same as in steel-to-steel connections. Refer to Section 2.2.1. Axial stiffness may vary based on properties of the embedded portion of the anchor (e.g. adhesive, cast-in-place, mechanical).

2.3.2 Shear

2.3.2.1 Shear in Flush-mounted Base Plates

Anchor bolts loaded in shear bear directly against the concrete surface, producing stress concentrations and potentially different behavior than in steel-to-steel connections. Eligehausen et al. (2006b) describe the general transfer of shear forces in a flush-mounted base plate. Any existing pretensioning in the anchor bolt generates compressive frictional resistance to shear between the base plate and concrete surface. Shear force greater than the frictional resistance causes the base plate to slip until the shear is transferred to the bolt. The bolt bears against the foundation until a concrete spall occurs, lowering the effective surface of the concrete and developing bending stresses and catenary tensile stresses in the anchor bolt in addition to the predominating shear stress. When steel failure is observed, the interaction of shear, tensile, and flexural forces within some anchor bolt length causes rupture as demonstrated in Figure 2-1 and described in Paulay et al. (1974).

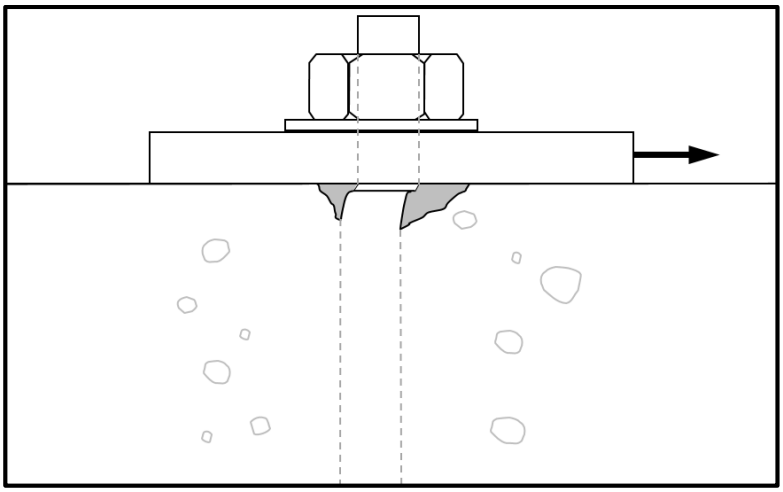

Figure 2-1. Illustration of steel shear failure of an anchor bolt in a flush-mounted base plate

Models accounting for the effects of the concrete support to an anchor bolt exposed to shear load have been developed assuming the anchor bolt is a beam supported by an elastic/elasto-plastic foundation. The first such model was proposed by Friberg (1940), which,

according to Eligehausen et al. (2006b), predicts failure loads on the order of half of experimental values. Given the complexity of these formulations, the inaccuracy of predictions, and that anchor bolt strength does not vary widely from steel-to-steel connections, however, it is standard practice to characterize steel shear failure in anchor bolt connections proportionally to the tensile strength of the steel as in steel-to-steel connections. Eligehausen et al. (2006b) proposes a constant of 0.6 to describe the relationship between shear and tensile capacity of anchor bolts installed in normal strength concrete as a result of the aggregation of German and American shear strength tests.

Grosser (2012) performed anchor bolt steel shear tests as part of a comprehensive research program on the connection strength of flush-mounted base plates studying concrete, steel, and combined failure modes. Material strength, bolt ductility, concrete strength, and embedment depths were investigated for their influence on steel shear strength.

In one set of tests, medium-strength concrete (4,600 psi), high-strength concrete (9,700 psi), and a rigid steel base were used as the anchor bolt foundation material for anchor bolts of three steel grades and three sizes. While concrete strength influenced the load-displacement and ultimate load, its influence on shear strength was not quantified due to the complexity of bolt bending forces within the depth of spall, particularly in the low-strength concrete, as discussed above. By inspection of reported COV values, the differences in ultimate strength due to concrete material do not appear to be statistically significant. Material strength and ductility, however, were correlated with the ultimate shear strengths; proposed correction factors were established with anchor bolt shear capacity inversely proportional to steel strength and directly proportional to steel ductility.

In a separate set of tests by Grosser (2012), the effect of embedment depth on anchor bolt shear strength was studied for low-strength (3,300 psi) and medium-strength (5,000 psi) concrete. In the low-strength concrete, anchor bolt shear strengths for embedment depths of 5 nominal diameters were approximately 20% lower than bolts installed with embedment depths of 8 bolt diameters. No difference, however, was observed in strength in the medium-strength concrete between the same embedment depth ratios. Ultimately, Grosser (2012) proposed Equation (2-5) to characterize flush-mounted anchor bolt shear strength, ${V^0}_{Rk,s}$, in design.

$$ {V^0}_{Rk,s} = k_{s1} * \mathrm{k_{s2}} * k_{s3} * A_s * f_{uk} \tag{2-5} $$

where
- k_{s1} = 0.6 for f_u < 500 MPa
  = 0.5 for 500 MPa ≤ f_u ≤ 1,000 MPa
  = 0.4 for f_u > 1,000 MPa
- k_{s2} = 1.0 for anchor bolts or unwelded headed studs
  = 1.2 for embed plates with headed studs
- k_{s3} = 0.8 for A_5 elongation < 16%
  = 1.0 for A_5 elongation ≥ 16%
- A_5 = rupture elongation measured across 5 bolt diameters
- A_s = cross-sectional area of steel
- f_{uk} = nominal characteristic ultimate tensile strength
- f_u = actual ultimate tensile strength

2.3.2.2 Shear in Ungrouted Stand-off Base Plates

The two previous studies on anchor bolt steel shear strength in ungrouted stand-off base plates utilized steel-to-steel connections. Thus, the influence of concrete on the connection behavior and strength was assumed by effective bending values by the respective authors.

Scheer et al. (1987) performed singly moment-restraining (flagpole) tests of anchor bolts at varying distances from the base material to the load application. Because this publication is in German, test details and conclusions were not explored. Based on this work, Eligehausen et al. (2006b) use Equation (2-6) to characterize the theoretical shear strength, $V_{u,s}$, of a stand-off base plate assembly purely as a function of tensile stresses due to the bolt moment. Figure 2-2

provides dimensions used in this formulation. The authors state that where the distance from the concrete surface to the center of shear loading is greater than one bolt diameter, any shear influence on bending moment at failure can be neglected.

$$V_{u,s} = \frac{\alpha_M * M_{u,s}}{l} \tag{2-6}$$

where α_M = correction factor for base plate rotation
= 1.0 when rotation is not restrained
= 2.0 when rotation is restrained
$M_{u,s}$ = average bending moment at failure = $1.7W_{el}f_y$
W_{el} = elastic section modulus of threaded portion of the bolt
f_y = measured steel yield stress
l = shear load lever arm = $e_1 + a_3$
e_1 = distance from concrete surface to base plate mid-thickness
a_3 = 0.5d when no nut is fastened to the concrete surface
= 0 when nut fastened to concrete surface

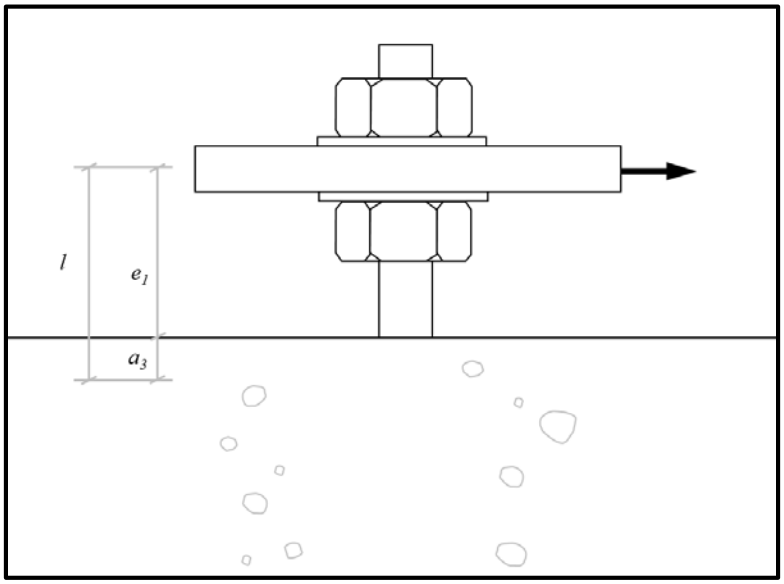

Figure 2-2. Dimensions used in Eligehausen et al. (2006b) for anchor bolt bending stresses

Lin et al. (2011) conducted physical and simulated tests of bolts with a moment arm in a steel-to-steel arrangement. The physical test setup included two 5/8 in. dia. B7 threaded rods loaded simultaneously in shear varying exposed lengths from 0.2 to 8 nominal bolt diameters with finger-tightened nuts. Two hole size conditions were tested, one with and one without 1/8

in. oversize. The test setup was arranged for vertical restraint of the bolts, which exists when grout pads, shim stacks or other stiff materials are placed below the base plate, but does not exist in ungrouted stand-off base plates.

Three zones of load displacement behavior were characterized for bolts with 2 diameter exposed lengths or greater: 1) an initial linear-elastic segment, 2) an approximately linear strain-hardening segment, and 3) tensile engagement of the bolt until rupture. Tensile contributions (Zone 3) to the observed failure strengths were significant due to the vertical restraint of the test specimens. Additional rotation within oversize holes allowed further tensile engagement, resulting in ultimate strengths between 16% percent and 36% higher than snug-hole counterparts for 2 diameter and 4 diameter exposed lengths, respectively.

Equation (2-7) characterizing the shear strength, V_{se}, of bolts with exposed lengths was proposed, adding the interaction of shear and moment as well as tension developed in the deformed anchor bolt to the equation by Eligehausen et al. (2006). The rotation angle, β, is estimated by summing any potential rotations from an oversize hole and from the rotations that would correspond to bold rupture from tensile strains due to bending within a plastic hinge. This was estimated using the tensile elongation of a bolt over the assumed length of the hinge, either 1/2 of the exposed length or one bolt diameter, whichever is less. Rotation due to the formation of the plastic hinge was taken as the curvature due to the strain multiplied by the bolt diameter. Any rotations allowed by the oversize holes was added to the plastic curvature for the β value in the second equation. The proposed equation fit the finite element analysis data well with the given constraints, with experimental data from oversized holes falling between two assumed values of bolt rotation.

$$V_{se} = f_{ya} A_{se,v} \sin(\beta) \frac{f_{ya} \cos(\beta)}{\frac{1}{0.9 A_{se,v}} + \frac{l}{3.4 S}} \quad (2\text{-}7)$$

where f_{ya} = yield strength of the bolt material
$A_{se,v}$ = cross-sectional area of bolt
β = bolt rotation with respect to initial shape (see above)
l = exposed length of the bolt
S = section modulus of the bolt

2.3.2.3 Shear in Grouted Stand-off Base Plates

Adihardjo and Soltis (1979) and Nakashima (1998) included cases of shear-only loading as part of their studies investigating combined tension and shear on stand-off base plates. In the shear-only cases, Adihardjo and Soltis observed shear *yield* strength of approximately 0.55 of the tension strength while Nakashima (1998) observed ultimate shear strengths between 0.6 and 0.7 of tension strength, both reporting high levels of displacement and grout cracking en route to failure. Further descriptions of these studies are provided in Section 2.3.3.3.

2.3.3 Combined Axial and Shear

2.3.3.1 Combined Axial and Shear in Flush-mounted Base Plates

For anchor bolts in flush-mounted base plates experiencing combined tension and shear, slight variations of have been proposed in the exponent of the elliptical equation given for steel-to-steel connections in Equation (2-4). McMackin et al. (1973) performed tests of combined tension and shear on anchor bolts, finding that an exponent of 5/3 fit the data appropriately. Similarly, Lotze et al. (2001) performed an extensive test program of individual anchor bolts subjected to combined tension and shear forces. The test setup used an angled member that reacted against the concrete block that contained anchor bolt specimens. Results were evaluated against different exponent values in the tension-shear interaction equation and the authors concluded that an exponent value of 1.67 (5/3) to 1.8 is appropriate for anchored connections to

concrete. ACI (2011) currently employs a 5/3 exponent for evaluating tension/shear interaction between both steel and embedment failure modes.

2.3.3.2 Combined Axial and Shear in Ungrouted Stand-off Base Plates

No experimental studies were found in the literature on combined axial and shear force applied to single-bolt connections with ungrouted stand-off base plates. Bolt group tests were performed by Kaczinski et al. (1998) as discussed in Section 2.4.2.

2.3.3.3 Combined Axial and Shear in Grouted Stand-off Base Plates

Adihardjo and Soltis (1979) studied the steel strength of single 0.5 in. dia. anchor bolts with 1 in. grout pads subjected to varying combinations of tension and shear. Failure was defined as yielding of the anchor bolt. Following this definition, tests were not run to anchor bolt steel rupture. Results were plotted against variants of the elliptical tension/shear interaction equation given in Equation (2-4). Tests with a low ratio of applied shear to applied tension agreed well with the interaction curves; however, as the ratio of shear load to tension load increased to 1 and beyond, yielding was lower than predicted by the interaction equations assuming a shear strength of 0.6 of the tension strength. The authors discussed the effects of moment within the bolts as the grout pad began to fail, allowing horizontal slip of the base plate.

Nakashima (1998) also performed single-anchor tests with combined tension and shear at various angles of applied load, including cases with direct tension and direct shear. Tests contained a 20 mm. base plate and 20 mm. grout pad. The effect of embedment depth and the influence of threads in the shear plane on the strength of anchors exposed to combined loads were also studied. It was found that test values exceeded the capacity predicted by the elliptical interaction equation between applied tension and shear stresses. Embedment depth did not significantly change the results, although it was noted that very short embedments produced slightly higher values. No observable difference was found between tests where the shear plane

was located within the threaded portion and where the shear plane was located at the intersection of the threaded and unthreaded portion of the bolts. Where the shear plane was in the shank, the values appear to be slightly higher than would be predicted by the increase in net area of the bolt.

2.4 Group Bolt Steel Strength in Steel-to-concrete Connections

In studies related to groups of anchors, the influence of axial and shear in the anchors are intertwined based on the magnitudes of applied moment, shear, and torsion forces on the structure. For this reason, the following discussions are not broken down into individual sections dealing with axial strength, shear strength, and combined axial and shear.

2.4.1 Flush-mounted Base Plates

Cook and Klingner (1992) described the work conducted in Cook (1989) on anchor bolt behavior and strength on a variety of multiple-bolt connections with square flush-mounted base plates. Varying combinations of shear and overturning moment using the test setup shown in Figure 2-3. Tests ranged from nearly pure shear applied to the base plate to predominantly overturning moment. ASTM A193 B7 threaded rod was used for all tests.

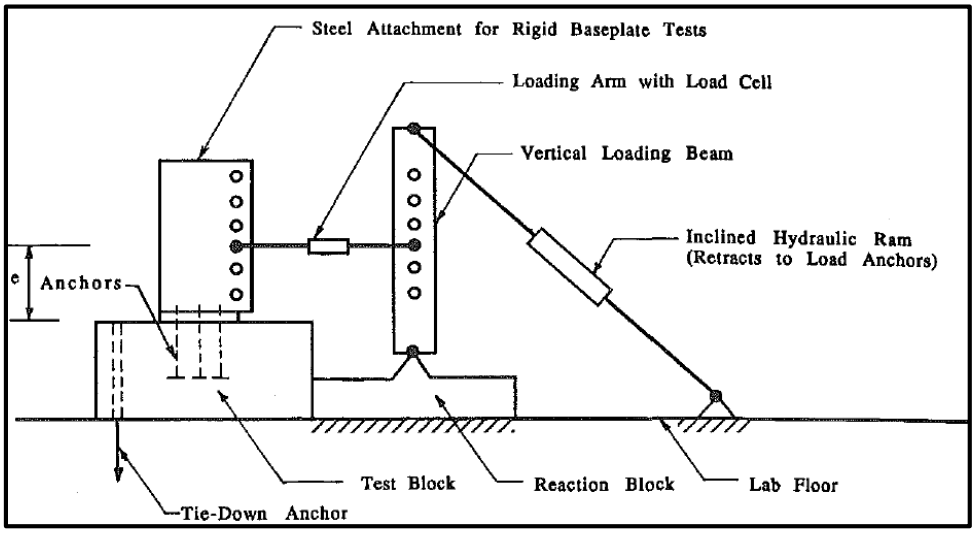

Figure 2-3. Schematic of test setup given in Cook and Klingner (1992)

Beyond moment-to-shear ratio, other parameters studied included different arrangements of anchor bolts, number of bolts, base plate flexibility, and friction contributions to the strength

of the connection. Cook and Klingner (1992) provided a model to characterize the shear strength of a group of anchor bolts, V_{ut}, applied at an eccentricity e. Based on critical values of e, ranges of shear- and moment-dominated behavior were defined. Shear-dominated behavior ($e < e''$) was defined as the range in which applied shear forces exceeded the resultant steel-to-concrete friction forces caused by the moment. For the shear-dominated range of eccentricities, Equation (2-8) was developed, which includes the elliptical representation of anchor bolt tension and shear forces of Equation (2-4). In moment-dominated behavior ($e > e''$), bolt shear did not contribute substantially to failure and the bolt group strength was characterized by Equation (2-9). While it did not affect the calculated value of bolt group steel strength, a second critical eccentricity e' defined the threshold between base plate slip and lack of slip due to friction. It was determined that the coefficient of friction between a steel base plate and concrete foundation can be taken as 0.4. As high hole tolerances, low steel ductility, and the number of anchors in line with applied load load can all affect the ability for the system to distribute load equally between multiple anchors, Cook and Klingner (1992) recommend that $\gamma = 0.5$ and 0.6 for multiple anchor bolt to concrete systems with adhesive and cast-in-place anchors, respectively.

$$V_{ut} = \gamma T_0 \frac{ma + \sqrt{n^2(a^2 + b^2) - m^2 b^2}}{a^2 + b^2} \tag{2-8}$$

$$V_{ut} = \frac{nT_0 d}{e} \tag{2-9}$$

where
γ = ratio of shear to tensile strength (assumed to be 0.5 for anchor bolts)
T_0 = ultimate tensile strength of the anchor
m = number of rows of anchors in the compression zone of bending
a = $1 - \frac{\mu e}{d}$
n = number of bolts
b = $\frac{\gamma e}{d}$
e = eccentricity of applied load; equal to ratio of base plate moment to shear
Critical eccentricities:
e'' = minimum eccentricity for connections with no tension-shear interaction

$= \frac{nd}{n\mu+m\gamma}$

e' = minimum eccentricity for connections experiencing no base slip

$= \frac{d}{\mu}$

d = distance from compressive reaction to tension anchors

μ = coefficient of friction between the base plate and concrete

2.4.2 Ungrouted Stand-off Base Plates

No studies were identified that have tested the ultimate capacity of multiple-bolt connections in ungrouted stand-off base plates. However, as part of a much larger study focusing on the fatigue performance of cantilever sign and signal structures, Kaczinski et al. (1998) applied low levels of load to ungrouted stand-off base plates in full-scale cantilever sign assemblies. The following were identified as variables affecting the performance of anchored base plate connections: misalignment of anchor bolts (i.e. out-of-plumbness), exposed length of the bolts, and nut tightness (i.e. pretensioning). Test specimens included a group of eight 1.5 in. diameter Grade 55 bolts installed at a 21 in. bolt circle diameter with bolt exposed lengths of 1 in. Two anchor bolt plumbness values (perfectly plumb and 1:20 out-of-plumb) and two base plate thicknesses (1 in. and 1.5 in.) were studied, producing four unique assemblies. Four ratios of Moment:Torsion:Shear were applied to each of the four assemblies. Using two of the load ratios and both plumbness values, additional tests were conducted with 3 in. anchor bolt exposed lengths. Load was applied monotonically in tension and compression to a reported half of the yield strength for every test.

To measure the effect of applied load on the anchor bolts, four uniaxial strain gages were installed at 90 degree intervals on the exposed portion of each anchor bolt. The authors acknowledged bolt bending from shear forces produced by direct shear and torsional base plate forces. To isolate bolt bending in tests with overturning moment and no applied torsion, strain gage readings on bolts positioned most closely to the neutral axis of the base plate overturning

moment were used. Calculated bolt bending stresses from strain gage readings were compared to theoretical bending moments assuming the bolts to be fixed-fixed beams with the direct shear load distributed equally between the eight bolts. Theoretical bending moments were reported as between 40% and 90% higher than calculated moments from strain gauge readings for the bolts with 3 in. exposed length. Greater discrepancy was reported between calculated and theoretical bolt bending moments in the 1 in. exposed length tests. On bolts with axial stress due to base plate overturning moment, bending stresses were less than ten percent of the total stresses for these bolts, leading to the conclusion that these stresses may be ignored for anchor bolt exposed length less than one bolt diameter. Although tests were performed with a relatively high torsion, it does not appear that the resulting bending stresses in the bolts from these types of tests were included in the assessment of the magnitude of bending stresses resulting from all sources of anchor shear compared to anchor axial stresses from overturning moment.

2.4.3 Grouted Stand-off Base Plates

Cook et al. (1995) and Cook et al. (2000a) studied linear load-displacement behavior of standoff base plate connections for sign/signal structures with and without grout pads below the base plate under high ratios load of moment to shear. Cook and Bobo (2001) synthesized this work, providing guidelines for required base plate thickness, required tensile stress area of bolts, and contributions to global signal rotation from base plate components.

Cook et al. (2000b) investigated corrosion of bolts with and without grout pads exposed to 14 weeks of rotating between saltwater immersion and free air exposure up to the base plate. The two grouts studied exhibited different water sorptivity levels. It was found that after 14 weeks, the bolts with grout lost nearly no section to corrosion, while the bolts that were ungrouted rusted significantly. Between the two grouts studied, no difference in weight loss was found. It was concluded that the properly installed grout protected the bolts rather than exacerbating corrosion.

Properly installed grout (as discussed within Section 4.2.2) was recommended to mitigate corrosion of anchors in standoff base plates. Kaczinski et al. (1998) stated that dry-pack grout pads should not be used based on the potential for corrosion from water pooling.

In the two published studies of anchor bolt group steel strength in grouted stand-off base plates, rectangular column base plate connections subjected varying combinations of tension and shear loading were used. Within individual tests in both studies, constant levels of tension were applied while shear was increased until anchor bolt steel rupture.

Gresnigt et al. (2008) discussed the shear strength of two- and four-anchor bolt grouted connections to square base plate with from tests conducted at TU-Delft in 1992. Four-bolt tests were performed with 20 mm (0.79 in.) dia., Grade 4.6 bolts at 130 mm x 130 mm spacing, while two-bolt tests were performed with 20 mm dia. grade 8.8 bolts at 130 mm spacing. Results from 22 tests were reported, six with no applied tension to the bolt group and 16 with applied tension ranging from 121 kN to 200 kN. All but six of the tests resulted in steel rupture.

Equation (2-10) was derived for calculating the elastic limit of anchor bolt shear resistance, F_h, based on tension forces developing by geometry of bolt bending and contributions from grout pad friction and elastic compression. Under the assumption that the grout pad does not provide significant resistance to bolt shear bearing, the model assumes a linear relationship between the applied load and displacement until bolt yielding corresponding to the value of δ_h, provided below. It is assumed that the grout responds linearly to the loads imposed on it throughout the model. Beyond the elastic limit of δ_h, bolt strains are assumed to be perfectly plastic, leaving only grout friction and compressive reactions providing additional resistance. Bolt rupture relies upon strains unique to different bolt types, which the analytical model does not take into account. Thus, while the model predicts behavior based on these assumptions, it does not predict ultimate

strength of the connection. Coefficients of friction, f_w, of 0.2 and 0.3 were proposed for sand-cement mortar and "special grout (e.g. Pagel IV)," respectively.

$$F_h = \frac{f_{y,b} A_{b,s}}{\sqrt{\delta_h^2 + v_r^2}} (\delta_h + f_w v_r) - f_w F_t \tag{2-10}$$

where
$f_{y,b}$ = yield strength of the bolt material
$A_{b,s}$ = cross-sectional area of bolt
δ_h = base plate horizontal displacement; elastic limit $= v_r \sqrt{\frac{2F_{y,b}}{E}}$
E = elastic modulus of the bolt
f_w = coefficient of friction between the grout pad and the base plate
v = grout pad thickness
v_r = effective grout pad thickness $= v + 0.5d_b$
d_b = nominal anchor bolt diameter
F_t = applied tensile force (assumed known)

Given the constraints of the model in predicting ultimate strength and that no trend was observed in bolt strength relative to grout pad thickness, a simplified approach was proposed for design. In this approach, constants accounting for the ductility of two materials were multiplied by the ultimate tensile strength of the bolt to approximate shear strength, as it was noted that the ultimate shear resistance of an anchor bolt is nearly independent of the thickness of the grout layer. Bolt tension forces were not accounted for. Despite the simplicity of the methodology, experimental results ranged from 1.4 to 2.6 times the predicted values of this simplified method. Results were compared against existing European standards utilizing the approach given in (2-6), which does not account for grout pad contributions to strength and takes the "lever arm" of bolt bending over a length from the center of the base plate to 0.5 bolt diameters below the concrete surface. Unsurprisingly, experimental results were 3.3 to 26.2 times the values predicted by the European standard method.

In a similar experimental approach, Gomez et al. (2011) studied cyclic shear transfer of a full-scale column connection to a concrete foundation under constant axial load. A W31x191

column was welded to a 34.5 in. by 67 in. by 2 in. thick base plate with four 2 1/16 in. diameter holes on a 24 in. square pattern. Two tests were conducted investigating ASTM F1554 Grade 55 anchor bolt strength, one with 7/8 in. dia. bolts and a 1.25 in. thick grout pad, the other with 1.25 in. dia. anchor bolts and a 1 in. thick grout pads below the base plate. Double plate washers were placed above the base plate on every anchor bolt, one with 0.25 in. thickness welded to the base plate and a second with 0.4 in. thickness that was not welded. No nuts were placed below the base plate, which was set and leveled using actuators in the test setup. Constant tension was applied to the bolt groups, 40 kips to the 7/8 in. bolt diameter test (31% of the tensile capacity of the bolt group) and 108 kips to the 1.25 in. bolt diameter test (39% of the tensile capacity of the bolt group). A cyclic displacement-controlled shear loading regimen was then applied to the bolt group until failure. For the 7/8 in. diameter anchor test the ultimate loads for each direction of loading were 30.2 kips and 28.2 kips, while for the 1.25 in. diameter anchor test the ultimate loads were 126 and 70.4 kips (averaging 98.2 kips). It was noted that the discrepancy in highest reported values for the two directions in the latter tests was likely due to eccentric bolt position within the oversize hole.

Results were compared to two calculations, both using the common elliptical interaction equation (2-4) between shear and tension stresses, where tensile stresses include applied axial force and maximum bolt bending stresses. Bolt bending stresses were taken as the moment in the rod over a length equal to the distance from the center of the welded plate washer to the top of the grout pad divided by the plastic modulus of the bolt. Notably, bolt rupture occurred at the bottom of the grout pad, the thickness of which was not included in the calculation of bolt bending stresses. Nonetheless, this calculation produced a predicted yield capacity of 11.4 kips and 36.9 kips for the two tests.

The second calculation added another component to the capacity from the first accounting for tension development in the bolts due to the geometry of loading. By geometry, the shear component of this contribution is equal to the constant tensile force applied to the bolt group multiplied by the proportion of the horizontal deflection over the length of bolt bending (top of the grout pad to the middle of the welded plate washer). This approach produced predictions of 26.5 and 75.3 kips when substituting the known bolt rupture displacements. Thus, as in Gresnigt et al. (2008), the model predicts post-yield *behavior* - albeit through a different mechanism of tensile contribution from the applied loads instead of from the grout pad - but not ultimate *strength* as no methodology was provided for determining ultimate displacement.

In addition to the tests that studied anchor bolt capacity, three tests investigated the friction characteristics of the base plate assembly with and without shim stacks, finding that previously established coefficients of friction are appropriate for steel base connections to grout with and without shim stacks. A grout-to-base plate coefficient of friction was found to be 0.46, similar to the 0.4 proposed by Cook and Klingner (1992).

CHAPTER 3
CODE COMPARISONS

3.1 Introduction

The American Association of State Highway and Transportation Officials (AASHTO 2013a), the American Concrete Institute (ACI 2011), and the American Institute of Steel Construction (AISC 2010) provide Load and Resistance Factor (LRFD) code provisions for the design of anchor bolts. Design bolt steel strength values including LRFD Φ factors from these code bodies are compared within this chapter for axial, shear, and combined axial and shear loads. In addition to these LRFD standards, AASHTO also provides an Allowable Stress Design (ASD) approach for highway sign, signal, and lighting structures (AASHTO 2013b). For the sake of comparison, all values given are taken for the threaded portion of the anchor bolt. If unthreaded properties are desired, the nominal area could be substituted (or reduction factors accounting for threads removed) in calculations to obtain gross section strengths. Beyond strength comparisons, allowable hole sizes for each code body and existing provisions accounting for the presence of both ungrouted and grouted stand-off base plates are discussed.

3.2 Steel Strength of Anchor Bolts in Tension

AASHTO (2013a) Section 6.13.2.10.2 specifies the design tensile strength, ϕT_n, as given in Equation (3-1). This conservatively assumes the net tensile area is 0.76 of the gross cross-sectional area.

$$\phi T_n = \phi 0.76 A_b F_{ub} \tag{3-1}$$

where ϕ = 0.8
A_b = unthreaded bolt cross-sectional area
F_{ub} = specified minimum tensile strength of the bolt

ACI (2011) Section D.5 specifies the design tensile strength, ϕN_{sa}, as given in Equation (3-2). For the sake of comparison to other codes, $A_{se,N}$ is taken as 0.75 of the gross area (the full definition is contained below). Ductile elements are defined by Appendix D as having a tensile test elongation equal to or exceeding 14% and an area loss of at least 30%. Brittle elements are those that do not meet one or both of the elongation or area reduction requirements in tensile testing.

$$\phi N_{sa} = \phi A_{se,N} f_{uta} \tag{3-2}$$

where ϕ = 0.75 for ductile steel as defined above
= 0.65 for brittle steel as defined above
$A_{se,N}$ = threaded bolt cross-sectional area $= \frac{\pi}{4}(d_a - \frac{0.9743}{n_t})^2$ [units in inches]
f_{uta} = specified tensile strength of anchor steel that shall be taken as no greater than 125,000 psi or $1.9 f_{ya}$
f_{ya} = specified yield strength of anchor steel

AISC (2010) Section J6 and Table J3.2 specify the design tensile strength, ϕR_{nt}, as given in Equation (3-3). The tensile area is assumed to be 0.75 of the unthreaded area.

$$\phi R_{nt} = \phi F_{nt} A_b \tag{3-3}$$

where ϕ = 0.75
F_{nt} = nominal tensile stress capacity $= 0.75 F_u$
A_b = unthreaded bolt cross-sectional area
F_u = specified minimum tensile strength

Table 3-1 provides a summary of resistance factors, nominal tensile strengths, and resulting design tensile strengths in terms of an assumed net tensile area, A_{se}, equal to 0.75 of the gross area and specified tensile strength F_{ut}.

Table 3-1. AASHTO (2013a), ACI (2011), and AISC (2010) bolt tension strengths

Code	Resistance (Strength Reduction) Factor	Nominal Tensile Strength	Design Strength
AASHTO (2013a)	0.80	$1.0 A_{se} F_{ut}$	$0.80 A_{se} F_{ut}$
ACI (2011)			
Ductile	0.75	$1.0 A_{se} F_{ut}$	$0.75 A_{se} F_{ut}$
Brittle	0.65	$1.0 A_{se} F_{ut}$	$0.65 A_{se} F_{ut}$
AISC (2010)	0.75	$1.0 A_{se} F_{ut}$	$0.75 A_{se} F_{ut}$

3.3 Steel Strength of Anchor Bolts in Shear

AASHTO (2013a) Section 6.13.2.12 specifies the design shear strength, ϕR_n, for ASTM F1554 anchor bolts with threads included in the shear plane as given in Equation (3-4). The basis for Equation (3-4) is discussed in AASHTO C6.13.2.7. The 0.48 multiplier for threads in the shear plane is based on a shear strength of 0.60 times the tensile strength of the bolt for threads not in the shear plane multiplied by 0.80 to account for the threads in the shear plane as observed by Yura et al. (1987). In Commentary Section C6.13.2.12 it is recommended to apply an additional 0.8 factor to the shear strength to account for bolt hole oversize and other factors from group effects using engineering judgment.

$$\phi R_n = \phi 0.48 A_b F_{ub} \tag{3-4}$$

where ϕ = 0.75
A_b = unthreaded bolt cross-sectional area
F_{ub} = specified minimum tensile strength of the bolt

ACI (2011) D.6.1 specifies the design shear strength, ϕV_{sa}, as given in Equation (3-5). See Section 3.2 for definitions of ductility.

$$\phi V_{sa} = \phi 0.6 A_{se,V} f_{uta} \tag{3-5}$$

where ϕ = 0.65 for ductile steel as defined in Section 3.2
= 0.60 for brittle steel as defined in Section 3.2
$A_{se,V}$ = $\frac{\pi}{4}(d_a - \frac{0.9743}{n_t})^2$ [for units in inches]
f_{uta} = specified tensile strength of anchor steel and shall be taken as no greater than 125,000 psi or $1.9F_{ya}$
f_{ya} = specified yield strength of anchor steel

AISC (2010) Section J9 and Table J3.2 specify the design shear strength, ϕR_{nv}, for anchor bolts as given in Equation (3-6). The 0.45 multiplier for the calculation of R_{nv} is a result of a 0.9 factor for group and hole oversize effects similar to the 0.8 factor discussed above in the AASHTO (2013a) approach. However, in AISC (2010) this factor was moved from 0.8 to 0.9

after several years of satisfactory connection performance. The 0.9 factor is applied to the 0.625 average bolt strength from Chesson et al. (1965) discussed in Section 2.1.2. To account for threaded area, the ratio of threaded shear strength to unthreaded shear strength is taken as 0.8 following recommendations by Yura et al. (1987) discussed in Section 2.1.2 in contrast to the AASHTO (2013a) and ACI (2011) assumptions that the shear area can be taken as the net tensile area in threaded regions. Thus, it follows that 0.625*0.9*0.8 = 0.45.

$$\phi R_{nv} = \phi F_{nv} A_b \tag{3-6}$$

where ϕ = 0.75
F_{nv} = nominal shear stress capacity $= 0.45F_u$
A_b = unthreaded bolt cross-sectional area
F_u = specified minimum tensile strength

Table 3-2 provides a summary of resistance factors, nominal shear strengths, and resulting design shear strengths for the threaded area in terms of the nominal bolt area, A_b, which is used in place of A_{se} because of the different assumptions about the ratio of unthreaded to threaded strength by the different codes. For comparison, this ratio is represented for ACI (2011) as 0.75, the approximate value of the threaded to unthreaded bolt area.

Table 3-2. AASHTO (2013a), ACI (2011), and AISC (2010) bolt shear strengths

Code	Resistance (Strength Reduction) Factor	Nominal Shear Strength	Design Strength
AASHTO (2013a)			
No group effect	0.75	$0.48A_bF_{ut}$	$0.36A_bF_{ut}$
With group effect	0.75	$0.38A_bF_{ut}$	$0.29A_bF_{ut}$
ACI (2011)			
Ductile	0.65	$0.6A_bF_{ut}$	$0.39A_bF_{ut}$
Brittle	0.60	$0.6A_bF_{ut}$	$0.36A_bF_{ut}$
AISC (2010)	0.75	$0.45A_bF_{ut}$	$0.34A_bF_{ut}$

3.4 Steel Strength of Anchor Bolts in Combined Tension and Shear

AASHTO (2013a) Section 6.13.2.11 specifies a reduced value of ϕT_n as given in Equation (3-7) accounting for shear present in the bolt. This is a factored rearrangement of the elliptical

relationship between tension and shear from Equation (2-4). For $\frac{P_u}{R_n}$ less than 0.33, the full value of T_n given in Equation (3-1) is allowed. No provisions are given for the shear strength under low levels of tension load, contrary to ACI (2011) and AISC (2010).

$$\phi T_n = \phi 0.76 A_b F_{ub} \sqrt{1 - \left(\frac{P_u}{\phi_s R_n}\right)^2} \tag{3-7}$$

where ϕ = 0.8
A_b = unthreaded bolt cross-sectional area
F_{ub} = specified minimum tensile strength of the bolt
P_u = factored shear force on the bolt
ϕ_s = 0.75
R_n = nominal shear resistance of the bolt (3-4)

ACI (2011) Section D.7 uses a linear interaction between bolt tension and shear forces as given in (3-8). At values of $\frac{V_{ua}}{\phi V_n} \leq 0.2$ the full tension strength of the anchor bolt may be taken as given in Equation (3-2). Similarly, at values of $\frac{N_{ua}}{\phi N_n} \leq 0.2$ the full shear strength of the anchor bolt may be taken as given in Equation (3-5).

$$\frac{N_{ua}}{\phi N_{sa}} + \frac{V_{ua}}{\phi V_{sa}} \leq 1.2 \tag{3-8}$$

where N_{ua} = factored tension force in the anchor bolt
ϕN_{sa} = tension capacity as calculated in (3-2)
V_{ua} = factored shear force in the anchor bolt
ϕV_{sa} = shear capacity as calculated in (3-5)

AISC (2010) Section J7 specifies the design available tension strength, ϕR_{nv}, in (3-9), using a linear relationship between tension and shear forces as in ACI (2011). Similar to ACI (2011), full tension and shear strength as calculated in Equation (3-3) and Equation (3-6), respectively are allowed for the anchor bolt if the other component of stress is less than 30% of its available non-combined stress capacity.

$$\phi R_n = \phi F'_{nt} A_b \quad (3\text{-}9)$$

where ϕ = 0.75

F'_{nt} = available tensile stress $= 1.3F_{nt} - \frac{F_{nt}}{\phi F_{nv}} f_{rv} \leq F_{nt}$

F_{nt} = nominal tensile stress as defined in (3-3)

F_{nv} = nominal shear stress as defined in (3-6)

f_{rv} = factored shear stress

3.5 Provisions for Steel Strength in Stand-off Base Plates

AASHTO (2013a) does not provide guidance on designing anchor bolt steel strength for ungrouted or grouted stand-off base plates. AASHTO (2013b) 5.17.4.3, however, accounts for stand-off explicitly based on work performed by Kaczinski et al. (1998) discussed in Section 2.4.2, stating that where the distance from the concrete surface to the bottom of the leveling nut exceeds one bolt diameter, bending in the anchor should be considered. Within the commentary, it is stated that bending moments developing in the anchor bolt from shear forces may be determined by modeling a doubly moment-restraining beam with length equal to the distance between the concrete surface and the bottom of the leveling nut. Stresses due to bolt bending are added to the tensile stress component of the elliptical interaction relationship provided in Equation (3-10) (or the compressive stresses in a similar compression/shear interaction). The commentary also states explicitly that bolt bending from bolt shear forces may be ignored for exposed lengths less than or equal to one anchor bolt diameter. AASHTO (2013b) 5.17.3.3 states that grout installed beneath the base plate may not be designed to contribute to connection strength in double-nut connections (those using leveling nuts). Thus, two double-nut connections, one with and one without a grout pad, would be designed using the beam model described above.

$$\left(\frac{f_v}{F_v}\right)^2 + \left(\frac{f_t}{F_t}\right)^2 \leq 1.0 \quad (3\text{-}10)$$

where f_v = factored shear stress
F_v = allowable shear stress
f_t = factored tensile stress from both axial bolt tension and bolt bending
F_t = allowable tensile stress

ACI (2011) D.6.1.3 states that 80% of the shear strength of an anchor group is maintained in the presence of a grout pad irrespective of grout pad height (base plate stand-off distance). No provisions currently exist for anchor bolt steel strength in ungrouted stand-off base plate connections.

Beyond stating in commentary that anchor bolt bending must be considered when shear is transferred through base plate bearing against anchor bolts, AISC (2010) does not provide guidance for ungrouted or grouted stand-off base plates. However, AISC *Design Guide 1* (Fisher and Kloiber 2006) provides an example using the interaction of tension forces in the anchor from direct tension and bolt bending with shear forces in the anchor in a base plate supported by a grout pad. Their calculation uses the same beam bending model as in AASHTO (2013b), but takes the length of the beam as the distance from the top of the grout to the middle of the grout pad. This assumes that anchor bolt length within the thickness of the grout pad does not contribute to bolt bending and also implies that grout pads shall not contribute to anchor bolt strength.

3.6 Hole Sizes

Table 3-3 provides anchor bolt hole size comparisons between AASHTO (2013a), AISC (2010), and current FDOT standards. ACI (20111) does not provide guidance on hole size. AASHTO (2013a,b) provides hole dimensions for both “shear holes” and “normal holes,” the former defined as those with anchor bolts designed to resist shear due to direct shear or torsion

forces on the base plate. AISC hole sizes for anchors, given in Table C-J9.1 (AISC 2010) align with the dimensions for AASHTO normal holes while AISC oversize holes for steel-to-steel connections align with AASHTO shear holes. To account for this relatively large oversize, AISC (2010) Section C-J9 states that if anchor bolts are to resist shear forces bolt bending must be considered, but does not provide any further guidance. FDOT hole sizes are taken as 0.5 inches greater than the bolt diameter following "General Notes" in Design Standards 11310 and 17745.

Table 3-3. Comparison of AASHTO (2013a,b), AISC (2010), and FDOT hole sizes

Bolt Dia. (in.)	Hole Dimensions (in.)			Hole Oversize (in.)			Hole:Bolt Ratio		
	AASHTO Shear	AISC	FDOT	AASHTO Shear	AISC	FDOT	AASHTO Shear	AISC	FDOT
0.5	0.63	1.06	-	0.13	0.56	-	1.26	2.13	-
0.625	0.81	1.19	-	0.19	0.56	-	1.30	1.90	-
0.75	0.94	1.31	-	0.19	0.56	-	1.25	1.75	-
0.875	1.06	1.56	-	0.19	0.69	-	1.21	1.79	-
1	1.25	1.81	1.5	0.25	0.81	0.5	1.25	1.81	1.50
1.25	1.56	2.06	1.75	0.31	0.81	0.5	1.25	1.65	1.40
1.5	1.81	2.31	2	0.31	0.81	0.5	1.21	1.54	1.33
1.75	2.06	2.75	2.25	0.31	1.00	0.5	1.18	1.57	1.29
2	2.31	3.25	2.5	0.31	1.25	0.5	1.16	1.63	1.25

CHAPTER 4
DEVELOPMENT OF EXPERIMENTAL PROGRAM

4.1 Introduction

The primary project objectives of quantifying reduction in anchor bolt steel strength in stand-off base plates and development of design and maintenance guidelines drove the development of the experimental program. Following the first objective, the major test variables were base plate stand-off distance and connection type (i.e. flush-mounted, ungrouted stand-off, and grouted stand-off base plates). Minor test variables considered were test method, hole oversize, bolt diameter, installation type (i.e. cast-in-place (CIP) vs. adhesive anchors), pretensioning of bolts, number of bolts per connection, and the presence of a fiber-reinforced polymer (FRP) retrofit around a grouted stand-off base plate. Other minor variables that were not considered for FDOT annular base plate applications but may influence the shear steel strength and behavior of anchor bolts in other types of stand-off base plates include bolt steel strength/ductility, location of the bolt threaded/unthreaded interface, concrete strength, base plate flexibility, grout material strength, grout pad installation technique (i.e. dry-packed vs. formed), and various grout pad size and shape parameters. These variables were not considered in this project since FDOT specifications for annular base plate applications significantly limit their variability.

The experimental program included three phases. Phases 1 and 2 were conducted at the University of Florida Structures Laboratory and Phase 3 was conducted at the Marcus H. Ansley Structures Research Center. Phase 1 employed a direct shear approach to study various parameters impacting the steel strength of anchor bolts in ungrouted stand-off base plates. Phase 2 included circular groups of 5/8 in. and 1 in. diameter anchor bolts loaded in torsion to investigate the impact of variables in both ungrouted and grouted annular stand-off base plate

connections. Phase 3 contained four full-scale circular groups of six 1.25 in. diameter bolts loaded predominantly in torsion.

4.2 Materials and Methods

4.2.1 Test Specimens

In all test specimens, anchor bolts were made with fully threaded ASTM F1554 Grade 55 steel headed with ASTM A563 heavy hex nuts. Embedment depths of 8.6, 7, and 16 bolt diameters for 0.625 in., 1 in., and 1.25 in. bolts, respectively, were assumed to have no impact on the results. All concrete used in the study was the FDOT Class IV Drilled Shaft mix with a specified 28-day compressive strength of 4,000 psi. Reinforcement within the blocks was provided only to prohibit failure modes other than anchor bolt steel fracture. All readings from instrumentation were taken using LabVIEW software. Distinguishing test specimen details for each of the three phases is provided within their respective sections.

4.2.2 Grout

The grout chosen was nonshrink with specified 28-day strength of 9,000 psi. FDOT Specification 934 for non-shrink grouts requires a 3-day compressive strength of 5,000 psi for 2 in. cube tests conducted in accordance with ASTM C109 (ASTM 2012), while the Technical Data Guide for the product chosen provides a minimum strength of 4,500 psi (corresponding to a 25-30 second flow cone time). It was determined that use of this nonshrink grout would be conservative.

For all grout pad installations a flow time of 20-25 seconds following ASTM C939 protocol (ASTM 2010b) was achieved following the methodology used in FDOT Report BC354 RWPO #4. Grout pads were installed in accordance with the Manufacturer's Printed Installation Instructions (MPII) and ASTM testing protocol was followed where practical. To prepare the concrete surface for grout pad placement, it was brushed of debris and blown with an air hose.

For 24 hours preceding grout installation the concrete surface was wetted with shop rags. Approximately one hour before grout placement, the shop rags were removed to achieve a "Saturated Surface Dry" (SSD) condition during grout placement.

To simulate the presence of an annular void in the test specimen's circular base plate, a cardboard circle with a diameter equal to the pipe outer diameter was cut and attached to the center of the underside of the base plate with tape as shown in Figure 4-1 (a). Circular Plexiglas forms were made with height equaling the distance from the concrete surface to the top of the base plate. Heat was applied as the form was wrapped around the base plate to achieve a circular bend in the strip and avoid cracking. Grout head pressure was insignificant for the range of grout pad heights, so packing tape was sufficient to connect matching ends of the form. A layer of putty was placed around the perimeter of the joint between the form and the concrete surface. Figure 4-1 (b) shows an installed form.

(a) (b)

Figure 4-1. Cardboard separator (a) and Plexiglas formwork (b) for grouted tests

The amount of grout needed was determined for every test and weighed using a digital scale. For a given weight of grout, 17% water by dry grout weight was measured and placed in a five-gallon bucket. The dry grout was poured into this water and the mix was blended for a minimum of five minutes. Water was then added and mixed in thoroughly until the 20-25 second flow time was reached. It was found that approximately 19% water by weight was ultimately

needed for the laboratory conditions. Because additional holes were present in the base plates for both Phase 2 and Phase 3 tests, grout was installed in a single pour through one of the additional holes using the flow cone attachment from the ASTM C939 (ASTM 2010b) method as shown in Figure 4-2.

(a) (b)

Figure 4-2. Performing the ASTM C939 flow cone test (a) and grout pad placement (b)

Immediately after placing a grout pad, 2 in. cubes were cast in copper molds treated with a light coat of WD-40 applied with shop rags. Cubes were prepared as specified by ASTM C942 (ASTM 2010a). Plexiglas sheets were then placed atop the gang mold to restrict water evaporation and the cubes were left near the grout pad. At 24 hours, the formwork for the grout pad and the cubes were removed. The grout pad was painted with two coats of the manufacturer's recommended curing compound per their recommendations. Although a moist cure condition is specified by ASTM C109 (ASTM 2012), the cubes were also painted with the curing compound to best reflect the condition of the installed grout pad specimen. After the second coat was dry, the grout pad and the cubes were wrapped in wet paper towels and left to sit as shown in Figure 4-3.

Figure 4-3. Grout pad and 2 in. cubes after wet-wrapping

Grout cubes were tested in compression following ASTM C109 protocol (ASTM 2012) immediately after corresponding torsion tests. For a displacement-controlled test, the tests ranged from 250-350 lb./sec. in the linear-elastic phase of the tests, after which the displacement rate was kept consistent until grout cube failure. For some of the Phase 2 grouted tests, additional grout cubes were made and treated by immersing them in water at 24 hours instead of painting. It was found that there were no significant differences in the strengths between the two treatment methods.

4.2.3 Fiber Reinforced Polymer (FRP)

One torsion test, T7, contained a 4 dia. grout pad and an FRP retrofit. Guidelines provided by the FRP manufacturer were followed for preparation and installation. The product had a design strength of 4.8 kips/in. of width per layer. The force required to be restrained by the FRP was calculated using two methods proposed in BD545-54, which both produced a one-layer minimum. Three layers were conservatively used.

Fiber strips were cut to a height equal to the distance from the concrete surface to the top of the base plate and a length equal to the circumference of the base plate plus an additional six inches. To impregnate dry fibers, the strips were spooled around a small section of PVC tubing. An epoxy bath was made using a small plastic tub lined with plastic sheeting. A fiber strip was

then unspooled into the tub, where a coat of epoxy was brushed on and rolled into the fibers using a toothed roller. The impregnated strip was then re-spooled. This process was repeated on the other side of the fibers, again unspooling and re-spooling in the same manner. This process is illustrated in Figure 4-4.

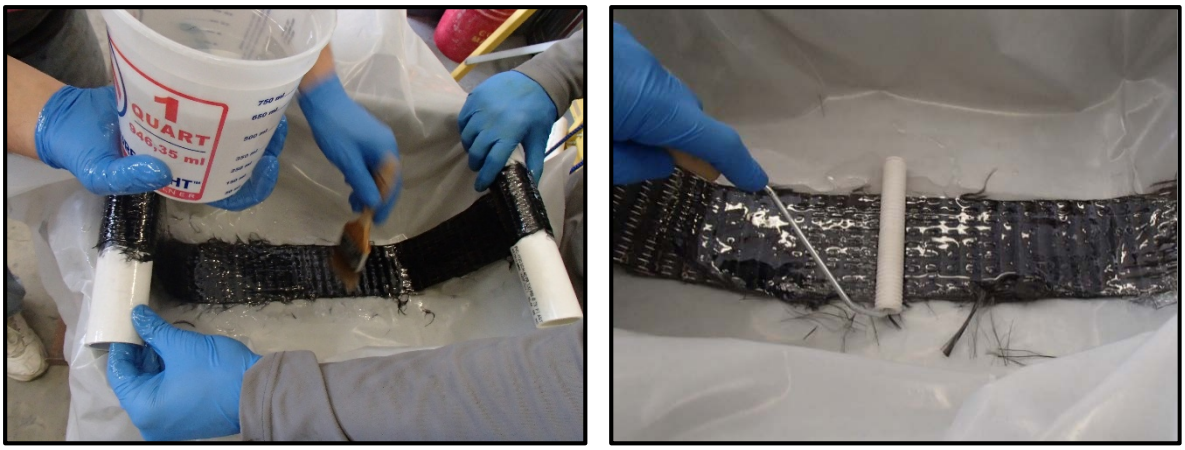

(a) (b)

Figure 4-4. Application of epoxy to fiber strips

FRP application to the grout pad is illustrated in Figure 4-5. The grout pad surface was first painted with a base coat of epoxy, after which the saturated layers of FRP were installed one at a time. To avoid material buildup, the starting point for each layer was set at 120 degrees from the previously installed layer.

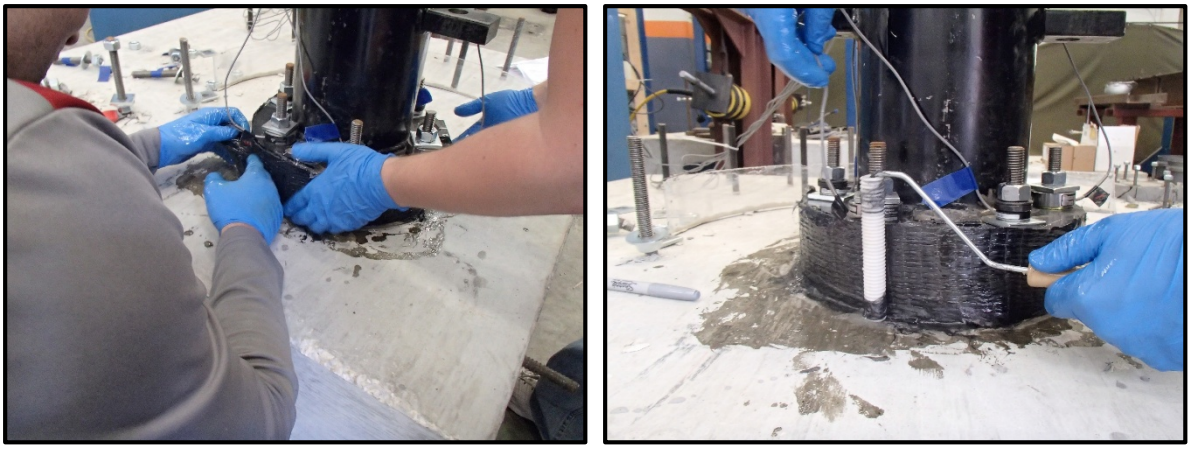

(a) (b)

Figure 4-5. FRP application to base plate

After the FRP had cured, it was found that excess epoxy material had settled at the interface between the concrete surface and the bottom of the grout pad, creating a “fillet.” It was believed that this might unconservatively contribute strength to the retrofitted grout pad that would not be accounted for in design, so an oscillating fine-toothed cutting tool was used to separate the concrete surface from the epoxy material as shown in Figure 4-6.

Figure 4-6. Cutting away excess epoxy material after cure

4.3 Phase 1: Direct Shear Testing

4.3.1 Experimental Design

The direct shear matrix is provided in Table 4-1. In total, 14 unique test series studied stand-off distance, single vs. double anchor bolts installed in a rectangular base plate, cast-in-place vs. adhesive anchor bolts, and 5/8 in. vs. 1 in. diameter bolts installed in tight (i.e. no oversize) holes. Two of the test series, DS10 and DS11, were not run to completion. This is discussed in the next chapter.

Table 4-1. Phase 1 test matrix

Set[a]	Reps	d_b (in.)	Hole Size (in.)	n	Anchor Type	Connection Type[b]	Top Nut Tightness[c]	$\frac{l_{BP}}{d_b}$	$\frac{l_{LN}}{d_b}$
DS1	8	0.625	0.63	1	CIP	FM	FT	0	*na*
DS2	6	0.625	0.63	1	CIP	U	FT	1.2[d]	0
DS3	2	0.625	0.63	1	CIP	U	FT	1.6	0.4
DS4	10	0.625	0.63	1	CIP	U	FT	2	0.8
DS5	4	0.625	0.63	1	CIP	U	FT	3	1.8
DS6	5	0.625	0.63	1	CIP	U	FT	4	2.8
DS7	4	0.625	0.63	2	CIP	FM	FT	0	*na*
DS8	5	0.625	0.63	2	CIP	U	FT	2	0.8
DS9	4	1	1.01	1	CIP	FM	FT	0	*na*
DS10	5	1	1.01	1	CIP	U	FT	2	0.75
DS11	2	1	1.01	1	CIP	U	FT	4	2.75
DS12	4	0.625	0.63	1	AD	FM	FT	0	*na*
DS13	5	0.625	0.63	1	AD	U	FT	2	0.8
DS14	2	0.625	0.63	1	AD	U	FT	4	2.8

na = not applicable
[a]DS = Direct Shear
[b]FM = Flush-Mounted base plate, U = Ungrouted stand-off base plate
[c]FT = Finger-Tightened
[d]Note: lowest possible stand-off with leveling nut

4.3.2 Test Setup

4.3.2.1 Structural Components

A 3D schematic of the test setup is shown below in Figure 4-7. The setup contained a 46.5 in. by 46.5 in. by 12 in. deep concrete block hosting multiple anchor bolt test specimens and resting on steel beam sections. A 7/8 in. diameter ASTM A193 B7 tension rod supplied load to the base plate through a telescoping through-hole hydraulic actuator supported by a reaction frame tied to a strong wall. The actuator was positioned on the back side of the steel frame

composed of two steel C channel sections with a 2 in. gap to allow the tension loading rod to pass through. On the loading end the concrete block bore against a steel channel section to restrain concrete breakout stresses and provide spacing. A system of steel beams tied to the strong floor of the laboratory was used to keep the system restrained against overturning moments during the test.

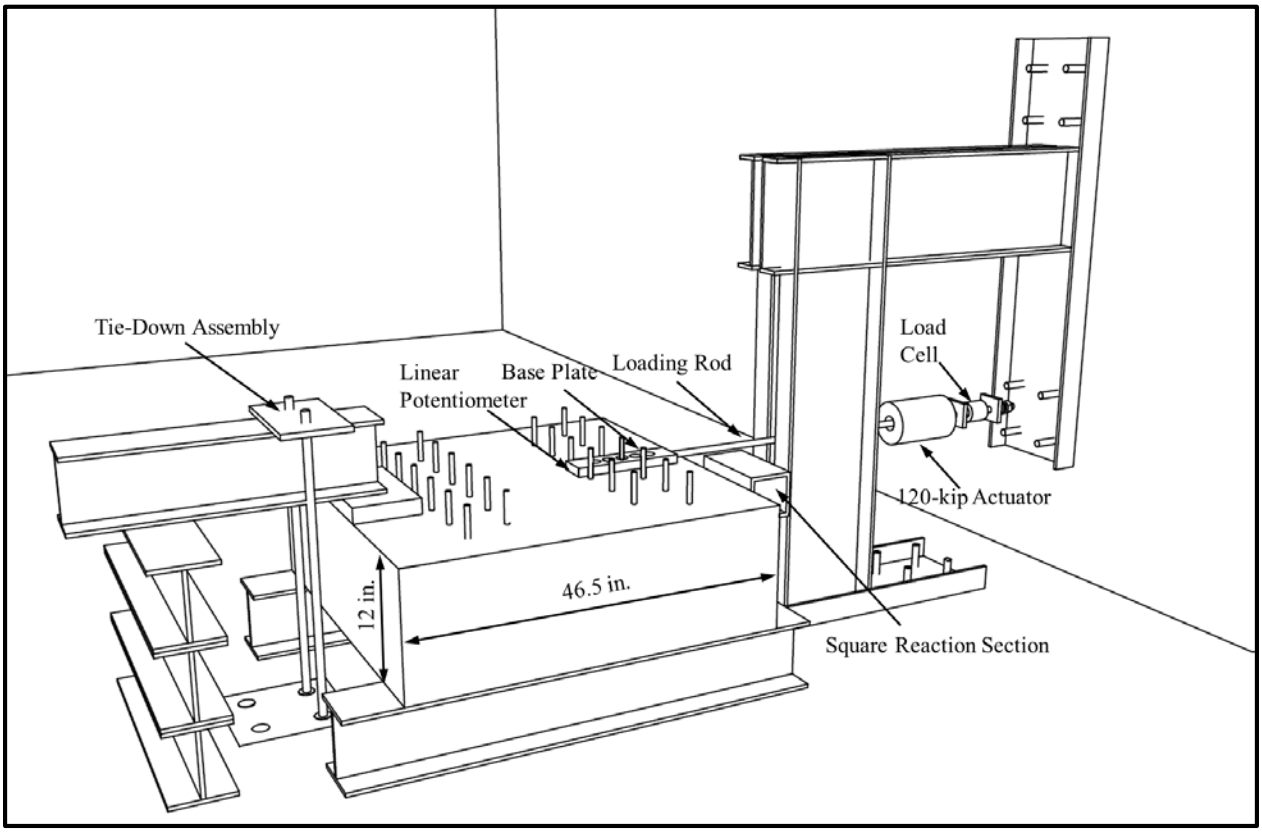

Figure 4-7. Phase 1 test setup

Checks were made on the double channel sections comprising the reaction frame to withstand shear, compression, and moment forces produced by the applied load from the actuator and the bearing reaction produced by the steel square reaction section. To maintain equilibrium in the test setup shown in Figure 4-7, the tie-down system needed to resist a moment equal to the loading eccentricity distance between the center of the base plate and the location of the bearing

reaction on the test block, so checks were made to ensure that the tension ties could restrain this moment.

The rectangular base plate was developed by Grosser (2012) and contained dimensions of 4 in. by 14.5 in. by 1.18 in. thick. In flush-mounted tests and double-bolt stand-off base plate tests the loading rod was threaded directly into the base plate. Single-bolt stand-off base plate tests, however, included a roller to restrain base plate rotation as shown in Figure 4-8. A clevis connection was used to release the bending forces in the loading rod. Nuts were installed in a "finger-tight" condition at approximately 20 in.-lb. Checks were made for net section fracture, tear-out, and bearing failure modes.

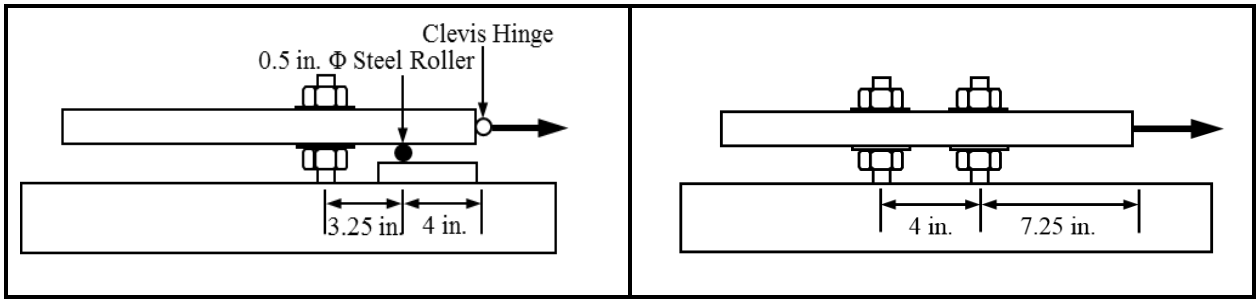

(a) (b)

Figure 4-8. Connection details for (a) single bolt and (b) double-bolt direct shear tests

Concrete blocks were designed with sufficient anchor bolt edge distance and effective depth to prohibit concrete breakout per ACI 318-11 without reinforcement. A mid-section perimeter of number 3 rebar was installed capable of supporting handling forces from self-weight.

Blocks were cast with anchor bolts installed upside-down in the formwork to accommodate the high number of bolt specimens and to achieve a formed flat concrete top surface. Holes were drilled through both the bottom sheet of plywood and a second reference piece of plywood as shown in Figure 4-9 to set the position and plumbness of anchor bolts. Embedment depth of the anchors was set by placing a nut above and a nut below the reference

sheet of plywood. Four coil loops were embedded at mid-depth of the slab to tie into for handling. A perimeter of #3 rebar was placed at mid-depth for handling precautions. ASTM A563 heavy hex nuts were placed on the embedded ends of the anchors and locked against rotation during concrete placement with a bead of adhesive. Two additional blank blocks were cast without anchors to allow for adhesive anchor installation. Blocks were wet-cured for seven days after pouring using a drip hose covered by painter's tarp and 4-mil plastic sheeting. After 28 days, formwork was removed. Two sets of cylinders were made, one cured alongside the test blocks in the lab and the other cured in a lime bath.

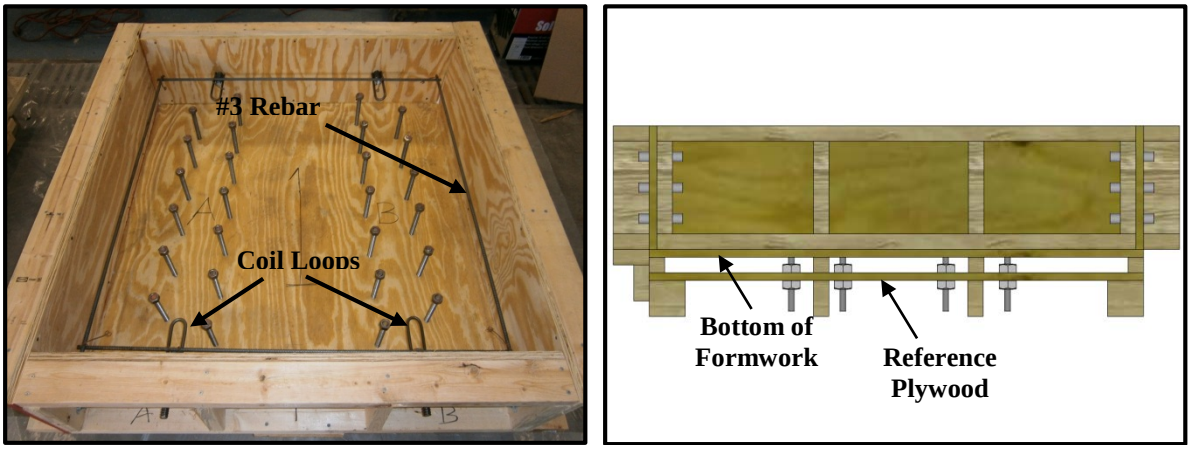

(a) (b)

Figure 4-9. Top view (left) and side view (right) of formwork

4.3.2.2 Instrumentation

Figure 4-10 indicates the locations of instrumentation used for direct shear testing. Load was measured by a through-hole 100 kip moment-compensating load cell located at the back end of the loading actuator with steel plates on either end of the load cell. Displacement was measured at the back end of the rectangular base plate with a linear potentiometer. The potentiometer, which contained a spring-retracting plunger, was connected to the back of the base plate through a stiff steel cord that fastened magnetically to the center of the top surface. In 42 of the 66 tests conducted, a 30 kip tension load cell was placed at the top of the anchor bolts.

The tests conducted without a tension load cell were all within datasets DS1, DS2, DS7 and DS8, which contained flush-mounted and $2d_b$ stand-off tests for single- and double-bolt tests and were run to determine if the load cell impacted test results. No difference in load-displacement behavior was found. Hence, all other 5/8 in. bolt tests contained tension load cells. A tension load cell was not used in 1 in. bolt tests.

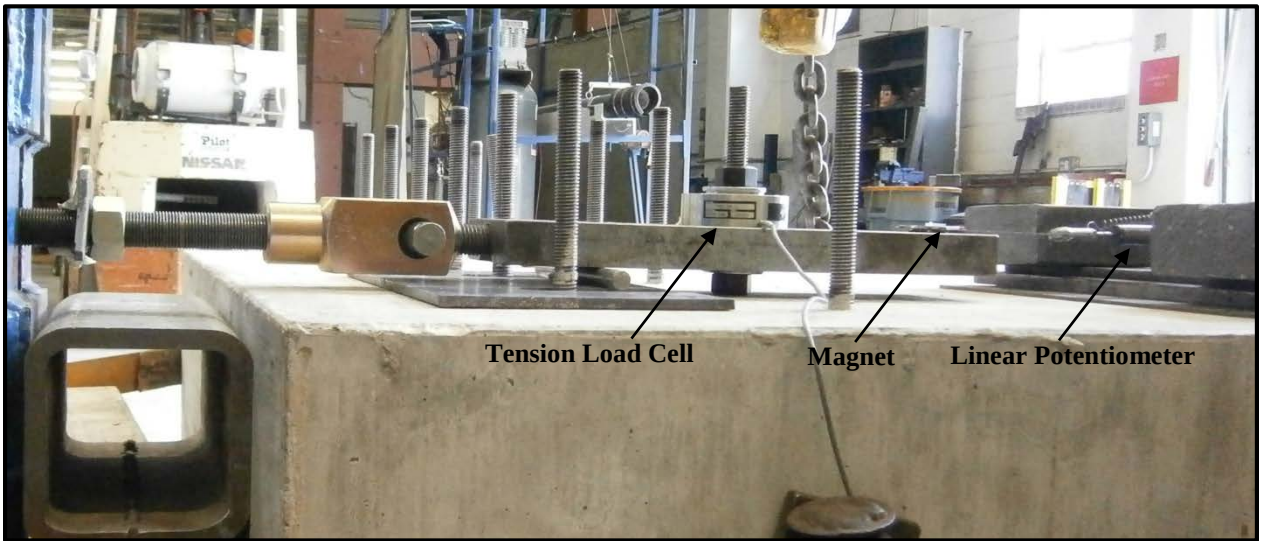

Figure 4-10. Instrumentation in Phase 1 testing

4.3.3 Test Procedure

To prepare every Phase 1 test, the concrete block was set into place onto two steel beams using an overhead crane, ensuring that the top surface of the block was level with steel shims below the block as necessary. Block position adjustments were made until the anchor bolt specimen was in-line with the loading rod. The block was then fastened on the back end using beams and tension ties in a snug-tight connection. The stand-off height of the test was then established, ensuring the distance from the concrete surface to the bottom of the base plate at the front and back of the base plate equaled the desired distance. The loading rod and actuator were set to collinearly with the mid-height of the base plate. All remaining instrumentation and test components (e.g. roller, clevis hinge) were installed. The top nut was set to a finger-tight

condition of 20 lb-in., after which the system was preloaded to approximately 100 lb. to engage components within the test setup.

The displacement-controlled loading procedure followed ASTM E488 protocol (ASTM 2010c), which states that failure should occur between 1 and 3 minutes from the beginning of the test. Due to the changing stiffnesses and resulting ultimate displacements for test specimens with different stand-off heights, the test displacement rate was estimated for every test to fall within this range of failure times. Consistent displacement rate was applied until anchor bolt rupture, ending an individual test.

4.4 Phase 2: Torsion Testing of Scaled Anchor Bolt Groups

Phase 2 torsion testing was added to the original test matrix for the following reasons: 1) A circular bolt pattern more accurately represents the field specimens studied in this research, making the results and retrofits more relevant and 2) Individual anchor bolts within the system are loaded in pure shear throughout the loading process without method-induced tension forces.

4.4.1 Experimental Design

The complete Phase 2 torsion test matrix is provided below in Table 4-2. Ten tests of groups of six 5/8 in. diameter anchor bolts included flush-mounted base plates, ungrouted base plates, grouted base plates, and a single test with an FRP-retrofitted grout pad. Effects of stand-off distance, connection type, and bolt pretensioning were investigated in these specimens, which were designed as scaled versions of existing FDOT mast arm and cantilever sign anchored base plate connections as discussed in the next section. Three additional test specimens containing 1 in. diameter bolts were included to investigate size effect.

Table 4-2. Phase 2 test matrix

Set[a]	Reps	d_b (in.)	Hole Size (in.)	n	Anchor Type	Connection Type[b]	Top Nut Tightness[c]	$\frac{l_{BP}}{d_b}$	$\frac{l_{LN}}{d_b}$
T1	2	0.625	0.81	6	CIP	FM	FT	0	*na*
T2	2	0.625	0.81	6	CIP	U	TOTN	2	0.8
T3	1	0.625	0.81	6	CIP	U	TOTN	4	2.8
T4	1	0.625	0.81	6	CIP	U	FT	2	0.8
T5	1	0.625	0.81	6	CIP	G	TOTN	2	0.8
T6	2	0.625	0.81	6	CIP	G	TOTN	4	2.8
T7	1	0.625	0.81	6	CIP	GF	TOTN	4	2.8
T8	1	1	1.25	3	CIP	U	FT	0	*na*
T9	1	1	1.25	3	CIP	U	TOTN	2	0.75
T10	1	1	1.25	3	CIP	U	TOTN	4	2.75

na = not applicable
[a]DS = Direct Shear, T = Torsion, FS = Full-scale
[b]FM = Flush-Mounted base plate, U = Ungrouted stand-off base plate, G = Grouted stand-off base plate, GF = Grouted stand-off base plate with FRP retrofit
[c]FT = Finger-Tightened, TOTN = Turn-of-the-Nut

4.4.2 Test Setup

4.4.2.1 Structural Components

A schematic of the Phase 2 test setup is given in Figure 4-11. Anchor bolt groups were installed in 46.5 x 46.5 x 12 in. deep reinforced concrete blocks. Independently operated hand pumps supplied hydraulic fluid to the actuators, which connected to the base plate assembly "loading wings" through 1 in. diameter ASTM A193 B7 threaded rods and 1 in. diameter clevis pin connections to produce torsion on the base plate and, ultimately, the anchor bolt group. Rolling reaction frames reacted against the opposite side of the concrete block via a 1.5 in. diameter ASTM A193 B7 tension rod sent through a PVC duct embedded in the concrete block. Because the system was self-reacting, no external tie-down support was necessary or used.

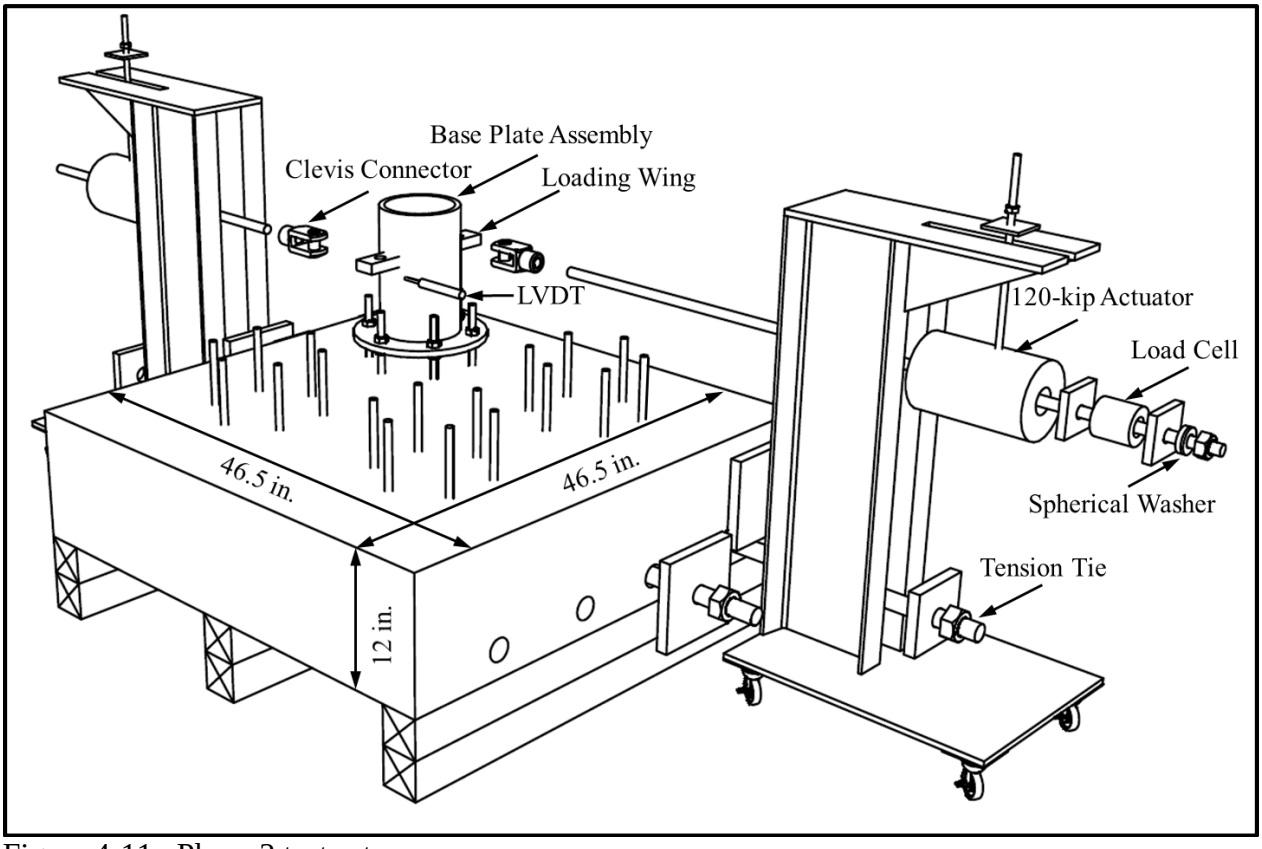

Figure 4-11. Phase 2 test setup

The 5/8 in. diameter bolt tests were designed as scaled versions of existing FDOT structures. Ratios of the bolt group radius and base plate thickness to nominal anchor bolt diameters were used as scaling parameters. To determine common ratios, a field survey of five mast arm assemblies was conducted, standard sizes for base connections in mast arm assemblies from a major supplier were obtained, the FDOT Cantilever Sign Program V5.1 (FDOT 2007) was used to produce several designs for highway cantilever signs, and a single cantilever sign specimen surveyed in BD545-54 were compiled. Table 4-3 provides the results and chosen dimensions for the test specimen. In contrast to the finger-tight top nut condition in Phase 1 testing, bolts in all but one of the stand-off base plate tests were pretensioned by the "turn-of-the-nut" method given in FDOT Specification 649. Flush-mounted tests, which included a Teflon layer below the base plate as in Phase 1, were not pretensioned to reduce additional contributions to strength from friction.

Table 4-3. Summary of scaling results for Phase 2 5/8 in. diameter bolt specimens

	Bolt Line Radius to Bolt Dia. Ratio	**Base Plate Thickness to Bolt Dia. Ratio**
UF Mast Arm Survey	6.1	1.0
Cantilever V5.1 Program	7.5	0.86
2012 FDOT Standard 17743	6.57-7.5	1.25-1.67
BD545-54 Specimen	9.0	0.6
Chosen Ratios	8	1

Base plate assembly dimensions and details are provided in Figure 4-12. The 12 in. HSS 7.5 X 0.5 pipe section was made of 55 ksi Carbon Steel DOM Mechanical Tube. The circular base plate and steel for the loading wing were made of grade 36 steel. All connections between assembly components were made with 3/8 in. fillet welds. For 2-bolt diameter spacing to the 5 in. bolt line radius, 3.75 in. and 6.25 in. radii to the outside of the pipe stub and the base plate, respectively, were chosen. To maintain the 1:1 base plate thickness to nominal anchor bolt diameter ratio for all tests, 3/8 in. thick plates were welded above holes for the 1 in. diameter

bolts. Hole diameters for both 5/8 in. and 1 in. diameter bolt tests were chosen per AASHTO (2013b) Table 5-5 for shear holes, defined as those with anchors subjected to shear forces due to base plate direct shear or torsion. After components were welded and holes cut, the entire assembly was case-hardened.

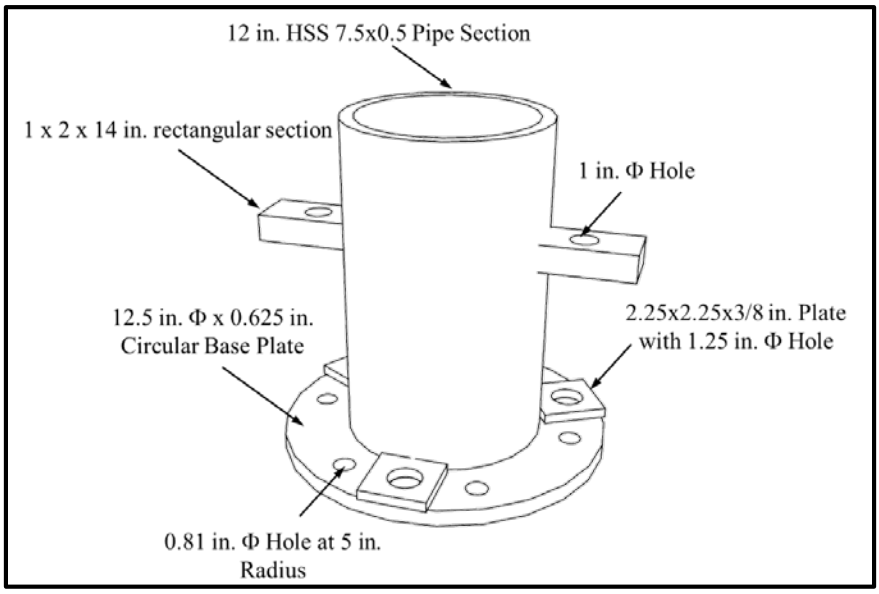

Figure 4-12. Base plate assembly components

Base plate assembly components were checked for structural capacity using the AISC Steel Construction Manual (AISC 2010). The pipe was designed to resist torsion forces from the loading couple along with combined moment, shear, and torsion forces that could be caused by extreme unequal loading from the actuators. The base plate was designed against net section fracture, tear-out, and bearing failure modes from anchor bolt forces on the holes. Loading wings were designed for moment and shear forces during loading in addition to the same bolt hole checks as performed on the base plate. Welds were all designed for ultimate shear stresses.

In the concrete block, top reinforcement was designed to restrain breakout forces from the anchor bolts. ACI 318 (ACI 2011) breakout calculations were modified to account for overlapping failure cones from shear forces from anchor bolts induced by the torsion load. These

forces could produce breakout cones in the direction of or perpendicular to the direction of load produced by an individual anchor bolt. As an example, Figure 4-13 provides one of the many cases considered for overlapping failure cones. Bottom block reinforcement accommodated minimum ACI 318-11 reinforcement requirements, temperature and shrinkage requirements, and was sufficient to withstand handling forces. Tension ties running through the bottom portion of the block were designed to transfer loads from the rolling frames to a compression reaction on the other side of blocks. Thorough checks were made of the combined effects on the block from the anchor bolt breakout forces and bearing forces from frame and tension tie reactions.

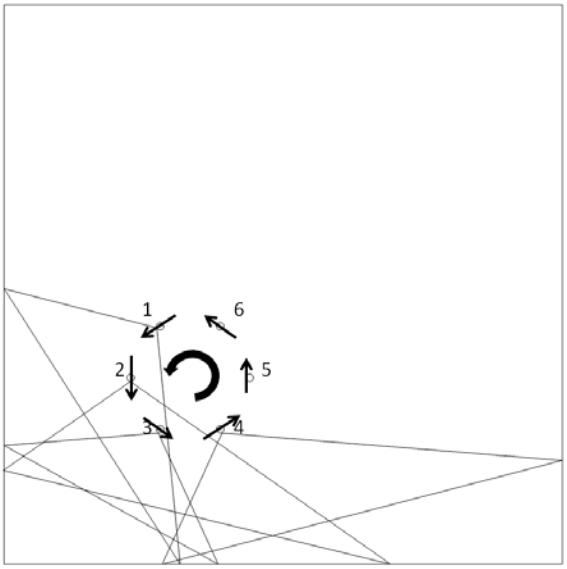

Figure 4-13. Example of design assumption of overlapping concrete failure cones

The cast-in-place anchor bolt installation technique from Phase I was again employed, with blocks cast upside-down and anchors passing underneath the formwork as described in Section 3.2.2.1. Specimens with groups of six 5/8 in. diameter bolts were installed four to a block while specimens with three 1 in. diameter bolts were cast one per block. 5/8 in. anchors were embedded 6 in. to the bottom of the bolt head (h_{ef} = 5.375 in.), while 1 in. anchors were embedded 8 in (h_{ef} = 7 in.). Number 4 rebar was used for all reinforcement bent into U shapes with 44 inch length and 8 in. legs. The bottom faces of all blocks contained five equally spaced

bars in both horizontal directions to satisfy minimum temperature and shrinkage reinforcement. The 2 in. diameter PVC pipes for tension reaction ties were installed three inches from the bottom face of the block to the center of the PVC. Blocks containing 5/8 in. diameter anchor specimens contained four bars in both horizontal directions on the top face, while those with 1 in. diameter anchors contained ten in each direction to restrain concrete breakout forces. All reinforcement contained a minimum cover of 1.5 in. Figure 4-14 shows completed formwork before the concrete pour and concrete blocks after formwork removal for blocks with 5/8 in. and 1 in. diameter bolt specimens.

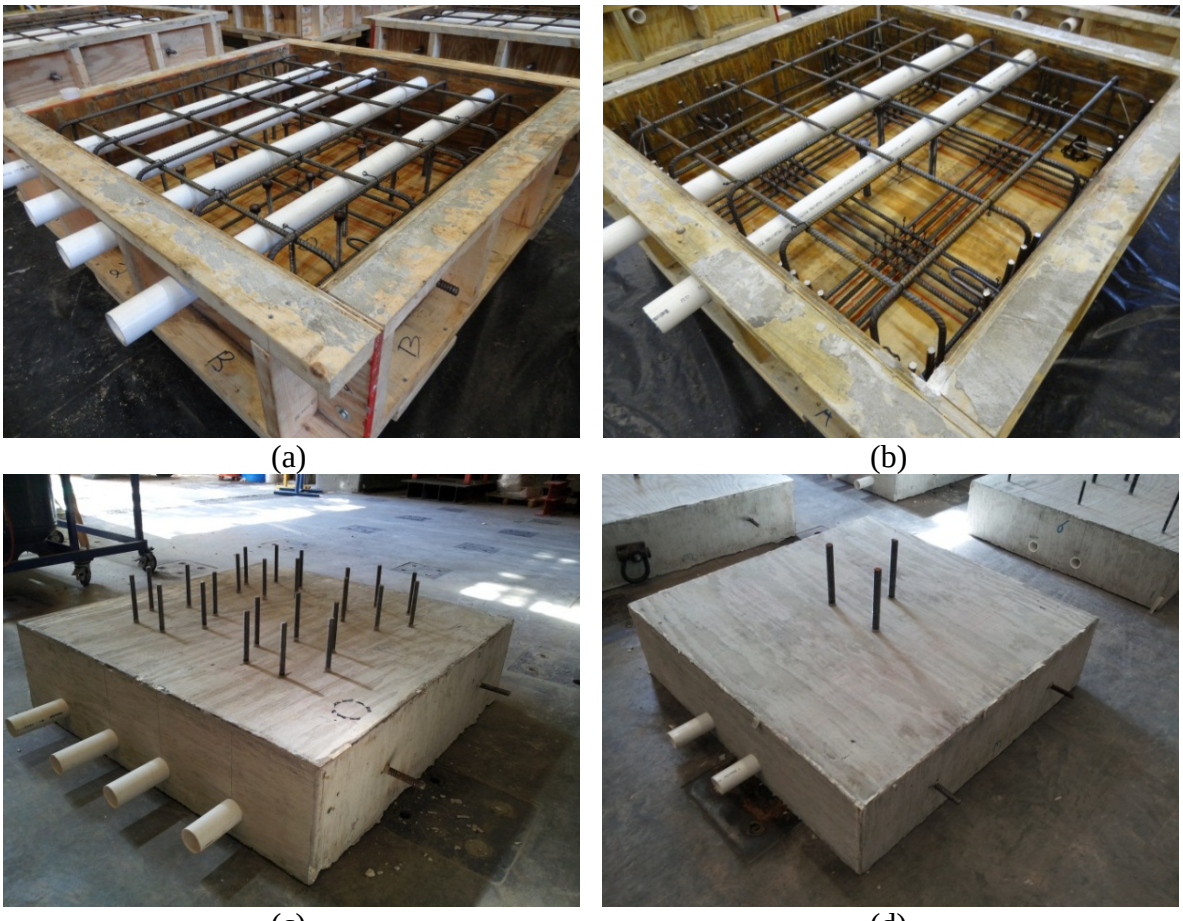

(a) (b)

(c) (d)

Figure 4-14. Reinforcement and completed blocks for 5/8 in. (a, c) and 1 in. (b, d) specimens

Rolling reaction frames were composed of two channel sections with a 3 in. gap for load application and restraint. The frames also contained 0.5 in. thick steel bottom plates with casters

and a 0.5 in. thick steel top plate to support identical telescoping through-hole hydraulic loading actuators. C10 x 15.3 channel sections were found sufficient to restrain moment forces assuming both a distributed load and a point load from the frame bearing reaction against the concrete block. The bottom platform was designed to balance the self-weight of the frames.

4.4.2.2 Instrumentation

Figure 4-15 (a) Figure 4-16 (a) display a view of a fully instrumented 5/8 in. diameter bolt test specimen. A plan view schematic of base plate instrumentation is provided in Figure 4-15 (b) and Figure 4-16 (b). The following instrumentation was implemented for all Phase II torsional testing:

- Two moment-compensating load cells installed behind the actuators (see Figure 4-7)
- Six donut load cells, one per anchor bolt, installed above the base plate with washers both above and below the cells. In the final 2 5/8 in. bolt tests conducted (T5 and T7), three new load cells were used with spherical washers placed above the cells (BT 1-6)
- Two horizontally oriented LVDTs installed behind base plate assembly loading wings (LVDT 1-2)
- Four vertically oriented LVDTs (LVDT 3-6)

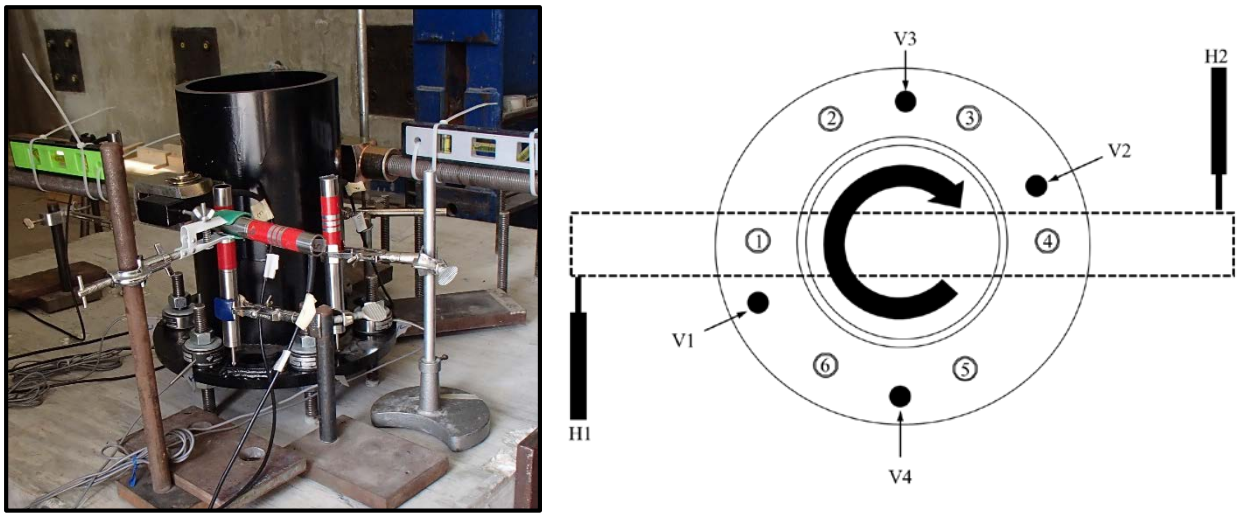

(a) (b)

Figure 4-15. (a) Fully instrumented 5/8 in. torsion specimen and (b) plan view detail of base plate assembly bolt numbers and instrumentation

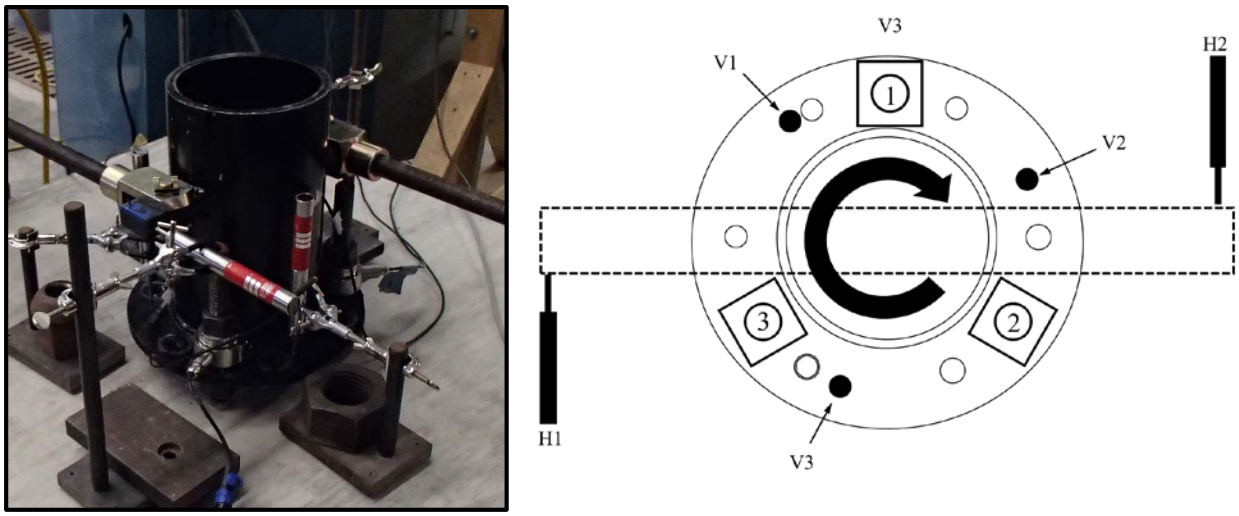

(a) (b)

Figure 4-16. (a) Fully instrumented 1 in. torsion specimen and (b) plan view detail of base plate assembly bolt numbers and instrumentation

4.4.3 Test Procedure

Figure 4-17 shows how independently operated hydraulic hand pumps were fed into the two loading actuators. The test procedure used for Phase 2 testing was broken into three distinct stages: Initial Setup, Final Instrumentation and Bolt Preloading, and Loading.

Figure 4-17. Hydraulic hand pumps used for torsion loading

Stage 1: Initial Setup

1. The concrete block with embedded anchor groups was placed supports, ensuring that the top surface of the concrete was level.
2. For tests other that were not flush-mounted, leveling nuts and washers were placed on the anchor bolts. For the flush-mounted tests, T1-A and T1-B, a 0.03 in. Teflon layer was placed on the concrete surface to reduce friction between the concrete and the base plate.
3. Stand-off distance was set as the distance from the top of the concrete surface to top of the leveling washer, with measurements made at the bearing end of every anchor bolt on the base plate. The base plate assembly was then seated on the washers. In the flush-mounted test, the base plate assembly was seated directly on the Teflon layer. For tests with grout, the grout pad was installed at this stage as described in Section 4.2.2.
4. The rolling reaction frames were secured to the concrete block by preloading the 1.5 in. diameter tension ties against the frames.
5. Actuators were attached to the reaction frames and loading rods were sent through the actuators and frames.
6. Actuator height was set by attaching levels to the loading rods, which were connected to the base plate assembly through a clevis connection.

Stage 2: Final Instrumentation Placement and Bolt Pre-loading

1. The LabVIEW program was run without recording data to view instrument readings.
2. LVDT plunger positions were set such that readings will stay in the linear range of the instrument output throughout the test.
3. Load cells were placed into testing position to finish preliminary setup.
4. Communication between instrumentation and the data acquisition system was verified.
5. Data recording began.
6. Anchor bolts were preloaded to FDOT specifications using the “turn-of-the-nut” method, defined as 1/3 turn past snug tight. For the flush-mounted test, T1, hand-tightness was used instead to minimize frictional forces in the base plate connection to the concrete.
    1. Snug tightness was performed as the AISC definition of the “full effort of an ironworker with an ordinary spud wrench.” Torque wrenches were not used due to compatibility constraints; therefore, snug tightness was performed as consistently as possible by the same test operator within and between tests with an approximate 100 lb. of effort applied at a 1 ft. torque arm. Bolts were snug tightened in a star pattern (e.g. bolts 1, 4, 2, 5, 3, 6).
    2. The operator repeated the previous step process in the same order to ensure that all bolts satisfied the definition of snug tightness.
    3. Anchors were marked to indicate when an additional 1/3 turn of the nut would be achieved. Every nut was turned to the final position in same order as for snug tightening using an extended lever arm for torque.
7. The position of every LVDT was checked or reestablished.
8. Enough preload was applied to the actuator load cells to set their position.

Stage 3: Loading

1. Two operators manned separate but identical hand pumps providing flow to their respective actuators. The LabVIEW user interface displayed load values for the actuators. These values

were used by the operators to maintain nearly equivalent load levels (within approximately 400 lb. at any given time) throughout the test.

2. The operators brought their loads into agreement between 1,000 and 2,000 lb. Step loading was applied in the linear range of each test in approximately 1,000 lb. increments with short pauses at the end of each load step to recover from any loading discrepancies. As the test transitioned into non-linear behavior, load was continually applied until failure. In some cases tests were stopped to take pictures, readjust LVDTs, and examine behavior.

4.5 Phase 3: Full-scale Anchor Bolt Groups under Predominantly Torsion Loading

4.5.1 Experimental Design

In total, four tests were conducted on groups of six 1.25 in. diameter anchor bolts under predominantly torsion loading as shown in Table 4-4. As a baseline, test FS1 was left ungrouted with exposed lengths equal to one bolt diameter. Test FS2 was grouted with identical dimensions to FS1. An "extreme" exposed length value of 3 nominal anchor bolt diameters was chosen in grouted tests FS3 and FS4. Tests FS1-FS3 contained a circular base plate while FS4 contained an annular base plate.

Table 4-4. Phase 3 test matrix

Set[a]	Reps	d_b (in.)	Hole Size (in.)	n	Anchor Type	Connection Type[b]	Top Nut Tightness[c]	$\frac{l_{BP}}{d_b}$	$\frac{l_{LN}}{d_b}$
FS1	1	1.25	1.75	6	CIP	U	TOTN	2.3	1
FS2	1	1.25	1.75	6	CIP	G	TOTN	2.3	1
FS3	1	1.25	1.75	6	CIP	G	TOTN	4.3	3
FS4	1	1.25	1.75	6	CIP	G	TOTN	4.3	3

[a]DS = Direct Shear, T = Torsion, FS = Full-scale
[b]FM = U = Ungrouted stand-off base plate, G = Grouted stand-off base plate
[c]FT = Finger-Tightened, TOTN = Turn-of-the-Nut

4.5.2 Test Setup

4.5.2.1 Structural Components

The test setup was designed to reuse the loading assembly from FDOT reports BD545-54, BDK75 977-04, and BDK75 977-32. The loading assembly, which was designed as a half-scale model in BDK545-54 for a failed cantilever sign structure, contained 12 1.75 in. diameter holes at a 10 in. bolt circle radius with a base plate thickness of 1 in. With FDOT's allowable 0.5 in. hole oversize, 1.25 in. anchors were conservatively chosen. Among the mast arm signal base plates surveyed in Gainesville, FL (discussed in Section 4.4.2.1), one specimen contained six 1.25 in. anchor bolts at a similar bolt circle radius to the loading assembly. The base plate thickness to bolt diameter ratio (0.8) fell within the range of values in Table 4-3. Thus, it was determined that the test design was conservative in representing existing structures.

Each test specimen was composed of a 6 ft. x 10 ft. x 3 ft. deep reinforced concrete block containing a single anchor bolt group in the center as shown in Figure 4-18. Blocks were tied to the strong floor using steel beams and 1.5 in. diameter threaded rods. Load was applied by a hydraulic actuator placed at a 9 ft. torsion arm through a steel pin connection.

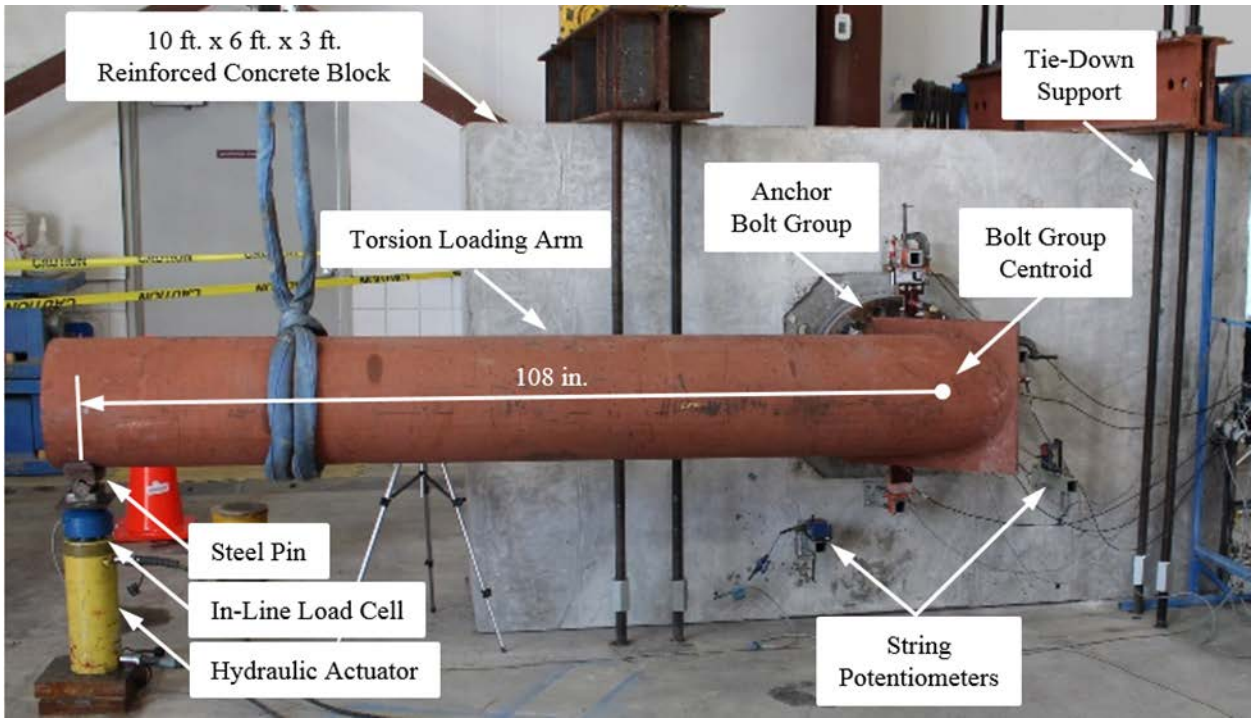

Figure 4-18. Phase 3 test setup

Details for the 10 ft. by 6 ft. by 3 ft. deep reinforced concrete blocks are given in Figure 4-19. Anchor bolts were positioned such that the pipe loading assembly, which was offset 15 degrees from the nearest bolt circle radius through one of the base plate holes. An 8 by 15 grid of Number 4 top reinforcement in the concrete blocks was designed to accommodate anchor bolt breakout forces as described for Phase 2 block specimens in Section 4.4.2.1. Bottom reinforcement duplicated the top reinforcement grid and was adequate for creep, shrinkage, and handling. A minimum cover of 3 inches was used for reinforcement. Additional #8 bars were placed at the top and bottom of the blocks to restrain block moment forces from the applied load and reactions.

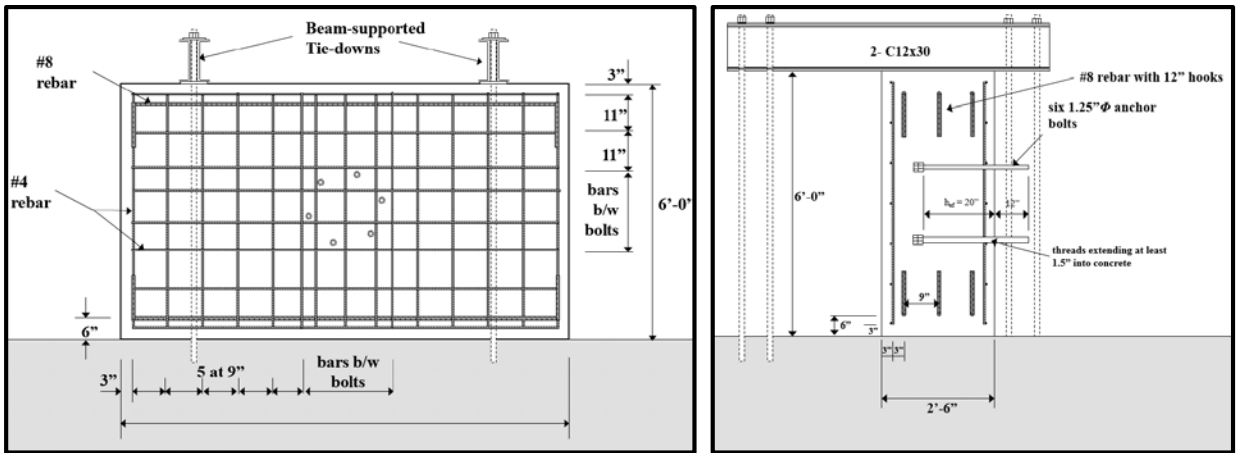

(a) (b)

Figure 4-19. Front (a) and side (b) views of anchor placement details for test specimen blocks

Figure 4-20 shows the formwork, reinforcement, and anchor bolt templates used. In the first block it was found difficult to level using conventional methods. The surface of the first block was ground with an angle grinder until a plane surface around the anchor bolts was achieved. For blocks 2 through 4 a plywood template (as shown) was placed around the bolt group to create a level surface to reference base plate stand-off height.

Figure 4-20. Full-scale anchor bolt and rebar and rebar placement before casting concrete

The loading assembly, shown in Figure 4-21 was composed of a 24 in. diameter, 1 in. thick circular base plate with 12 1.75 in. diameter holes. For test FS4, a 15.5 in. diameter circle was

cut out of the center of the base plate. The base plate was welded to HSS 16.000 x 0.500 steel pipe assembly containing a 23 in. stub welded to a 120 in. loading arm.

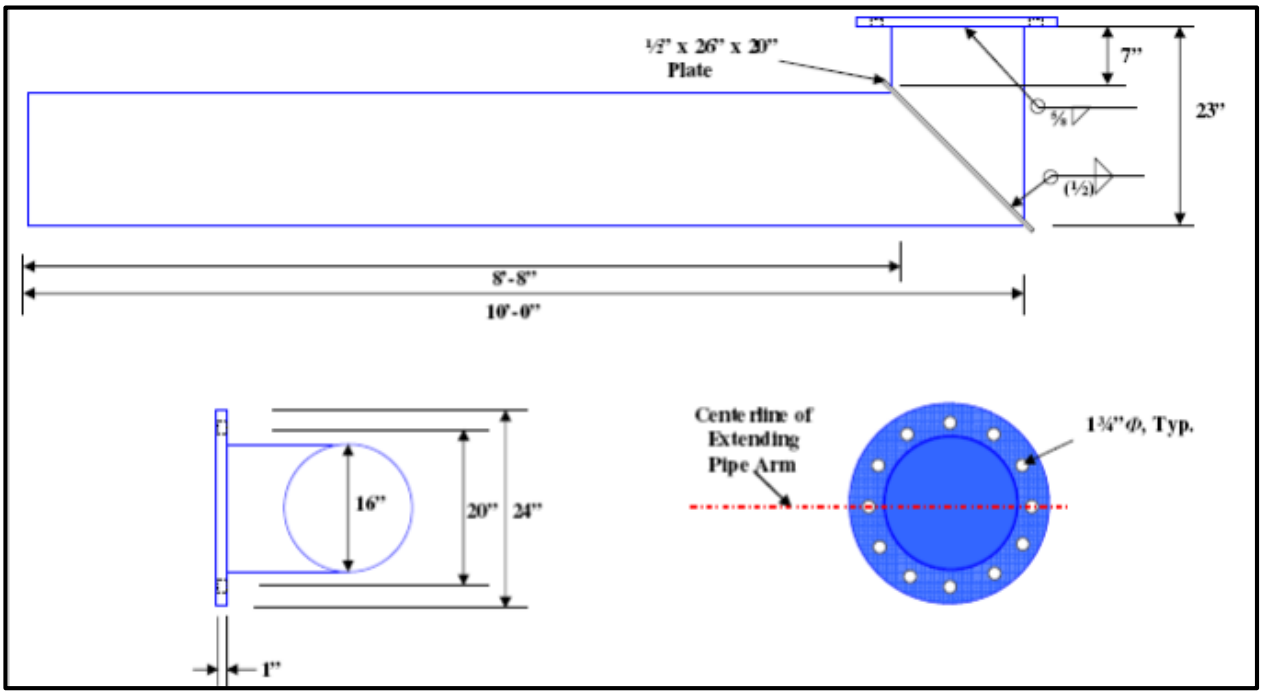

Figure 4-21. Schematic of full-scale loading apparatus (from Cook and Halcovage 2007)

4.5.2.2 Instrumentation

Figure 4-22 displays a view of a fully instrumented test specimen and a plan view schematic of base plate instrumentation within the test setup. The following instrumentation was implemented for all Phase 3 full-scale testing:

- A load cell threaded into the loading actuator (see Figure 4-18)
- Six donut load cells installed on anchor specimens directly above the base plate assembly
- Two horizontally oriented LVDTs installed at base plate mid-height (H1 and H2)
- Three vertically oriented LVDTs (V1-V3)
- Two string potentiometers tangential to the base plate mid-thickness (SP1 and SP2)

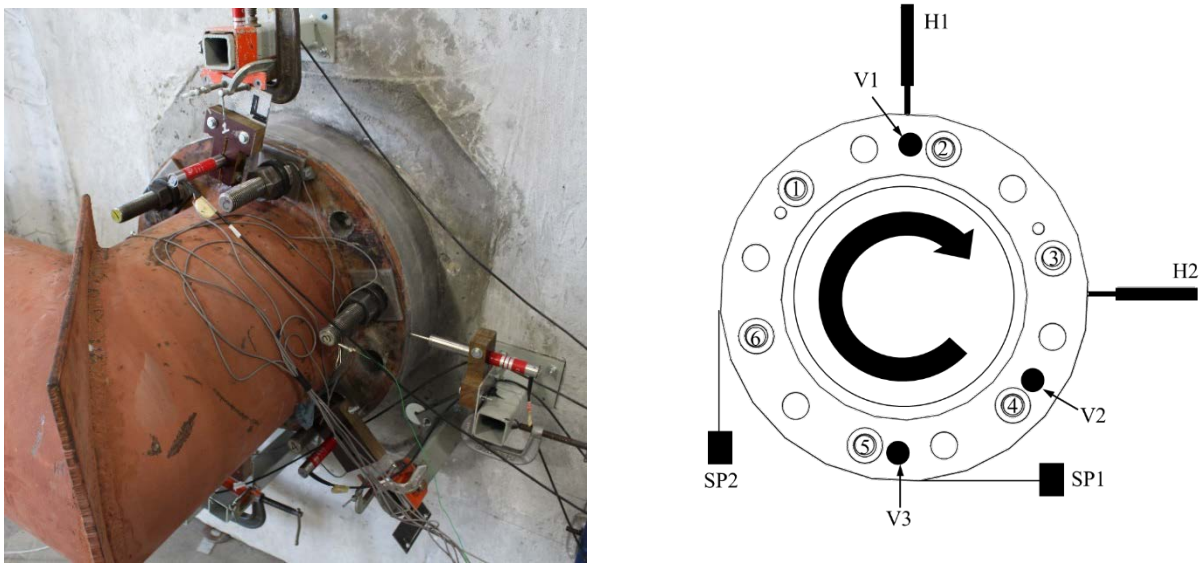

(a) (b)

Figure 4-22. (a) Fully instrumented full-scale specimen and (b) plan view detail of base plate assembly bolt numbers and instrumentation

4.5.3 Test Procedure

To prepare for tests, the loading assembly was installed for every test with the block resting on the opposite face from the location of the anchor bolts. Procedural stages 1 and 2 described for Phase 2 testing were followed where applicable for setting stand-off distance and recording pre-loaded values in the bolt tension load cells. Concrete bug holes directly below the base plate were filled with putty so that grout would not fill these spaces and contribute mechanically to the shear strength of the grout pad (note: none were present in Phase 2 testing). After the anchor bolts were preloaded, grout was installed and treated in applicable tests following the methodology presented in 3.1.2.2. After the grout pad had cured for a minimum of 24 hours the concrete block was moved into the test position, instrumentation was installed, and the tie-down system was set in place.

Tests were displacement-controlled by through an electric hydraulic pump manned by an operator. In the linear-elastic portion of each test the loading rate was set at approximately 150 lb. per second on the 9 ft. loading arm, equivalent to a torque rate of approximately 100 kip-

in./second. Displacement rate was increased slightly through the much larger inelastic phase of test behavior. At the loading arm, displacements nearing 30 inches were observed as the anchor bolts deformed, requiring in-test adjustment of the loading actuator. During adjustment periods, the loading arm was supported by an overhead crane while the actuator was retracted and reset. A shorter actuator was used at the beginning of the test and replaced by a taller actuator after one or two stroke cycles. Other than stopping for actuator adjustment, the consistent quasi-static displacement was continued until anchor bolt rupture.

CHAPTER 5
EXPERIMENTAL RESULTS AND DISCUSSION

5.1 Introduction

This chapter provides a summary and discussion of the test results for all three phases of the project. Individual load-displacement results are presented in Appendix A for the Phase 1 direct shear tests, Appendix B for the Phase 2 torsion tests, and Appendix C for the Phase 3 Torsion and bending tests.

5.2 Phase 1: Direct Shear Testing

Table 5-1 provides a summary of Phase 1 results. Two of the datasets, DS10 and DS11, do not contain result values; this is discussed in subsequent paragraphs. Datasets DS7 and DS8 contained two bolts per test. Thus, the $V_{u,bolt}$ value reported represents the ultimate shear load divided by two. The 28-day concrete strength for Phase 1 was 4,990 psi. All 5/8 in. and 1 in. bolts were from the same batch. Ultimate tension strengths, T_u, of anchor bolt threaded rod specimens, were determined according to ASTM F606 methodology (ASTM 2011) using the UF Structures Laboratory Instron machine. Ultimate displacements, δ_u, correspond to the value of $V_{u,bolt}$ for each test. A limited number of bending depths, l_b, defined as the distance from the concrete surface to the deepest point below the surface of the concrete where the anchor experienced any bending deformations, were taken from cored anchor bolt specimens from datasets DS1 through DS8.

Figure 5-1 displays load-displacement behavior for representative tests within the Phase I test program. Flush-mounted tests performed nearly identically between 5/8 in. cast-in-place (CIP), 5/8 in. adhesive (AD), and 1 in. bolt tests. At $2d_b$ and $4d_b$ base plate stand-off, however, differences emerged. Behavior and stiffness between CIP and AD single-bolt equivalents was approximately equivalent with slightly greater $V_{u,bolt}$ values observed in the AD tests. While not

investigated in detail, the higher strengths observed in adhesive tests may be a result of greater surface area from the larger diameter annular adhesive ring bearing against the concrete surface.

Table 5-1. Summary of Phase 1 anchor bolt ultimate load and displacement results

Set	Reps	$\frac{l_{BP}}{d_b}$	$\frac{l_{LN}}{d_b}$	T_u (kip)	$V_{u,bolt}$ (kip)	COV	$\frac{V_{u,bolt}}{T_u}$	δ_u (in.)	$\frac{\delta_u}{d_b}$	l_b (in.)
DS1	8	0	*na*	21.1	12.3	3%	0.59	0.18	0.29	0.56
DS2	6	1.2	0	21.1	11.3	1%	0.54	0.56	0.89	0.64
DS3	2	1.6	0.4	21.1	9.8	*na*	0.46	0.77	1.23	0.66
DS4	10	2	0.8	21.1	7.9	6%	0.37	0.72	1.15	0.73
DS5	4	3	1.8	21.1	5.6	6%	0.27	0.64	1.03	0.52
DS6	5	4	2.8	21.1	4.4	10%	0.21	0.74	1.18	0.47
DS7	4	2	0.8	21.1	11.4	5%	0.54	0.17	0.272	0.54
DS8	5	4	2.8	21.1	6.9	3%	0.33	0.64	1.024	0.72
DS9	4	0	*na*	55.8	33.5	1%	0.60	0.31	0.31	-
DS10[a]	5	2.0	0.75	55.8	27.2	19%	0.49	1.64	1.64	-
DS11[a]	2	4.0	2.75	55.8	19.4	*na*	0.35	1.85	1.85	-
DS12	4	0.0	*na*	21.1	12.2	3%	0.58	0.18	0.288	-
DS13	5	2.0	0.8	21.1	9.2	5%	0.44	0.75	1.2	-
DS14	2	4.0	2.8	21.1	5.1	5%	0.24	0.83	1.328	-

na = not applicable
- = unavailable
[a]Note: results discarded. Refer to discussion below.

For 5/8 in. bolt specimens, double-bolt stand-off tests (DS8) demonstrated earlier stiffness degradation than single-bolt tests. In double-bolt stand-off tests, the base plate was free to displace vertically over its entire length. The roller in single-bolt tests, however, restrained base plate vertical movement and rotation, preventing anchor bolt "flagpole" action. As the stand-off bolt deformed horizontally the restraint of downward base plate movement caused a tension force to develop in the single anchor resulting in increased stiffness and strength.

Representative curves for the 1 in. diameter stand-off tests are shown below in gray. In the 1 in. diameter tests the roller prevented downward movement at its location but permitted plate rotation at the location of the anchor. As a result, the anchor bolt experienced "flagpole" rotation while still adding tension force to the anchor to balance the compressive reaction from vertical restraint at the roller. Because the roller restrained downward movement of the base plate at one location yet allowed the anchor to experience "flagpole" action, the anchor essentially turned

into a truss tension element with the roller acting as the truss compression strut. Thus,large tension forces developed in the anchors resulting in significantly increased capacity. Since this type of base plate restraint is not representative of what would occur in annular base plate connections, direct shear testing was abandoned for 1 in. bolts. The results of all 1 in. bolt tests with stand-off (DS10 and DS11) were not used in developing design models.

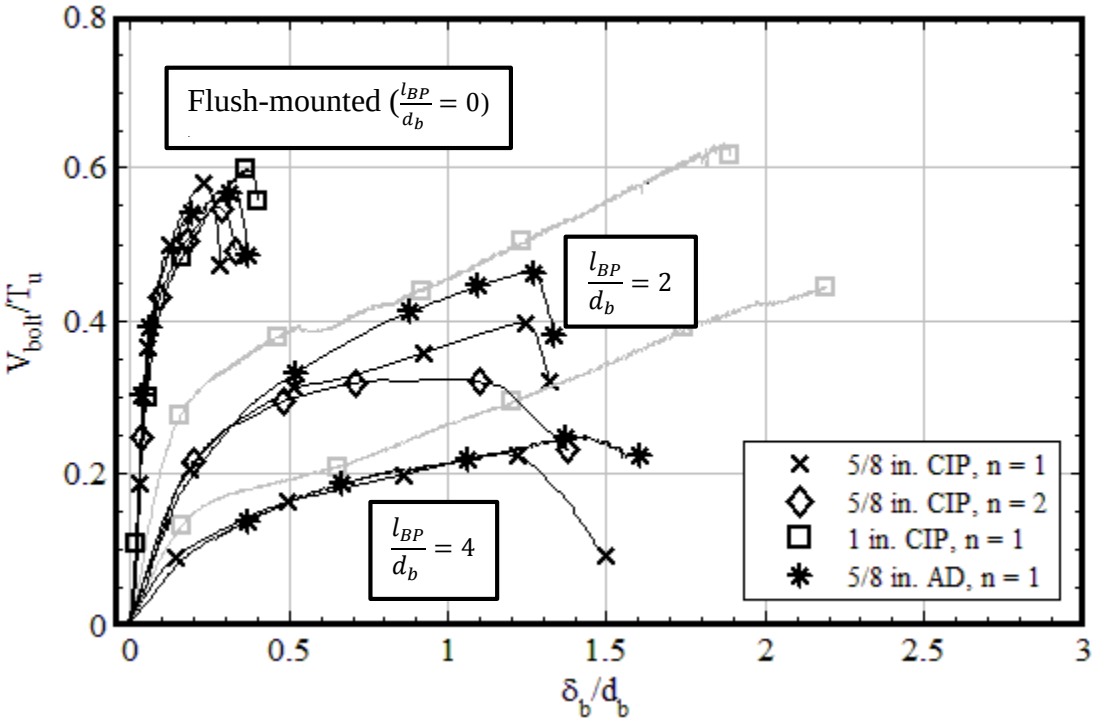

Figure 5-1. Load-displacement behavior of representative Phase 1 tests

Multiple repetitions within Phase 1 datasets allow for statistical classifications of which sets are statistically equivalent and which are statistically different. Results from an analysis of variance (ANOVA) test were used in a Tukey-Kramer test that tells which datasets can be considered statistically different or equivalent. The analytical approach is described below along with the results from both analyses.

A one-factor ANOVA test evaluates the means of three or more samples sets (generically known as “treatments”). The statistical null hypothesis is that *all* means are statistically equivalent, but the test does not distinguish *which* sample sets are statistically different if the null

hypothesis is rejected (hence the need for the Tukey-Kramer comparison below). To test the hypothesis, an F statistic is obtained as shown below in Equations (5-1) through (5-5). The F statistic is compared against a tabulated critical F value for a chosen acceptable probability of Type 1 Error, α. If the calculated F value exceeds the tabulated F value (resulting in a P-value less than α), the null hypothesis is rejected and the conclusion is made that not all means are statistically equivalent.

$$F = \frac{MST}{MSE} \tag{5-1}$$

$$MST = \frac{SST}{t-1} \tag{5-2}$$

$$MSE = \frac{SSE}{N-1} \tag{5-3}$$

$$SST = n\sum_{ij}(\bar{y}_{i.} - \bar{y}_{..})^2 \tag{5-4}$$

$$SSE = \sum_{i}(y_{ij} - \bar{y}_{i.})^2 \tag{5-5}$$

where
MST = Mean Square Treatment
MSE = Mean Square Error
SST = Between Treatment Sum of Squares
SSE = Sum of Squares for Error
t = number of treatments
n = number of samples within each treatment
N = total number of samples in the experiment
y_{ij} = j^{th} sample taken from treatment i
$\bar{y}_{i.}$ = mean of the samples in treatment i
$\bar{y}_{..}$ = mean of all samples in the experiment

All Phase 1 datasets excluding those not representative of field conditions (stand-off 1 in. tests DS10 and DS11) and sets with fewer than three repetitions (DS3 and DS14) were considered in an ANOVA test with $\alpha = 0.05$ (95% confidence). Results of the analysis are given

in Table 5-2. Unsurprisingly, the test produced a statistically significant result that *at least one dataset is different from at least one other*.

Table 5-2. Analysis of variance between selected Phase 1 datasets

Source of Variation	*SS*	*df*	*MS*	*F*	*P-value*	*F crit*
Between Groups	0.938	9	0.104	312.464	1.68E-37	2.10
Within Groups	0.015	45	0.0003			
Total	0.953	54				

If, as in Table 5-2, an ANOVA test results in statistical differences, further analysis is needed to determine which means are statistically different. The Tukey-Kramer Honestly Significant Difference (HSD) is one such method that accounts for multiple sample sizes, as were contained in Phase 1 datasets. α, df_E, and MSE values from the ANOVA test are utilized in the HSD method to find significance in results. The test places the difference between any two means in the experiment against an HSD value calculated by Equation (5-6).

$$HSD = q_{dfE,t,\alpha} * \sqrt{\frac{MSE}{n}} \tag{5-6}$$

where $q_{dfE,t,\alpha}$ = taken from the Student's t-distribution table
df_E = number of degrees of freedom for error in the ANOVA test
t = is the and is the total number of means in the ANOVA test
MSE = Mean Square Error taken from the ANOVA
n = number of samples in each sample population

HSD values are calculated for each dataset (differences are fully dependent on sample size). If the absolute value of the difference between any two datasets is greater than the combined HSD values of the two datasets, the null hypothesis that any two means are statistically equivalent is rejected and it is concluded that *the two means are different.*

Table 5-3 indicates which datasets are statistically different or equivalent from conducting the Tukey-Kramer analysis. Within groups of datasets containing the same installation type and varying stand-off distances (single-anchor cast-in-place datasets DS1 through DS6, double-

anchor cast-in-place datasets DS7 and DS8, and adhesive anchor datasets DS12 and DS13), the strength of the bolts decreased with increased stand-off distance. Thus, it is confirmed statistically that all values of stand-off distance produce lower anchor bolt strengths. Flush-mounted and $2d_b$ stand-off distance tests were conducted for multiple installation types. All installation types for flush-mounted datasets were statistically equivalent except for the double-bolt DS7, where its normalized shear strength was lower than both the normalized shear strength of the 5/8 in. single-bolt cast-in-place (DS1) and 1 in. bolt (DS9) sets. At $2d_b$ stand-off, however, adhesive anchors (DS13) are statistically stronger than 5/8 in. single anchors (DS1), which are in turn statistically stronger than the two-bolt 5/8 in. anchor tests (DS8), although the latter two are nearly statistically equivalent.

In summary, the statistical analysis concludes that:

- strength decreased with all stand-off distance increments tested
- adhesive anchors in stand-off base plates were stronger than equivalent cast-in-place anchors
- single-bolt tests normalized by bolt tension strength were slightly stronger than double-bolt tests (per bolt)

Table 5-3. Statistical differences between selected Phase 1 datasets using Tukey-Kramer analysis

Dataset	$\frac{V_{u,bolt}}{T_u}$	*Different from…*								
		DS1	*DS2*	*DS4*	*DS5*	*DS6*	*DS7*	*DS8*	*DS9*	*DS12*
DS1	0.59	-	-	-	-	-	-	-	-	-
DS2	0.54	Y	-	-		-	-	-	-	-
DS4	0.37	Y	Y	-	-	-	-	-	-	-
DS5	0.27	Y	Y	Y	-	-	-	-	-	-
DS6	0.21	Y	Y	Y	Y	-	-	-	-	-
DS7	0.54	Y	N	Y	Y	Y	-	-	-	-
DS8	0.33	Y	Y	Y	Y	Y	Y	-	-	-
DS9	0.60	N	Y	Y	Y	Y	Y	Y	-	-
DS12	0.58	N	Y	Y	Y	Y	N	Y	N	-
DS13	0.44	Y	Y	Y	Y	Y	Y	Y	Y	Y

5.3 Phase 2: Torsion Testing of Scaled Anchor Bolt Groups

Phase 2 results are summarized in Table 5-4. One test, T6-A, was not run to ultimate load. Values provided for T6, then, reflect only results from test T6-B. The 28-day concrete strength for Phase 2 blocks was 6,360 psi. Grout strengths were 5,360 psi, 7,480 psi, and 6,230 psi for T5, T6-B, and T7, respectively. All 5/8 in. bolts were from the same unique batch to Phase 2. 1 in. bolts were from the same batch as in Phase 1. Expressions of V_{bolt} for Phase 2 reflect the average of the two load cell readings adjusted for loading rod geometry and distributed equally among the bolts in a given test. As in Phase 1 δ_u values correspond to $V_{u,bolt}$ for each test. The expression of displacement as a distance rather than a systemic rotation was chosen for comparison to Phase 1 tests and proportion to bolt diameter. Displacement values were calculated by adjusting the linear LVDT readings (refer to the instrumentation locations in Figure 4-15) to the equivalent distance traveled along the bolt circle using geometry and adjusting the radius from the center of the base plate to the LVDT locations to the radius of the bolt circle.

Table 5-4. Summary of Phase 2 anchor bolt ultimate load and displacement results

Test	Reps	$\frac{l_{BP}}{d_b}$	$\frac{l_{LN}}{d_b}$	T_u (kip)	$V_{u,bolt}$ (kip)	$\frac{V_{u,bolt}}{T_u}$	δ_u (in.)	$\frac{\delta_u}{d_b}$
T1	2	0	Na	20.7	11.1	0.54	0.3	0.3
T2	2	2	0.8	20.7	6.5	0.31	0.56	0.56
T3	1	4	2.8	20.7	4.6	0.22	0.73	0.73
T4	1	2	0.8	20.7	7.4	0.36	0.6	0.6
T5	1	2	0.8	20.7	10.9	0.53	0.56	0.56
T6	2[a]	4	2.8	20.7	13.1	0.63	1.03	1.03
T7	1	4	2.8	20.7	14.8	0.71	0.44	0.44
T8	1	0	Na	55.8	31.7	0.57	0.39	0.39
T9	1	2	0.75	55.8	18	0.32	0.88	0.88
T10	1	4	2.75	55.8	10.5	0.19	1.57	1.57

na = not applicable

[a]T6-A was not run to ultimate load. All T6 results reflect T6-B.

Figure 5-2 displays load-displacement behavior of representative ungrouted Phase 2 tests. Flush-mounted tests demonstrated initial slip through the hole oversize followed by linear-elastic

behavior. T1-B stiffness degraded at a lower displacement and failed at lower ultimate load ($0.51T_u$) than T1-A ($0.56T_u$), presumably from less favorable bolt position within the holes.

Ungrouted stand-off base plate tests demonstrated linear-elastic behavior to approximately $0.15T_u$and $0.08T_u$ for $2d_b$ and $4d_b$ tests, respectively, followed by a ductile inelastic phase as the bolts deformed laterally over their exposed lengths. Strength and behavior between 5/8 in. and 1 in. bolts were nearly identical. Ultimate displacements of the $2d_b$ and $4d_b$ tests were on the order of one bolt diameter for both with the exception of the 1 in. diameter $4d_b$ torsion test (T10), which showed greater deformation with respect to d_b.

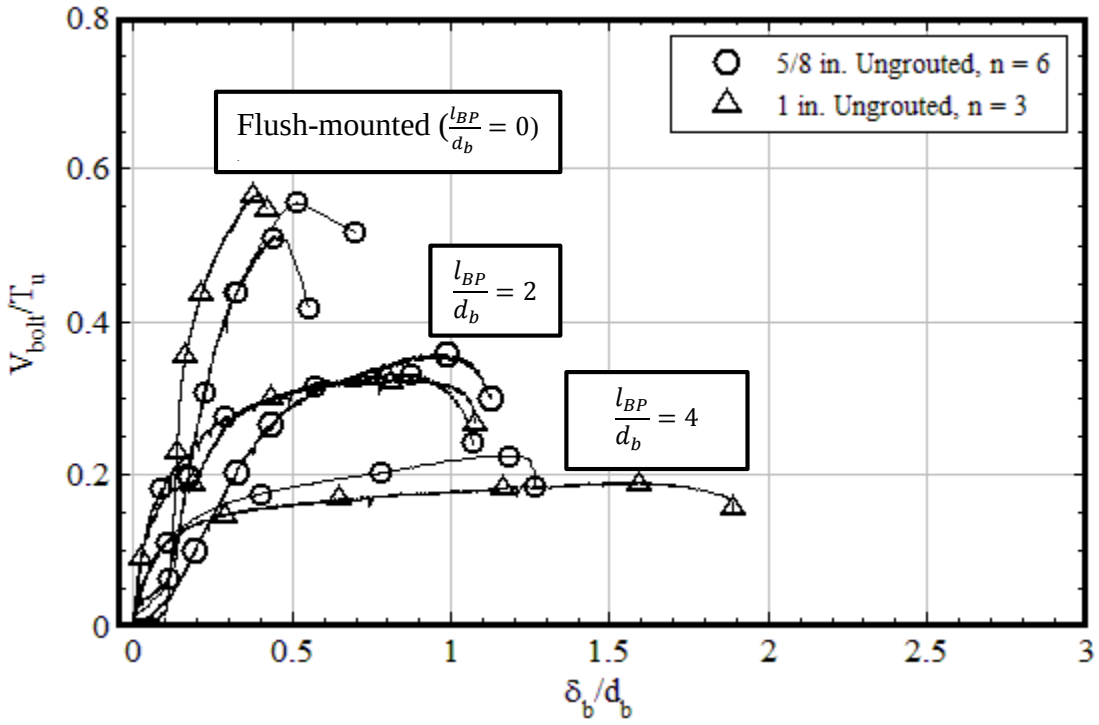

Figure 5-2. Load-displacement behavior of representative ungrouted Phase 2 tests

Figure 5-3 shows anchor bolts in pretensioned test T2-B and the non-pretensioned test T4 tests after failure. The leveling nuts in both tests underwent rotation en route to ultimate strength, but it is clear that the magnitude of T4 rotation exceeded that in T2-B, as would be expected. While the difference in $V_{u,bolt}$ is slight and statistical inferences cannot be made, the tests

represent the average strength of six bolts and the difference between the two tests may indicate more than the spread of data. It is hypothesized that the additional bolt deformation between the leveling nut and the base plate allowed greater overall ductility, resulting in small amounts of additional tension pickup by bolt the angled geometry of the displaced bolt. Referring back to Figure 5-2, base plate slip occurred immediately in T4, while no slip is apparent throughout the T2-B curve. T4 linear elastic stiffness was lower, likely due to additional bolt bending within the thickness of the base plate. Surprisingly, however, the inelastic phase was stiffer in T4 than T2 and the ultimate load was higher ($0.36T_u$vs. $0.31T_u$). Thus, the consequences of absence/loss of pretension in ungrouted double-nut stand-off base plate connections may not be critical beyond serviceability considerations, similar to conclusions made by Kulak et al. (1987) with respect to flush-mounted steel-to-steel connections.

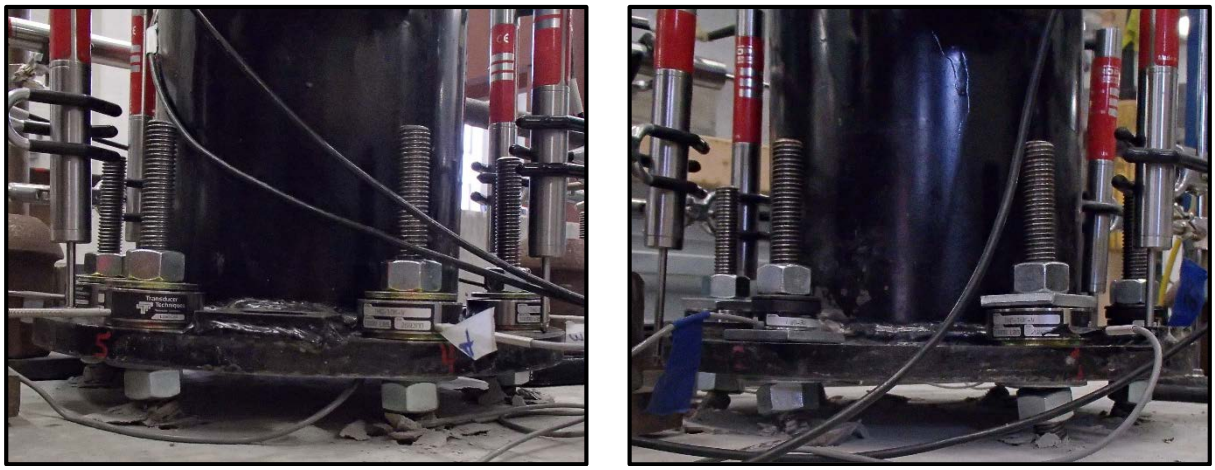

(a) (b)

Figure 5-3. Anchor bolts in failed condition for (a) pretensioned T2-B and (b) non-pretensioned T4 ungrouted $2d_b$ base plate tests

Load-displacement behavior of grouted stand-off base plate tests is provided in Figure 5-4. General behavior of grouted tests without the FRP retrofit is discussed in Section 5.5.1 coupled with the discussion of grouted tests from Phase 3 testing. Initial behavior of the grouted $4d_b$ stand-off torsion test with an FRP retrofit, T7, was similar to other grouted tests. With load less

than approximately $0.3T_u$, there was rotation of the base plate relative to the FRP wrap. After initial grout cracking at approximately $0.3T_u$, radial grout material displacement was restrained by the FRP perimeter. Subsequent test rotation was shared equally between the base plate assembly and the retrofitted grout pad until an explosive failure, with all of the anchor bolts completely sheared away at the top surface of the grout pad at slightly greater than $0.7T_u$. The higher result than flush-mounted shear strength was attributed to the combination of the restraint of the grout pad from crack propagation, the leveling nuts immediately below the grout pad surface producing greater bearing area (no local spalls in front of anchor bolts were observed), and friction between the grout pad and the base plate. While only one FRP-retrofitted test was performed, this result shows promise for bringing anchor bolts in existing ungrouted and grouted stand-off base plates to flush-mounted strength or higher at low levels of ultimate displacement.

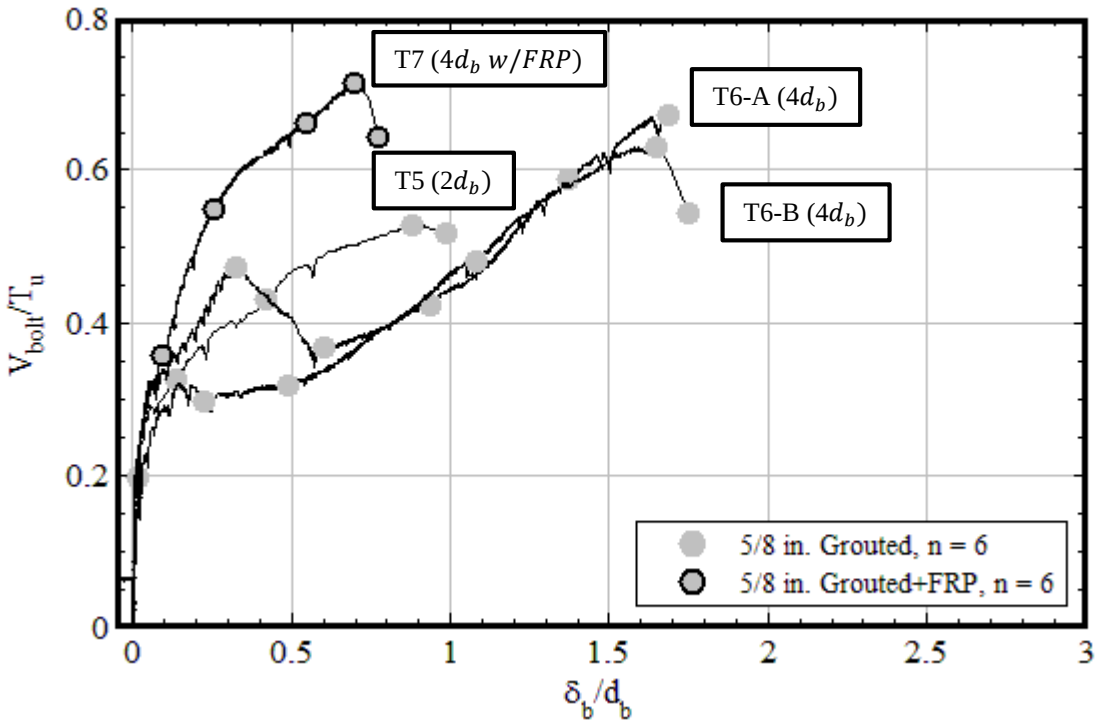

Figure 5-4. Load-displacement behavior of grouted Phase 2 tests

Figure 5-5 shows in-test grout cracking and post-test grout top surfaces following base plate removal for $2d_b$ and $4d_b$ stand-off grouted tests. Torsional cracks originating at the

location of bolt bearing on the grout pad were observed within tests (Figure 5-5 (a) and (c)). Plan views in Figure 5-5 (b) and (d) show tensile cracking within the compression struts between bolts along the bolt circle and within the center of the base plate. As these cracks propagated, grout material displaced radially. The central circular indentation in top views indicates the location of the cardboard circle inserted to simulate an annular base plate connection in the circular base plate as discussed in Section 4.2.2. Figure 5-6 shows the grout top surface of FRP-retrofitted $4d_b$ stand-off test T7. Evidence of microcracking patterns similar to the unretrofitted tests can be seen. However, the system equilibrated as the FRP engaged, prohibiting further crack propagation.

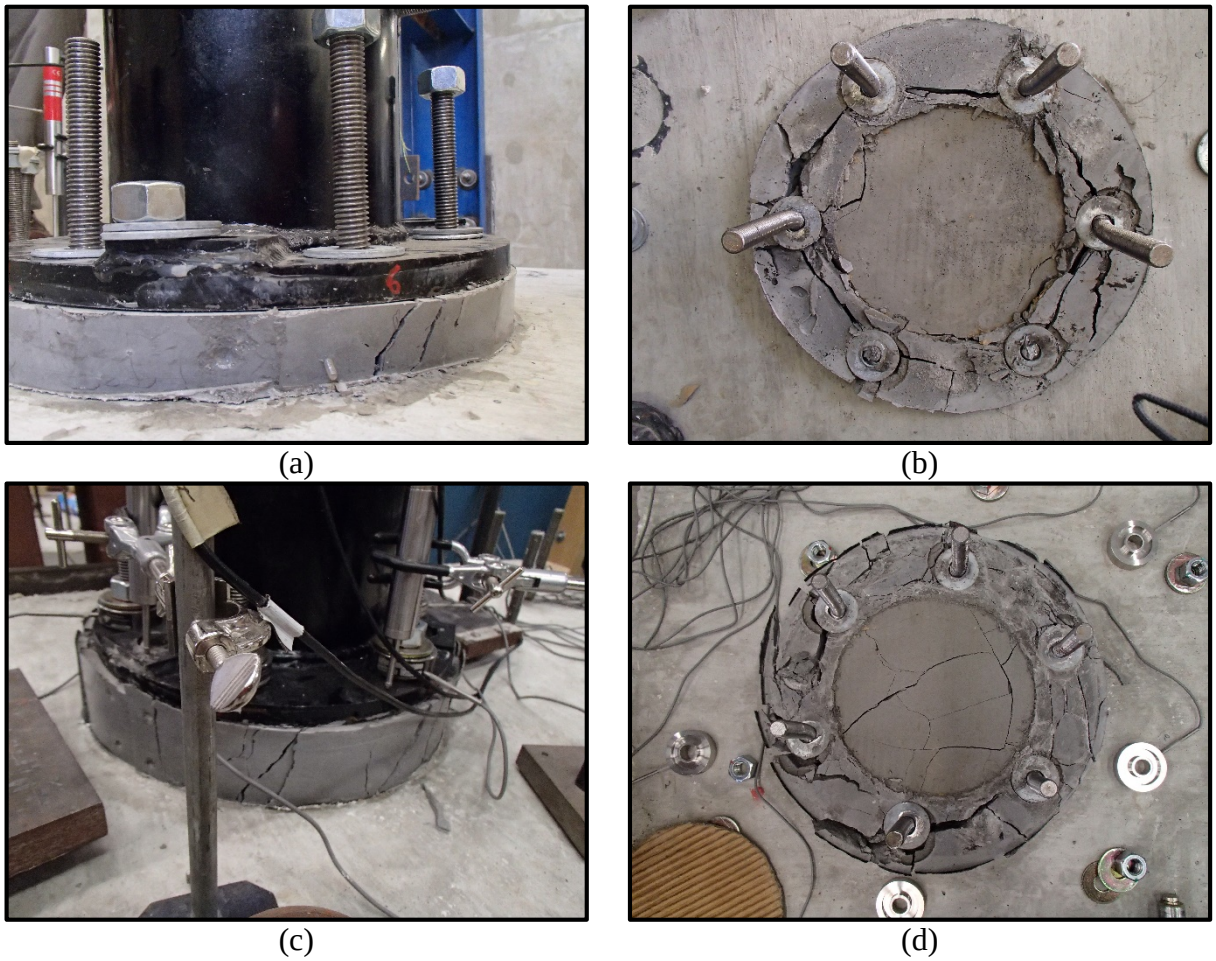

(a) (b) (c) (d)

Figure 5-5. (a, c) In-test grout cracking and (b, d) post-test grout surface for T5 ($2d_b$ base plate stand-off) and T6-A ($4d_b$ base plate stand-off)

Figure 5-6. Post-test grout surface for T7 (FRP-retrofitted $4d_b$ base plate stand-off)

Table 5-5 provides ultimate displacement values from vertically oriented LVDTs, with positive values indicating downward base plate movement. Readings were not taken for T2-A. Values were negligible in flush-mounted and ungrouted $2d_b$ tests, while ungrouted $4d_b$ tests showed much greater vertical displacement. In general, grouted vertical displacements were negligible, but slight *upward* movement was observed in $2d_b$ test T5. Load vs. vertical displacement graphs are provided for every test in Appendix B.

Table 5-5. Vertical base plate displacements in Phase 2 tests

Test	V1	V2	V3	V4	Average
T1-A	-0.011	0.000	0.035	0.001	0.006
T1-B	0.007	-0.036	0.013	-0.024	-0.005
T2-B	0.038	-0.015	0.016	-0.012	0.007
T3	0.083	0.081	0.119	0.058	0.085
T4	-0.007	0.008	-0.014	0.001	-0.003
T5	-0.031	-0.079	-0.054	-0.054	-0.054
T6-A	0.008	-0.008	0.031	0.008	0.014
T6-B	0.042	-0.004	0.009	0.033	0.020
T7	-0.029	-0.008	-0.036	-0.013	-0.021
T8	-0.017	-0.013	0.012	*na*	-0.006
T9	0.006	-0.009	0.022	*na*	0.006
T10	0.266	0.271	0.378	*na*	0.305

na = not applicable

5.4 Phase 3: Full-scale Anchor Bolt Groups under Predominantly Torsion Loading

Phase 3 results are summarized in Table 5-6. 28-day concrete strengths for the four blocks were 6,590 psi, 7,160 psi, 7,140 psi, and 8,460 psi and grout strengths for FS2 through FS4 were 9,100 psi, 9,010 psi, and 8,170 psi, respectively. All of the 1.25 in. bolts were from the same batch. Expressions of V_{bolt}, as in Phase 2, reflect geometrically adjusted values, in this case adjusted for the angle of loading with respect to the tangent of the pivoting loading arm. Contributions to bolt stresses by overturning moment from the short pipe section were negligible and are not reflected in the results. Again, ultimate displacements, δ_u, correspond to the value of $V_{u,bolt}$ for each test. Displacement values were calculated by adjusting the average of the two string potentiometer readings from their base plate radius location to the bolt circle radius.

Table 5-6. Summary of Phase 3 anchor bolt ultimate load and displacement results

Test	Reps	$\frac{l_{BP}}{d_b}$	$\frac{l_{LN}}{d_b}$	T_u (kip)	$V_{u,bolt}$ (kip)	$\frac{V_{u,bolt}}{T_u}$	δ_u (in.)	$\frac{\delta_u}{d_b}$
FS1	1	2.3	1	84.4	27.1	0.32	1.89	1.52
FS2	1	2.3	1	84.4	59.1	0.7	2.12	1.7
FS3	1	4.3	3	84.4	46.9	0.56	3.57	2.86
FS4	1	4.3	3	84.4	52.8	0.63	2.53	2.02

Load-displacement behavior of all Phase 3 tests is provided in Figure 5-7. The ungrouted test, FS1, demonstrated similar behavior to ungrouted Phase 2 results. The magnitude of ultimate load for this $2.3d_b$ stand-off ($1d_b$ exposed length) test, $0.32T_u$, fell between the values for the $2d_b$ and $4d_b$ stand-off Phase 2 tests. Test FS4, which contained the modified base plate with the circle cut out of the center, demonstrated behavior similar to Phase 2 and Phase 3 grouted tests with a circular base plate and a strength greater than its circular base plate counterpart FS3. Thus, it has been determined that results from the circular base plate tests with the cardboard filler in the annular area are valid representations of annular base plates. A detailed description of grouted test behavior is grouped with Phase 2 results in Section 5.5.1.

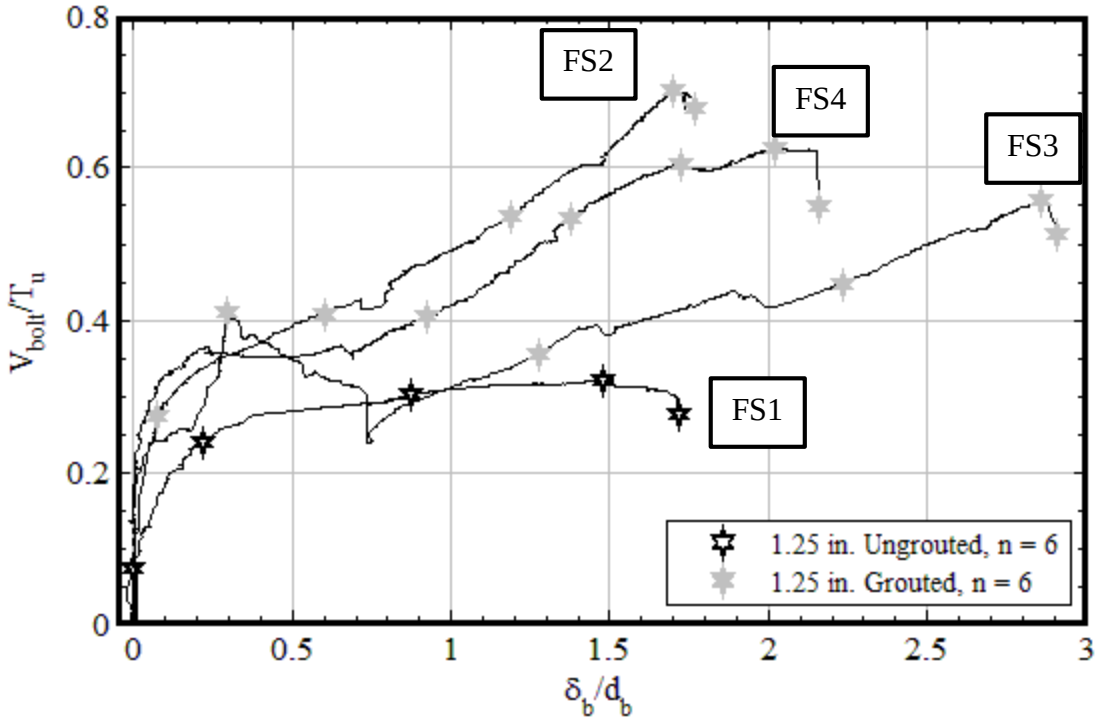

Figure 5-7. Load-displacement behavior of Phase 3 tests

Figure 5-8 shows the displaced anchor bolts in ungrouted test FS1. While bolts were fully pretensioned using the turn-of-the-nut method, significant leveling nut rotation on the order of that observed in the non-pretensioned Phase 2 test T4 occurred. As discussed in Section 5.3, it is expected that leveling nut rotation may produce slightly higher failure load values and higher end-of-test stiffness than a fully rigid (rotationally) leveling nut.

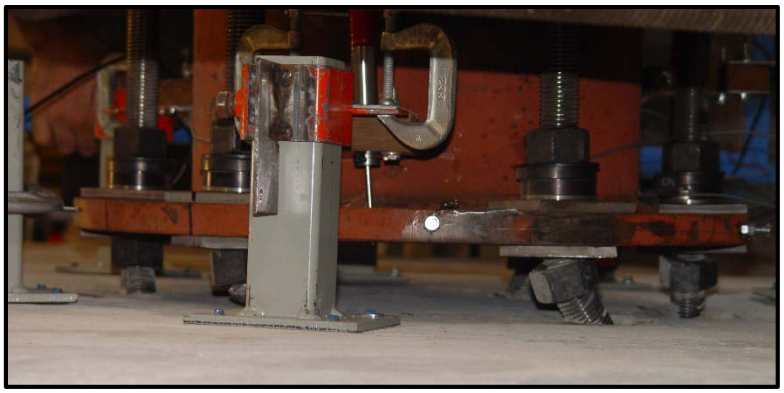

Figure 5-8. FS1 anchor bolts in failed condition

Figure 5-9 displays in-test grout pad cracking and post-test top views of the grout pads for tests FS2, FS3, and FS4. With the connection oriented 90 degrees to its in-service condition (i.e.,

anchor bolts parallel to the floor), fragments of grout material outside of the bolt circle fell away during post-test removal of the loading assembly. Remaining grout outside of the bolt circle was manually removed, explaining its absence in the top views.

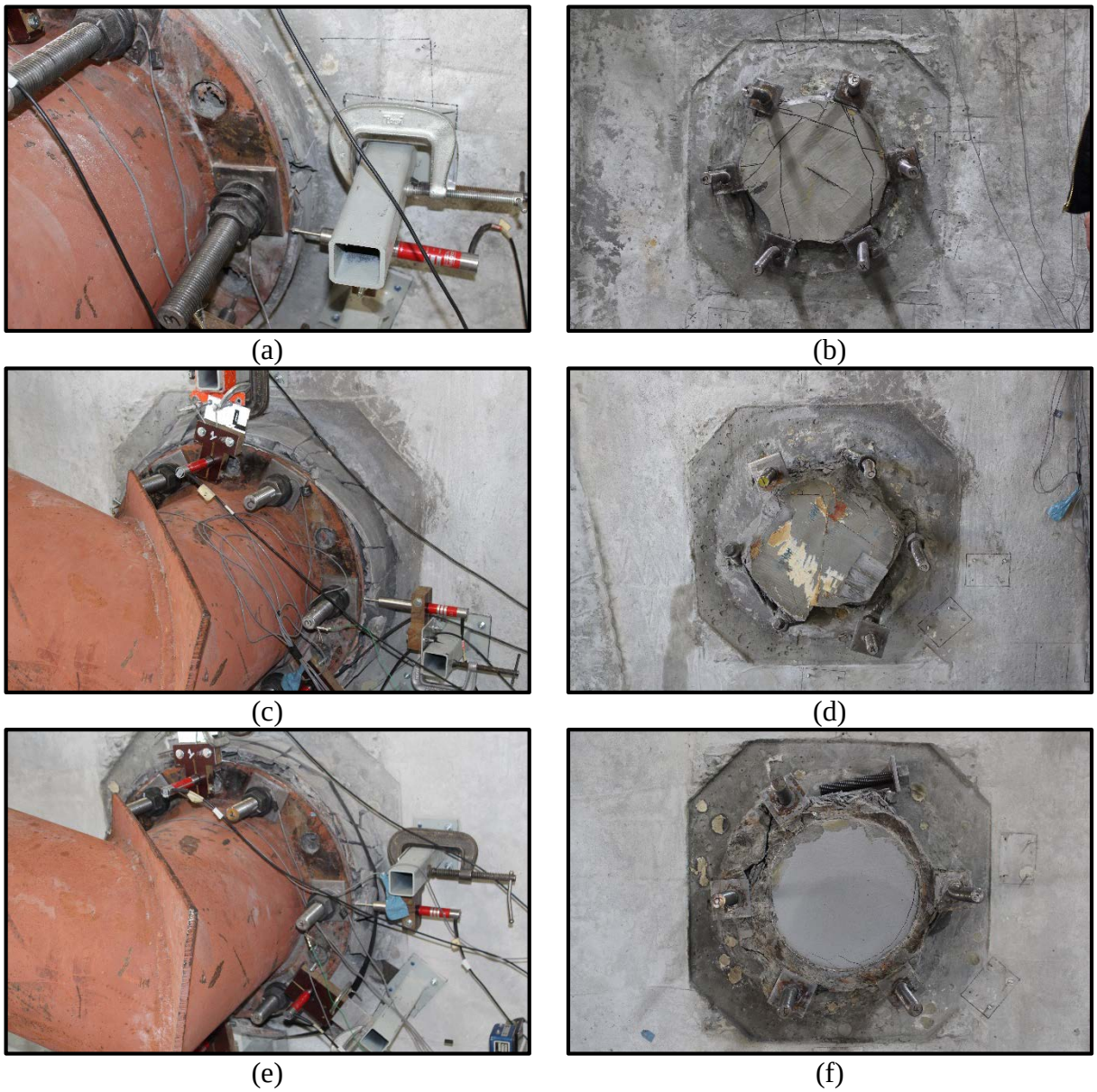

(a) (b) (c) (d) (e) (f)

Figure 5-9. (a, c, e) In-test grout cracking and (b, d, f) post-test grout surfaces for FS2, FS3, and FS4

Displacements corresponding to ultimate load from the three vertically oriented (parallel to anchor bolts) and two horizontally oriented (orthogonal to anchor bolts) LVDTs arranged according to Figure 4 22 are provided in Table 5 7. Load vs. vertical and horizontal LVDT

displacements are provided for every test in Appendix C. Positive values for vertical LVDTs indicate base plate movement toward the concrete at a given location. Positive readings for H1 and H2 indicate upward and rightward base plate movement, respectively. The greatest vertical and horizontal displacements were observed in FS3, which also experienced the greatest overall displacement. In contrast to the Phase 2 ungrouted stand-off test T2-B, the ungrouted stand-off test FS1 showed relatively large downward displacements, which were restrained in the grouted counterpart FS2.

Table 5-7. Vertical and horizontal base plate displacements (in.) in Phase 3 tests

Test	V1	V2	V3	V Average	H1	H2
FS1	0.103	0.182	0.039	0.108	0.279	0.101
FS2	0.048	-0.015	-0.010	0.008	0.215	-0.138
FS3	0.342	0.209	0.185	0.245	0.335	0.050
FS4	0.191	0.069	-0.019	0.080	0.190	0.006

5.5 General Discussion

5.5.1 General Behavior

Flush-mounted tests displayed initial linear-elastic behavior until concrete spalling at the bearing side of the anchor bolt, after which stiffness degraded continuously until ultimate load was reached. Anchor bolt failure surfaces were smooth, indicating predominantly shear slipping of the steel lattice on the material level. Hole oversize effects were pronounced in flush-mounted tests; this is discussed in Sections 5.3 and 5.5.3.

Ungrouted stand-off base plates contained linear-elastic initial behavior until bolt yielding and concrete spalling, where stiffness degraded into an extended plastic phase of behavior through ultimate load. Anchor bolts failed predominantly below the leveling nut, sometimes sharing failure between this location and at the concrete surface. Failure planes were rough, clearly showing tensile rupture and a demarcation between locations of tension and compression fields from bending over the bolt cross-section. Test method contributions to behavior are discussed in the ensuing section.

Grouted stand-off base plate tests exhibited markedly different behavior than their flush-mounted equivalents. Initial behavior in all cases was extremely stiff until the bond between grout pads and the surface of the concrete was overcome, engaging the anchor bolts in shear at approximately $0.1T_u$. A phase of stiffness roughly equivalent to the linear-elastic portion of flush-mounted tests in Figure 5-1 commenced, ending in grout cracking. At this point, behavior diverged between tests within both Phase 2 and Phase 3. T5 and FS2, which contained the lower levels of stand-off within their respective phases, transitioned smoothly into an approximately linear inelastic range, the stiffness degrading only moderately until failure. Tests T6-A, T6-B, FS3, and FS4, those containing higher levels of stand-off within their respective phases, were split equally into two distinct patterns of behavior. Shortly after grout cracking, T6-B and FS4

entered a phase of stiffness approximately parallel to the ungrouted $4d_b$ stand-off test, T3. Following significant deformation, these tests transferred into a final phase of elevated stiffness leading to ultimate load. T6-A and FS3, however, contained another phase of increased stiffness and associated strength gain immediately following grout cracking, reaching local maxima and subsequently losing load until displacements roughly equivalent to transition into a the final phase of elevated stiffness observed in tests T6-B and FS4. It is believed that while the base plate rotated the grout pad restrained downward displacement of the base plate, enabling the anchors to develop axial strains as well as flexural strains and shear strains as they became more inclined. The tension in the inclined anchors then contributed to shear capacity in two ways. The vertical "clamping" component of the anchor tension provided a friction force at the interface while the horizontal component provided direct resistance to the shear. The resulting increase in shear strength is then the result of the combined effects of the friction from the vertical component of the tension, the horizontal component of the tension, the anchor bending, and the anchor shear strength. These resulting effects of the grout pad at large base plate rotations generated significant additional connection stiffness and strength until anchor bolt rupture, which occurred below the leveling nut in all cases except for test T3, in which failure occurred at the interface between the base plate and the grout pad. Post-cracking stiffness observed in T6-A and FS3 may have been caused by interlock between cracked grout pieces that, when overcome, caused the tests to retrograde to the baseline behavior observed in T6-B and FS4 equivalents. The ultimate loads of all grouted tests ranged from approximately $0.55T_u$ to $0.7T_u$, all above the ACI (2011) ultimate strength $0.48T_u$ resulting to an 0.8 factor applied to the $0.6T_u$ shear strength. These results suggest that the ACI (2011) factor is conservative and appropriate as a design basis.

5.5.2 Experimental Method Comparisons

Figure 5-10 compares the behavior of direct shear and torsion tests. Note that direct shear tests contained tight holes and bolts were not pretensioned, while torsion tests contained oversize holes and turn-of-the-nut bolt pretension. Flush-mounted torsion tests T1-A and T1-B exhibited nearly identical load-displacement behavior to flush-mounted Phase 1 tests (dataset DS1) aside from initial slip in their 30% oversize holes.

In ungrouted stand-off base plate tests, slip through oversize holes and differences in ultimate load were less pronounced than in flush-mounted tests. Stiffnesses in the inelastic phase of single-bolt $2d_b$ and $4d_b$ stand-off direct shear tests are observably higher than in the torsion tests due to the deflected geometry of the direct shear test setup, discussed in detail in Section 5.2. Double-bolt direct shear test behavior (DS8 tests), however, closely resembled that seen in torsion tests. Because the magnitudes of ultimate load were commensurate between Phase 1 and Phase 2 equivalents, it is believed that Phase 1 ultimate load values are applicable to the shear strength of field-installed annular base plate connections and valid for comparison.

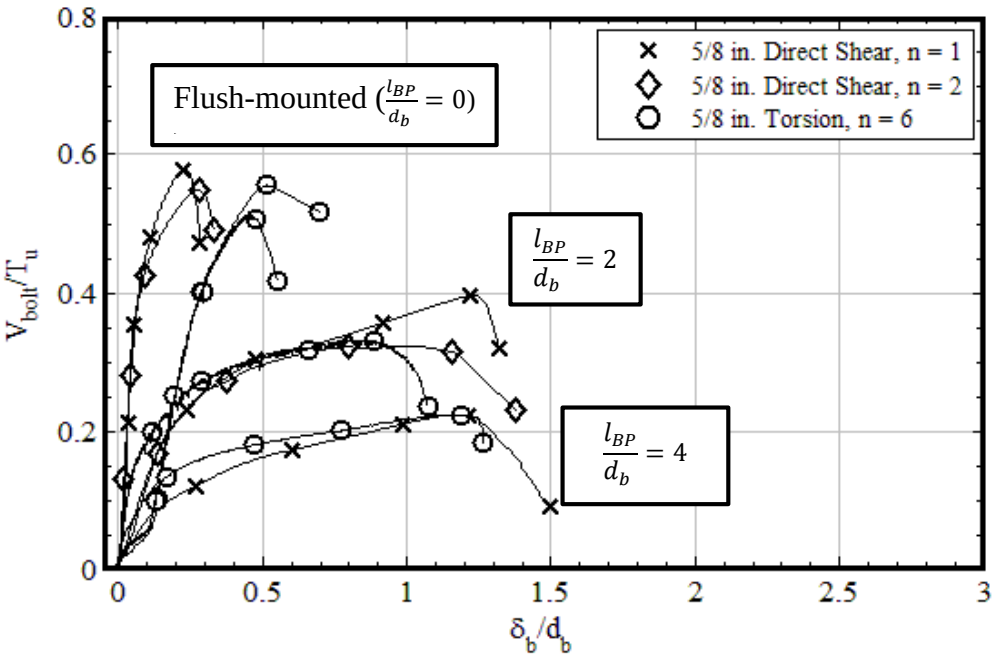

Figure 5-10. Comparisons between Phase 1 and Phase 2 ungrouted load-displacement behavior

5.5.3 Effect of Minor Test Variables

While the interaction of minor test variables cannot be quantified without further investigation, inferences of their impact on testing can be gleaned from observation of failure load and load-displacement behavior. Potential contributions to the results from the study's major test variables of stand-off distance and connection type were identified for the following minor study variables.

- **Test Method.** Refer to the discussion in Section 5.5.2.
- **Hole Oversize.** Flush-mounted torsion tests with oversize holes (T1-A and T1-B) showed obvious slip through the hole oversize in the early stages of the tests. As discussed in Section 5.3, flush-mounted shear strength may be adversely affected by unfavorable anchor bolt positioning within oversize holes. The lower value observed in test T1-B ($0.51T_u$) is in good agreement with the AASHTO (2013a) commentary recommendation for a 0.8 factor for oversize holes. While evidence of slip is seen in load-displacement curves for stand-off tests, especially the non-pretensioned T4 test, no adverse effects from hole oversize on ultimate strengths were observed in stand-off base plate tests.
- **Anchor Bolt Diameter.** Aside from flush-mounted 5/8 in. torsion tests (see hole oversize discussion), ultimate loads normalized by respective T_u values were comparable between equivalent ungrouted stand-off tests with 5/8 in. and 1 in. diameter bolts. Thus, it is concluded that the results are representative of the full range of anchor bolt diameters in ungrouted annular base plates. Grouted tests with 5/8 in. and 1.25 in. diameter bolts exhibited similar load-displacement behavior at comparable stand-off distances.
- **Bolt Pretensioning.** Refer to the discussion in Section 2.2.1.
- **FRP Grout Pad Retrofit.** Refer to the discussion in Section 5.3

Other variables inherent in the testing including base plate thickness and straight-line (Phase 1) vs. circumferential (Phases 2 and 3) in-test displacement, were determined to have had minimal impact on the results.

5.5.4 Comparisons to Existing Codes

Equations within this section are expressed for an individual bolt positioned for worst-case values of tension and resolved shear within a stand-off base plate exposed to global shear (V_{group}), overturning moment (M_{group}), torsion (T_{group}), and axial (N_{group}) forces.

AASHTO (2013b) states that anchor bolt exposed lengths may be accounted for using a model of a doubly moment-restrained beam free to displace laterally and axially, placing resulting axial stresses from secondary bolt bending into the axial stress component as shown in Equation (5-7) for tension. This method is applied to both ungrouted and grouted base plates with l_{LN} greater than one bolt diameter. Equations (5-7) through (5-12) demonstrate a conservative interpretation of this method for the steel strength of anchor bolts in annular base plates.

$$\left(\frac{f_{t,1} + f_{t,2}}{F_t}\right)^2 + \left(\frac{f_v}{F_v}\right)^2 \leq 1 \tag{5-7}$$

$f_{t,1}$ is defined as the individual bolt tensile stress from global equilibrium, conservatively assumed to be oriented perpendicular to the axis of overturning moment in Equation (5-8), while $f_{t,2}$ is defined as the individual bolt tensile stress produced by bolt bending over the exposed length as shown in Equation (5-10). f_v is simply equal to a shear force per bolt, V_{bolt}, taken as the highest possible shear force on an individual anchor bolt as shown in Equation (5-12), divided by the effective shear area, A_{se}.

$$f_{t,1} = \frac{M_{group}}{S_{group}} + \frac{N_{group}}{(n)(A_{se})} \tag{5-8}$$

$$S_{group} = \frac{n * r_{group}}{2} \tag{5-9}$$

$$f_{t,2} = \frac{m_2}{S_{bolt}} \tag{5-10}$$

$$m_2 = \frac{V_{bolt} l_{LN}}{2} \tag{5-11}$$

$$V_{bolt} = \frac{V_{group}}{n} + \frac{T_{group}}{(r_{group})(n)} \tag{5-12}$$

where $f_{t,1}, f_{t,2}, f_v, M_{group}, N_{group}, V_{group}, T_{group}, V_{bolt}, A_{se}$ are defined in the text above
F_t = tensile stress capacity of bolt material
F_v = shear stress capacity of bolt material
S_{group} = section modulus of the bolt group
n = number of bolts in the group
r_{group} = radius of the bolt group
m_2 = bolt-level moment produced by V_{bolt} acting over l_{LN}
S_{bolt} = section modulus of the bolt = $\pi d_b^3/32$
l_{LN} = distance between the concrete surface and the bottom of the leveling nut

The implementation of these equations into FDOT design guidelines is provided in Appendix D. For comparison to test data in this section, F_t is taken as the measured ultimate strength $F_{u,t}$, F_v is taken as $0.6F_{u,t}$ in accordance with AASHTO (2013a) and AASHTO (2013b), and S_{bolt} is replaced by Z_{bolt}, the plastic section modulus of the bolt, which is equal to $d_b^3/6$. Solving for V_{bolt} using Equations (5-7) through (5-12) and subsequent definitions yields the predicted shear capacity value, $V_{u,predicted}$, given in Equation (5-13), noting that $f_{t,1} = 0$ for the test data.

$$V_{u,predicted} = F_{u,t}\sqrt{\frac{1}{\frac{l_{LN}^2}{4{Z_{bolt}}^2} + \frac{1}{0.36A_{se}^2}}} \tag{5-13}$$

For grouted base plates, the ACI 318 (2011) 0.8 shear strength reduction factor results in $F_{v,GR} = (0.8)(0.6)$ and, thus, Equation (5-14). With $f_{t,1} = 0$, the predicted strength value reduces to $V_{u,predicted} = 0.48A_{se}F_{u,t}$.

$$\left(\frac{f_{t,1}}{F_t}\right)^2 + \left(\frac{f_v}{F_{v,GR}}\right)^2 \leq 1 \tag{5-14}$$

Table 5-8 provides mean values for each experimental dataset against AASHTO (2013b) predicted ultimate values and proposed modifications. Proposed modifications to AASHTO (2013b) used in Table 5-8 are as follows:

- The AASHTO (2013b) beam bending methodology given in Equation 3 is applied to all ungrouted tests with exposed anchor bolt length.
- The AASHTO (2013a) 0.8 shear resistance reduction factor for oversize holes is applied to F_v for ungrouted stand-off base plate tests.
- Grouted tests are treated as flush-mounted (i.e., no bolt bending considerations) with the ACI (2011) 0.8 shear strength reduction factor and no additional reduction factor for oversize holes.

In Figure 5-11, ungrouted results are shown superimposed by AASHTO (2013b) code-predicted ultimate strength and two predictive curves for all values of l_{LN} using Equation (5-13) with $F_v = 0.6F_{u,t}$ (Tight Holes) and $F_v = 0.48F_{u,t}$ (Oversize Holes; replace $0.36A_{se}^2$ with $0.23A_{se}^2$), respectively. Figure 5-12 shows grouted test results against the AASHTO code-predicted ultimate strength and the ACI (2011) predicted ultimate strength. Figure 5-13 normalizes ungrouted results by the AASHTO (2013b) code-predicted strength and Figure 5-14 normalizes ungrouted test results by the applicable proposed modifications for each test. In Figure 5-11 and Figure 5-12, separate x-axes are given for l_{BP} and l_{LN}. However, because the difference between l_{BP} and l_{LN} is defined by the combined thickness of the leveling nut and leveling washer, exposed lengths of DS9 and T8-10 and stand-off distances for full-scale results are not properly reflected by the figures. Refer to Figure 5-7 for these values. The results indicate that significant strength reduction occurs at *all* stand-off distances. The beam model from AASHTO (2013b) accounting for bending stresses in calculating shear strength of anchor bolts is a good model for the experimental results. It is believed that the more conservative predictions at higher stand-off do not account for additional tensile component strength pickup from the angle

of the deflected bolt. Grouted results all contained strengths above the ACI (2011) ultimate strength, showing no trends between the stand-off distances tested.

Table 5-8. Comparisons between results, AASHTO (2013b), and proposed ultimate strengths

Phase	Set	$\frac{l_{BP}}{d_b}$	$\frac{l_{LN}}{d_b}$	$\frac{F_v}{F_T}$ (proposed)	$V_{u,bolt}$ (kip)	AASHTO (Code-Specified)		AASHTO (Proposed Modifications)	
						$V_{u(6)}$ (kip)	$\frac{V_{u,bolt}}{V_{u(6)}}$	$V_{u,proposed}$ (kip)	$\frac{V_{u,bolt}}{V_{u,proposed}}$
1	DS1	0	na	0.6	12.3	12.7	0.97	12.7	0.97
1	DS2	1.2	0	0.6	11.3	12.7	0.89	12.7	0.89
1	DS3	1.6	0.4	0.6	9.8	12.7	0.77	10.6	0.93
1	DS4	2	0.8	0.6	7.9	12.7	0.62	7.7	1.03
1	DS5	3	1.8	0.6	5.6	12.7	0.44	4.0	1.38
1	DS6	4	2.8	0.6	4.4	2.7	1.65	2.7	1.65
1	DS7	0	na	0.6	11.4	12.7	0.90	12.7	0.90
1	DS8	2	0.75	0.6	6.9	12.7	0.55	7.7	0.90
1	DS9	0	na	0.6	33.5	33.5	1.00	33.5	1.00
1	DS12	0	na	0.6	12.2	12.7	0.96	12.7	0.96
1	DS13	2	0.8	0.6	9.2	12.7	0.73	10.6	1.20
1	DS14	4	2.8	0.6	5.1	2.7	1.90	2.7	1.90
2	T1	0	na	(0.8[a])(0.6)	11.1	12.4	0.89	10.0	1.11
2	T2	2	0.8	(0.8[a])(0.6)	6.5	12.4	0.52	6.8	0.95
2	T3	4	2.8	(0.8[a])(0.6)	4.6	2.6	1.75	2.6	1.77
2	T4	2	0.8	(0.8[a])(0.6)	7.4	12.4	0.59	6.8	1.08
2	T5	2	0.8	(0.8[b])(0.6)	10.9	12.4	0.88	10.0	1.10
2	T6	4	2.8	(0.8[b])(0.6)	13.1	2.6	4.95	10.0	1.31
2	T7	4	2.8	(0.8[b])(0.6)	14.8	2.6	5.61	10.0	1.49
2	T8	0	na	(0.8[a])(0.6)	31.7	33.5	0.95	26.8	1.18
2	T9	2	0.75	(0.8[a])(0.6)	18.0	33.5	0.54	18.7	0.97
2	T10	4	2.75	(0.8[a])(0.6)	10.5	7.3	1.45	7.2	1.47
3	FS1	2.3	1	(0.8[a])(0.6)	27.1	26.9	1.01	25.0	1.08
3	FS2	2.3	1	(0.8[a])(0.6)	59.1	26.9	2.19	40.5	1.46
3	FS3	4.3	3	(0.8[a])(0.6)	46.9	10.4	4.52	40.5	1.16
3	FS4	4.3	3	(0.8[a])(0.6)	52.8	10.4	5.08	40.5	1.30

[a]reduction factor for oversize holes per AASHTO (2013a)
[b]reduction factor for grouted base plates per ACI (2011)

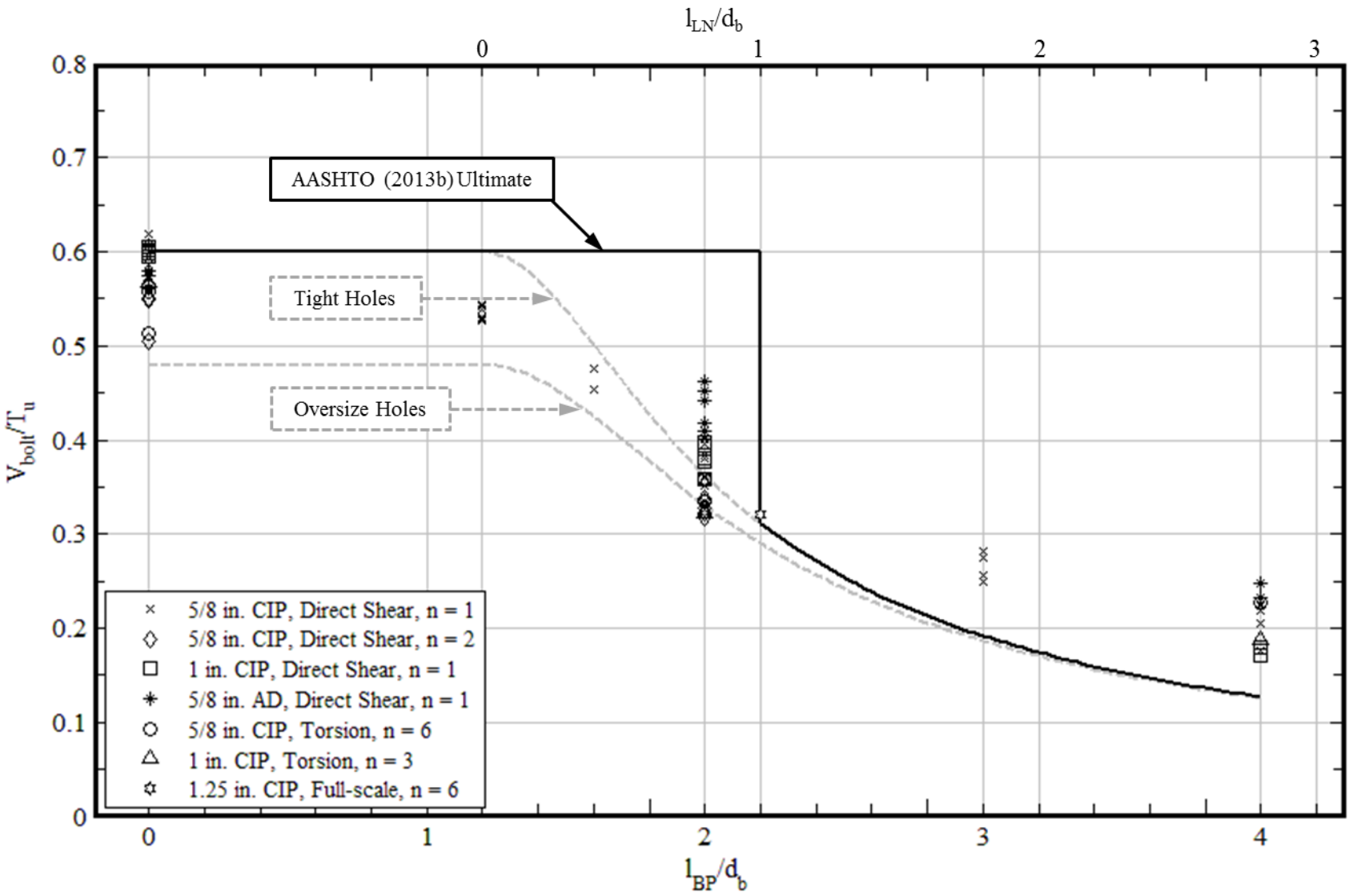

Figure 5-11. Summary of all ungrouted test results

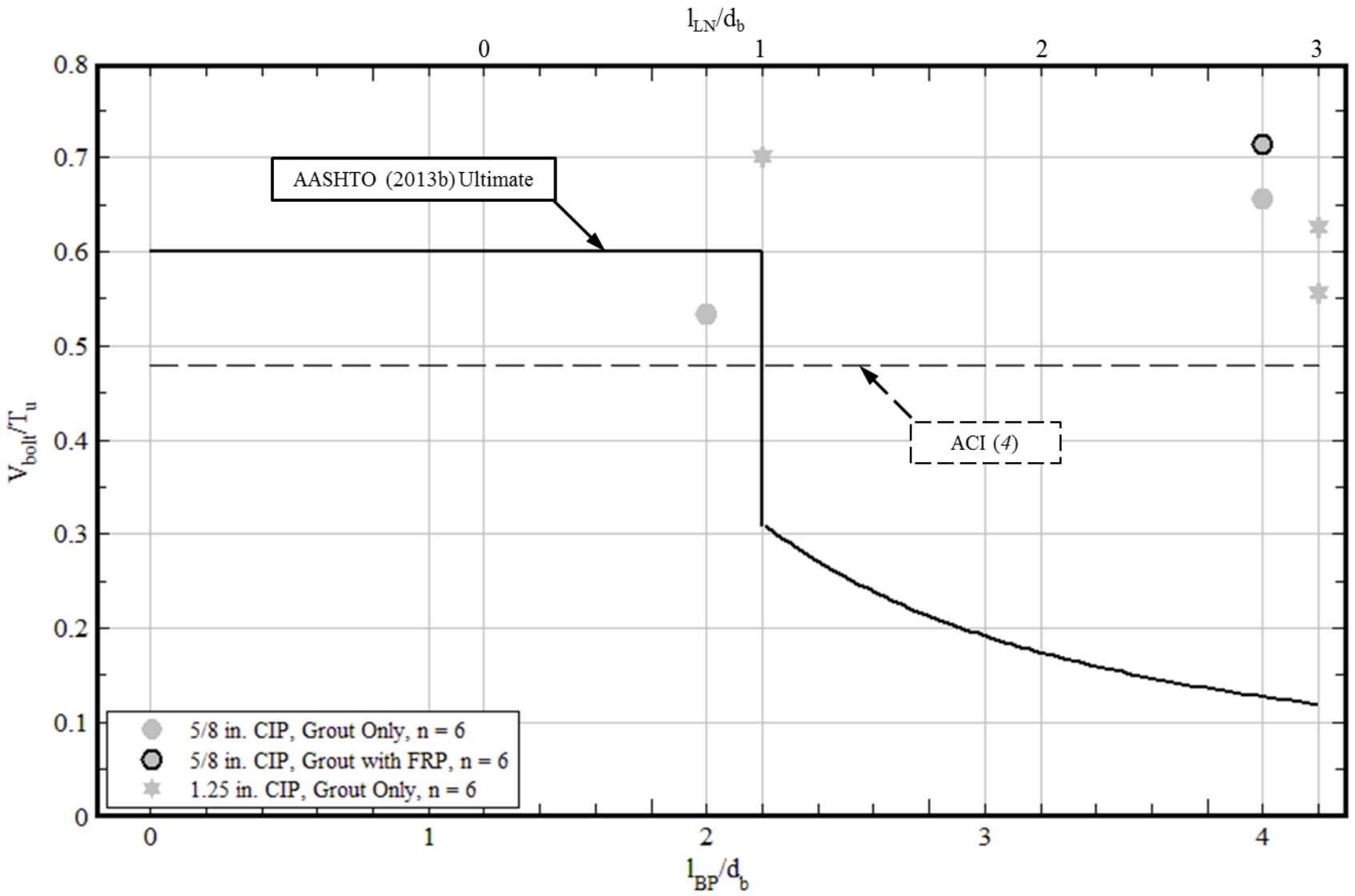

Figure 5-12. Summary of all grouted test results

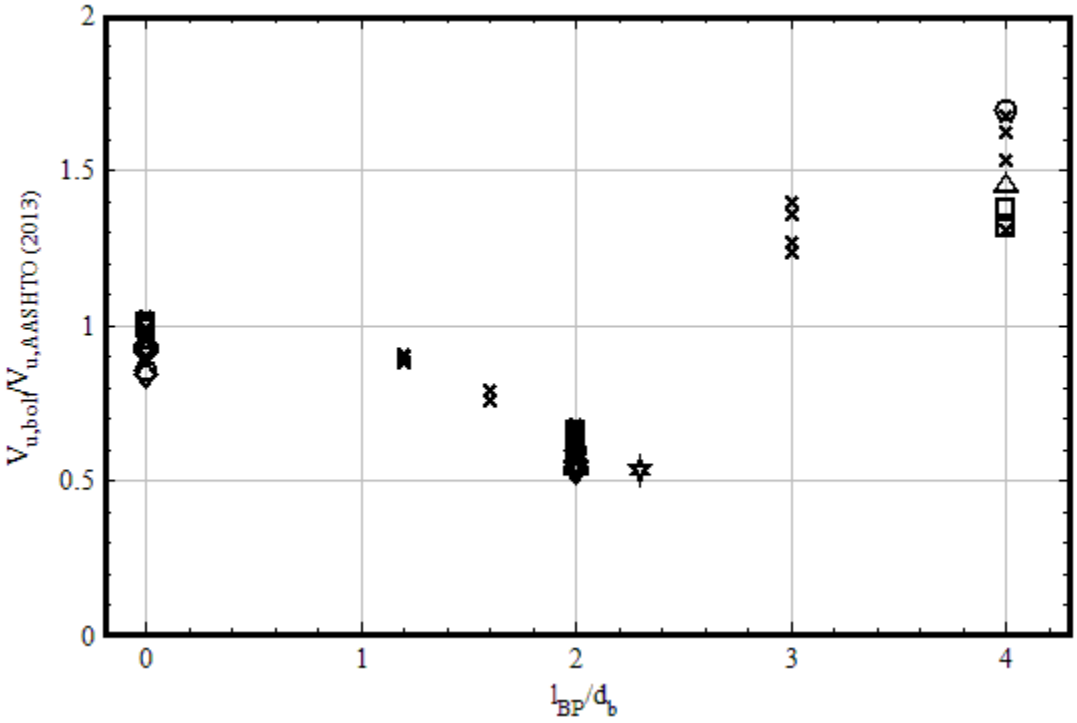

Figure 5-13. Summary of ungrouted results normalized by AASHTO (2013b) ultimate strength

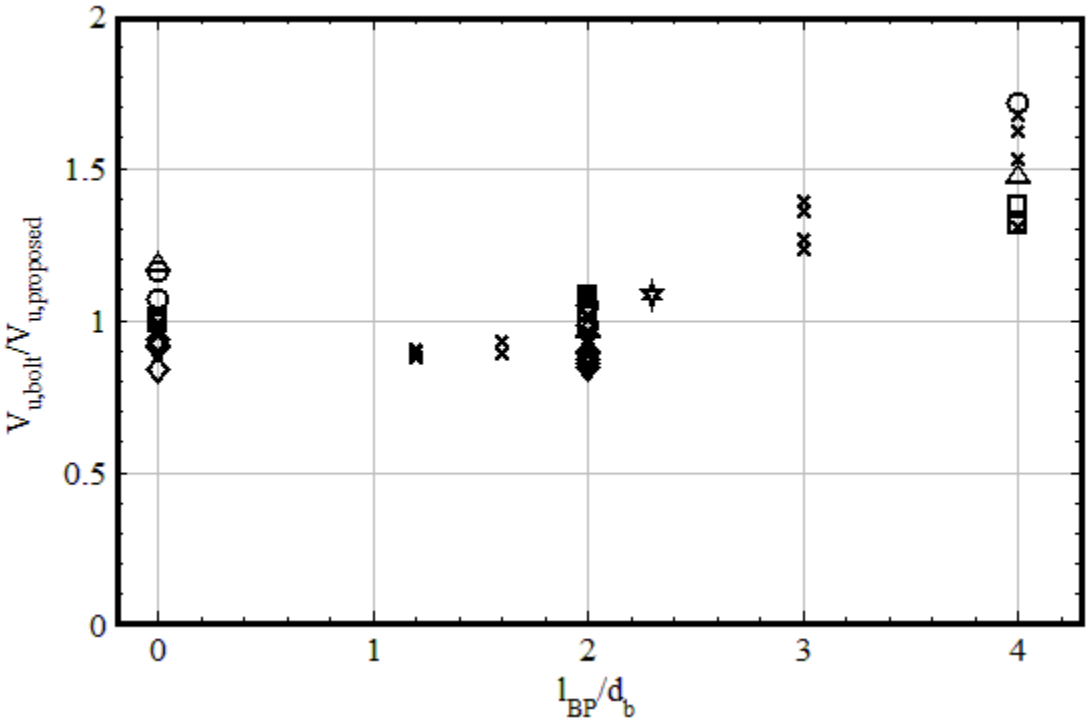

Figure 5-14. Summary of ungrouted results normalized by proposed ultimate strength

CHAPTER 6
SUMMARY, CONCLUSIONS, AND RECOMMENDATIONS

6.1 Summary

Anchor bolts in stand-off base plates connecting cantilever sign and signal structures to concrete may experience high shear load, which acts over the stand-off distance and produces bolt bending stresses in addition to shear stresses. In existing standards, anchor bolt steel strength in ungrouted stand-off base plates is either not accounted for explicitly (AISC 2010 and ACI 2011) or built with unconservative assumptions for certain conditions (AASHTO 2013b). Grout contributions to strength are not allowed in the design of double-nut connections (AASHTO 2013b), left to the user to account anchor bolt bending (AISC 2011), or used as a basis for adjustment with a simple reduction factor compared to flush-mounted connections (ACI 2011).

The study reported herein studied the steel shear strength and behavior of anchor bolts in ungrouted and grouted stand-off base plate connections to concrete with emphasis on double-nut connections seen in annular base plates for sign and signal structures. Three phases of experimental testing were undertaken studying various parameters relevant to such connections.

In Phase 1, direct shear methodology was employed to establish relationships between stand-off distance and ultimate steel shear strength. Influences from installation method (cast-in-place vs. adhesive anchors) and number of bolts (single- vs. double-bolt connections) on bolt steel strength in stand-off base plates were also investigated. All anchor bolts in Phase 1 were finger-tightened and installed in holes without oversize. Statistically significant differences were found between anchor bolts at *all* levels of stand-off distance, including within the permissible range by AASHTO (2013b) for ignoring strength reductions caused by bolt bending. Adhesive anchors were found to be slightly statistically stronger than cast-in-place anchors. Minor differences in the behavior, but not the strength, of double-bolt vs. single-bolt tests attributable to

a roller used to restrain base plate rotation in single-bolt but not double-bolt tests were observed. The slightly different behavior, however, did not translate to differences in ultimate strength.

Phase 2 comprised evaluation of ungrouted and grouted circular groups of 5/8 in. and 1 in. diameter anchor bolts in a torsion testing approach. Stand-off distance, influence of grout, bolt pretensioning, size effect, and the presence of a fiber-reinforced polymer (FRP) wrap were investigated for their influence on strength and behavior. In contrast to Phase 1, tests were run with "shear hole" oversize values provided in AASHTO (2013b) and nuts were tightened with the turn-of-the-nut method (one-third turn past snug-tight). The strength of flush-mounted torsion tests were slightly less than direct shear counterparts, which was attributed to anchor bolt placement within the oversize holes in Phase 2. Stand-off base plate tests contained ultimate load values similar to Phase 1 equivalents, with behavior more closely resembling Phase 1 double-bolt tests. Grouted tests contained higher shear strengths than the ACI (2011) ultimate load value but at considerable displacements that may not be serviceable. In the three grouted tests run, no difference in ultimate strength was observed between two stand-off distances. However, different load displacement behavior was observed, with much greater displacement and pronounced phases of load-displacement behavior in the two tests run at higher stand-off. A single test conducted with an FRP retrofit around the perimeter of the grout pad and the base plate exhibited the highest strength of all tests in the study at significantly lower displacements than other grouted tests, resulting in shear failure of the anchor bolts at the top of the grout pad surface.

Phase 3 contained four full-scale tests containing circular groups of six 1.25 in. diameter bolts, three with grout pads and one left ungrouted. Two tests were conducted at the AASHTO (2013b) maximum permissible leveling nut stand-off distance (exposed length) of one bolt diameter between the concrete surface and the bottom of the leveling nut, one ungrouted (FS1)

and one grouted (FS2). The final two tests contained a more extreme exposed length of three bolt diameters. The effects of a circular vs. annular grouted base plate were studied by removing a concentric circle from the circular base plate (used in FS1-FS3) in the final test (FS4). Similar reduction in the strength was seen in the ungrouted test FS1 to Phase 1 and Phase 2 results. Grouted test behavior and strength were consistent with Phase 2 tests, even in the annular base plate (all Phase 2 tests contained a circular base plate). It was determined that results from both phases are valid representations of field annular base plate connections.

6.2 Conclusions

Results from the study lead to the following conclusions:

- *All* values of base plate stand-off distance in ungrouted double-nut connections result in reduced steel shear strength of the anchor bolts relative to the exposed length of the anchor bolt between the concrete surface and the bottom of the leveling nut. The AASHTO (2013b) allowance for ignoring bolt bending for exposed lengths less than one bolt diameter is unconservative in predicting ultimate strength in ungrouted stand-off base plates. The beam bending model given by AASHTO (2013b) suggested for greater values of exposed length is appropriate for exposed lengths of at least three anchor bolt diameters.

- The AASHTO (2013a) group connection reduction factor of 0.8 is appropriate for ungrouted flush-mounted and stand-off base plate tests.

- Properly installed nonshrink grout pads significantly increase the steel shear capacity of anchor bolts in stand-off base plates, albeit at high levels of connection deformation. The ACI (2011) anchor bolt shear strength reduction factor of 0.8 for anchor bolt steel shear strength in grouted stand-off base plates compared to flush-mounted base plates is conservative. Existing AASHTO (2013b) specifications stating that a grout pad shall not be factored in the strength of the connection may be overly conservative.

- Adhesive anchors are at least as strong and stiff as cast-in-place anchors in stand-off base plates under short-duration static shear loading.

- While the absence of pretensioning in a double-nut connection allows slip at low levels of load, ultimate loads not affected.

- An adequately designed FRP wrap around *both* the grout pad and the base plate perimeter restricts grout pad crack propagation, returning the steel shear strength of anchor bolts to at least the flush-mounted shear strength.

6.4 Design and Maintenance Recommendations

It is recommended that AASHTO (2013b) be modified to mandate that anchor bolt bending stresses be included in its beam bending model to anchor bolts in *all* ungrouted annular stand-off connections as in Equation (5-7) and to explicitly apply the 0.8 shear strength reduction factor for hole oversize from AASHTO (2013a) to F_v in Equation (5-7).

The application of Equation (5-14) for the steel strength of anchor bolts in grouted annular base plate is recommended for properly installed high-strength nonshrink grout pads with a thickness of up to four nominal anchor bolt diameters.

Retrofit installation of properly installed high-strength nonshrink grout pads is recommended below all existing cantilever sign and signal supports with ungrouted annular stand-off base plates with grout pads satisfying Equation (5-14). In such structures where it is undesirable to install a grout pad, it is recommended that the steel strength of the anchor bolts be reevaluated using Equation (5-7) and retrofitted/lowered/reinstalled as necessary.

Draft FDOT Design Guidelines are presented in Appendix D. Draft FDOT Maintenance Guidelines are presented in Appendix E.

6.5 Recommendations for Future Work

The following recommendations are made for future work related to the steel strength of anchor bolts in stand-off base plate connections:

- Development of an expanded model for the steel shear strength of anchor bolts in ungrouted stand-off base plates using an adjusted effective exposed length and accounting for secondary geometry of anchor bolts.
- Stand-off anchor bolt group steel strength tests under combined loading (producing varying levels of tension and shear forces on anchor bolts) and with different bolt configurations (e.g. rectangular patterns).
- Investigation of the influence of anchor bolt material strength and ductility.

- Investigation of the effects of concrete strength on the steel strength of anchor bolts in stand-off base plates.

- Investigation of the influence of various grout pad parameters on anchor bolt steel strength including grout pad height, edge distances, strength, and influence of dry-packing vs. formed methods.

- Further testing on FRP retrofits on grouted base plate connections, particularly with rectangular base plates and investigating the effects of different levels of coverage (e.g. only on the grout pad).

REFERENCES

Adihardjo, R. and Soltis, L. (1979). "Combined shear and tension on grouted base details." *AISC Engineering Journal*, 16(1), 23-26.

American Association of State Highway and Transportation Officials (AASHTO). (2013a). *LRFD bridge design specifications*, 6th Ed., AASHTO, Washington, DC.

American Association of State Highway and Transportation Officials (AASHTO). (2013b). *Standard specifications for structural supports for highway signs, luminaires and traffic signals (LTS-6)*, 6th Ed., AASHTO, Washington, DC.

American Concrete Institute (ACI). (2011). *Building code requirements for structural concrete and commentary*, ACI 318-11, ACI, Farmington Hills, MI.

American Institute of Steel Construction (AISC). (2010). *Steel construction manual*, 14th Ed., AISC, Chicago, IL.

ASTM. (2010a). "Standard test method for compressive strength of grouts for preplaced-aggregated concrete in the laboratory." *C942-10*, ASTM, West Conshohocken, PA.

ASTM. (2010b). "Standard test method for flow of grout for preplaced-aggregate concrete (flow cone method)." *C939-10*, ASTM, West Conshohocken, PA.

ASTM. (2010c). "Standard test method for strength of anchors in concrete elements." *E488/E488M-10*, ASTM, West Conshohocken, PA.

ASTM. (2011). "Standard specification for determining the mechanical properties of externally and internally threaded fasteners, washers, and rivets." *F606-11*, ASTM, West Conshohocken, PA.

ASTM. (2012). "Standard test method for compressive strength of hydraulic cement mortars (using 2-in. or [50-mm] cube specimens)." *C109-12*, ASTM, West Conshohocken, PA.

Chesson, E., Faustino, N. L., and Munse, W.H. (1965). "High-strength bolts subjected to tension and shear." ASCE *Journal of the Structural Division*, 91(ST 5) 155-180.

Cook, R. A. (1989). "Behavior and design of ductile multiple-anchor steel-to-concrete connections." Ph.D. Dissertation, University of Texas at Austin, Austin, TX.

Cook, R. A. and Bobo, B. J. (2001). "Design guidelines for annular base plates." *FDOT Report BC354-04*, FDOT, Tallahassee, FL.

Cook, R. A. and Dalton, S. A. (2011). "Base connections for signal/sign structures." *FDOT Report BDK75 977-32*, FDOT, Tallahassee, FL.

Cook, R. A., Ellifritt, D. S., Schmid, S. E., Adediran, A., and Beese, W. (1995). "Design procedure for annular base plates." *FDOT Report 0510697*, FDOT, Tallahassee, FL.

Cook, R. A. and Halcovage, K. M. (2007). "Anchorage embedment requirements for signal/sign structures." *FDOT Report BD545-54*, FDOT, Tallahassee, FL.

Cook, R. A.,and Jenner, K. L. (2010). "Alternative support systems for cantilever signal/sign structures." *FDOT Report BDK75 977-04*, FDOT, Tallahassee, FL.

Cook, R. A. and Klingner, R. E. (1992). "Ductile multiple-anchor steel-to-concrete connections." *Journal of Structural Engineering*, 118(6) 1645-1665.

Cook, R. A., Tia, M., Fisher, K. B., and Darku, D. D. (2000a). "Use of grout pads for sign and lighting structures part 2 – corrosion study." *FDOT Report BB-512*, FDOT, Tallahassee, FL.

Cook, R. A., Tia, M., Fisher, K. B., and Darku, D. D. (2000b). "Use of grout pads for sign and lighting structures part 1 – structural evaluation." *FDOT Report BB-512*, FDOT, Tallahassee, FL.

Dexter, R. J., and Ricker, M. J. (2002). "Fatigue-resistant design of cantilevered signal, sign, and light supports." *NCHRP Report 469*, National Cooperative Highway Research Program, Transportation Research Board of the National Academies, Washington, DC.

Eligehausen, R. and Balogh, T. (1995). "Behavior of fasteners loaded in tension in cracked reinforced concrete." *ACI Structural Journal*, 92(3), 365-379.

Eligehausen, R., Cook, R.A, and Appl, J. (2006a). "Behavior and design of adhesive bonded anchors." *ACI Structural Journal*, 103(6), 822-831.

Eligehausen, R., Mallée, R., and Silva, J. F. (2006b). *Anchorage in concrete construction*. Ernst & Sohn, Berlin, DE.

Federal Highway Administration (FHWA). (2002). *Guidelines for the installation, inspection, maintenance and repair of structural supports for highway signs, luminaries, and traffic signals*, U. S. Department of Transportation, Washington, DC.

Fisher, J. M. and Kloiber, L. A. (2006). *AISC Steel Design Guide 1: base plate and anchor rod design*, 2nd Ed., American Institute of Steel Construction, Chicago, IL.

Florida Department of Transportation (FDOT). (2007). Cantilever Overhead Sign Program (Version 5.1) [Software]. Available from http://www.dot.state.fl.us/structures/Programs/setupCantileverV5.1.exe

Fouad, F. H., Davidson, J. S., Delatte, N., Calvert, E. A., Chen, S. E., Nunez, E., and Abdalla, R. (2003). "Structural supports for highway signs, luminaires, and traffic signals." *NCHRP Report 494*, National Cooperative Highway Research Program, Transportation Research Board of the National Academies, Washington, DC.

Friberg, F. (1940). "Load and deflection characteristics of dowels in transverse joints of concrete pavements." Presented at the Highway Research Board 20th Annual Meeting.

Fuchs, W., Eligehausen, R., and Breen, J. (1995). “Concrete capacity design (CCD) approach for fastening to concrete.” *ACI Structural Journal*, 92(1), 73-94.

Gomez, I. R., Kanvinde, A. M., and Deierlein, G. G. (2011). “Experimental investigation of shear transfer in exposed column base connections.” *AISC Engineering Journal*, 48(4), 245-264.

Gresnigt, N., Romeijn, A., Wald, F., and Steenhuis, M. (2008) “Column bases in shear and normal force.” *HERON*, 53(1) 87-108.

Grosser, P. R. (2012). “Load-bearing behavior of anchorages subjected to shear and torsion loading in uncracked concrete.” Ph.D. Dissertation, University of Stuttgart, Stuttgart, DE.

Kaczinski, M. R., Dexter, R. J., and Van Dien, J. P. (1998). “Fatigue-resistant design of cantilevered signal, sign and light supports.” *NCHRP Report 412*, National Cooperative Highway Research Program, Transportation Research Board of the National Academies, Washington, DC.

Kulak, G. L., Fisher, J. W., and Struik, J. H. A. (1987). *Guide to design criteria for bolted and riveted joints*, 2nd Ed., American Institute on Steel Construction, Chicago, IL.

Lin, Z., Petersen, D., Zhao, J., and Tian, Y. (2011). “Simulation and design of exposed anchor bolts in shear.” *International Journal of Theoretical and Applied Multiscale Mechanics*, 2(2), 111-129.

Lotze, D., Klingner, R. E., and Graves III, H. L. (2001). “Static behavior of anchors under combinations of tension and shear loading.” *ACI Structural Journal*, 98(4), 525-536.

McMackin, P. J., Slutter, R. G., Fisher, J. W. (1973). “Headed steel anchor under combined loading.” *AISC Engineering Journal*, 10(2), 43-52.

Nakashima, S. (1998). “Mechanical characteristics of exposed portions of anchor bolts in steel column bases under combined tension and shear.” *Journal of Constructional Steel Research*, 46(1), 262-263.

Paulay, T. Park, R. Phillips, M. H. (1974). “Horizontal construction joints in cast-in-place reinforced concrete.” *ACI Special Publication 42-27.*

Scheer, J., Peil, U., and Nölle, P. (1987). “Screws under planned bending (in German).” Institut für Stahlbau, Braunschweig, DE.

Wallaert, J. J. and Fisher, J. W. (1965). “Shear strength of high-strength bolts.” *ASCE Journal of the Structural Division*, 91(ST3), 99-125.

Yura, J., Frank, K., and Polyzois, D. (1987). “High strength bolts for bridges.” *U.S. Department of Transportation Federal Highway Administration*, Washington, D.C.

APPENDIX A
LOAD-DISPLACEMENT BEHAVIOR OF PHASE 1 TESTS

This appendix contains the load-displacement behavior of Phase 1 tests. Tension load cell readings, while not necessarily representative of actual tensile stresses in the bolts, are also provided for 5/8 in. cast-in-place datasets DS1 through DS6. 1 in. bolt tests are presented together and adhesive anchor tests are superimposed with comparable datasets.

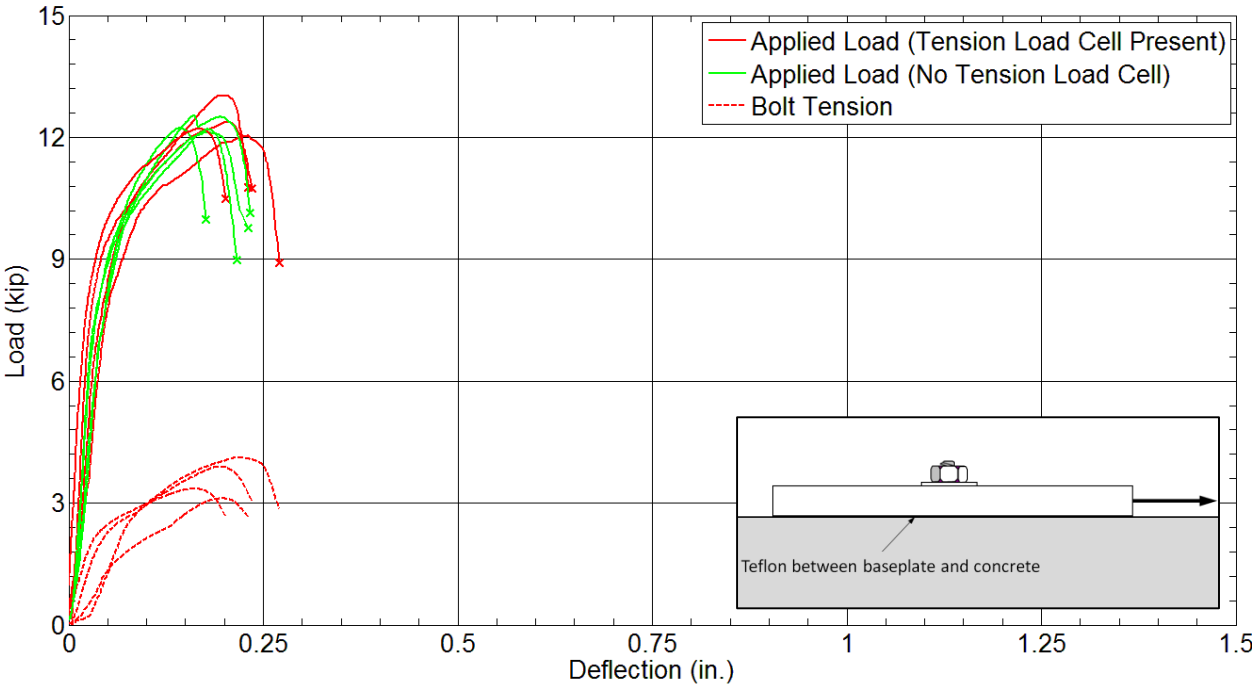

Figure A-1. DS1 (flush-mounted base plate, 5/8 in. bolts, n = 1) applied load and bolt tension vs. displacement

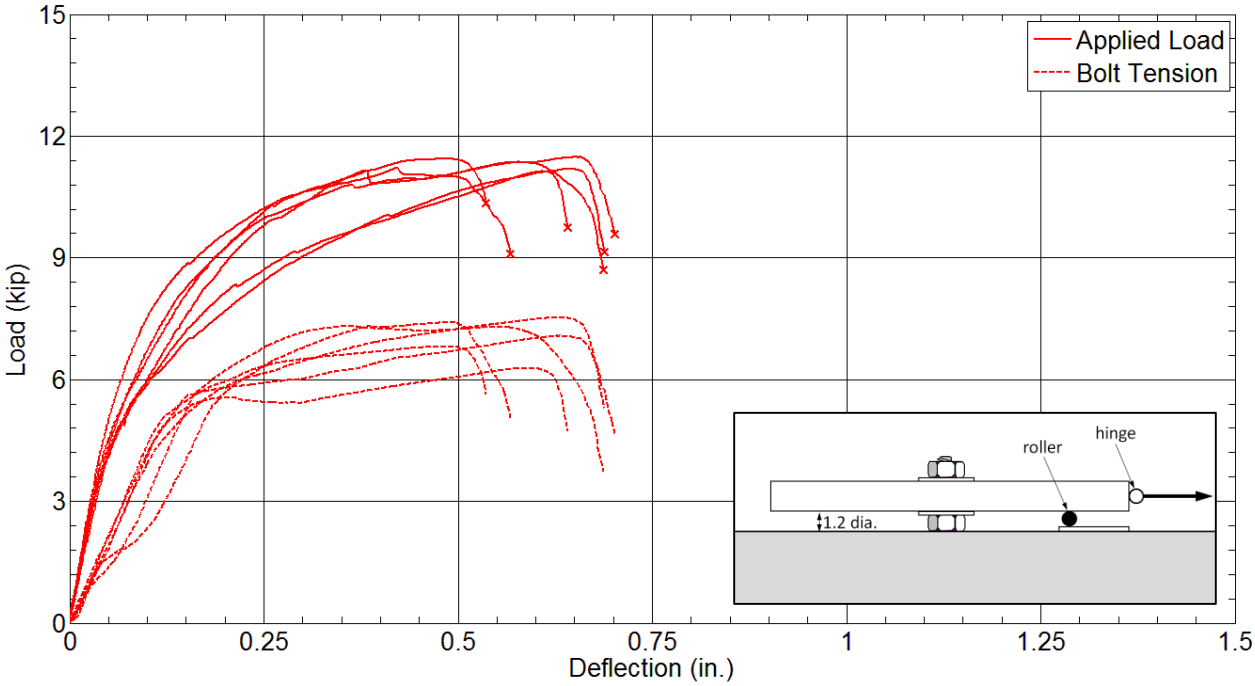

Figure A-2. DS2 (ungrouted 1.2 dia. stand-off base plate, 5/8 in. bolts, n = 1) applied load and bolt tension vs. displacement

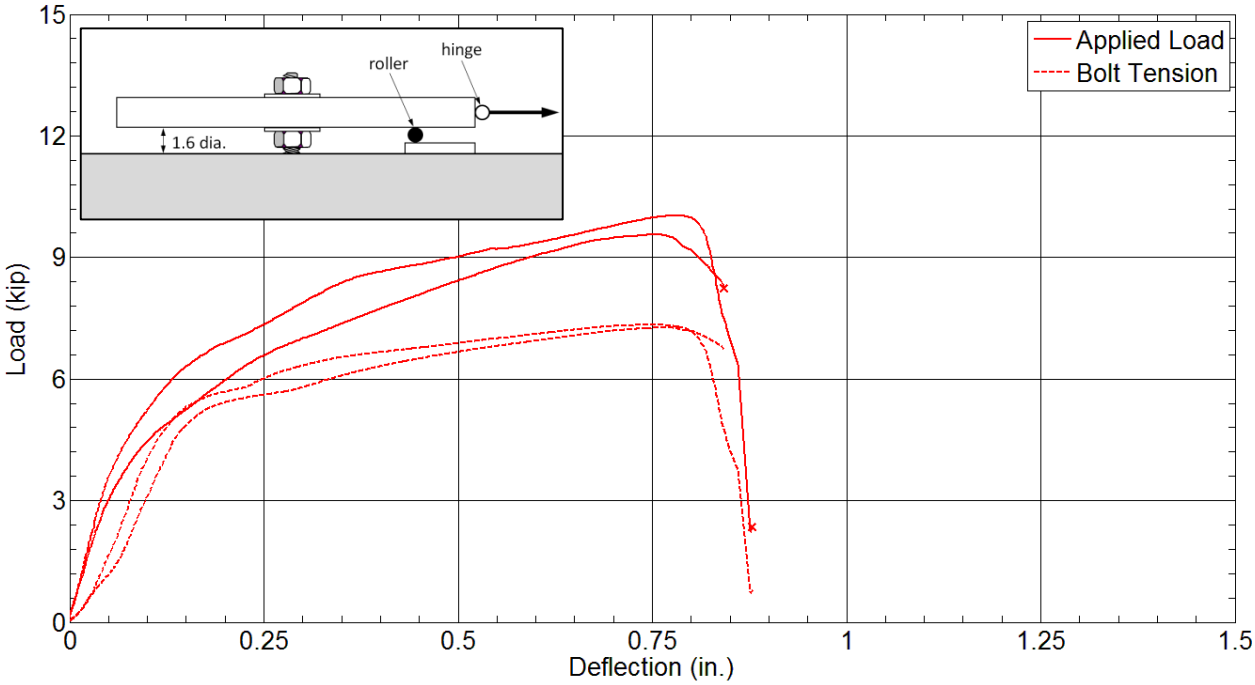

Figure A-3. DS3 (ungrouted 1.6 dia. stand-off base plate, 5/8 in. bolts, n = 1) applied load and bolt tension vs. displacement

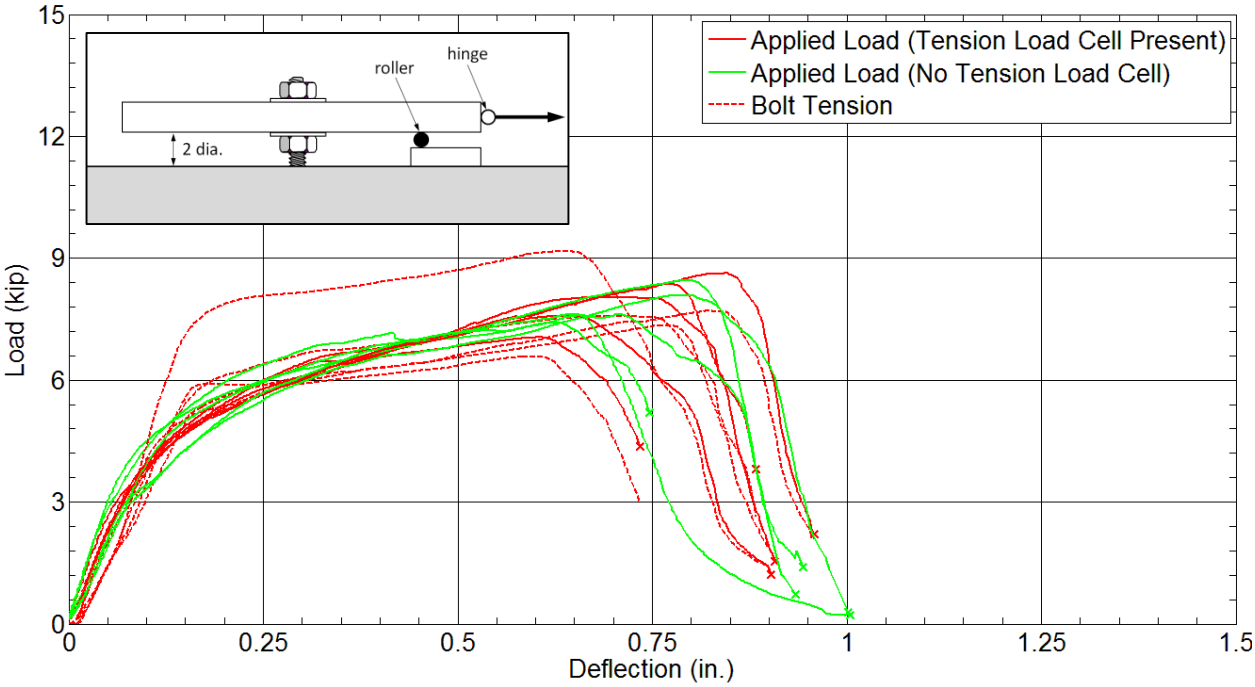

Figure A-4. DS4 (ungrouted 2 dia. stand-off base plate, 5/8 in. bolts, n = 1) applied load and bolt tension vs. displacement

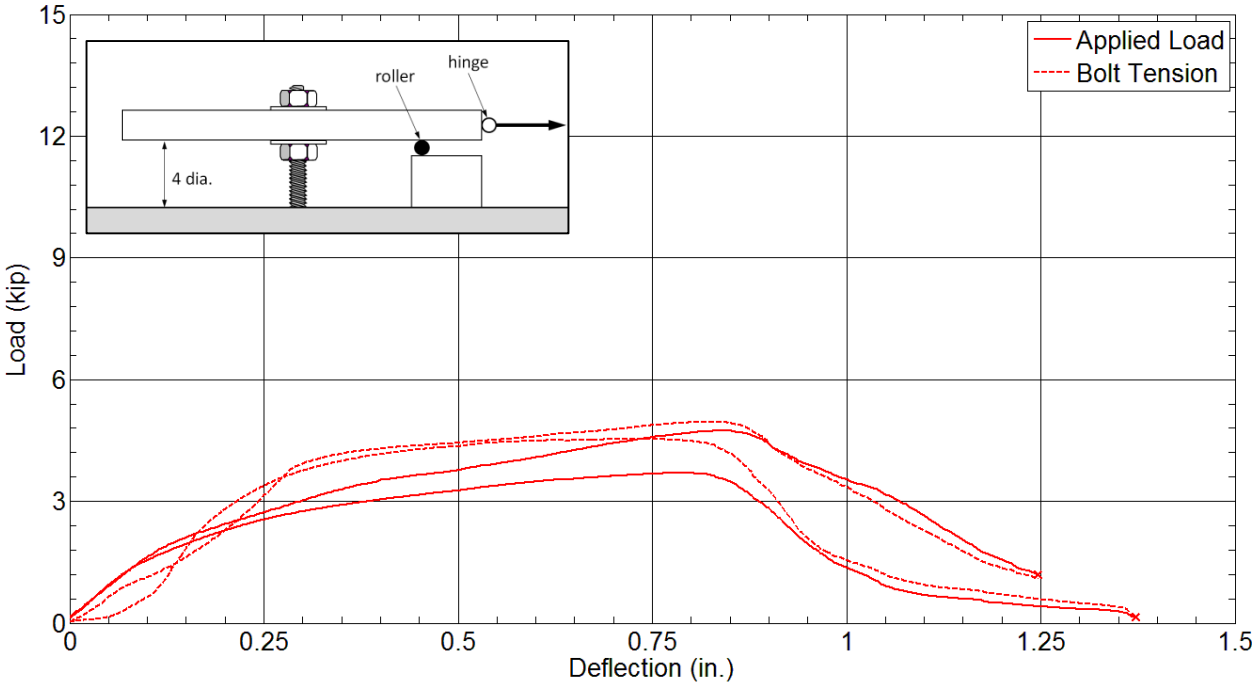

Figure A-5. DS6 (ungrouted 4 dia. stand-off base plate, 5/8 in. bolts, n = 1) applied load and bolt tension vs. displacement

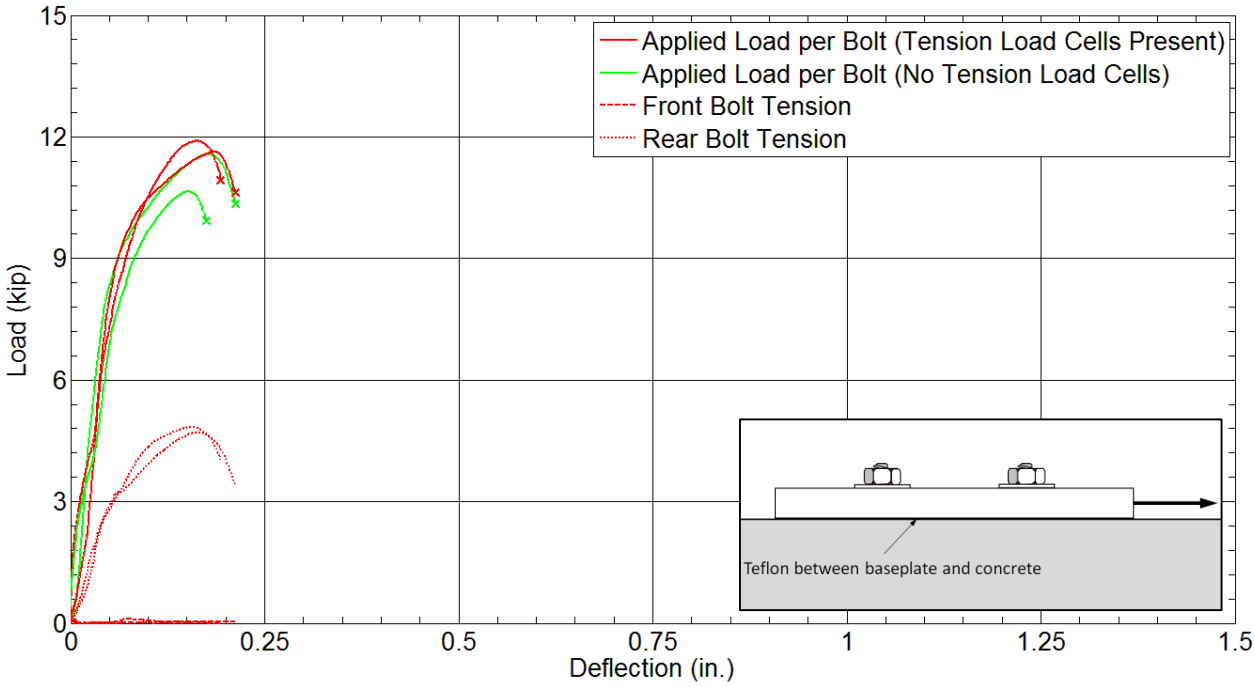

Figure A-6. DS7 (flush-mounted base plate, 5/8 in. bolts, n = 2) instrumentation schematic

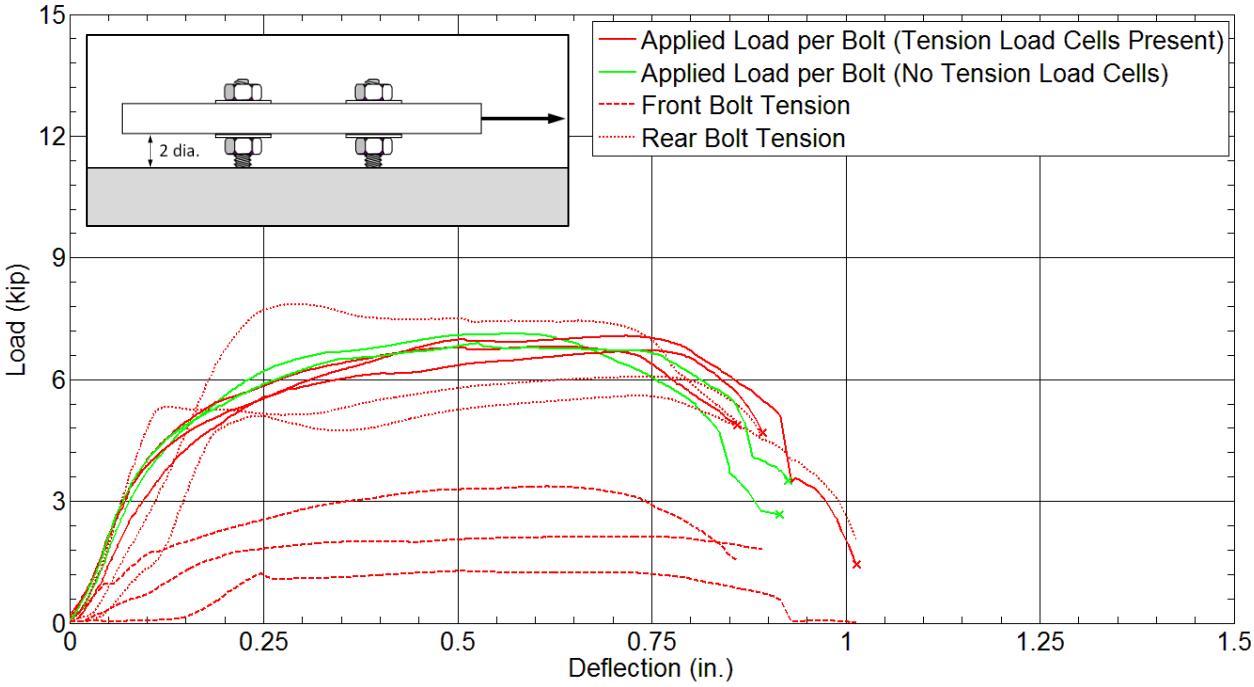

Figure A-7. DS8 (ungrouted 2 dia. stand-off base plate, 5/8 in. bolts, n = 2) applied load and bolt tension vs. displacement

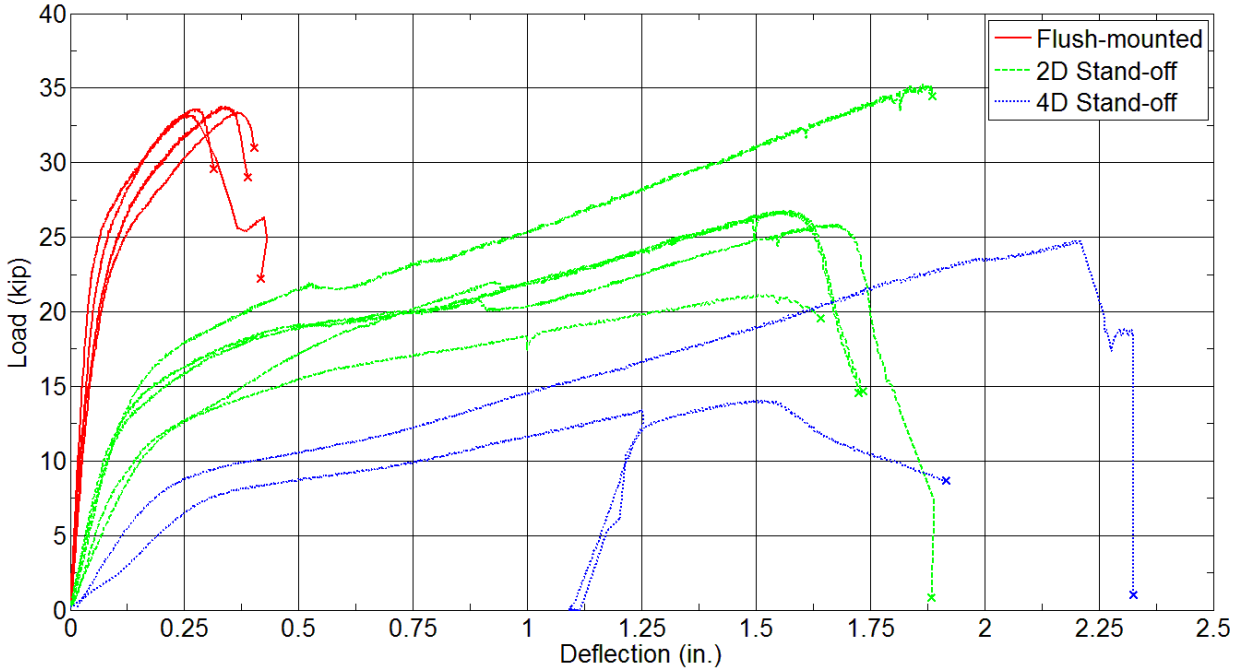

Figure A-8. DS9, DS10, and DS11 (flush-mounted, ungrouted 2 dia. stand-off base plate, and 4 dia. ungrouted stand-off base plate, 1 in. bolts, n = 1) applied load and bolt tension vs. displacement

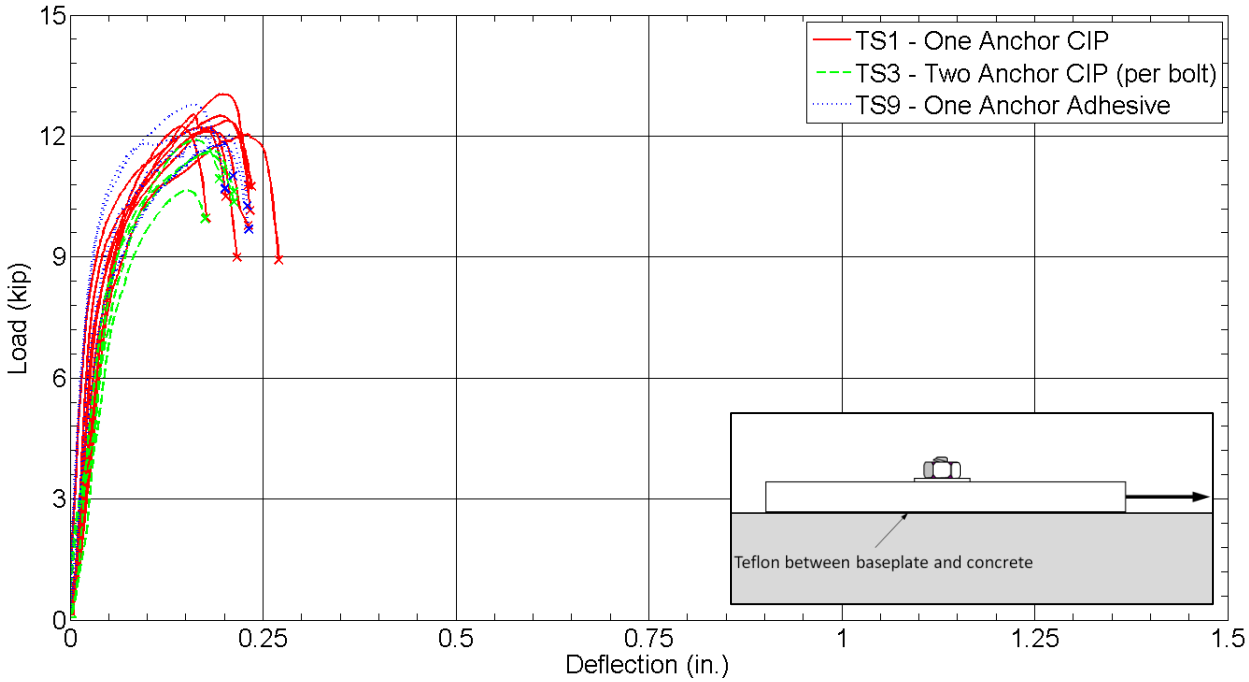

Figure A-9. DS8 (flush-mounted base plate, 5/8 in. bolts, n = 1, adhesive installation) applied load vs. displacement with comparable datasets

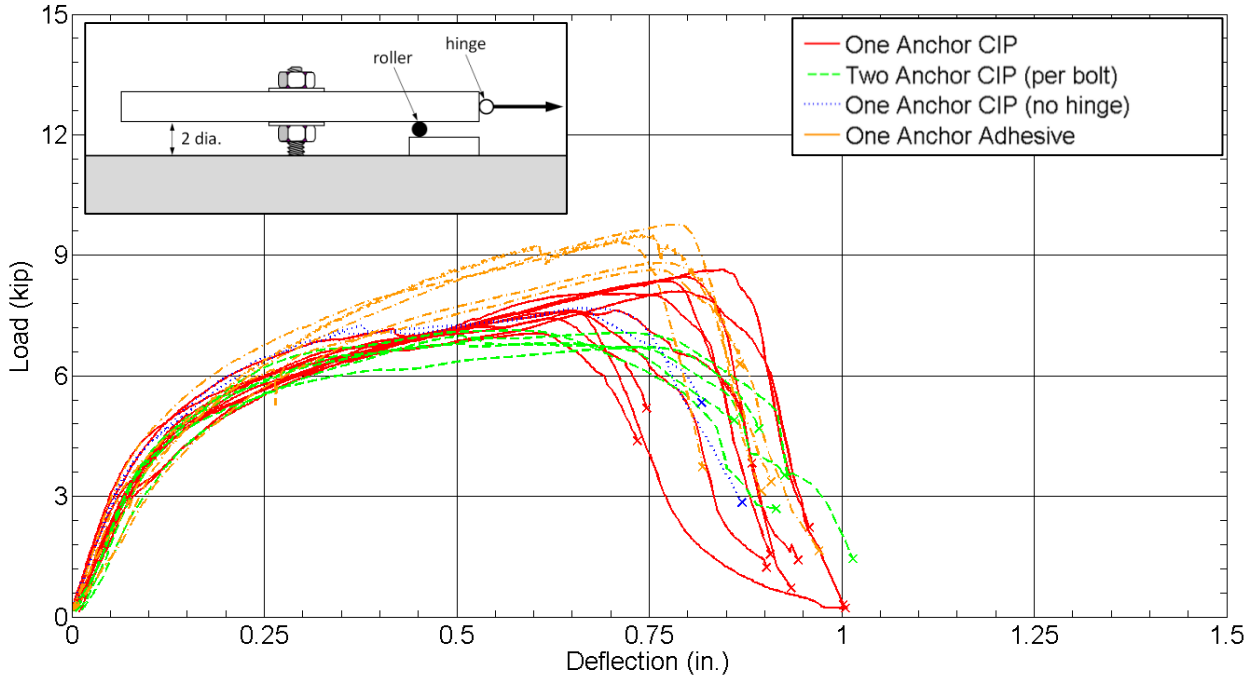

Figure A-10. DS13 (ungrouted 2 dia. stand-off base plate, 5/8 in. bolts, n = 1, adhesive installation) applied load vs. displacement with comparable datasets

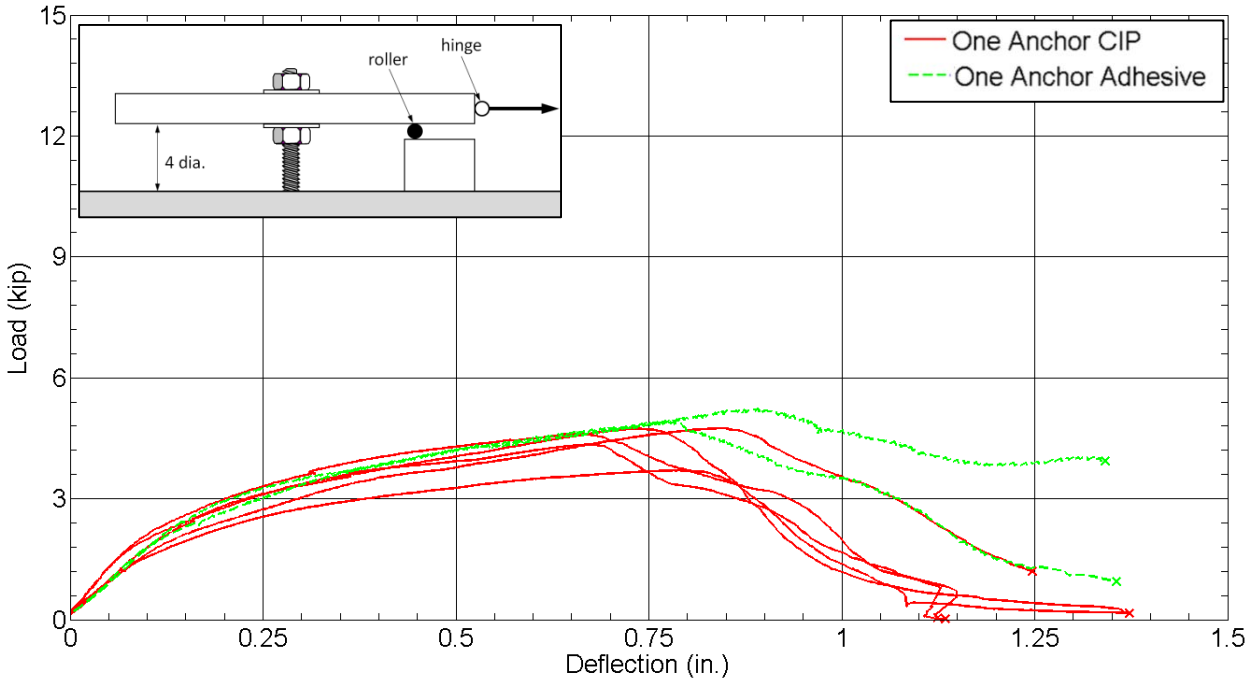

Figure A-11. DS14 (ungrouted 2 dia. stand-off base plate, 5/8 in. bolts, n = 1, adhesive installation) with DS6 CIP applied load vs. displacement

APPENDIX B
LOAD-DISPLACEMENT BEHAVIOR OF PHASE 2 TESTS

This appendix contains the locations of instrumentation, individual actuator loads producing torsion on the bolt group vs. bolt displacement, bolt tension vs. bolt displacement graphs for every bolt tension load cell, and average applied actuator load vs. displacement of every vertically oriented LVDT. Due to initial improper calibration of actuator load cells, the first tests conducted (T1-A, T2-A, and T3) show imbalanced applied loads between the two actuators to varying degrees. The values presented represent corrected values after load cell recalibration; failure loads for these tests are the average of the two actuator readings at ultimate load. Despite many calibrations, tension load cells proved to be unreliable in providing consistent and reasonable readings between and within tests. However, their data are valuable for characterizing individual bolt behavior within tests. For this reason, readings are represented as values normalized by the maximum reading of *all bolts within an individual test.* Vertical displacement readings were not taken for T2-A. In some cases, vertical LVDTS may have been disturbed or fallen off of an edge (e.g. V3 in T1-A and V1 in T6-B). However, this was rare.

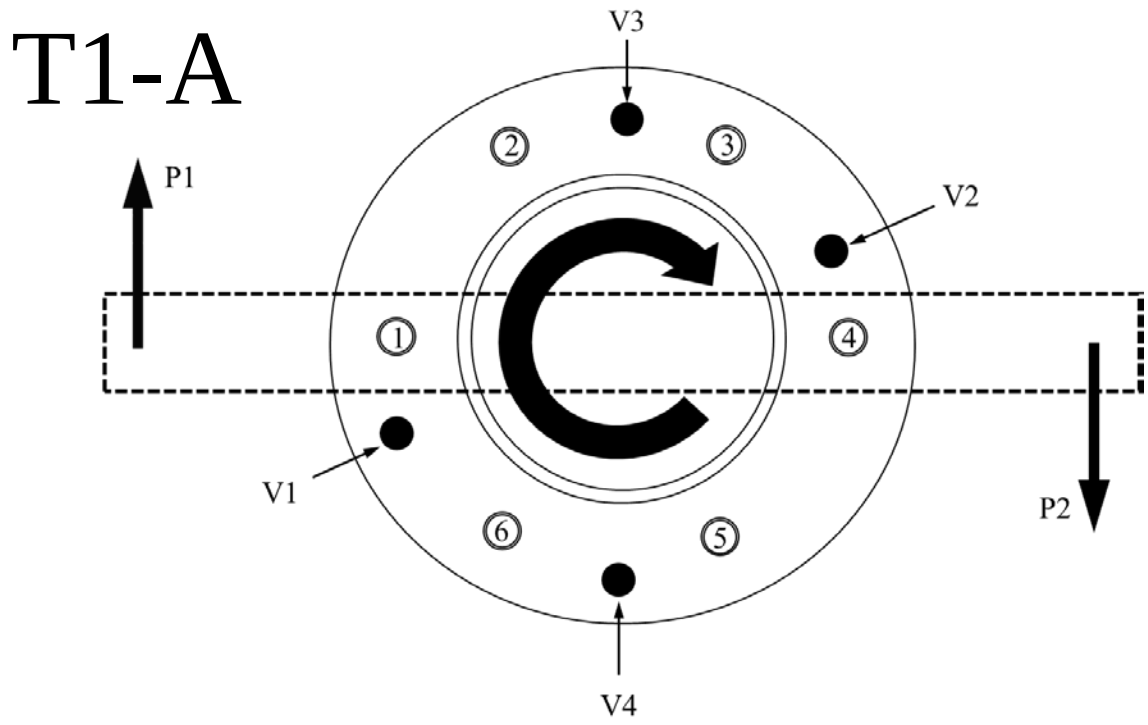

Figure B-1. T1-A (flush-mounted base plate, 5/8 in. bolts, n = 6) instrumentation schematic

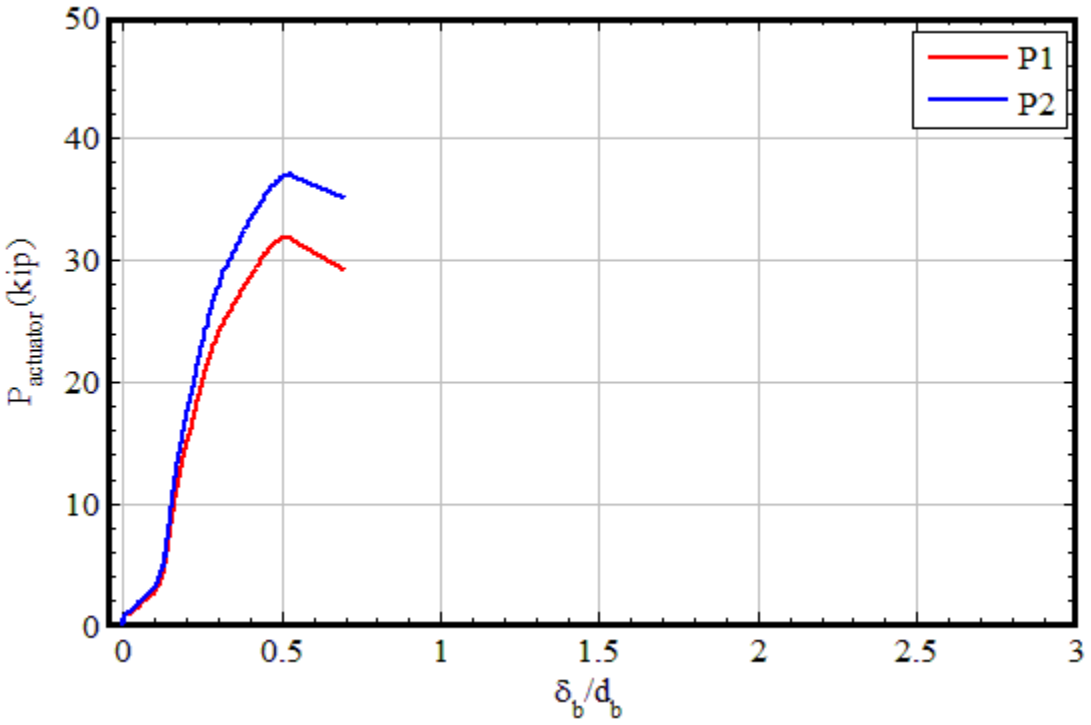

Figure B-2. T1-A individual actuator loads vs. bolt displacement

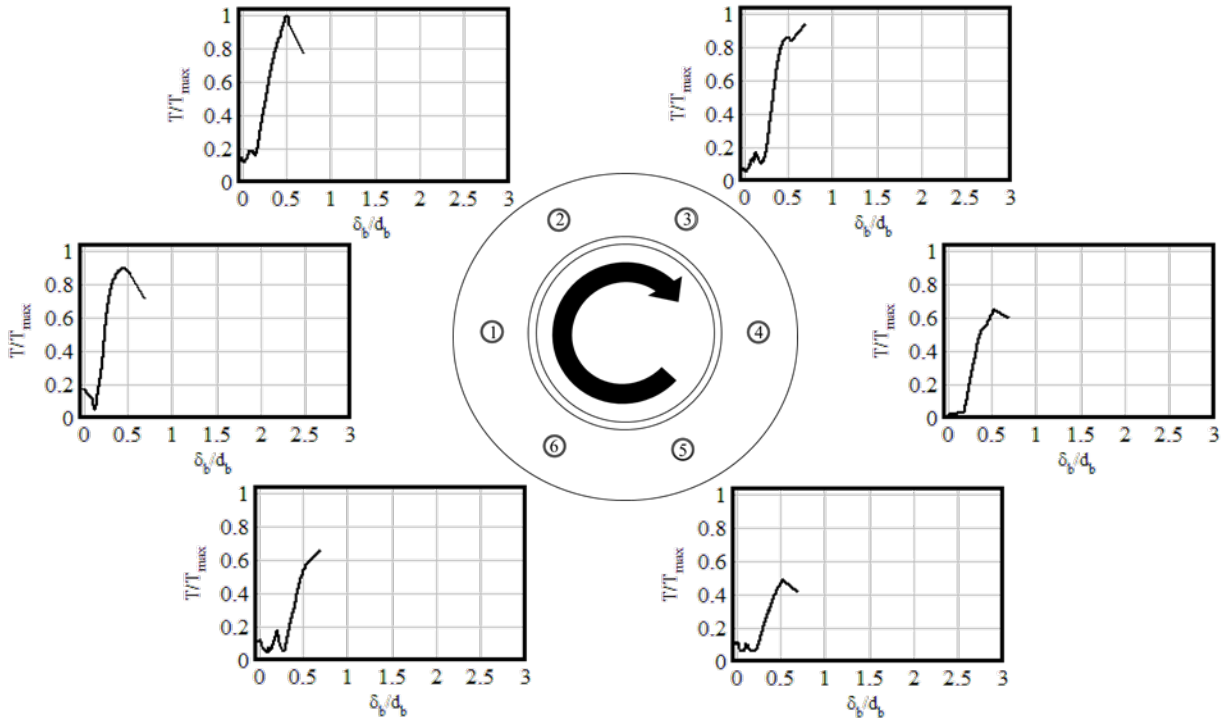

Figure B-3. T1-A bolt tensions vs. bolt displacement

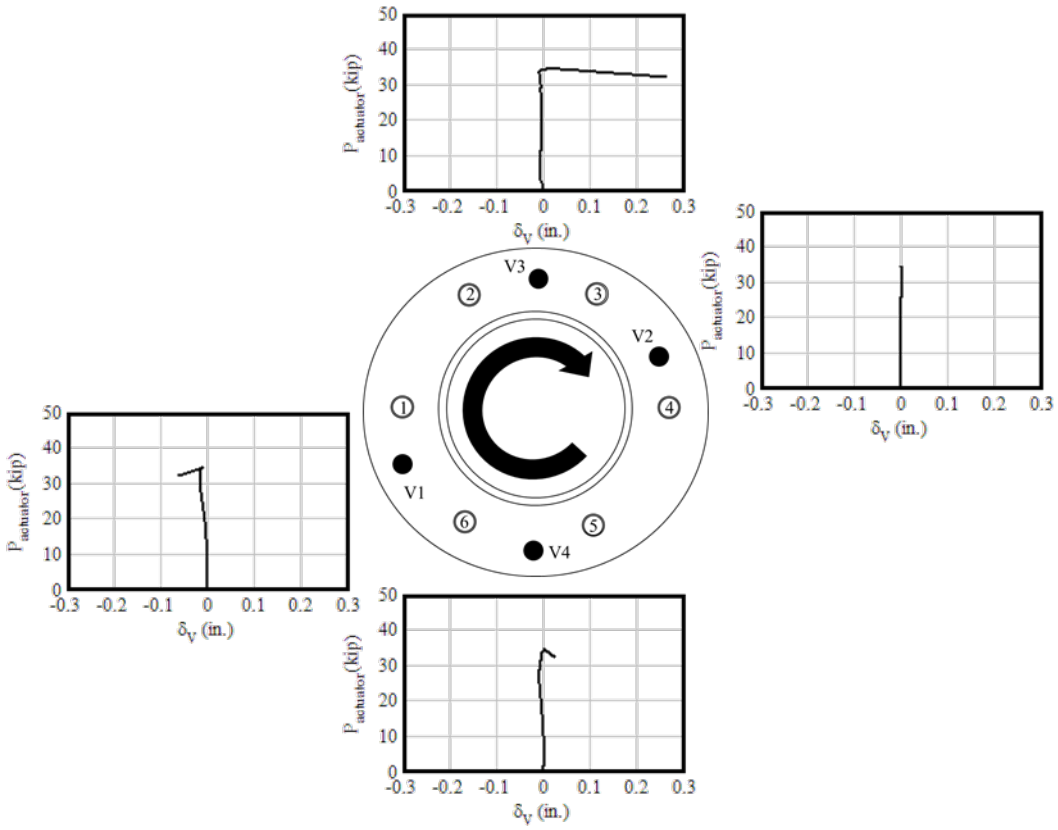

Figure B-4. T1-A average applied load vs. vertical displacements

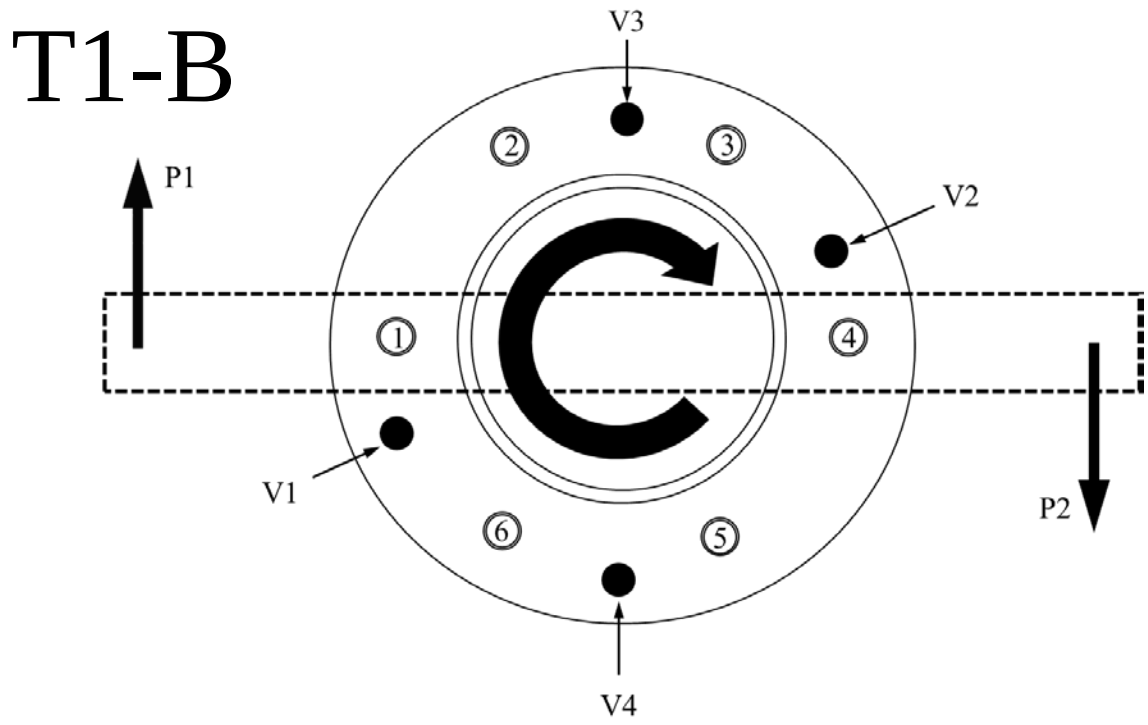

Figure B-5. T1-B (flush-mounted base plate, 5/8 in. bolts, n = 6) instrumentation schematic

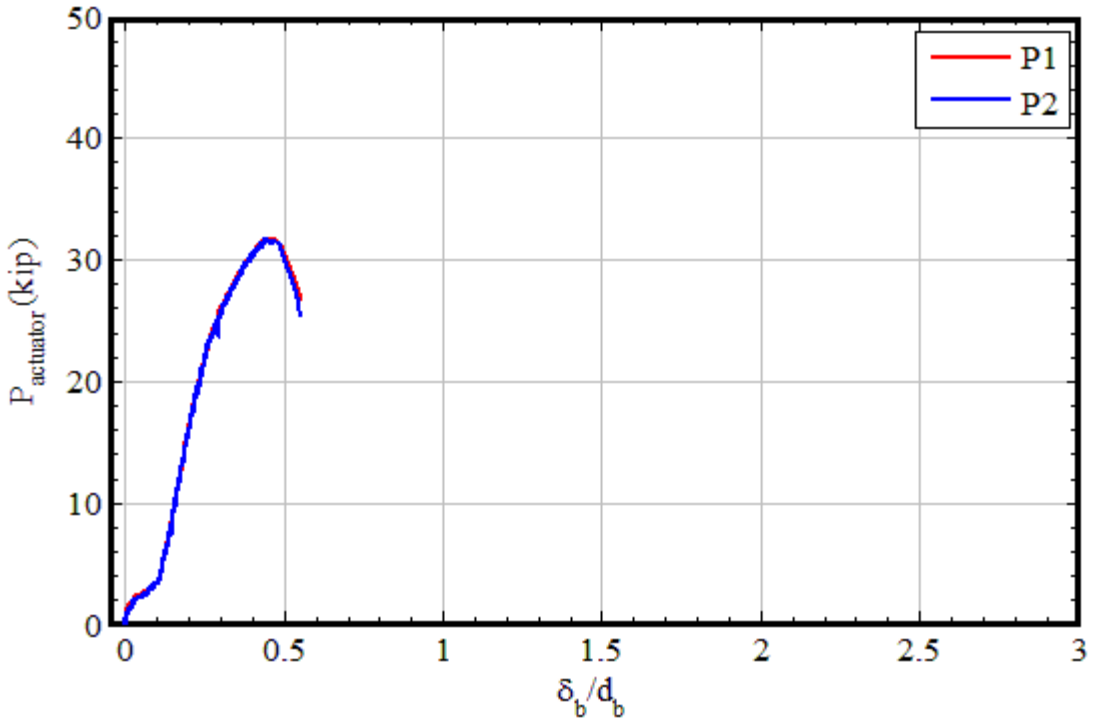

Figure B-6. T1-B individual actuator loads vs. bolt displacement

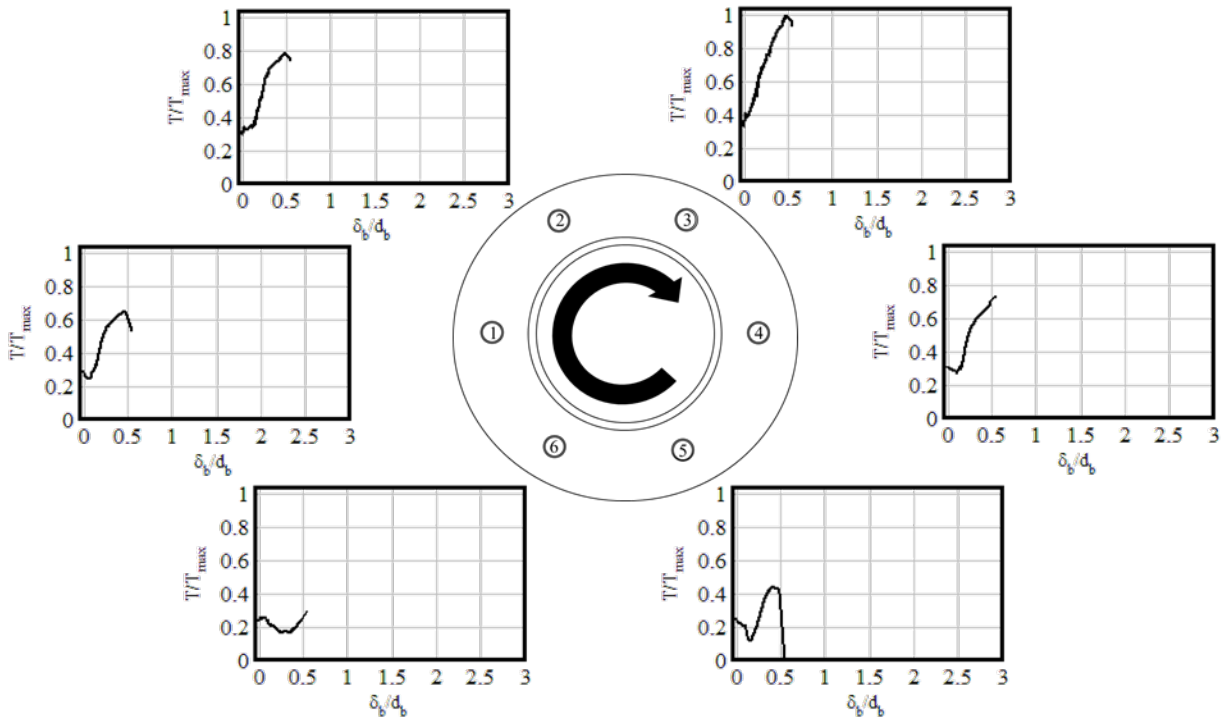

Figure B-7. T1-B bolt tensions vs. bolt displacement

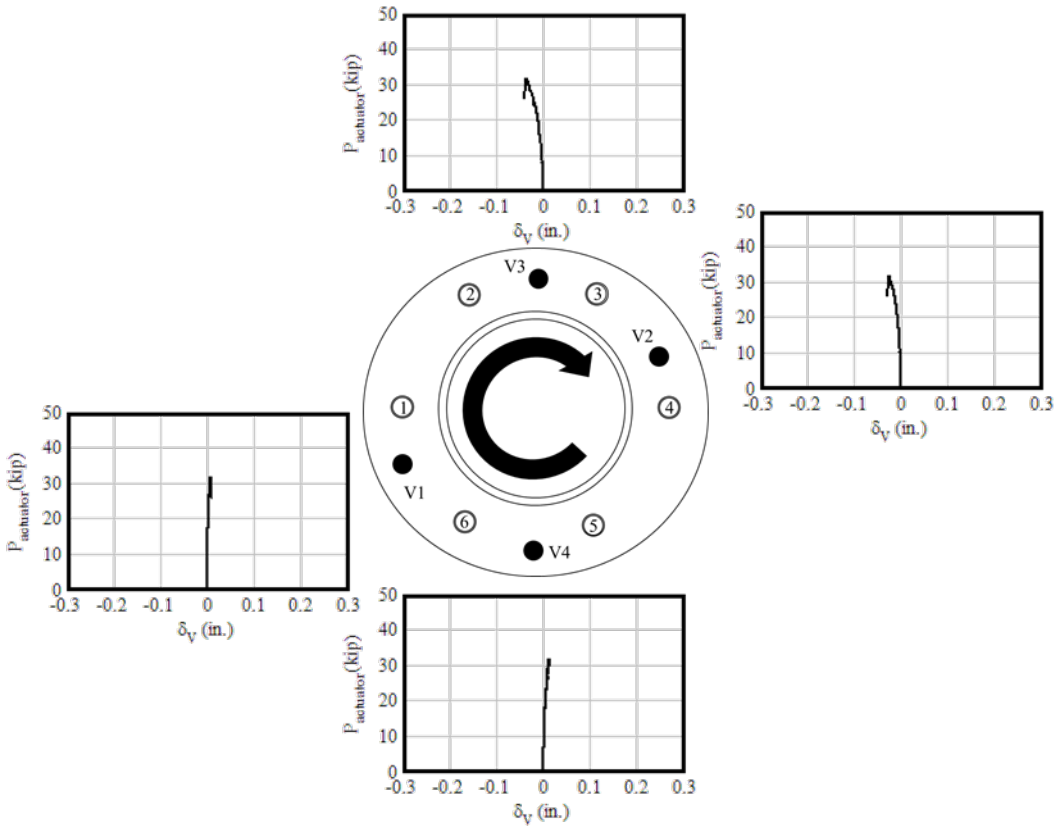

Figure B-8. T1-B average applied load vs. vertical displacements

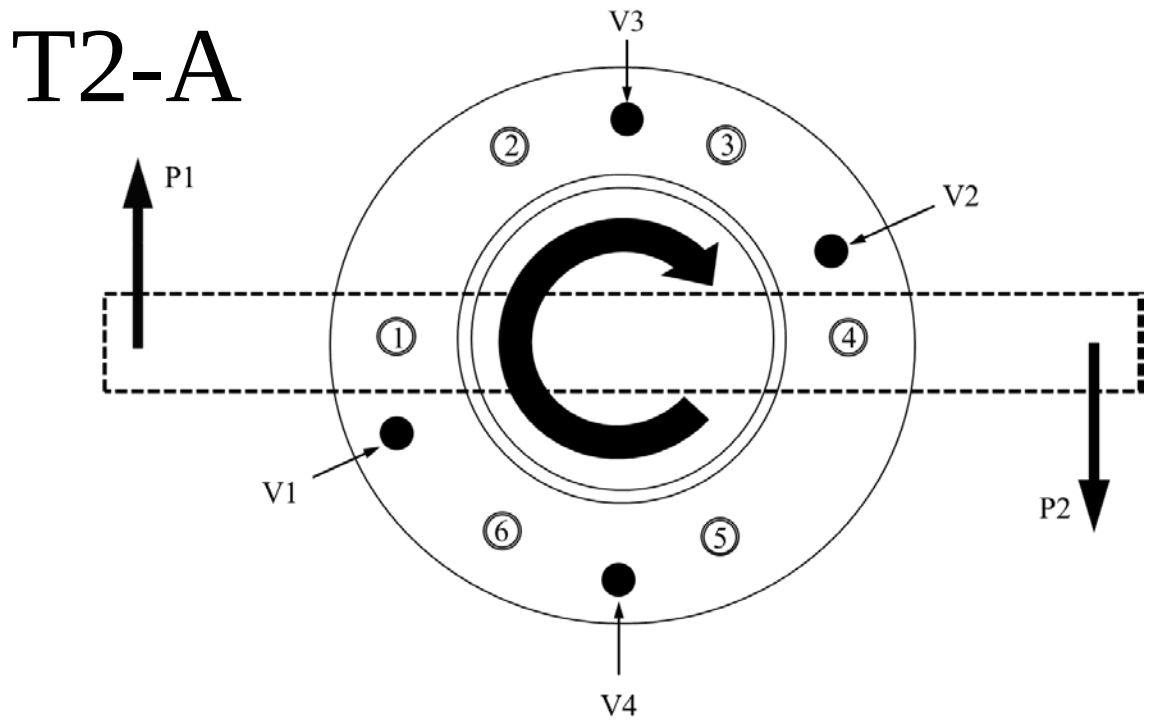

Figure B-9. T2-A (ungrouted 2 dia. stand-off base plate, 5/8 in. bolts, n = 6) instrumentation schematic

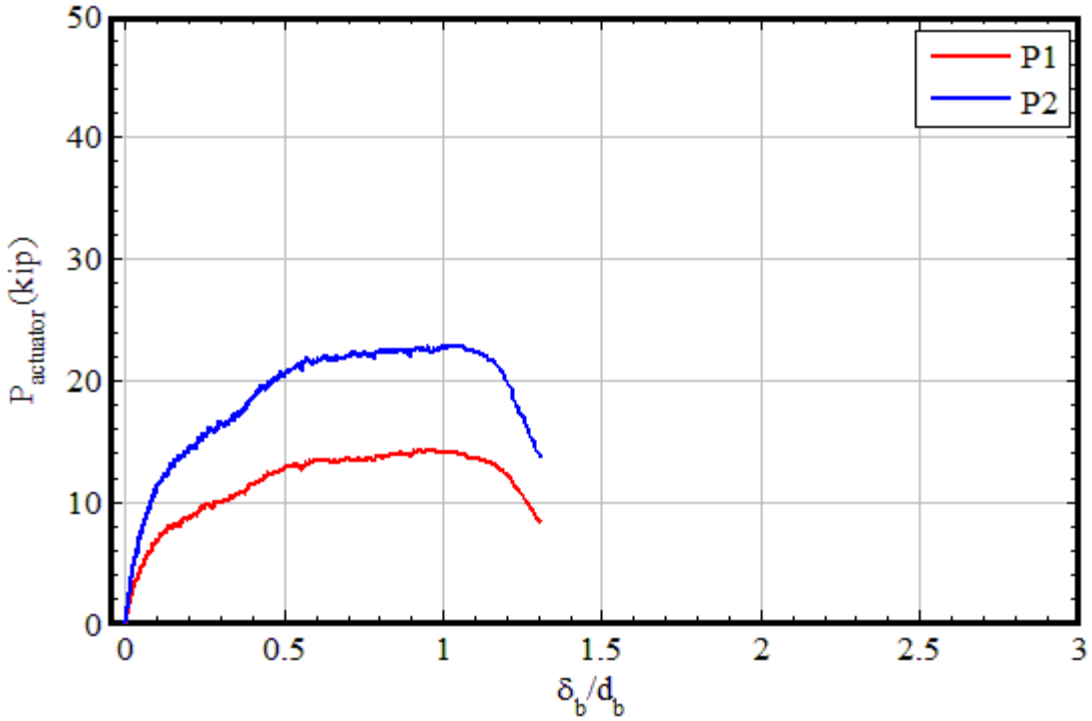

Figure B-10. T2-A individual actuator loads vs. bolt displacement

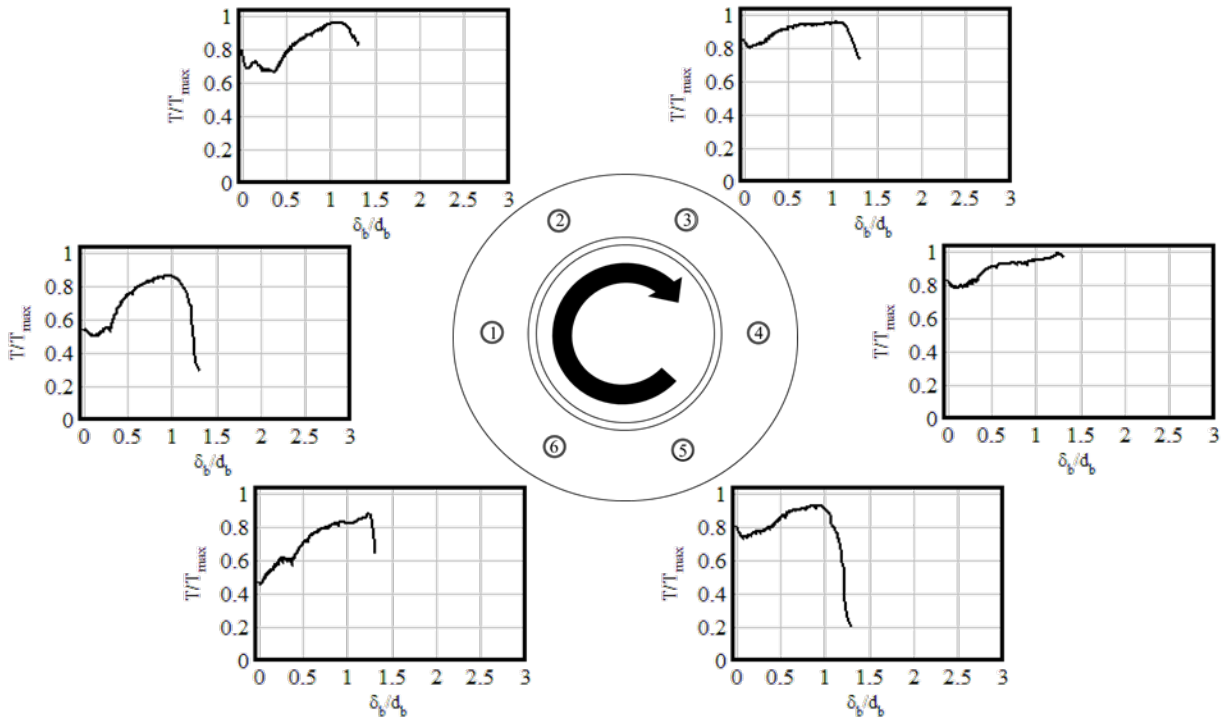

Figure B-11. T2-A bolt tensions vs. bolt displacement

Note: Vertical displacement not recorded for test T2-A.

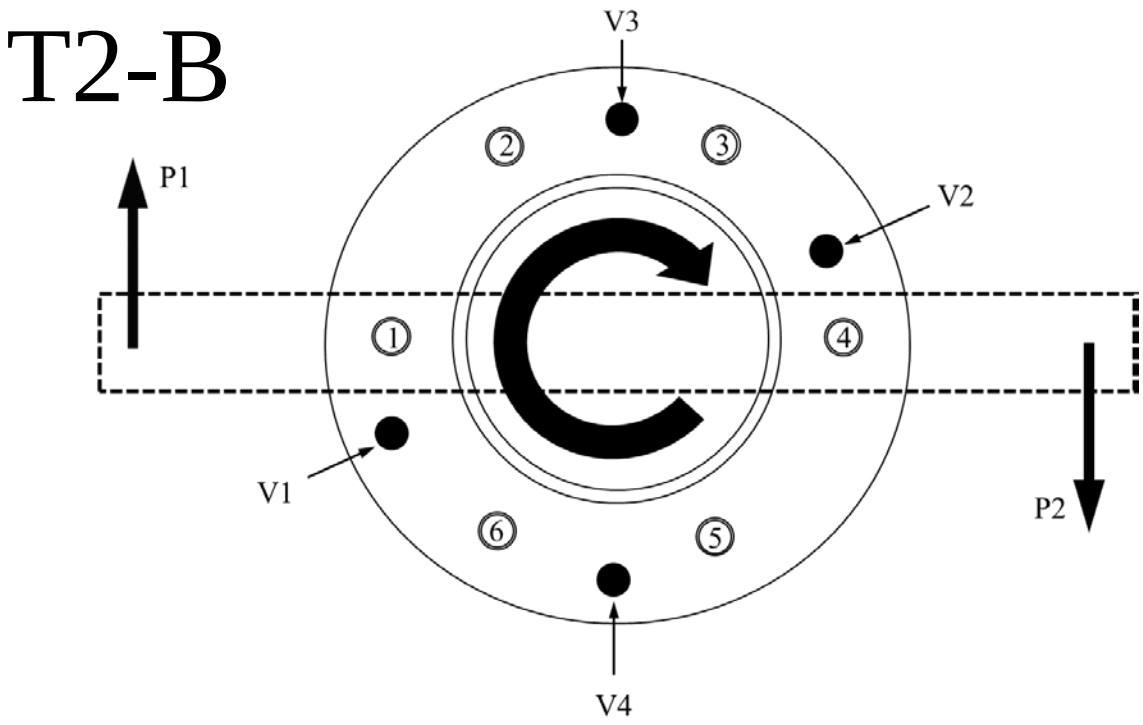

Figure B-12. T2-B (ungrouted 2 dia. stand-off base plate, 5/8 in. bolts, n = 6) instrumentation schematic

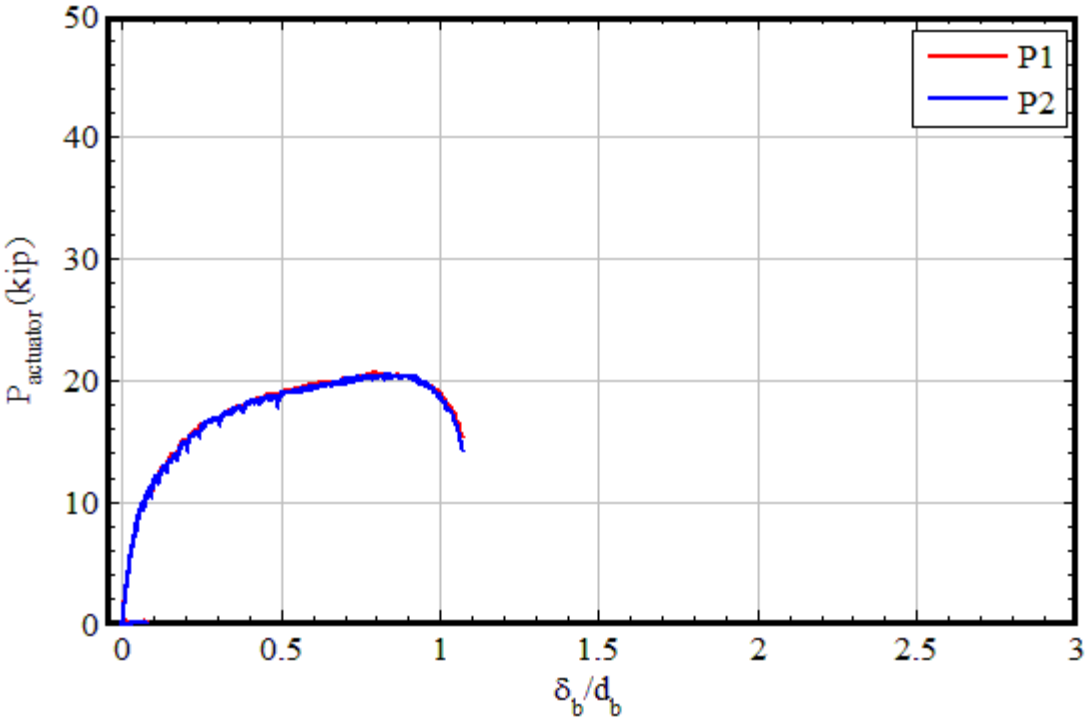

Figure B-13. T2-B individual actuator loads vs. bolt displacement

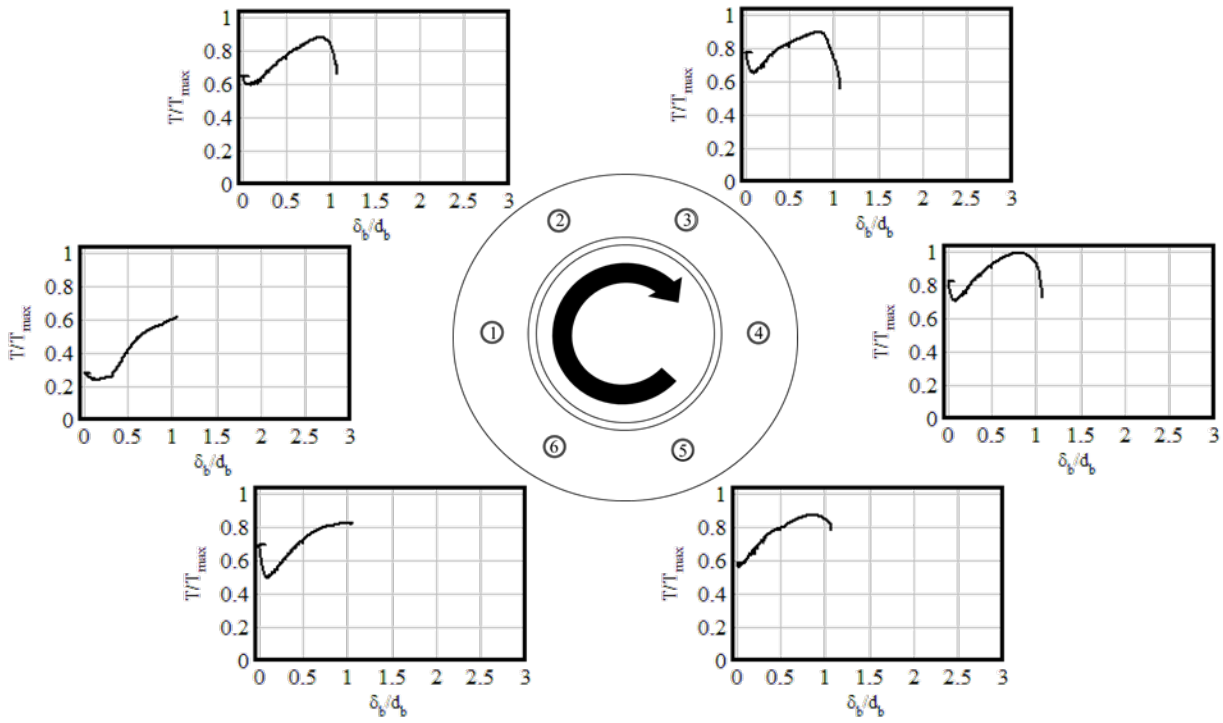

Figure B-14. T2-B bolt tensions vs. bolt displacement

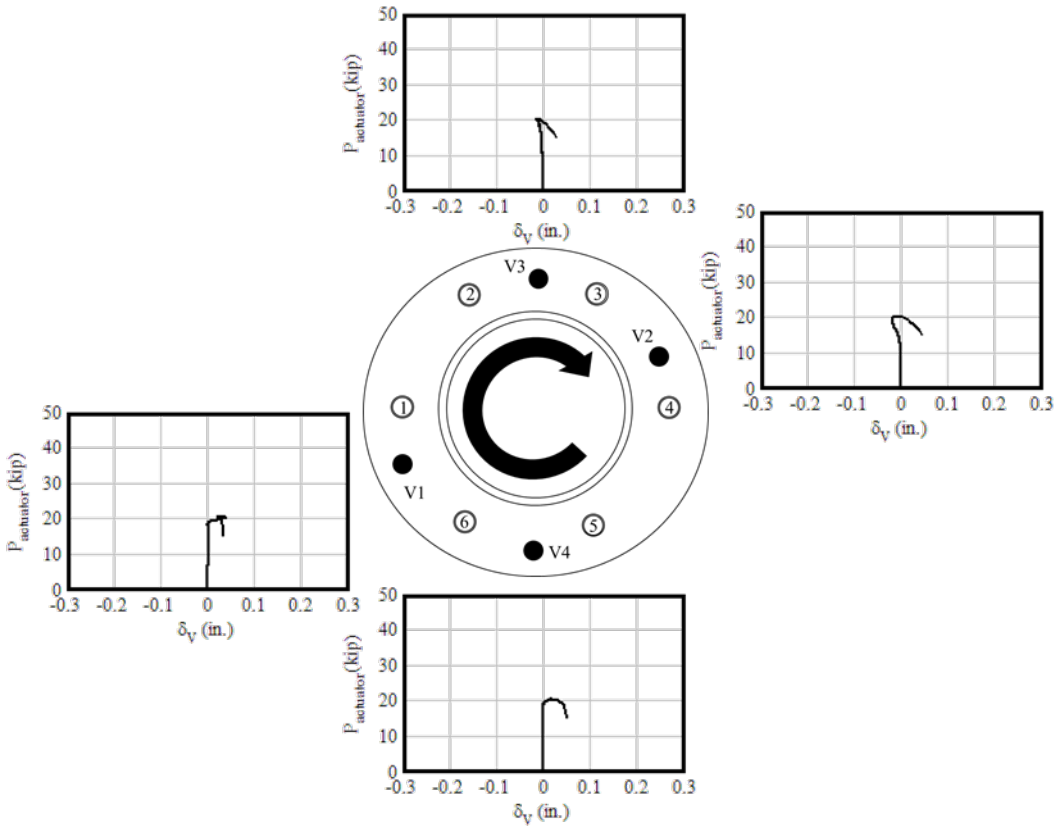

Figure B-15. T2-B average applied load vs. vertical displacements

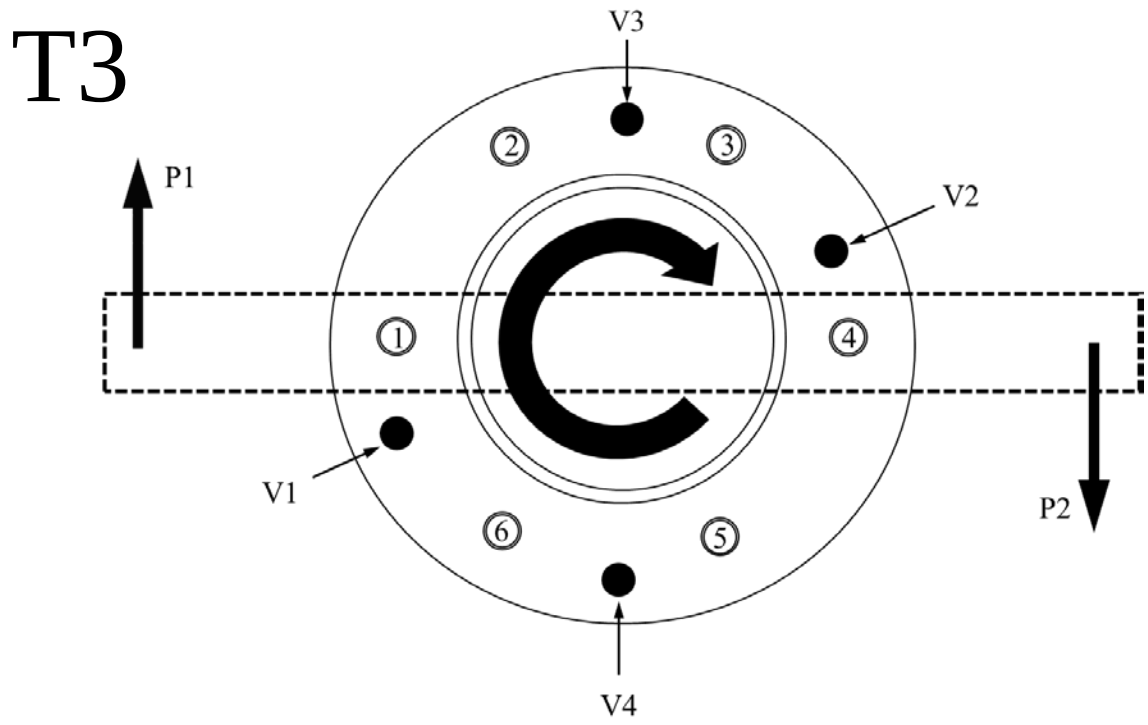

Figure B-16. T3 (ungrouted 4 dia. stand-off base plate, 5/8 in. bolts, n = 6) instrumentation schematic

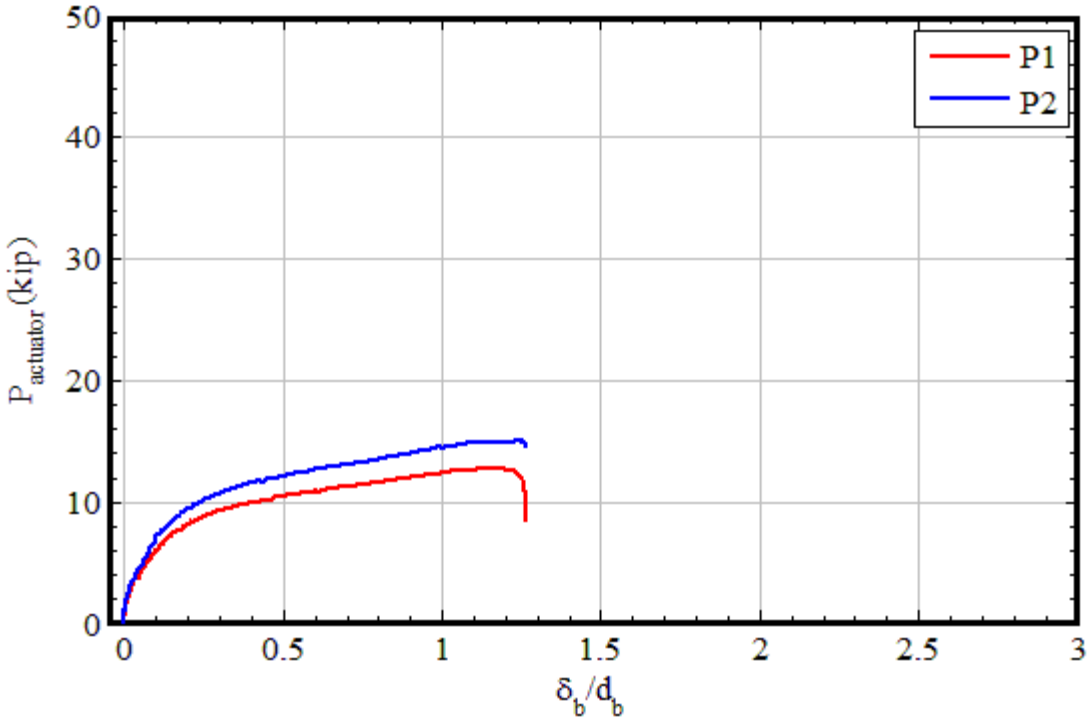

Figure B-17. T3 individual actuator loads vs. bolt displacement

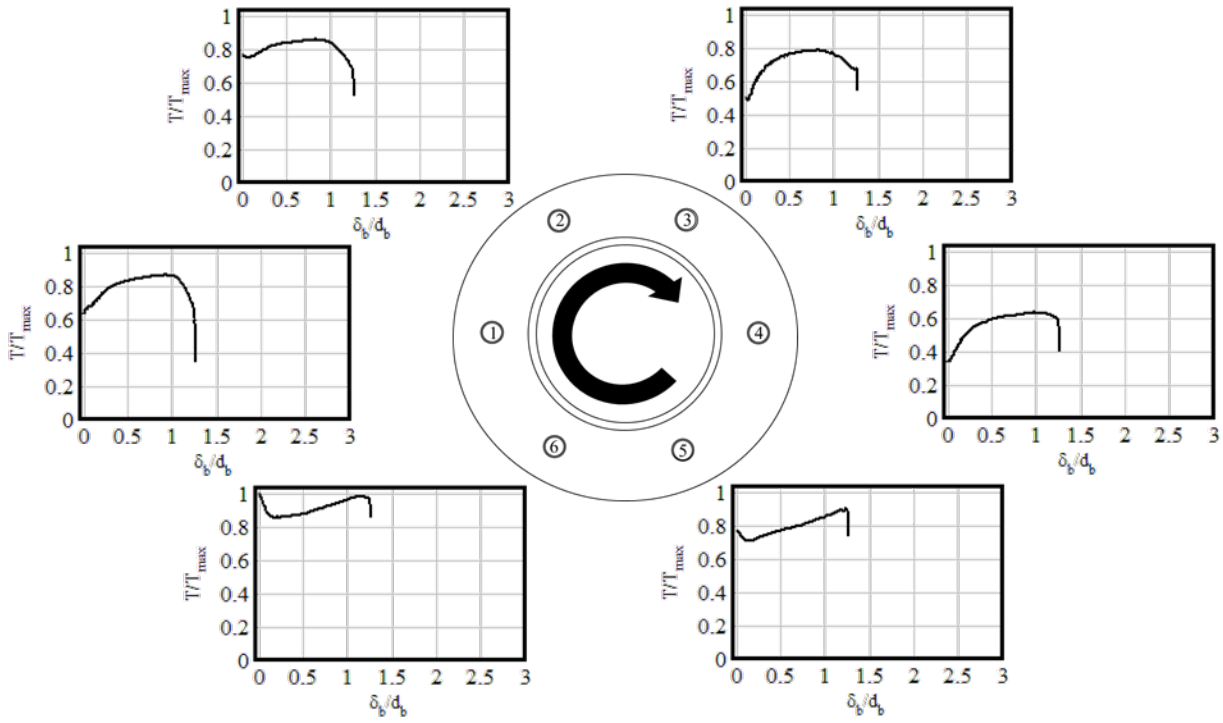

Figure B-18. T3 bolt tensions vs. bolt displacement

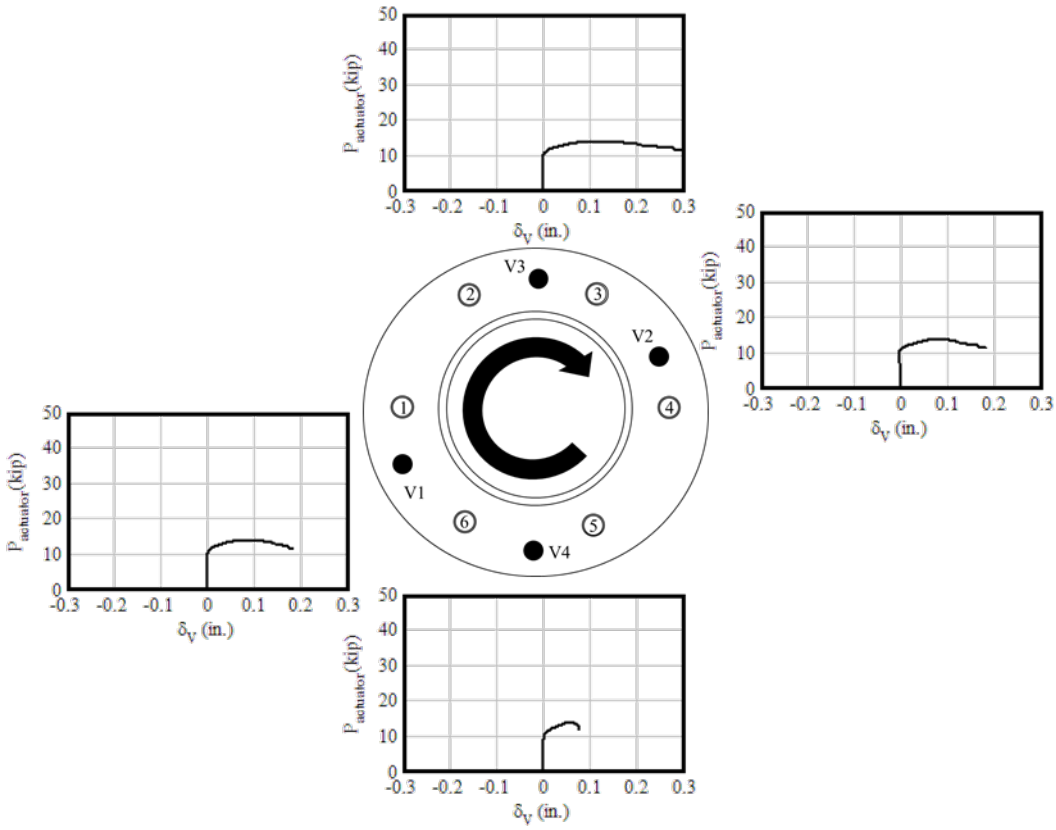

Figure B-19. T3 average applied load vs. vertical displacements

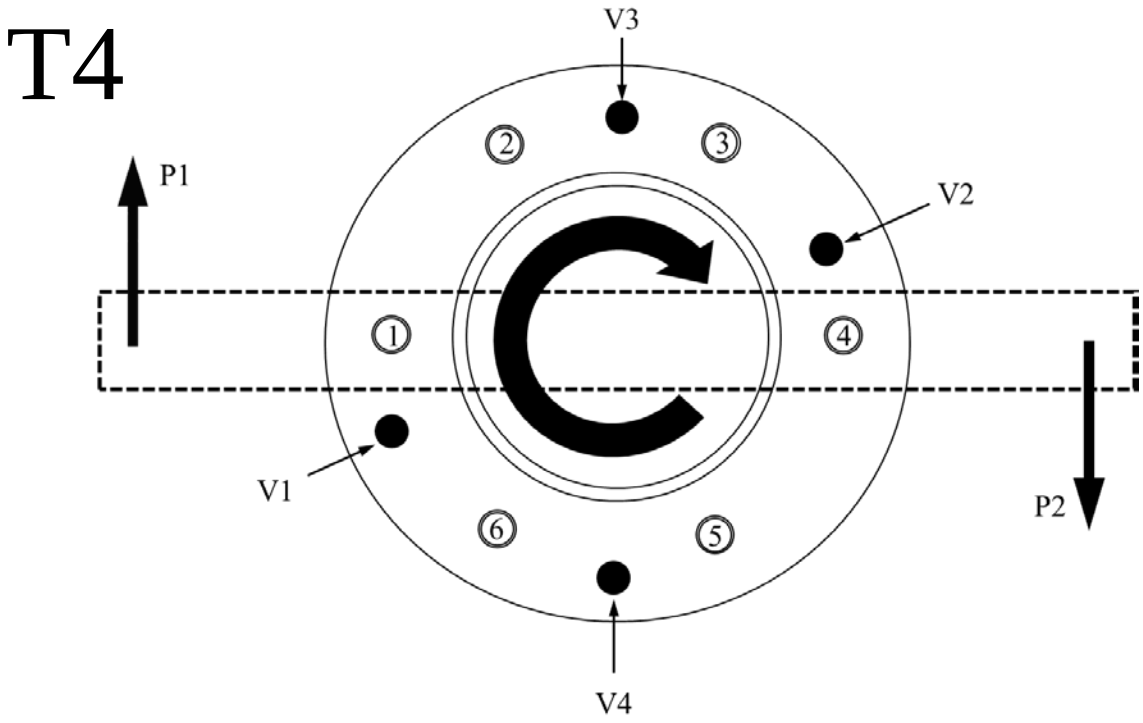

Figure B-20. T4 (ungrouted 2 dia. stand-off base plate, 5/8 in. bolts, n = 6, no pretension) instrumentation schematic

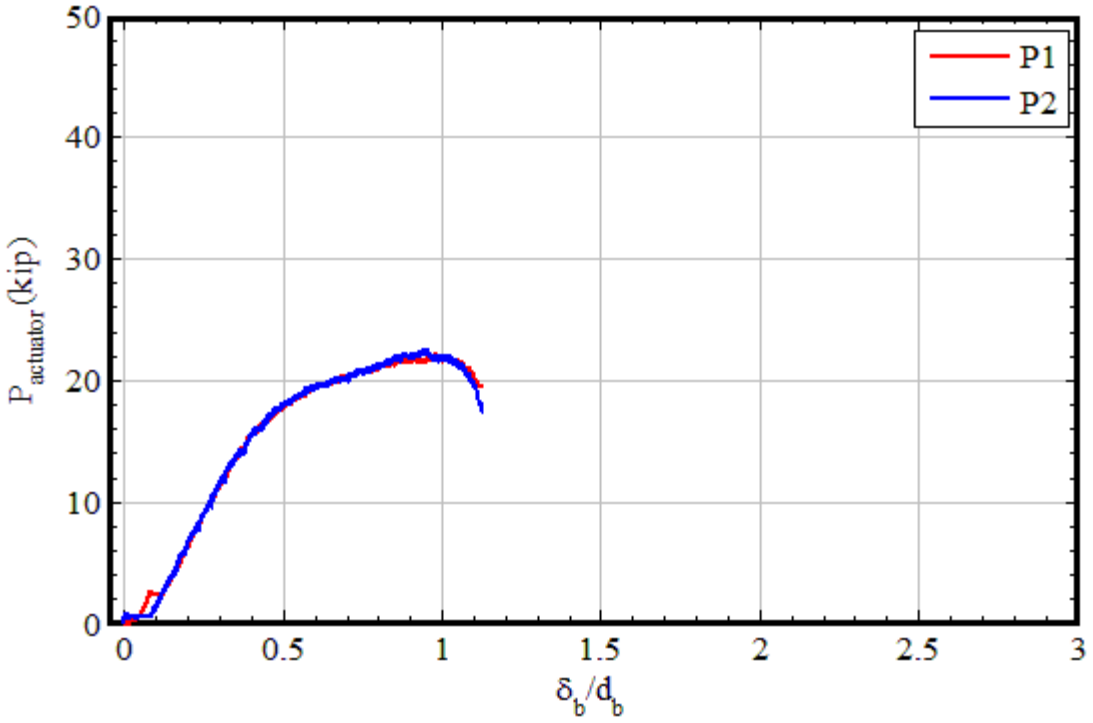

Figure B-21. T4 individual actuator loads vs. bolt displacement

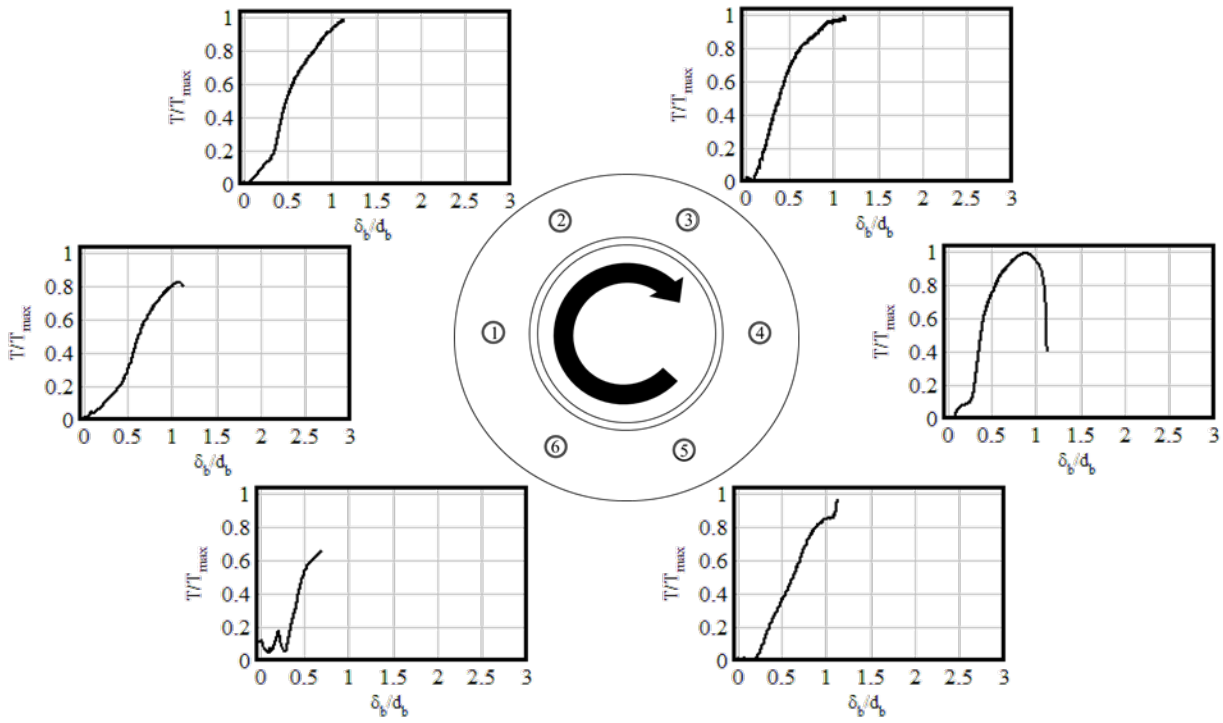

Figure B-22. T4 bolt tensions vs. bolt displacement

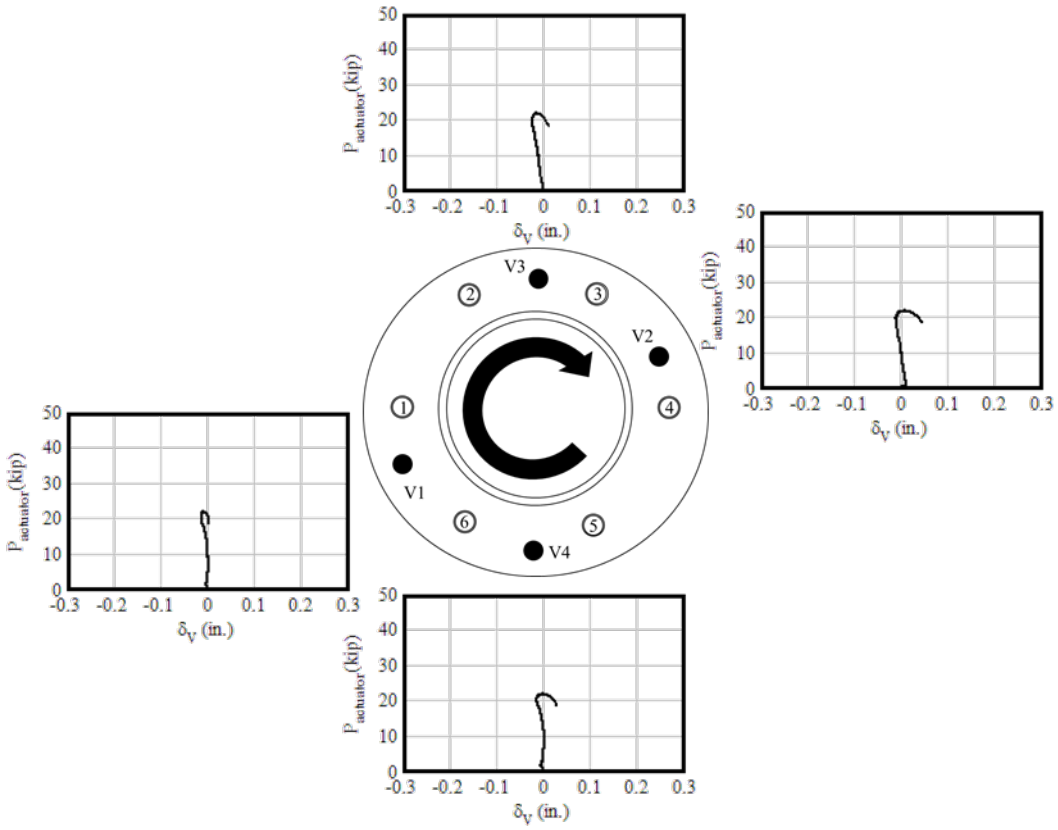

Figure B-23. T4 average applied load vs. vertical displacements

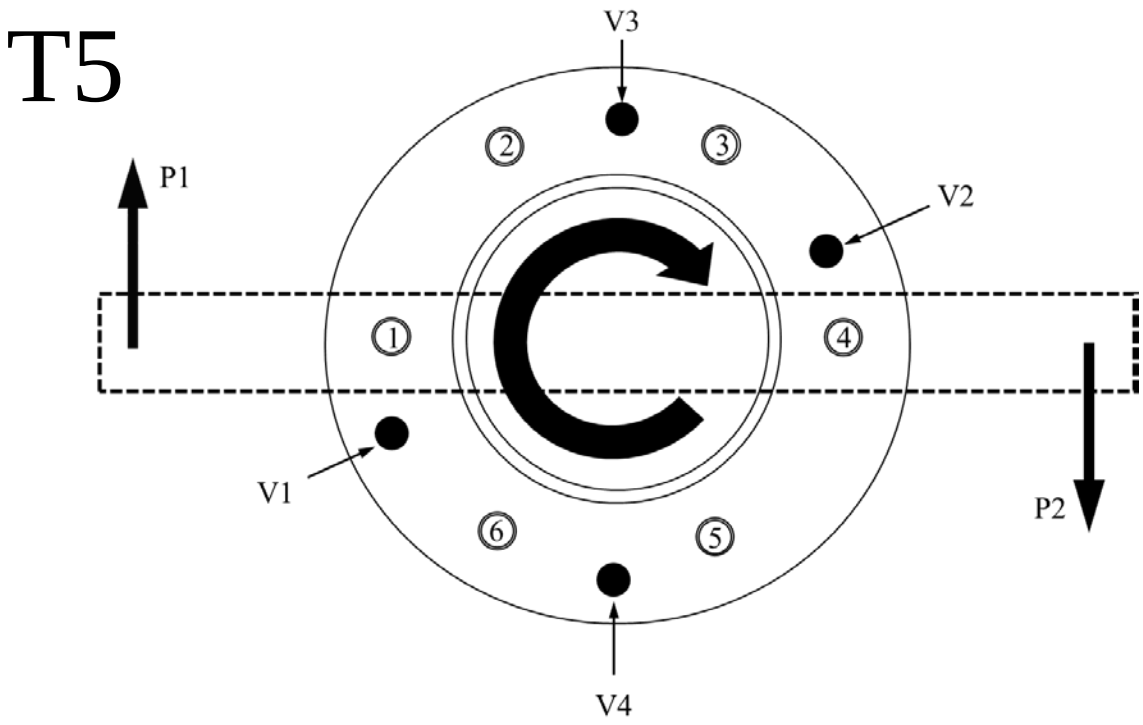

Figure B-24. T5 (grouted 2 dia. stand-off base plate, 5/8 in. bolts, n = 6) instrumentation schematic

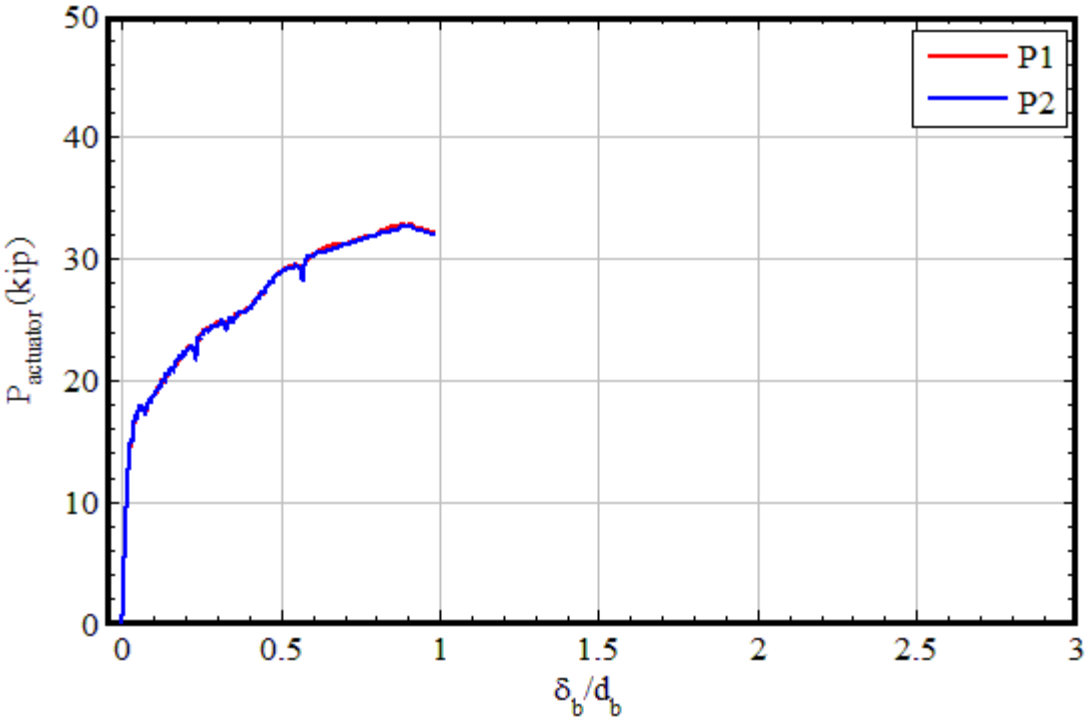

Figure B-25. T5 individual actuator loads vs. bolt displacement

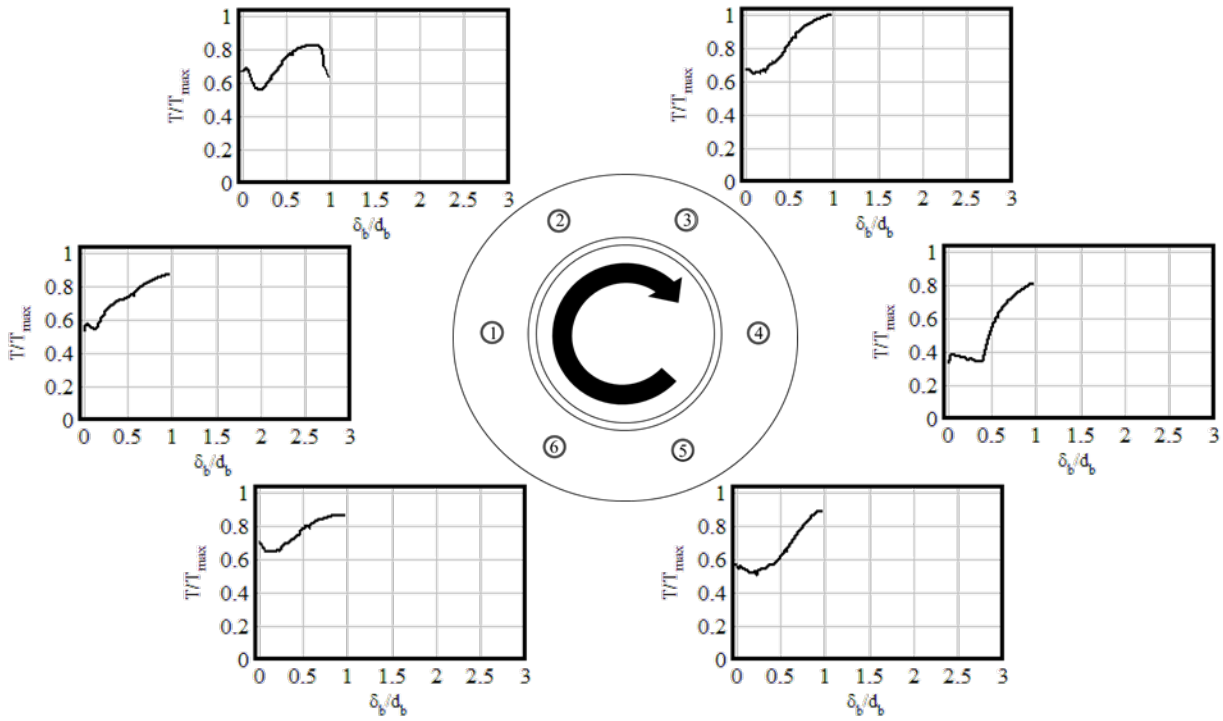

Figure B-26. T5 bolt tensions vs. bolt displacement

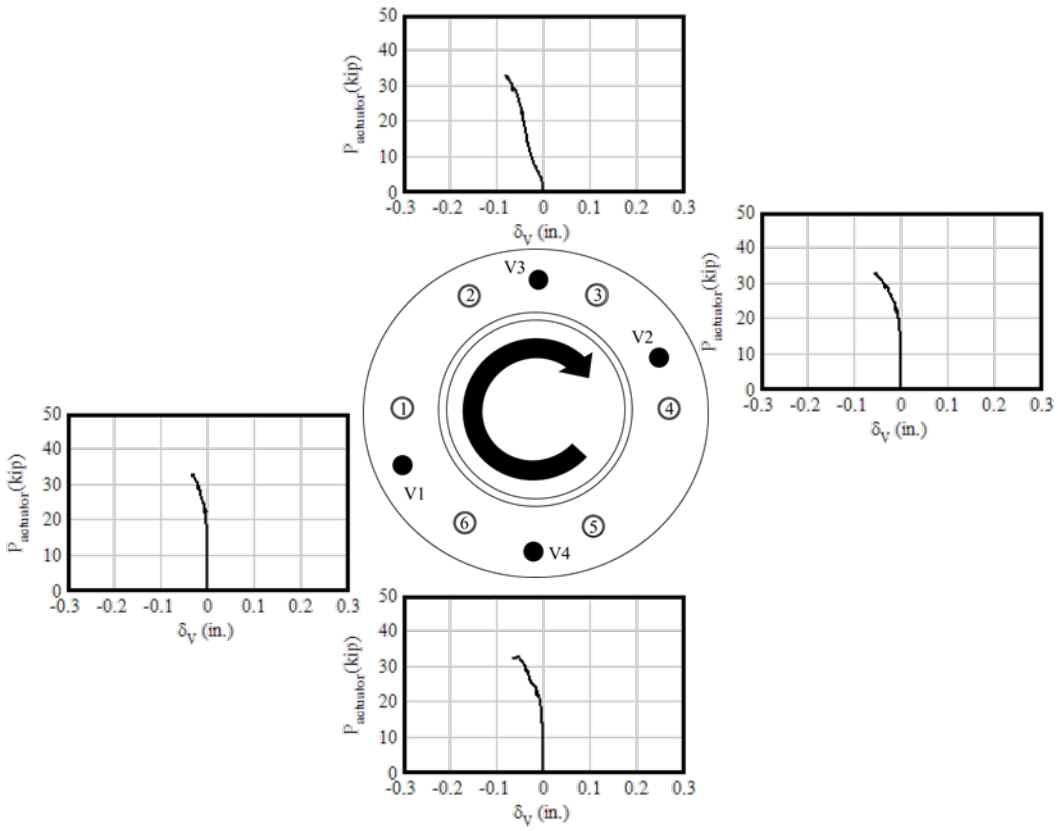

Figure B-27. T5 average applied load vs. vertical displacements

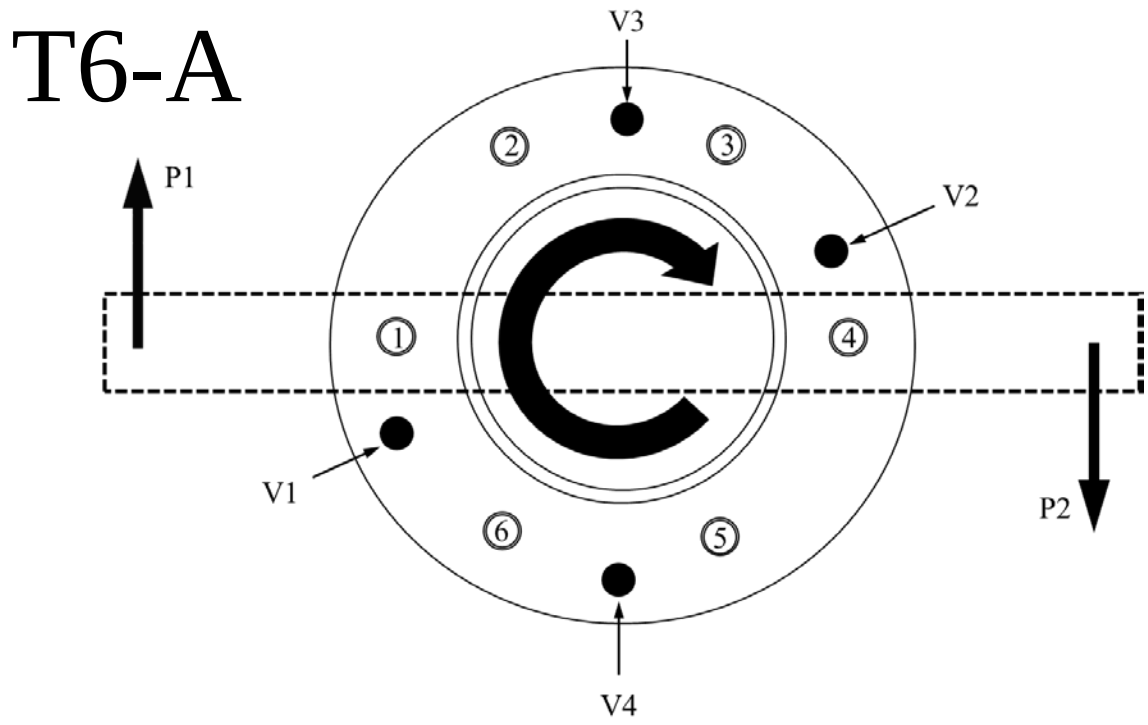

Figure B-28. T6-A (grouted 4 dia. stand-off base plate, 5/8 in. bolts, n = 6) instrumentation schematic

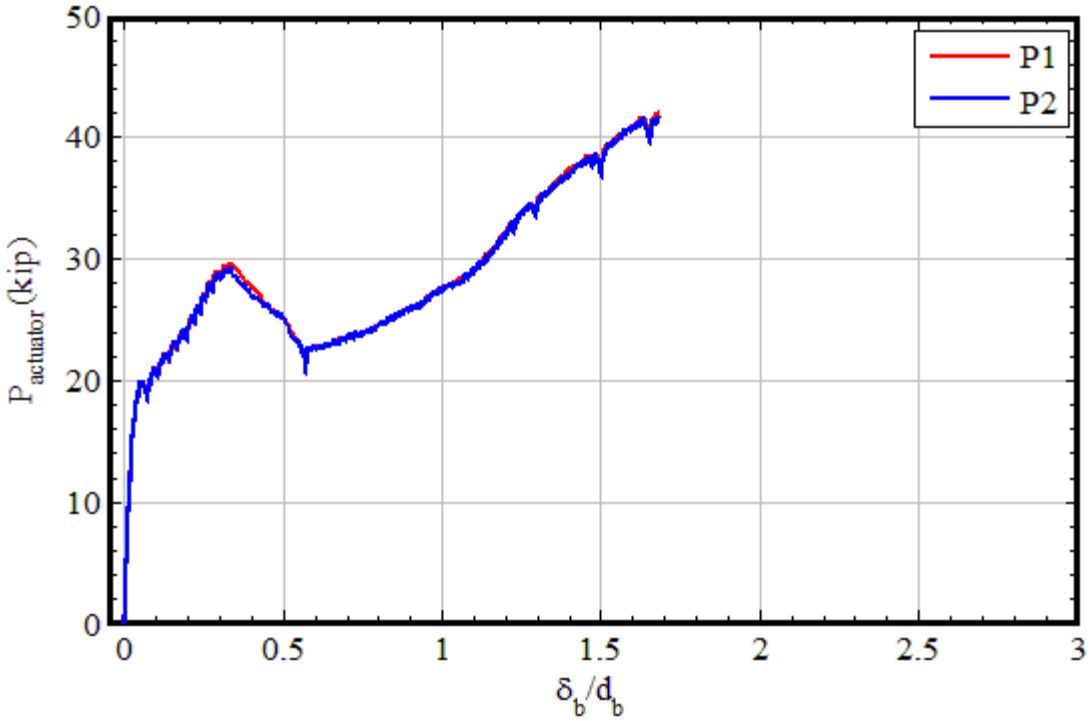

Figure B-29. T6-A individual actuator loads vs. bolt displacement

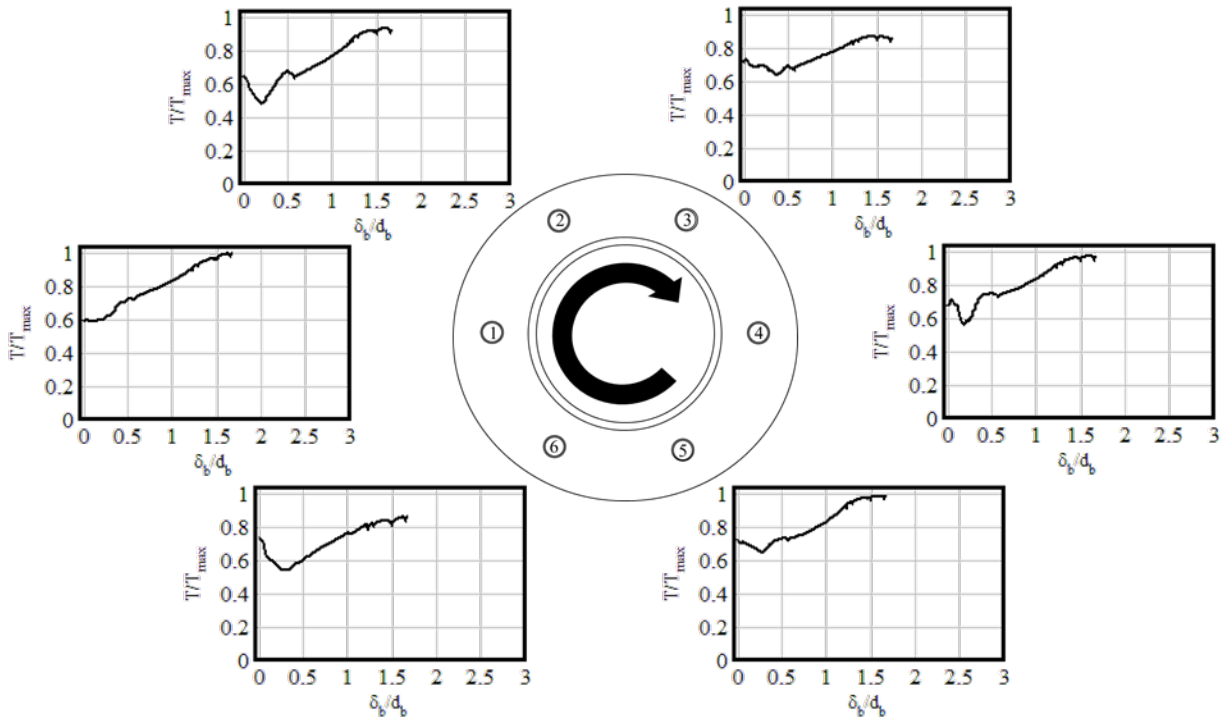

Figure B-30. T6-A bolt tensions vs. bolt displacement

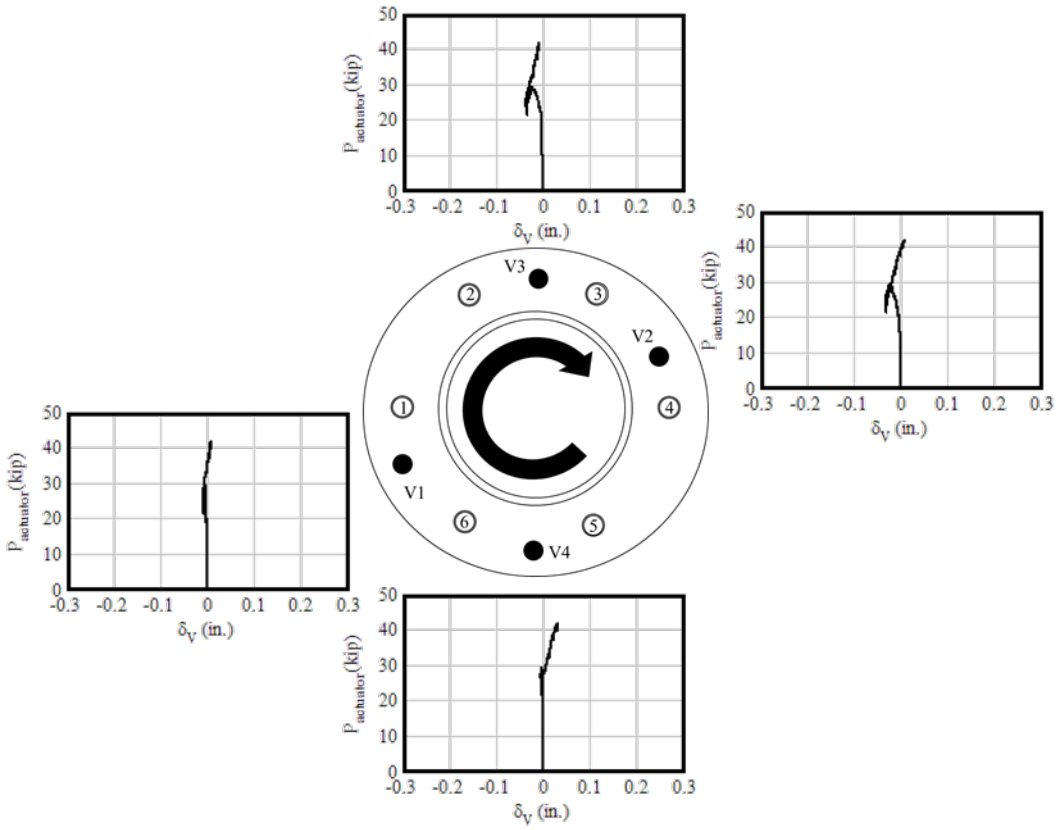

Figure B-31. T6-A average applied load vs. vertical displacements

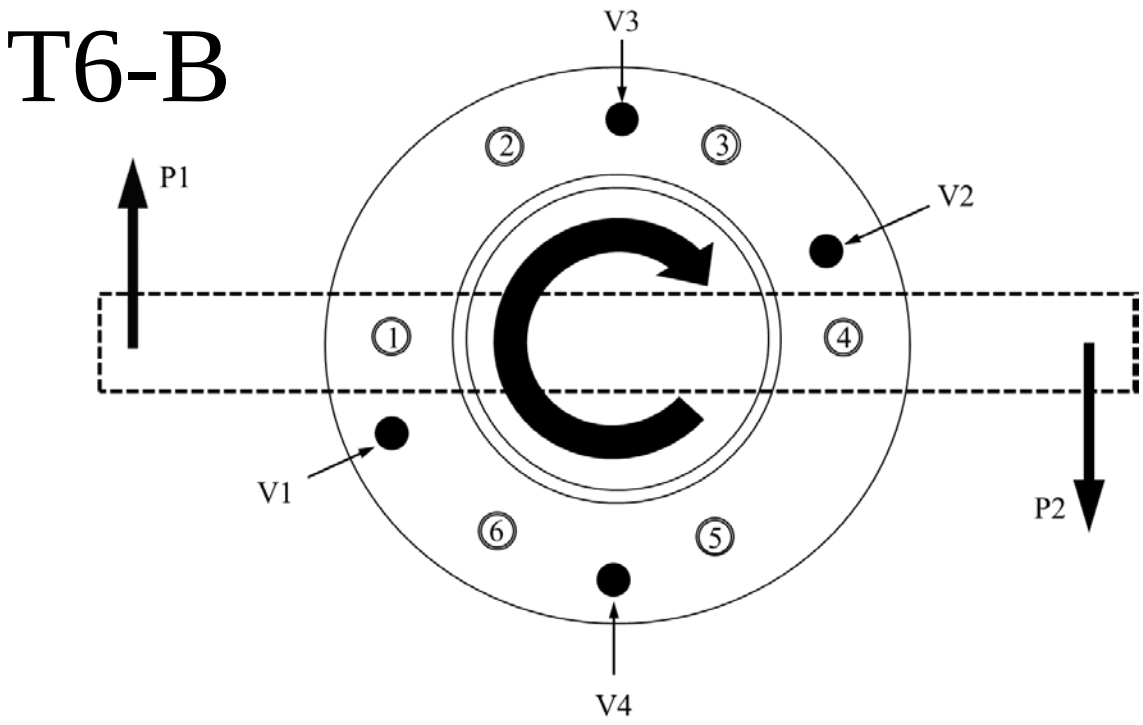

Figure B-32. T6-B (grouted 4 dia. stand-off base plate, 5/8 in. bolts, n = 6) instrumentation schematic

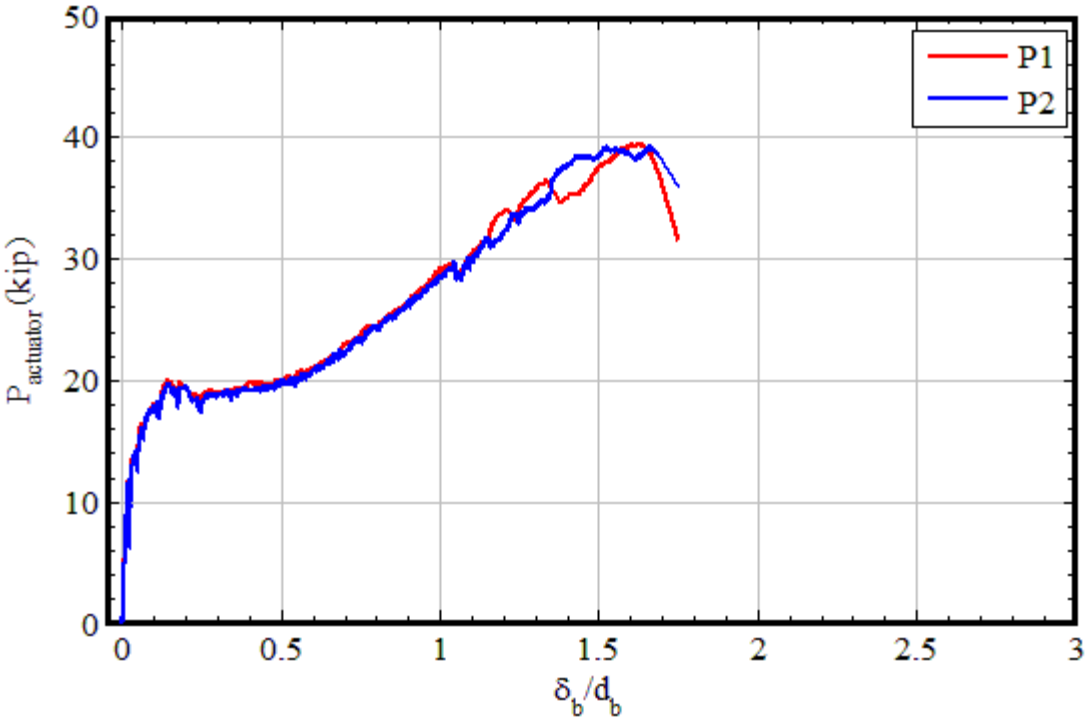

Figure B-33. T6-B individual actuator loads vs. bolt displacement

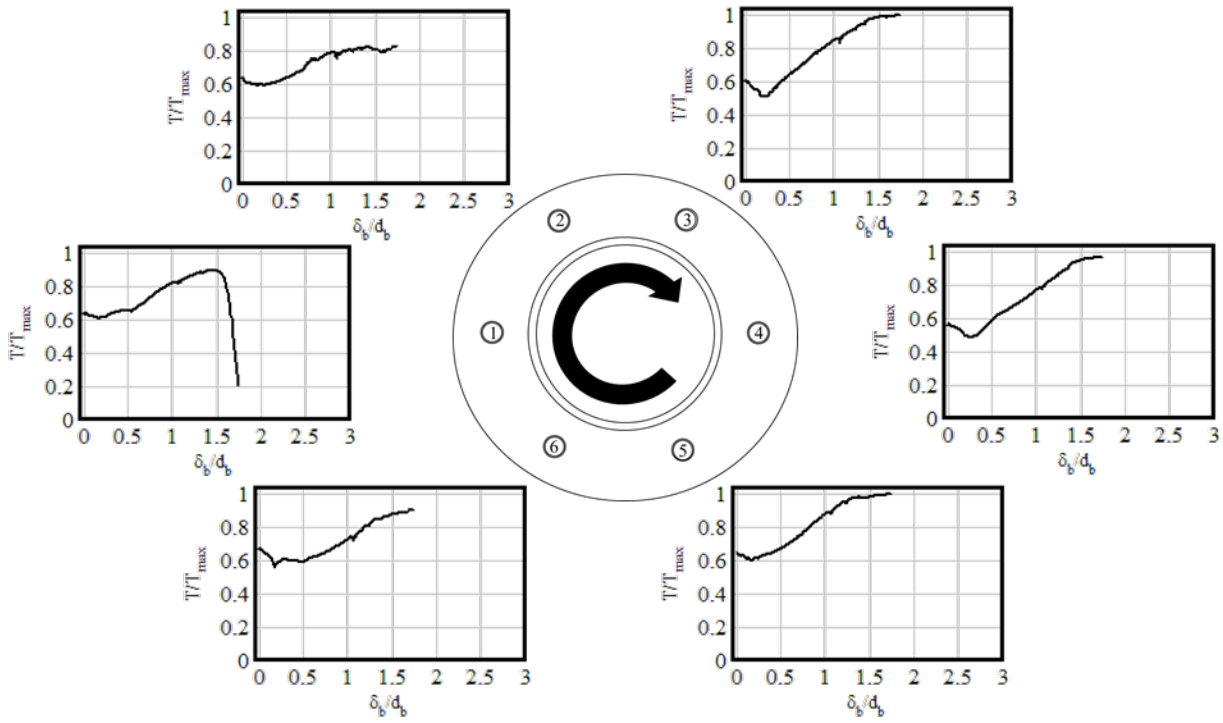

Figure B-34. T6-B bolt tensions vs. bolt displacement

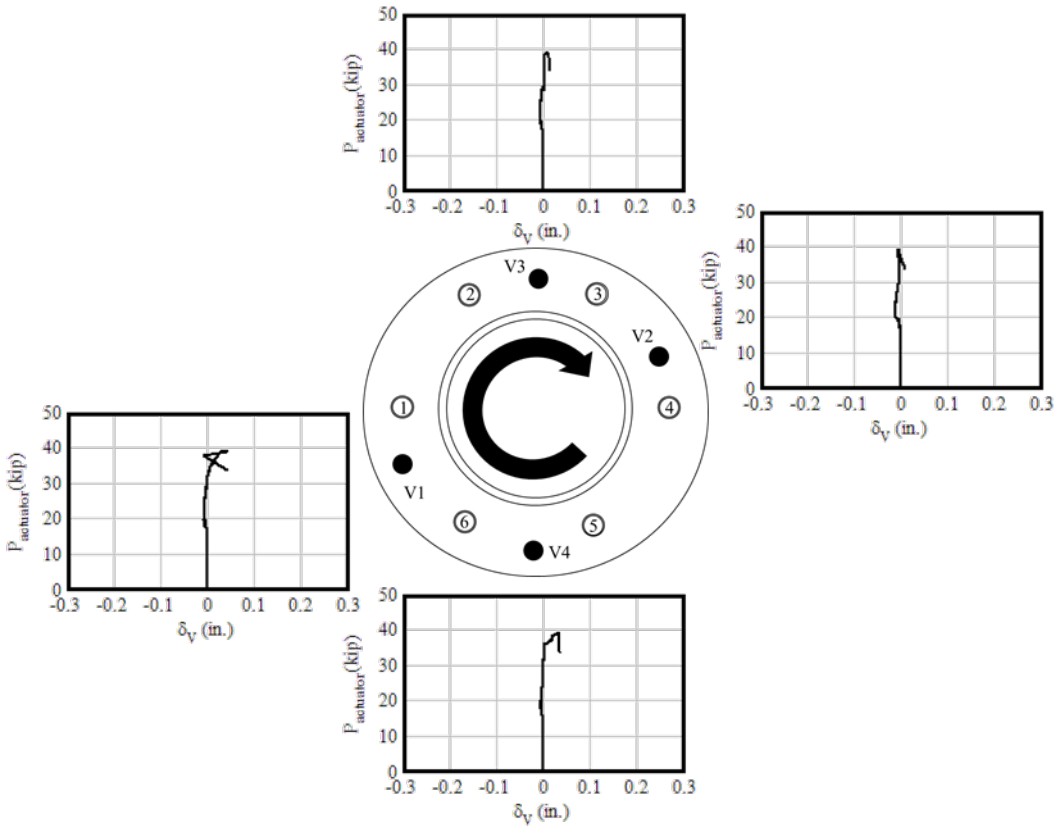

Figure B-35. T6-B average applied load vs. vertical displacements

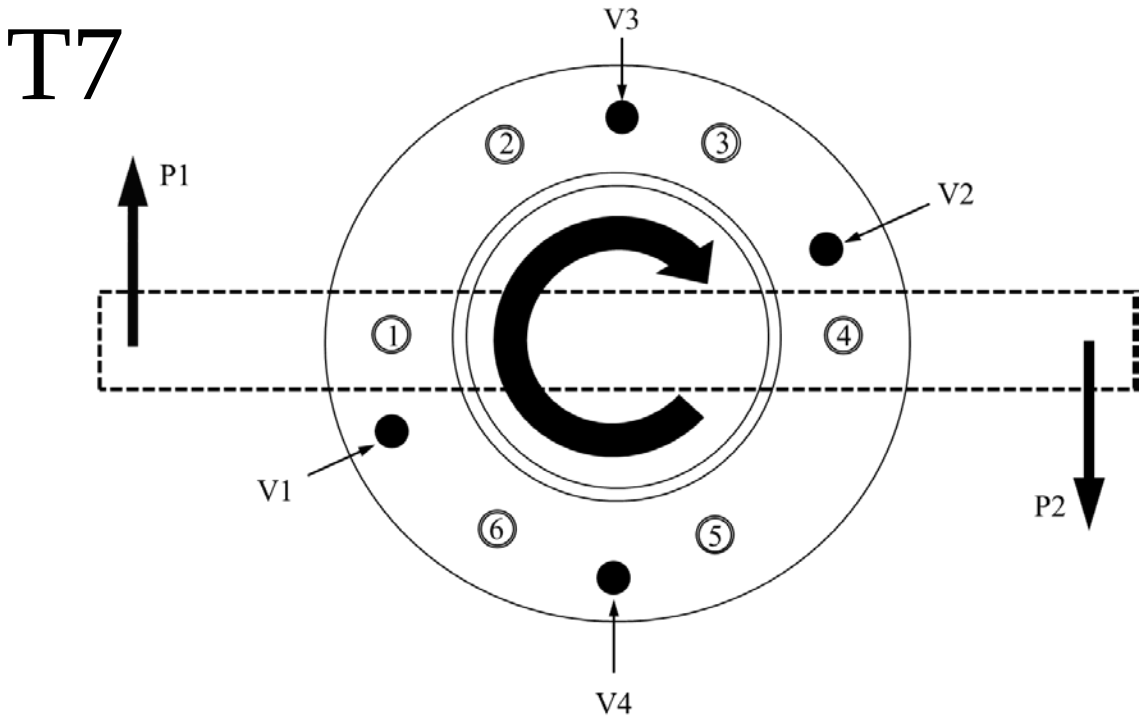

Figure B-36. T7 (grouted 4 dia. stand-off base plate with FRP wrap, 5/8 in. bolts, n = 6) instrumentation schematic

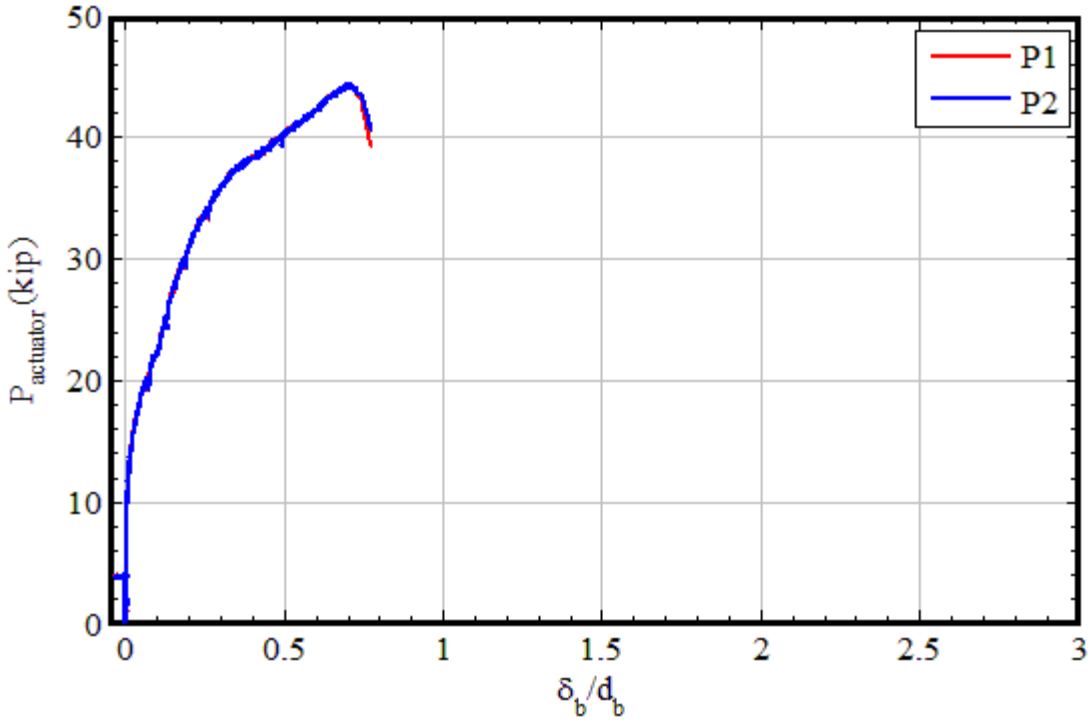

Figure B-37. T7 individual actuator loads vs. bolt displacement

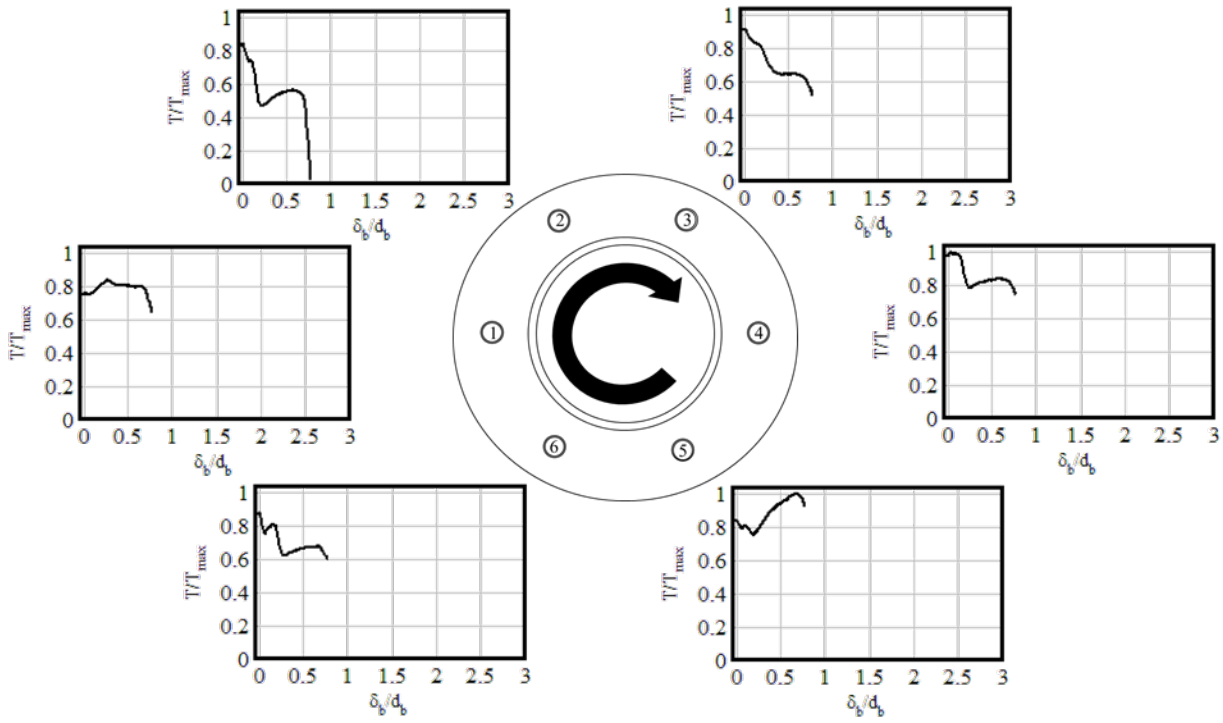

Figure B-38. T7 bolt tensions vs. bolt displacement

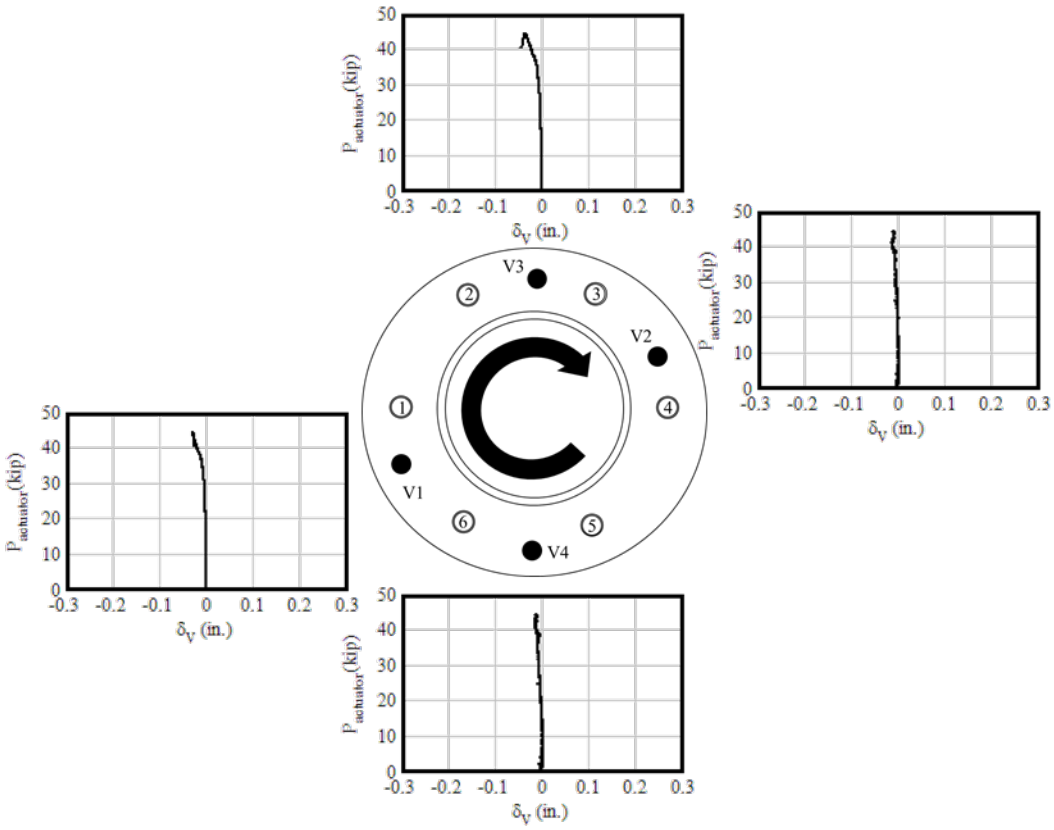

Figure B-39. T7 average applied load vs. vertical displacements

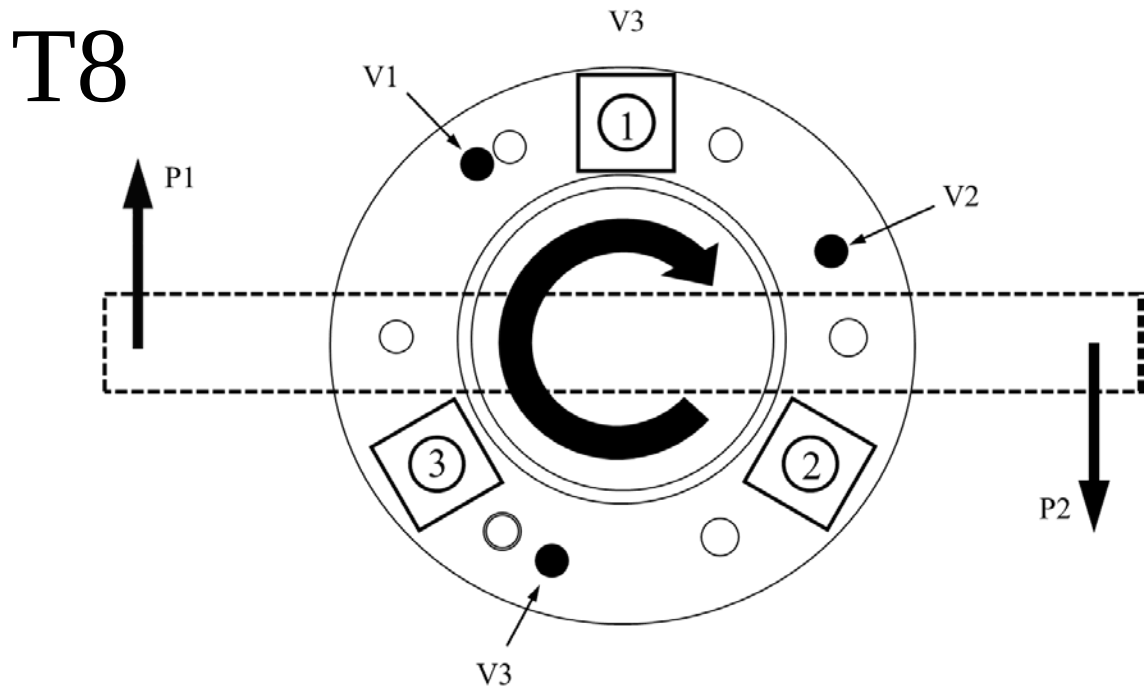

Figure B-40. T8 (flush-mounted base plate, 1 in. bolts, n = 3) instrumentation schematic

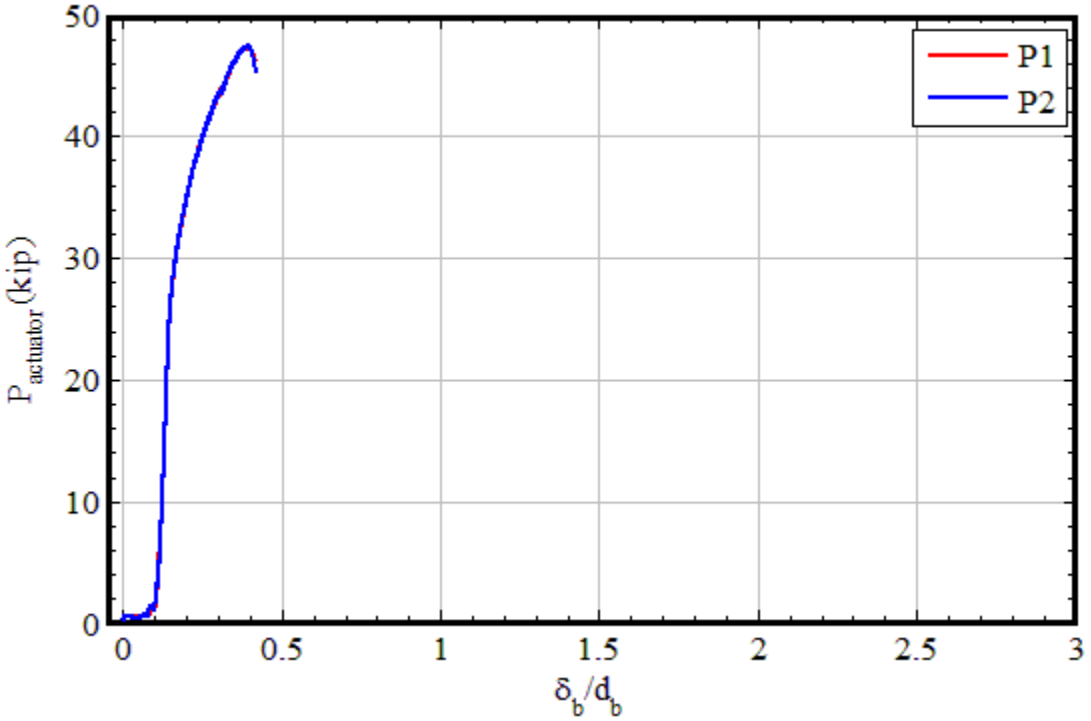

Figure B-41. T8 individual actuator loads vs. bolt displacement

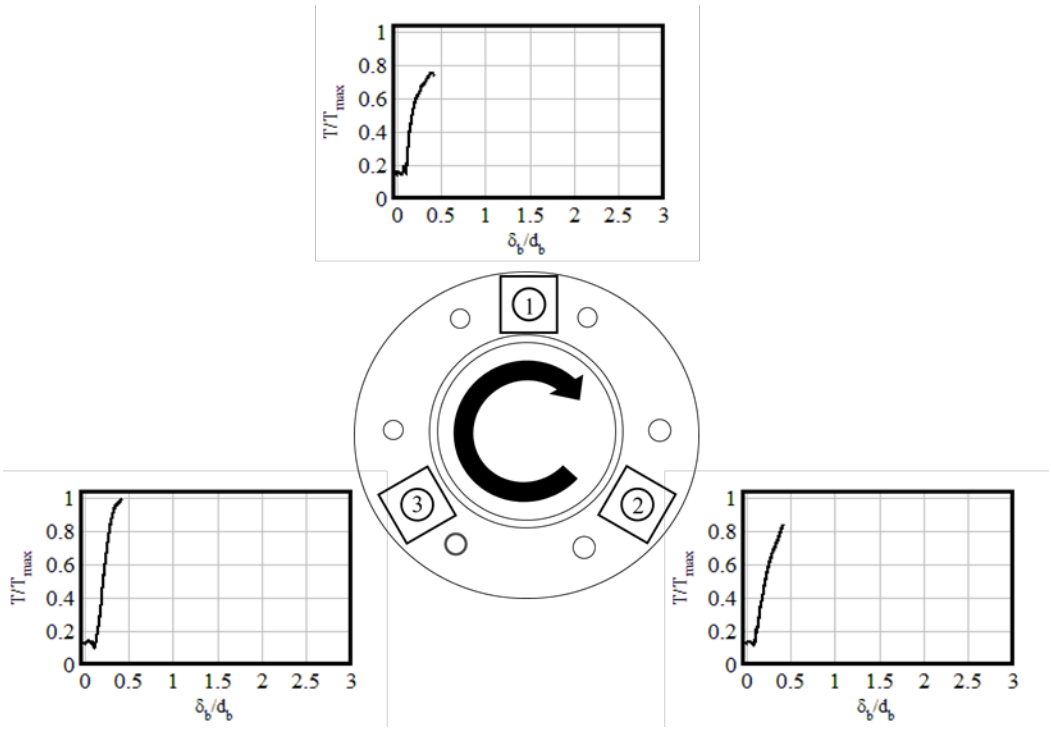

Figure B-42. T8 bolt tensions vs. bolt displacement

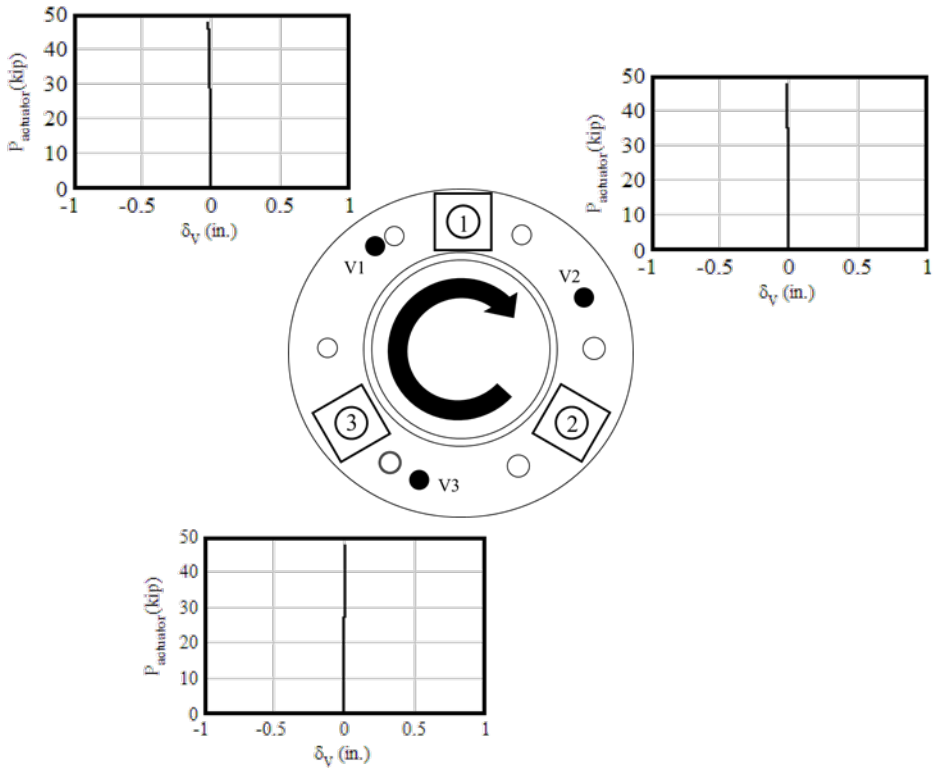

Figure B-43. T8 average applied load vs. vertical displacements

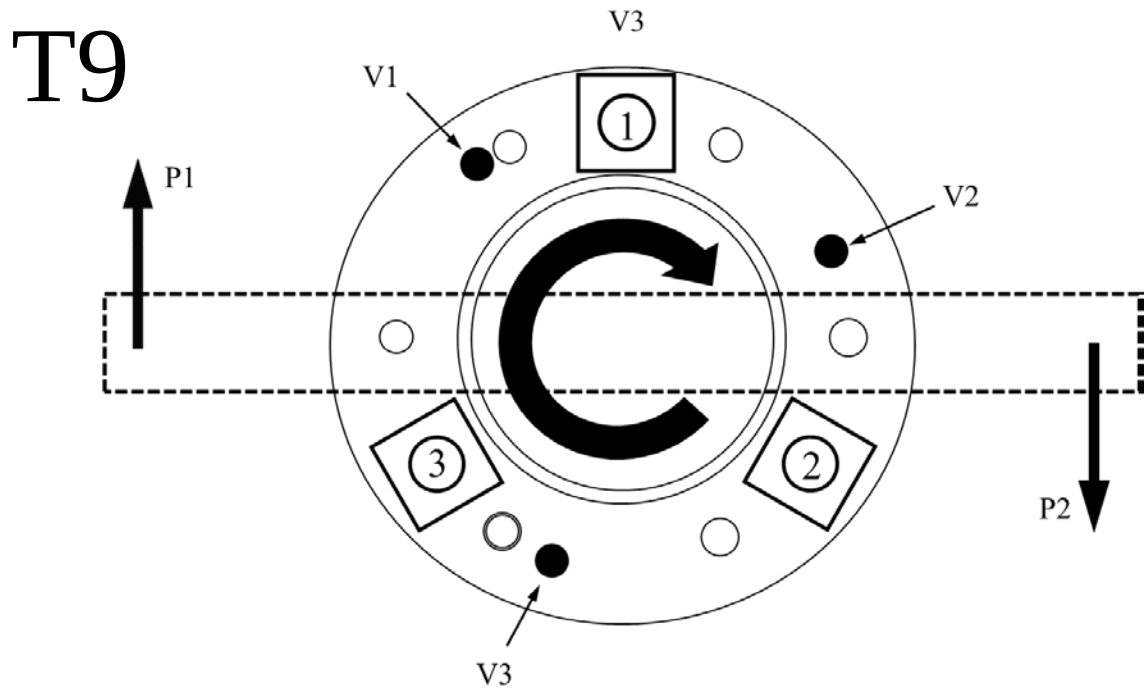

Figure B-44. T9 (ungrouted 2 dia. stand-off base plate, 1 in. bolts, n = 3) instrumentation schematic

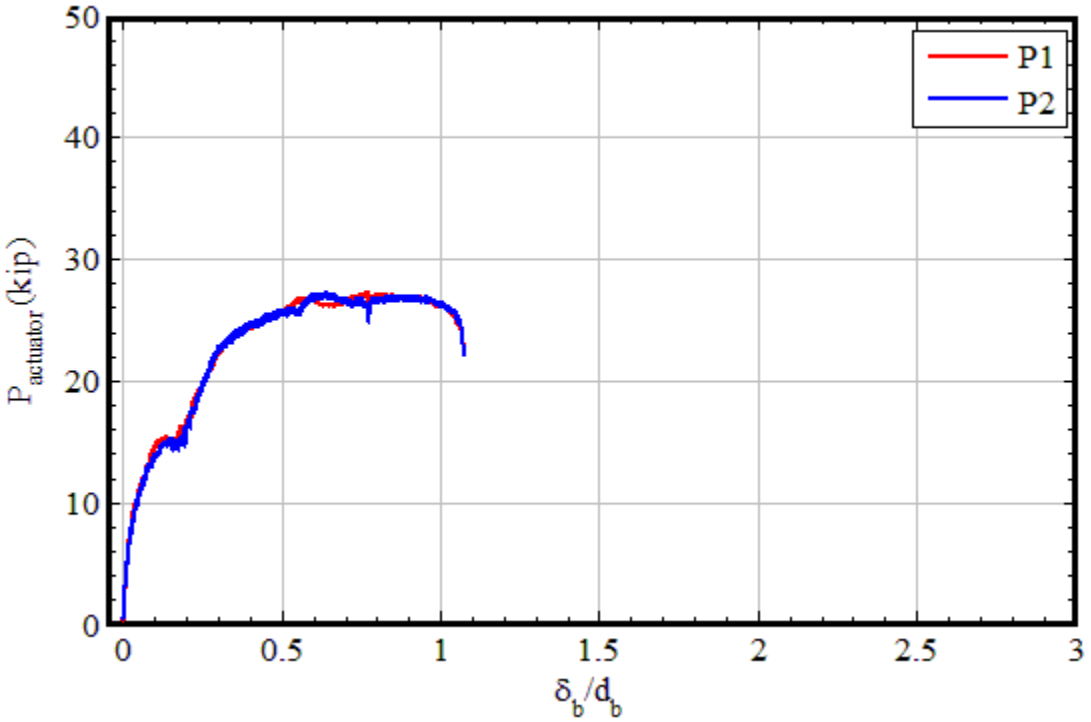

Figure B-45. T9 individual actuator loads vs. bolt displacement

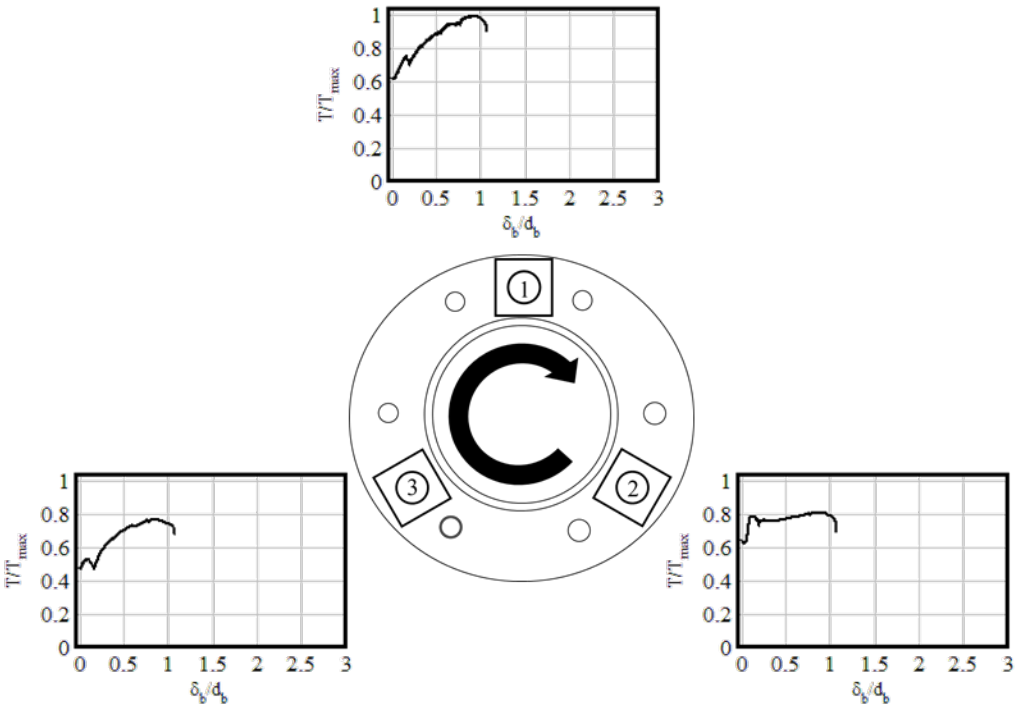

Figure B-46. T9 bolt tensions vs. bolt displacement

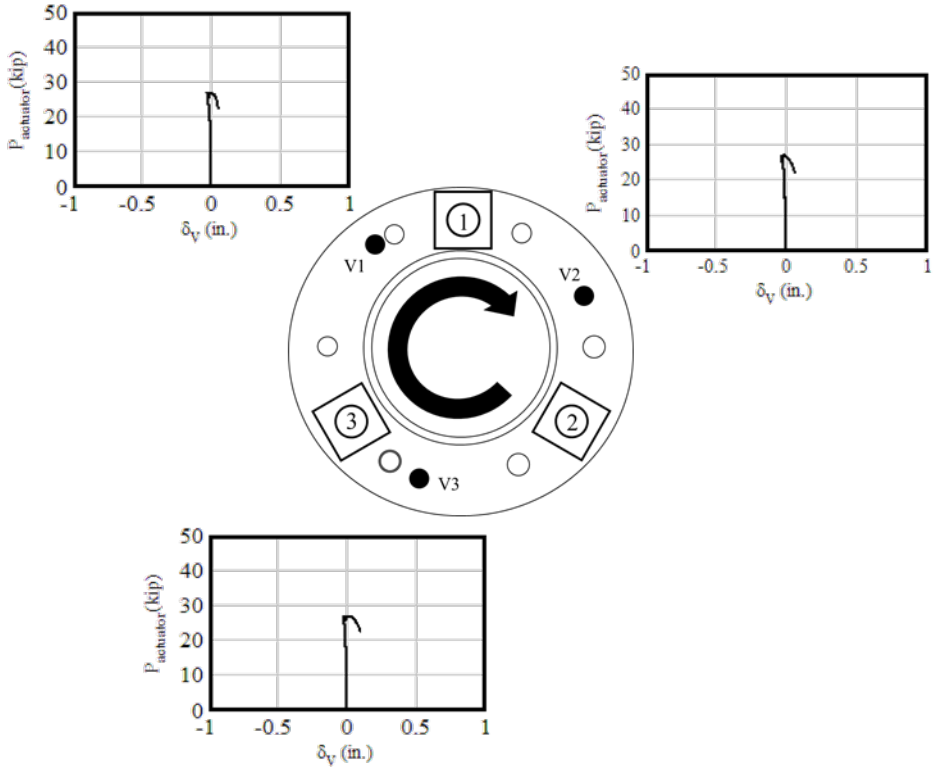

Figure B-47. T9 average applied load vs. vertical displacements

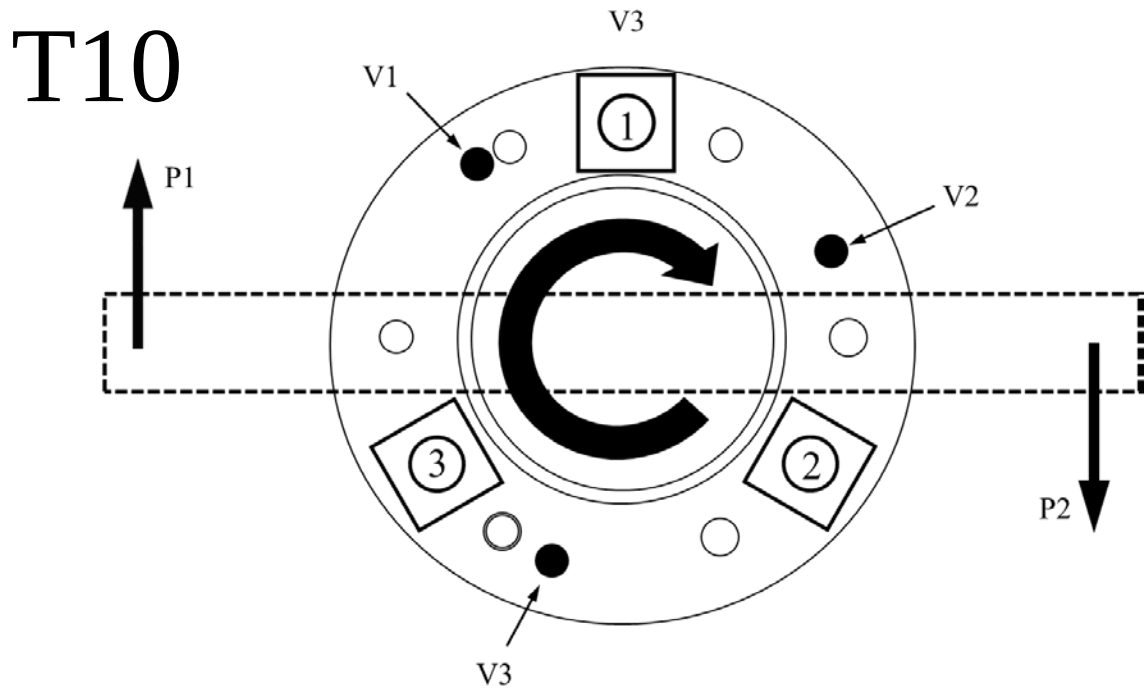

Figure B-48. T10 (ungrouted 4 dia. stand-off base plate, 1 in. bolts, n = 3) instrumentation schematic

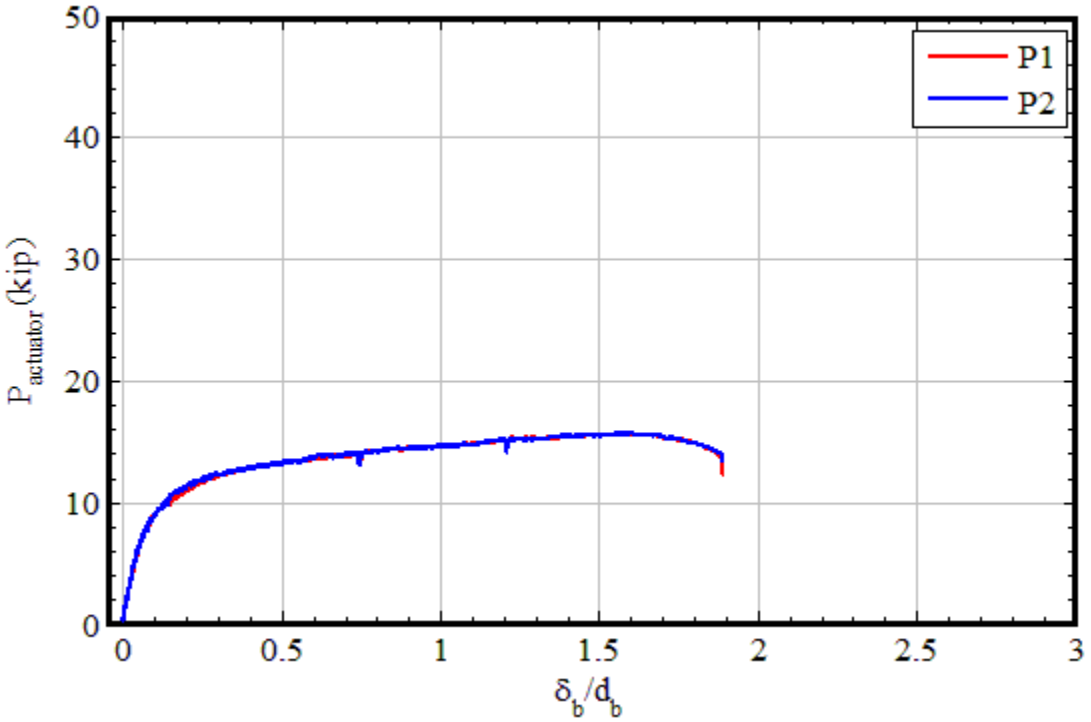

Figure B-49. T10 individual actuator loads vs. bolt displacement

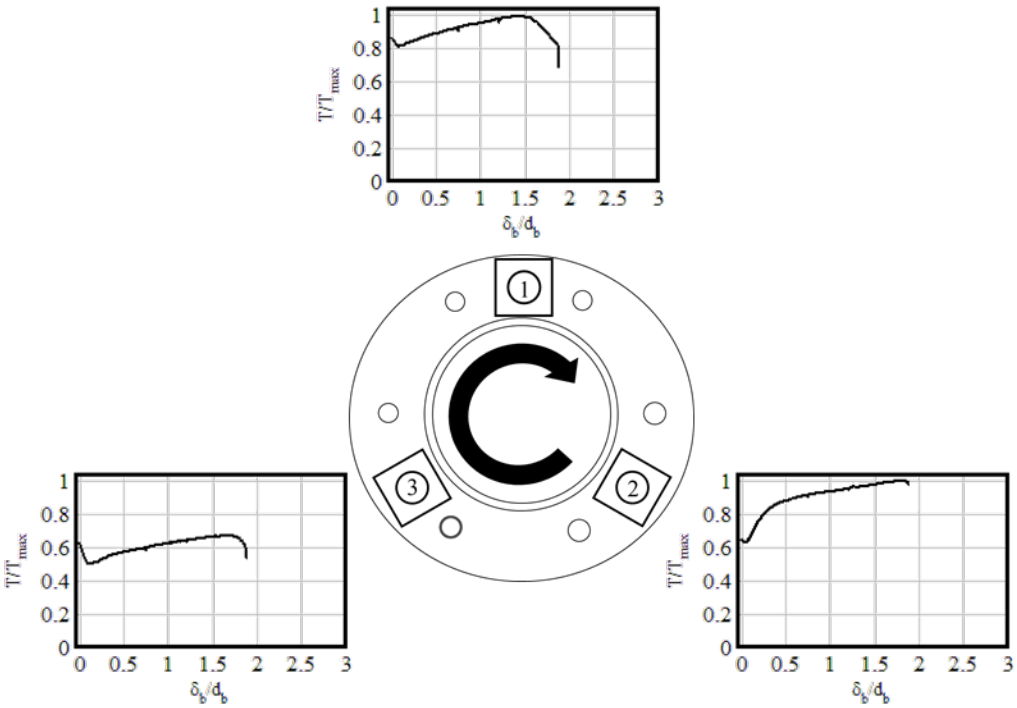

Figure B-50. T10 bolt tensions vs. bolt displacement

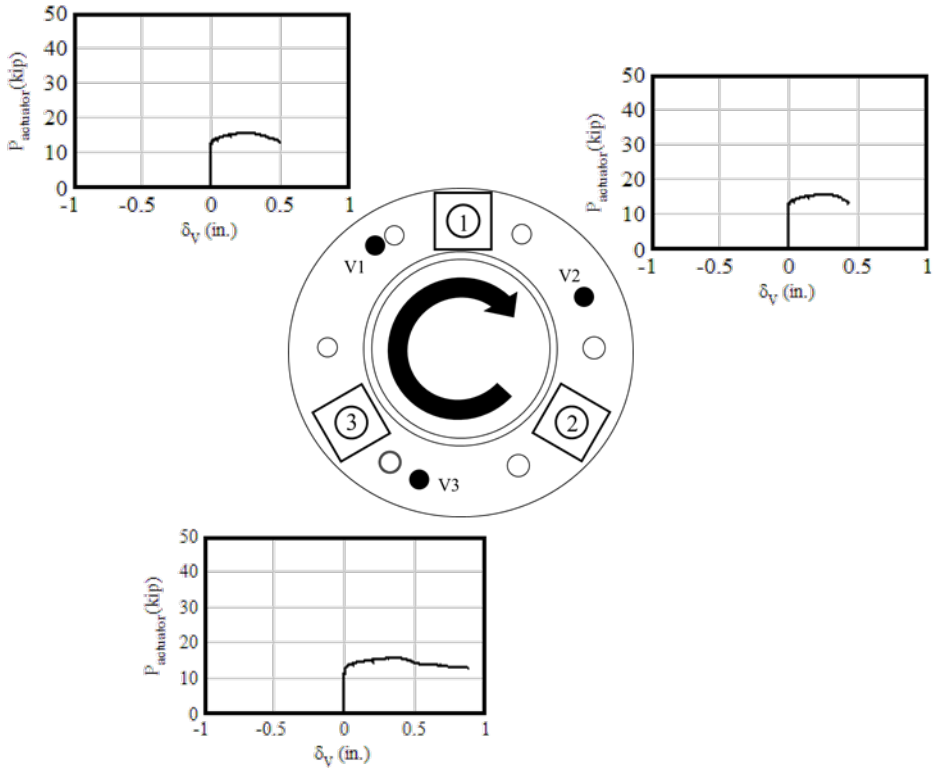

Figure B-51. T10 average applied load vs. vertical displacements

APPENDIX C
LOAD-DISPLACEMENT BEHAVIOR OF PHASE 3 TESTS

This appendix contains the locations of instrumentation, applied actuator load vs. bolt displacement from string potentiometer readings, bolt tension vs. bolt displacement graphs for every tension load cell, and applied actuator load vs. displacement for every vertically and horizontally oriented LVDT. Test FS1 contained a different vertical LVDT layout than the three subsequent tests; at the end of the test LVDT V1 was run into by the pipe loading apparatus, making its position unviable. Thus, the vertically oriented LVTDs were shifted away from the movement of the pipe in the remaining tests. For the same reasons presented in the Appendix B description, bolt tension readings are represented as values normalized by the maximum reading of all bolts within an individual test.

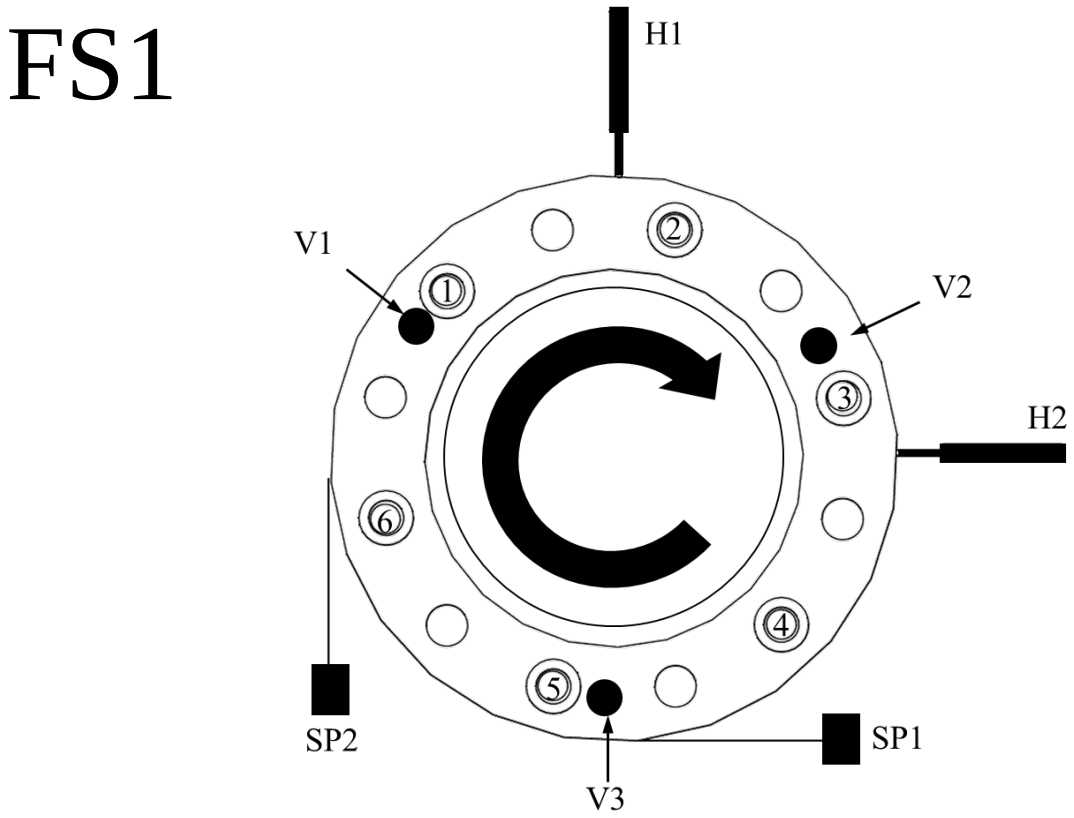

Figure C-1. FS1 (ungrouted 2.3 dia. stand-off base plate, 1.25 in. bolts, n = 6) instrumentation schematic

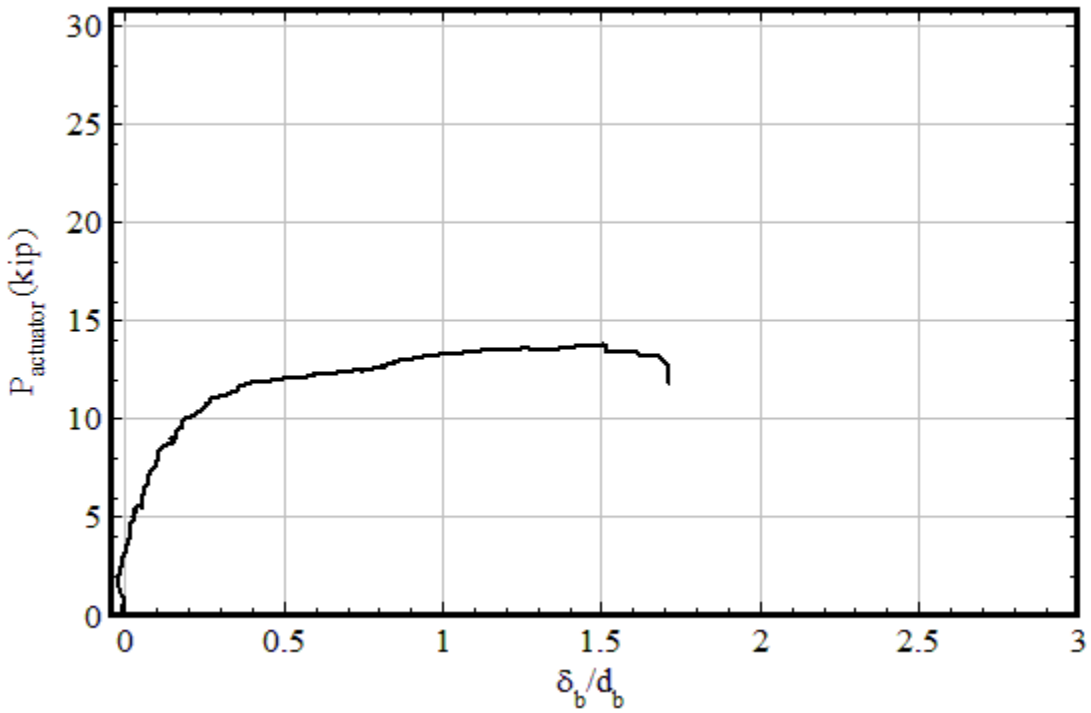

Figure C-2. FS1 actuator applied load vs. average bolt displacement

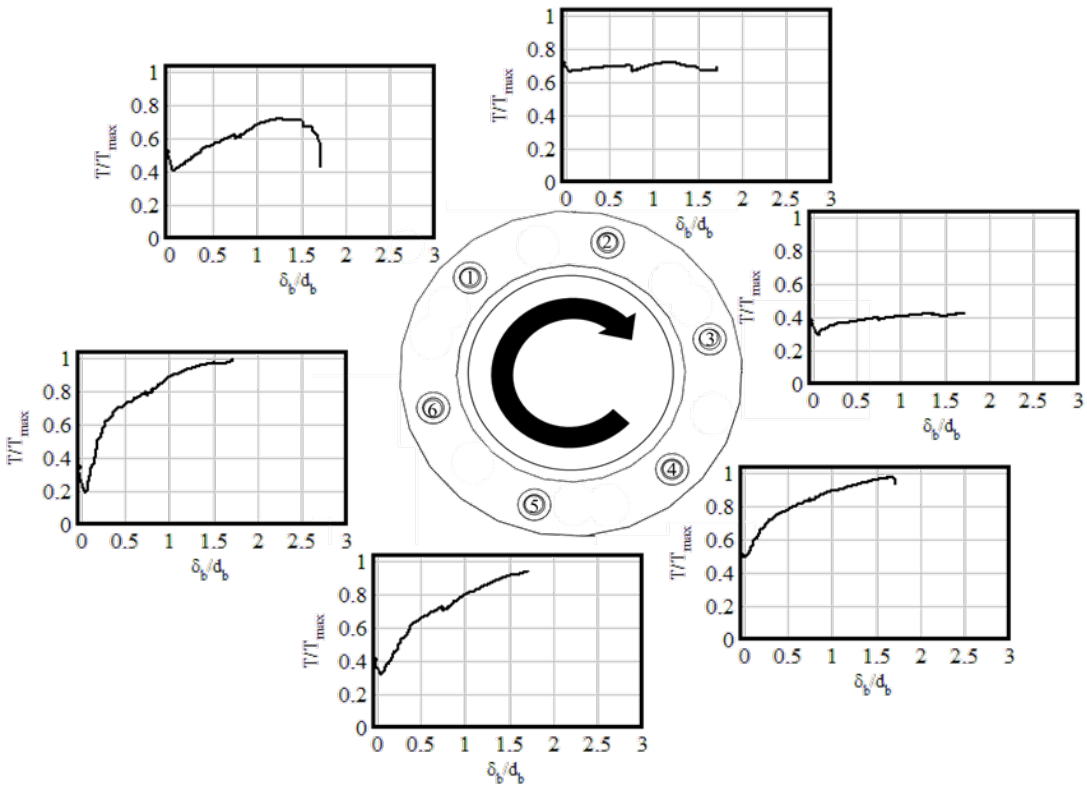

Figure C-3. FS1 bolt tensions vs. bolt displacement

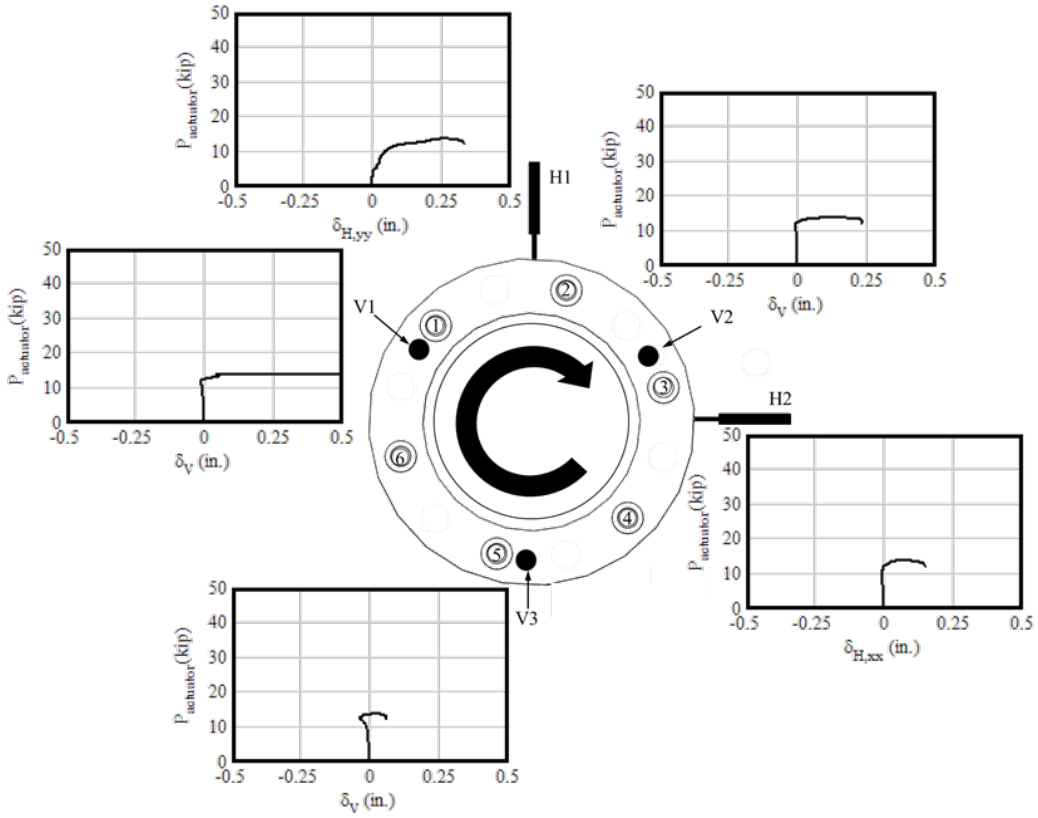

Figure C-4. FS1 applied load vs. vertical and horizontal displacements

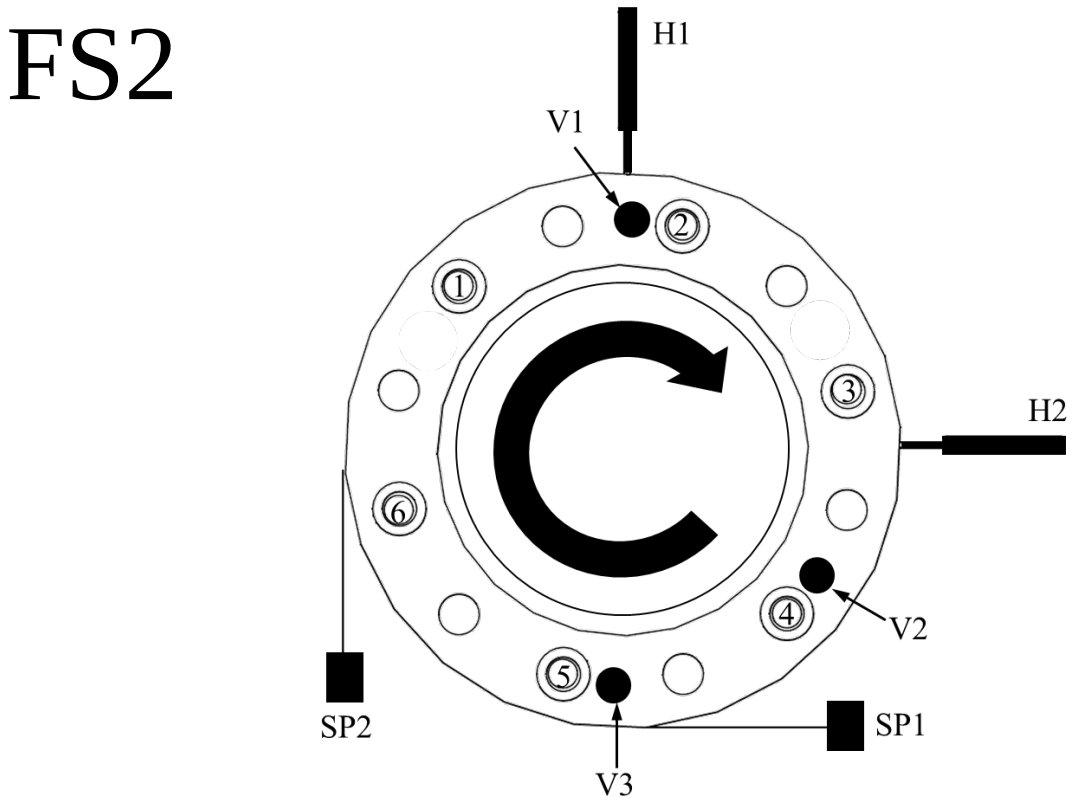

Figure C-5. FS2 (grouted 2.3 dia. stand-off base plate, 1.25 in. bolts, n = 6) instrumentation schematic

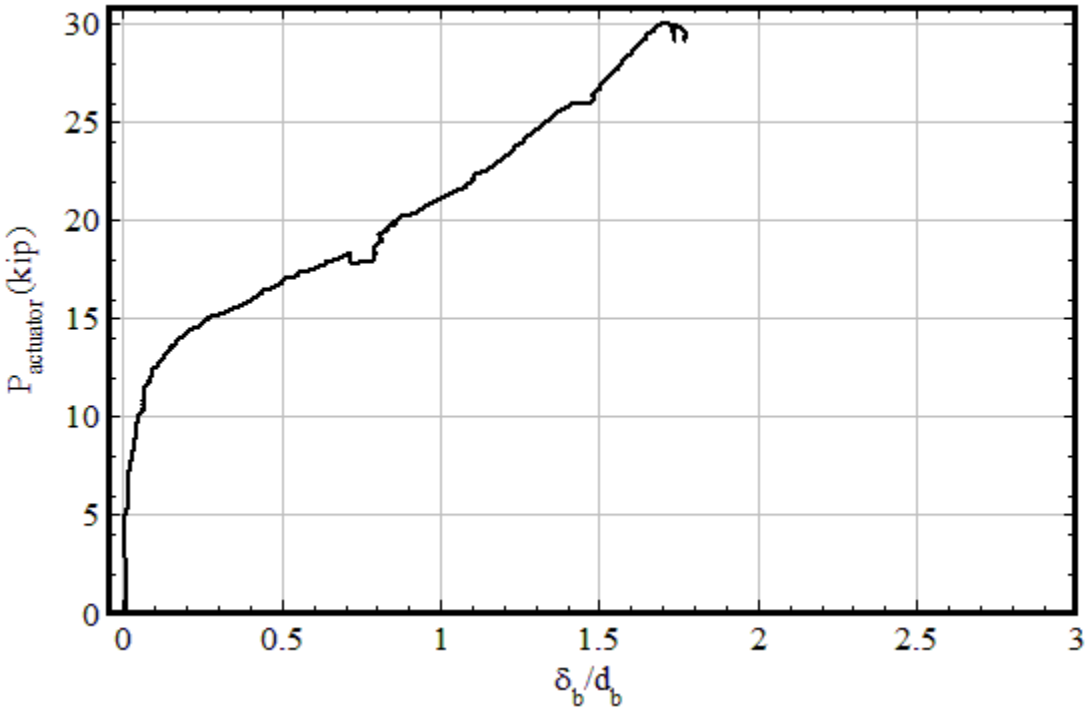

Figure C-6. FS2 individual actuator loads vs. average bolt displacement

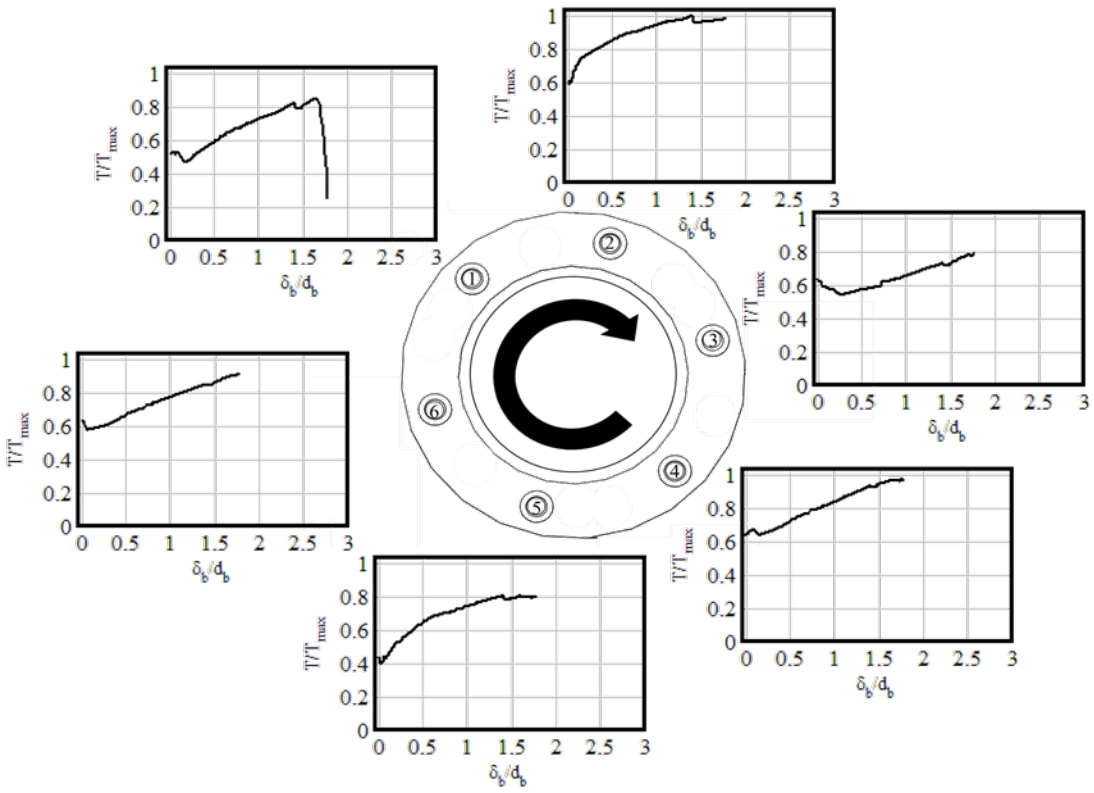

Figure C-7. FS2 bolt tensions vs. bolt displacement

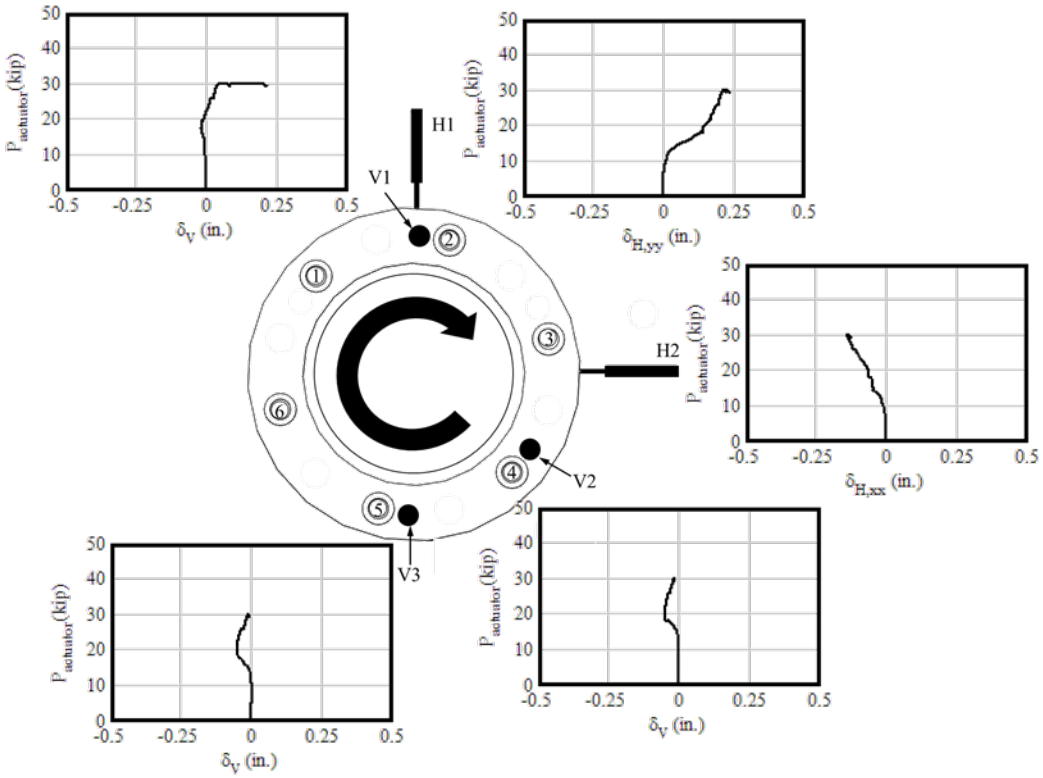

Figure C-8. FS2 applied load vs. vertical and horizontal displacements

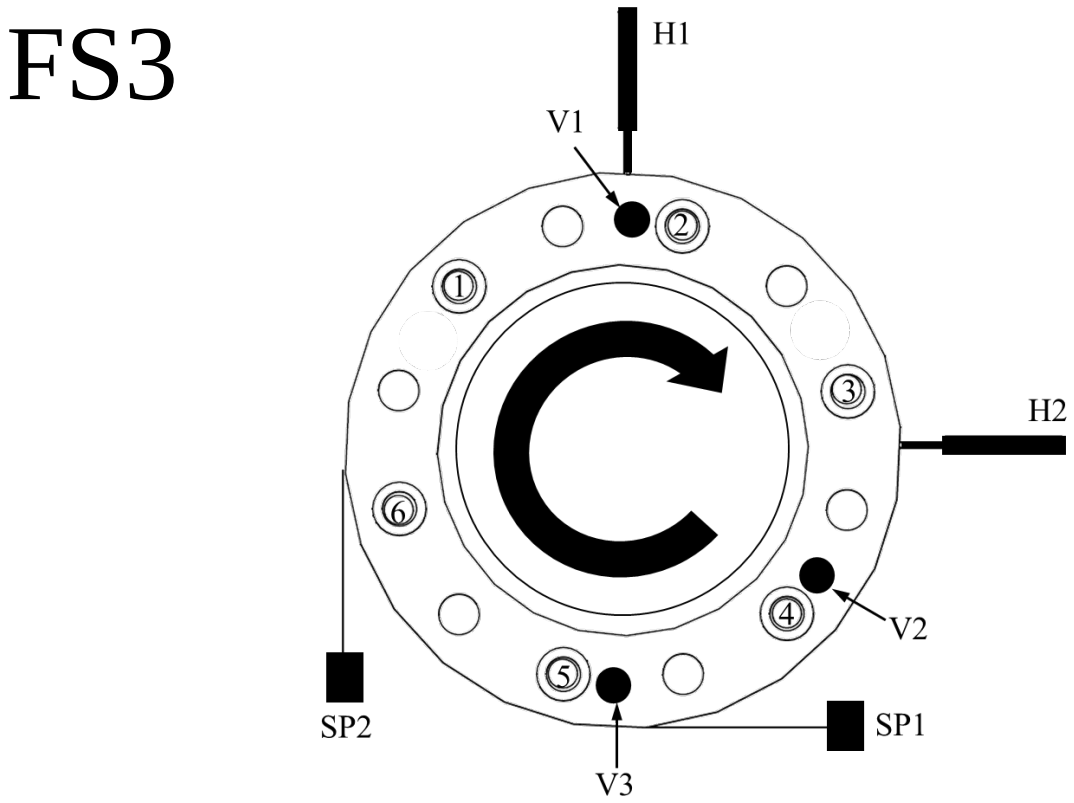

Figure C-9. FS3 (grouted 4.3 dia. stand-off base plate,1.25 in. bolts, n = 6) instrumentation schematic

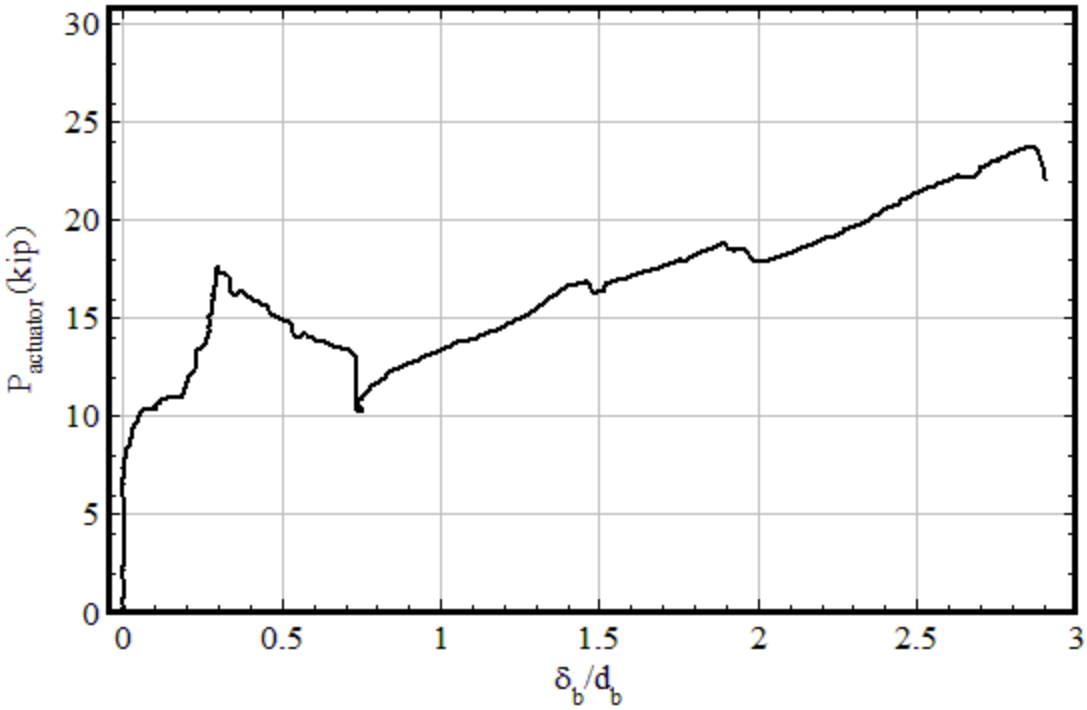

Figure C-10. FS3 actuator load vs. average bolt displacement

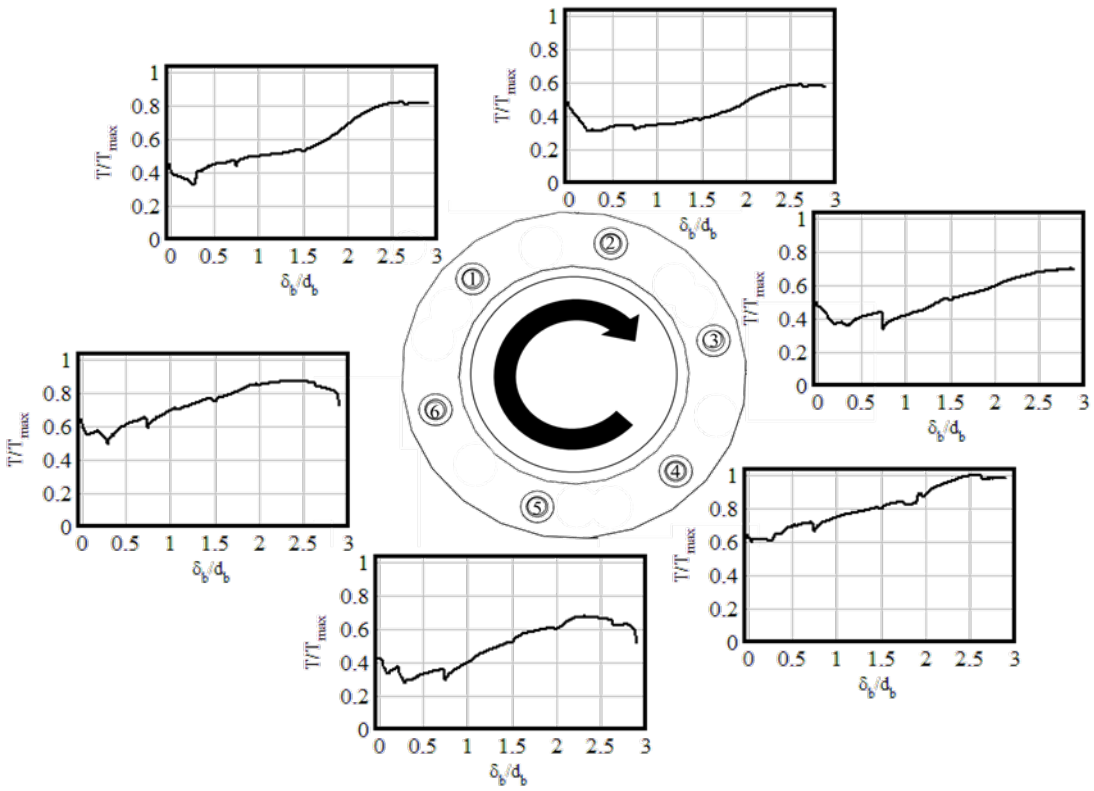

Figure C-11. FS3 bolt tensions vs. bolt displacement

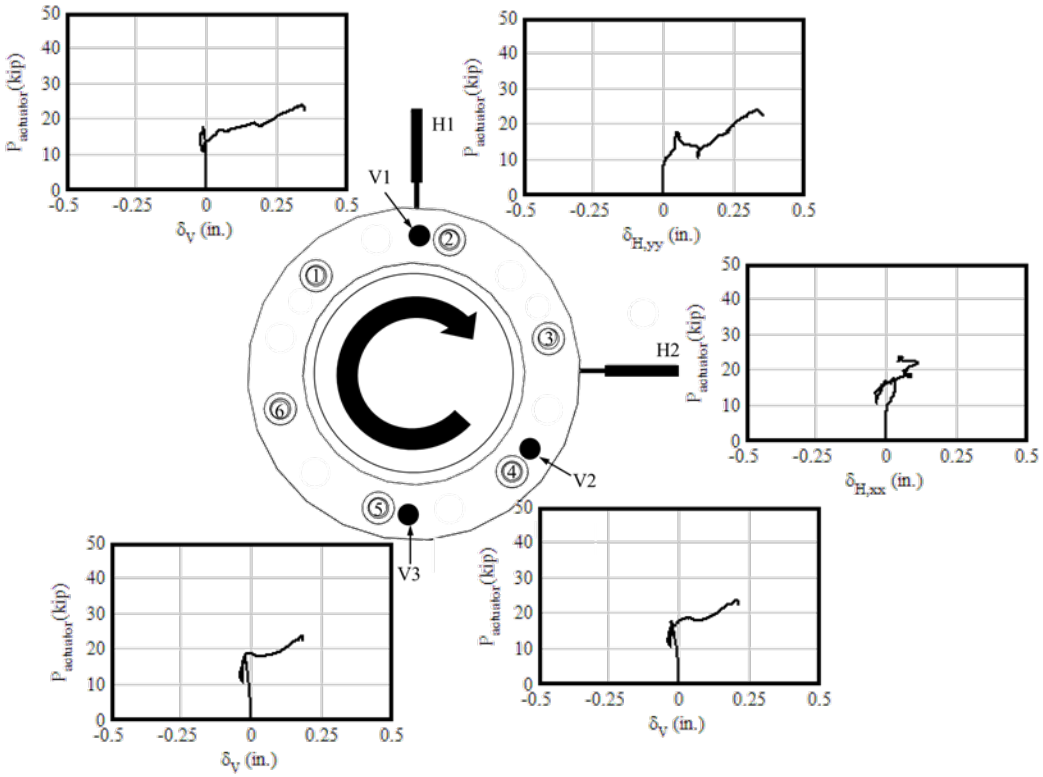

Figure C-12. FS3 applied load vs. vertical and horizontal displacements

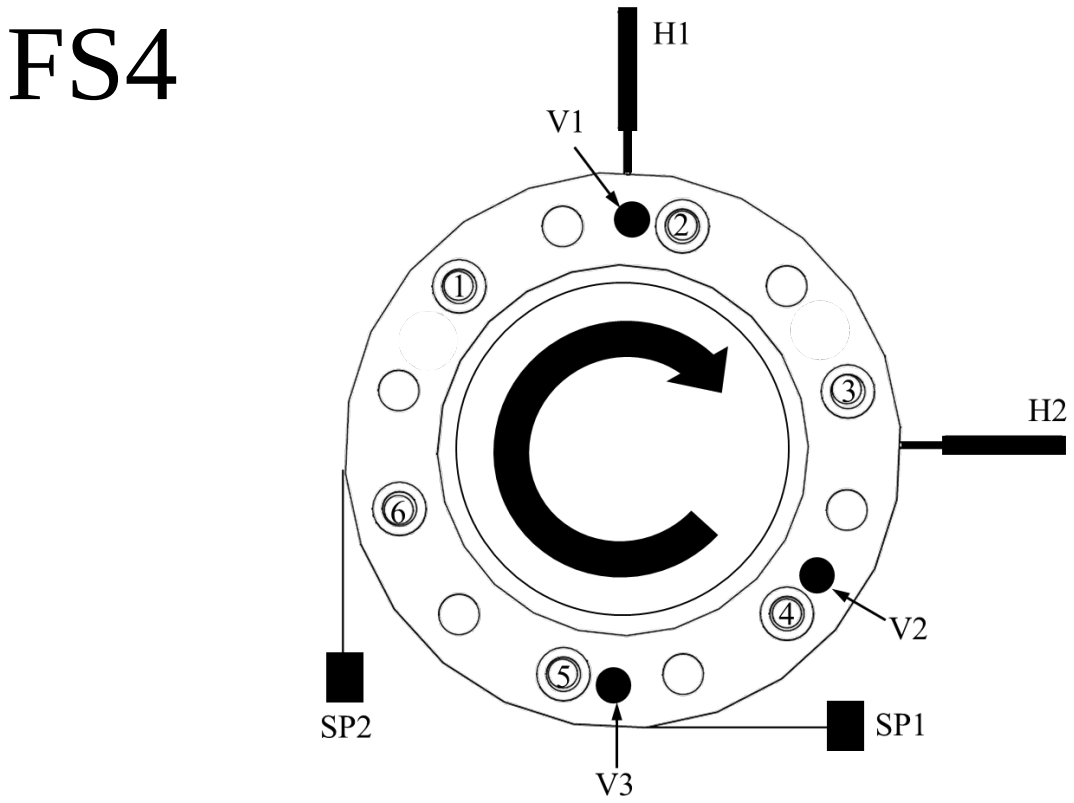

Figure C-13. FS4 (grouted 4.3 dia. stand-off base plate, 1.25 in. bolts, n = 6) instrumentation schematic

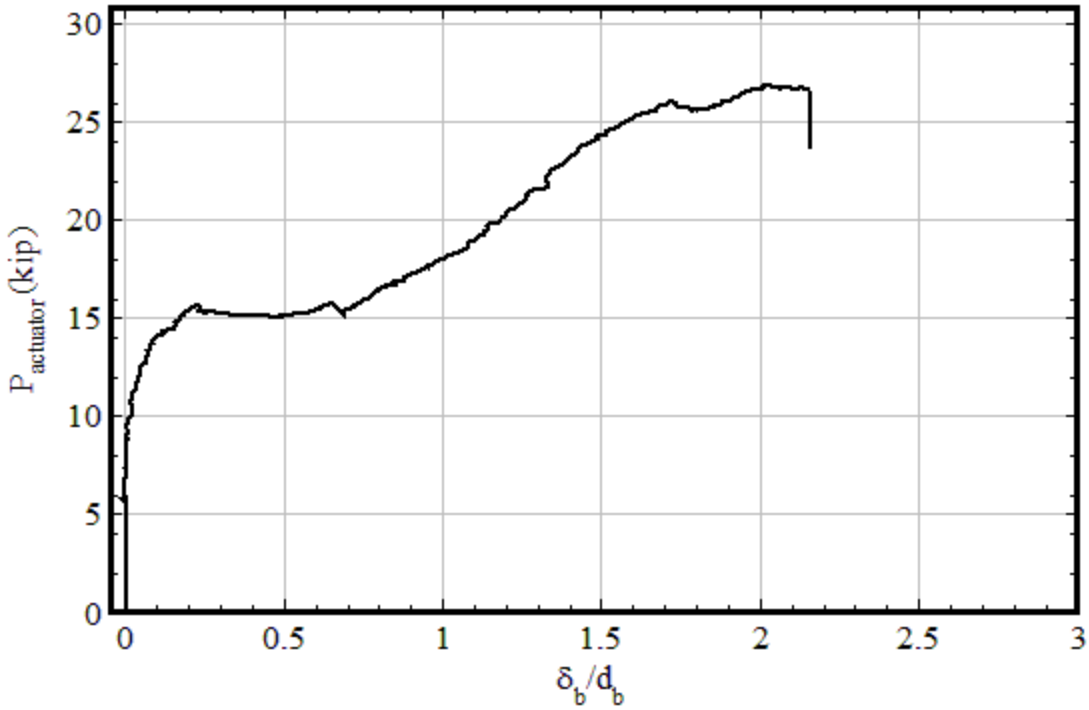

Figure C-14. FS4 actuator load vs. average bolt displacement

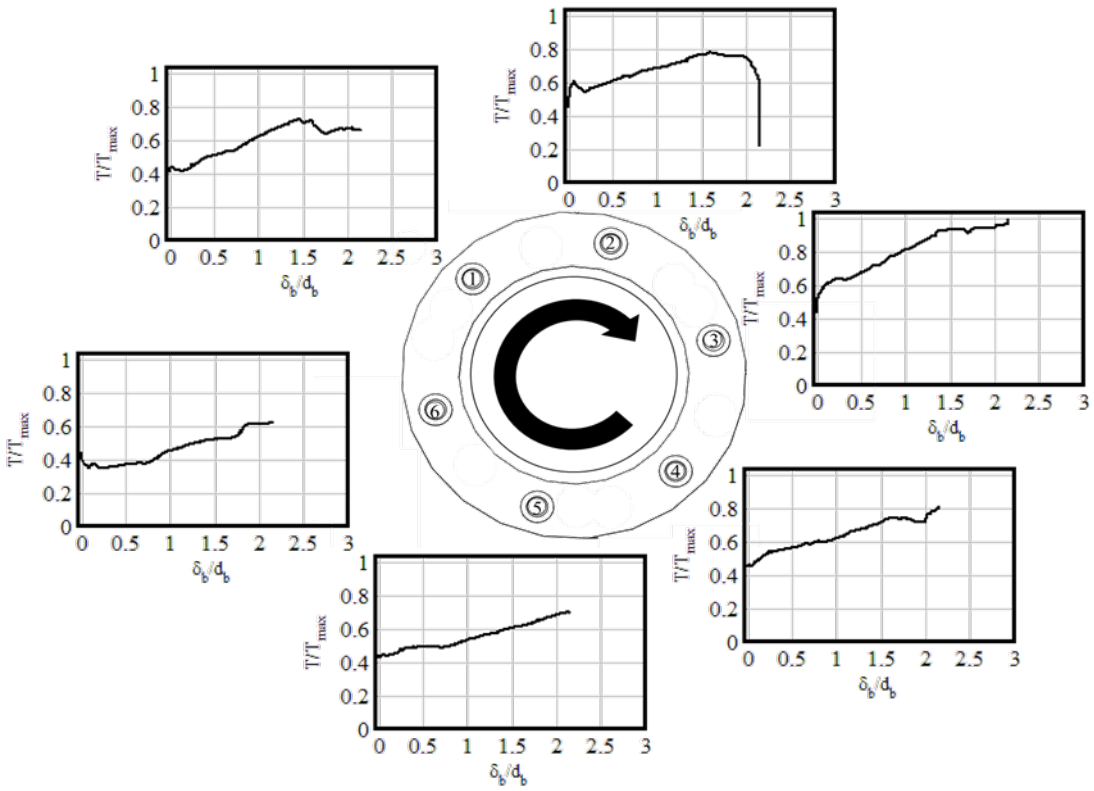

Figure C-15. FS4 bolt tensions vs. bolt displacement

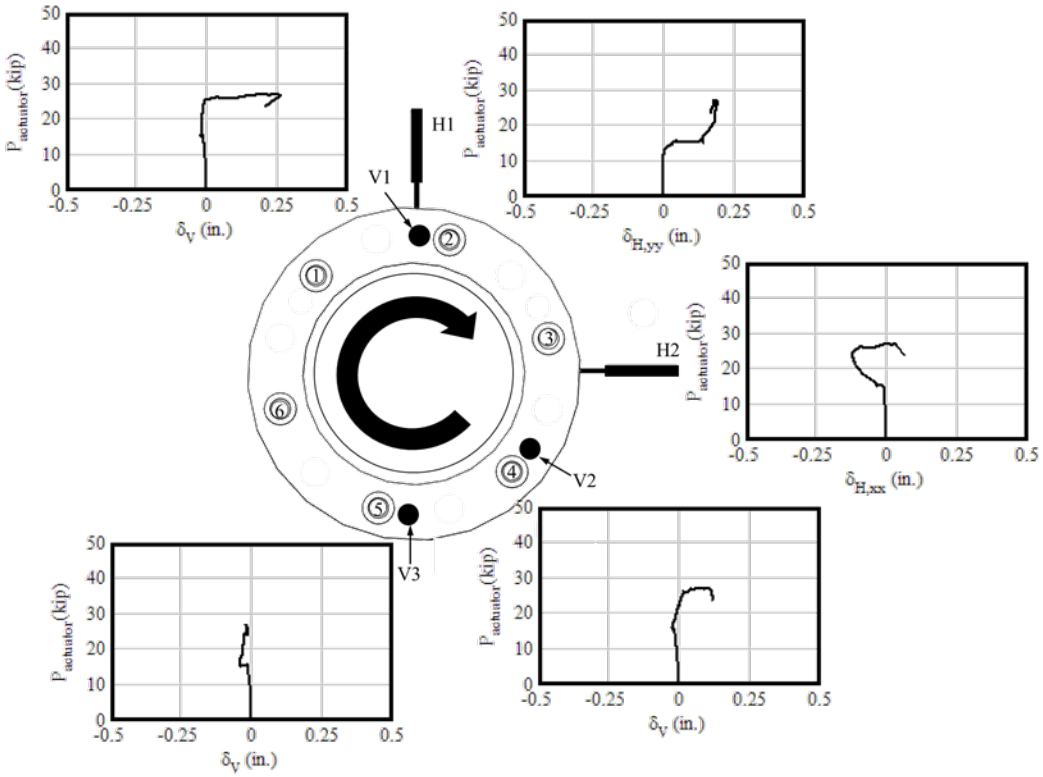

Figure C-16. FS4 applied load vs. vertical and horizontal displacements

APPENDIX D
DRAFT DESIGN GUIDELINES FOR STEEL STRENGTH OF ANCHOR BOLTS

1.x ANCHOR BOLT STEEL STRENGTH IN ANNULAR BASE PLATES

1.x.1 General

Scope: This document covers LRFD design for the steel strength of anchor bolts in FDOT structures using annular base plates, which fall into any one of the following three categories:

A. ***Flush-mounted Base Plates.*** The base plate is set directly onto the concrete surface. Nuts and/or washers fasten the base plate to anchor bolts.
B. ***Ungrouted Stand-off Base Plates.*** Leveling nuts and washers are placed on the anchor bolts protruding from the concrete. The base plate is set on the leveling nuts, then nuts and washers are installed on the anchor bolts extending through the top of the base plate. This is often called a "double-nut" connection.
C. ***Grouted Stand-off Base Plates.*** The base plate is first leveled on leveling nuts. After the base plate has been erected and fastened, a non-shrink grout pad is placed between the base plate and the concrete surface.

1.x.2 Determination of Anchor Bolt Steel Strength in Annular Base Plates

A. Notation

$N_{ua,g}$ = factored axial force acting on the base plate. [kips]
$V_{ua,g}$ = resolved factored direct shear acting on the base plate. [kips]
$V_{uax,g}$, $V_{uaz,g}$ = factored direct shear components acting on the base plate. [kips]
$M_{ua,g}$ = resolved factored moment acting on the base plate. [kip-in]
$M_{uax,g}$, $M_{uaz,g}$ = factored overturning moment components acting on the base plate. [kip-in]
$M_{uay,g}$ = factored torsion force acting on the base plate. [kip-in]

n = number of anchor bolts in group.
r_g = radius of bolt group (bolt group centroid to centroid of anchor bolts). [in]
I_g = moment of inertia of anchor bolt group. [in^3]
d_a = nominal anchor bolt diameter. [in]
n_t = number of threads per inch for the anchor bolt.

d_e = effective diameter of the threaded portion of an anchor bolt $= d_a - \frac{0.9743}{n_t}$. [in]
A_e= net effective area of the threaded portion of an anchor bolt $= \frac{\pi}{4} * {d_e}^2$. [$in^2$]
Z_a= plastic section modulus of the threaded portion of an individual anchor bolt $= \frac{d_e^3}{6}$. [in^3]
N_{ua} = maximum individual anchor bolt normal force. [kips]
V_{ua} = maximum individual anchor bolt shear. [kips]
$V_{ua,V}$ = individual anchor bolt shear due to base plate direct shear. [kips]
$V_{ua,T}$ = individual anchor bolt shear due to base plate torsion. [kips]

l_{LN} =distance from the surface of the concrete to the bottom of the leveling nut in ungrouted stand-off base plates. Equal to 0 in flush-mounted base plates and grouted stand-off base plates. [in]

Commentary: Grout below the base plate stiffens the connection and, after grout cracking, restrains downward displacement of the base plate, generating significantly higher anchor bolt steel shear strengths than in ungrouted stand-off base plates with the same stand-off distance. No reduction from flush-mounted strength is taken for grouted stand-off base plates.

$F_{u,t}$ = specified ultimate tensile capacity of anchor bolts. [ksi]
$F_{na,N}$ = nominal axial strength of anchor bolts. [ksi]
$F_{na,V}$ = nominal shear strength of anchor bolts. [ksi]
$f_{ua,N}$ = maximum individual bolt axial stress. [ksi]
$f_{na,V}$ = maximum individual bolt shear stress. [ksi]

$\Phi_N = 0.80$ axial resistance factor
$\Phi_V = 0.75$ shear resistance factor

$$N_{ua} = \frac{N_{ua,g}}{n} + \frac{M_{ua,g}}{2r_b}$$

Commentary: The maximum normal force acting on an anchor is produced by the superimposition of the base plate axial force shared by all anchors in the group (this will typically be negative for compression from dead load) and the highest axial load on any one anchor in the group due to base plate overturning moment.

The axial force due to moment is derived from $M_{ua,g}cAe/I_g$ *for the bolt group assuming that the most extreme bolt is oriented perpendicular to the neutral axis of bending (i.e.* $c = r_g$*);*

where:

$$M_{ua,g} = \sqrt{{M_{uax,g}}^2 + {M_{uaz,g}}^2}$$

$$V_{ua} = V_{ua,V} + V_{ua,T}$$

where:

$$V_{ua,g} = \sqrt{{V_{uax,g}}^2 + {V_{uaz,g}}^2}$$

$$V_{ua,V} = V_{ua,g}/n$$

$$V_{ua,T} = \frac{M_{uay,g}}{nr_g}$$

Commentary: The calculation of V_{ua} *assumes the maximum possible shear force by superimposing circumferentially oriented torsional shear with direct shear forces.*

B. Interaction of Tension and Shear Stresses

The following interaction equation for tension and shear stresses must be satisfied:

$$\left(\frac{f_{ua,V}}{\Phi_V F_{na,V}}\right)^2 + \left(\frac{f_{ua,N}}{\Phi_N F_{na,N}}\right)^2 \leq 1.0$$

Commentary: An elliptical relationship between axial and shear stresses against limiting values of each has been found to be appropriate for design of anchor bolts. Using the interaction equation with maximum values for tension and shear is conservative since these may not occur on the same anchor. In cantilever structures anchor bolt shear force is dominated by base plate torsion shared equally by all of the anchors, making the conservatism minimal while acknowledging minor contributions from base plate direct shear. In other structures the torsion component is dropped and the calculation represents the actual shear force on the most highly loaded anchor.

where:

$$F_{na,N} = F_{u,t}$$
$$F_{na,V} = 0.5F_{u,t}$$
$$f_{ua,N} = \frac{N_{ua}}{A_e} + \frac{V_{ua} l_{LN}}{2Z_a}$$
$$f_{ua,V} = \frac{V_{ua}}{A_e}$$

Commentary: Shear loads on ungrouted stand-off base plates from global direct shear and torsion cause an internal moment forces to develop in anchor bolts, resulting in significant losses in strength and stiffness. Bending stresses are calculated with a beam model of length equal to the exposed length of the bolt (from the top of the concrete surface to the bottom of the leveling nut) restrained on both sides from rotation but free to displace laterally. l_{LN} *is equal to zero for flush-mounted base plates and grouted stand-off base plates.*

APPENDIX E
PROPOSED 649-7 GROUTING PROCEDURE

649-7 Structural Grout Pads.

On mast arm support structures, place a structural grout pad using grout meeting the requirements of Section 934 and listed on the QPL. Obtain the services of a representative, employed or certified by the manufacturer of the grout, to be present on site to verify that the installation of the first grout pad complies with the manufacturer's instructions.

Prior to grout placement, flush the top of the foundation with clean water to remove any dirt and debris and prepare the concrete surface in accordance with the manufacturer's recommendations. Remove all freestanding water before beginning the grouting operation.

Use a watertight, non-absorbent steel, wood, or plastic form with a form release agent applied to all interior surfaces. Maintain a 2 inch ± 1 inch clearance between the form and the base plate. Extend the form a minimum of 1 inch above the bottom of the base plate. Place a temporarily sealed, 1" diameter PVC drain pipe in the area beneath the base plate. The PVC pipe shall extend horizontally from the face of the form to the approximate center of the pole, then vertically 90 degrees to the elevation of the bottom of the base plate. Attach a head box with a 45 degree slope on the form for grout placement.

Mix the grout to a fluid state in accordance with the manufacturer's instructions. Use only potable water and fresh unopened full bags of grout. Test the fluidity of the grout using the ASTM C 939 Flow Cone Method. Use fluid grout that meets the efflux time of 20 to 30 seconds. Do not use plastic (dry-pack) or flowable grout. Discard grout with efflux times less than 20 seconds.

Pour the fluid grout from only one side of the base plate through the head box until the grout has filled the entire form and extends 1/4 inch ± 1/8 inch above the bottom of the base plate. Do not allow the grout to enter the PVC drain pipe. Do not use mechanical means to push or vibrate grout. Clean excess grout off the base plate after the grout has reached initial set (two to four hours). Cure the grout in accordance with the manufacturer's instructions and Section 925. Remove the forms after verifying the grout is self supporting by penetration with a pointed masons trowel or other sufficient tool. Unseal the PVC drain pipe and ensure water inside the pole drains freely out of the pipe.